DISRUPTION OF COMPLEX ENTERIC COMMENSAL MICROBIAL COMMUNITIES AND THEIR MUTUALISTIC FUNCTIONS WITH THE HOST CONTRIBUTES TO THE SEVERITY OF COMMON INTESTINAL DISORDERS AND SERVES AS A PROMISING THERAPEUTIC TARGET

Christopher Dennis Packey

A dissertation submitted to the faculty at the University of North Carolina at Chapel Hill in partial fulfillment of the requirements for the degree of Doctor of Philosophy in the Microbiology and Immunology Department in the School of Medicine.

Chapel Hill
2013

Approved by:

R. Balfour Sartor

Scott E. Plevy

Christian Jobin

Chris Dekaney

Bo Wang

Virginia Miller

ABSTRACT

Christopher Dennis Packey: Disruption of complex enteric commensal microbial communities and their mutualistic functions with the host contributes to the severity of common intestinal disorders and serves as a promising therapeutic target
(Under the direction of R. Balfour Sartor)

Many people were surprised when the Human Genome Project revealed that the human genome contains only about 20,000 protein-coding genes, comparable to the number in the fruit fly genome. The complexities of human health and disease may lie in the human microbiota, the constellation of microbes living inside and on the body that harbors at least 3.3 million non-redundant genes.

The human gut is the natural environment for a diverse and dynamic microbial ecosystem. A better understanding of the human intestinal microbiota and how to manipulate it safely may lead to better ways to prevent harm and promote health. An overall goal of this work was to generate data that guides the design and implementation of diagnostic and therapeutic strategies that intentionally manipulate the human microbiota to optimize its performance in the context of an individual's physiology.

We utilized novel, high-throughput technologies with next-generation gene sequencing and powerful bioinformatics analysis tools integrated with metagenomics, gnotobiology and microbiota transplantation to provide deep insights into the composition, structure and activities of the gut microbiota over time in rodents and humans with injury and inflammation in the small

intestine and colon. We characterized significant shifts in the composition of the microbiota in several forms of intestinal disease, including irritable bowel syndrome, spontaneous, chronic, immune-mediated colitis, and radiation enteropathy. We identified interventions that alter dysbiosis and the course of intestinal disease, including antibiotics, probiotics and fecal microbiota transplantation. Host innate immune molecules including antimicrobial peptides produced by cells in the small intestinal mucosa contribute to phenotypes.

Our studies have improved the knowledge of how the host and bacteria interact during intestinal inflammation and injury and how the microbiota responds and is regulated. Given the abrupt rise in incidence of intestinal disorders that appears to have coincided with socioeconomic development and dietary changes, expeditious progress in this area of research is crucial in order to impede the dramatic acceleration of the prevalence of these diseases. These data may yield valuable clinical tools in restoring a healthy microbiota to prevent or treat intestinal disorders without administering broad, immunosuppressive medications that are accompanied by severe side effects.

ACKNOWLEDGEMENTS

This work is dedicated to my parents, Dennis and Julie, for all of their unconditional love and encouragement throughout my life. They were the best parents that anyone could hope for. From attending every little league baseball game, to staying up all night to help me with science fair projects, to selling hundreds of boxes of grapefruits and oranges at the hospital for a school contest every year, I can never thank my parents enough for everything that they have done for me. Everything that I do in my career is dedicated to them.

I would also like to thank my mentor, Dr. R. Balfour Sartor, for offering tireless guidance and endless wisdom throughout my years at UNC.

While there are many other people at UNC that I would like to thank for their help along the way, I need to convey special gratitude to Dr. Bo Wang, Dr. Eugene Orringer, and Dr. Susan Henning, who were extremely supportive of me.

TABLE OF CONTENTS

LIST OF FIGURES AND TABLES

Introduction

The incidence of some important gastrointestinal (GI) disorders is increasing, including that of irritable bowel syndrome (IBS), radiation enteropathy, and the inflammatory bowel diseases (IBD). These three sets of intestinal diseases share some key features: They are associated with a similar group of symptoms, (nausea, abdominal pain, changes in bowel habits) (1-3), they are common reasons for seeking treatment (4-6), they have a high correlation with poor health-related quality of life (7-9), they are responsible for substantial costs to society (10-12), and intestinal microbes may contribute to their development (13-15).

IBS is the most common cause of lower GI illness (16). Diarrhea-predominant IBS (D-IBS) accounts for approximately 40% of all IBS patients and has an estimated 5% prevalence in the general population (1). D-IBS is defined by abdominal pain and diarrhea, in the absence of organic disease that is likely to explain the symptoms (16). It is a symptom-based condition that lacks biomarkers that can be used for diagnostic or monitoring purposes.

Intestinal radiation injury is a significant clinical issue that is increasing in prevalence due to improved survival of cancer patients and increased availability of radiotherapy as an affordable treatment. Radiation therapy is a part of the treatment regimen for approximately 70% of all cancer patients (17). GI radiation injury is an important problem for two main reasons. First, it limits the dose that is administered to the patient, which can compromise efficacy of treatment and malignancy cure rate. Second, it can lead to the radiation GI syndrome, which is the cause of initial morbidity and mortality following a nuclear accident, terrorist attack or other large dose radiation exposure. Radiation enteropathy is still a significant problem despite efforts to decrease damage to normal intestinal tissue by utilizing physical maneuvers, tissue expanders, prophylactic surgical techniques, and optimized planning and delivery techniques (5). Biological

strategies have been largely ineffective, as today there is still no prophylactic or therapeutic agent available that is proven to mitigate the acute and chronic symptoms of GI radiation injury or to allow safe radiation dose escalation for better control of malignancies. This is, in large part, due to the fact that relatively little is known about the pathophysiology of radiation intestinal injury.

IBD, immune-mediated disorders that include Crohn's disease and ulcerative colitis, have been steadily increasing in incidence in North America and Northern Europe since World War II, with rates doubling during several decades (6). Rapid increases in incidence are now also being recorded in Southern Europe, Australia, New Zealand, Japan, South Korea, China, and India. It has been proposed that IBD will emerge as a worldwide epidemic in the near future. Unlike IBS and radiation enteropathy, it is well established that commensal gut bacteria play a critical role in the pathogenesis of IBD (18, 19). However, exactly what role they play is still in need of further clarification (20).

Some researchers had predicted in the past that the human genome might be comprised of more than 100,000 genes. So many were surprised when the Human Genome Project revealed that the human genome contains only about 20,000 protein-coding genes, comparable to the number in the fruit fly genome. The complexities of human health and disease may lie in the human microbiota, the constellation of microbes living inside and on the body that harbors at least 3.3 million non-redundant genes (21).

My studies focus on the role of commensal bacteria in the pathogenesis of the aforementioned three intestinal disorders. The GI tract has a large mucosal interface (300-400 m^2) that has structures and functions for the immunological recognition of the external

environment (19). This tract is the principal site of permanent microbial colonization in the human body, teeming with 10-100 trillion microorganisms that exceed the total number of host cells by at least one order of magnitude (22). Most of these microbes belong to the domain Bacteria. 98% of genes in the human gut microbiome are bacterial, and the gut is home to at least 1150 prevalent bacterial species (21). Yet, only seven to nine of the 55 phyla of the domain Bacteria are detected in the human intestine (21, 23-25). More than 90% of all phylotypes (sequences with 97% identity, assumed to represent a single species) belong to two divisions: Bacteroidetes and Firmicutes (24). The other divisions that have been consistently found in samples from the human distal gut are Proteobacteria, Verrucomicrobia, Actinobacteria, and Fusobacteria.

The concept of the gut microbiota as a regulator of health and disease is not a new one. In fact, Elie Metchnikoff hypothesized over a century ago that toxic colonic microbes that accelerate senescence could be replaced with beneficial microbes for the betterment of the host (26). Metchnikoff may have provided the foundation for the notion of probiotics when he advertised claims of improved health upon introducing sour milk to his diet, following the example of notoriously long-enduring Eastern European farmers who consumed large quantities of acrid dairy products (27).

The relationship between the mammalian host and microorganisms that colonize the intestinal tract is the product of a lengthy and complex co-evolution. Experimental studies in germ-free animals have revealed the importance of commensal microbial communities for normal host growth and development and for the maintenance of health. There are important anatomical and physiological differences between germ-free and colonized animals, and reconstitution of germ-free animals with a microbiota from conventional counterparts restores

most of the deficiencies (28). The main functions of the gut microbiota are ascribed into three categories: Metabolic, protective and trophic functions (29). Germ-free mice are immunodeficient and highly susceptible to infections caused by pathogens or opportunistic organisms (30-33).

Certain organisms, such as *Lactobacillus* spp. (34) and *Faecalibacterium prausnitzii* (35), are considered beneficial for health. The gut community also harbors organisms that have the capacity for adverse effects, via their gene products, metabolic outputs, or potential for pathogenicity (36). The balance of benefit and harm for the host therefore depends on the overall state of the microbial community in terms of its species composition, diversity and distribution (37, 38). While there is significant inter-individual variation in the composition of the microbiota, fecal microbiota profiles in healthy adults seem to have substantial stability over time (38-40).

Not surprisingly then, a "dysbiosis", or imbalanced state of the gut microbial ecosystem, including overgrowth of more "pro-inflammatory" commensals and loss of protective microbes, has been associated with several diseases, including IBD (18, 41), obesity (42) and metabolic syndrome (43, 44). However, how changes in microbial communities contribute to disease etiology remains poorly defined.

The study of isolated bacteria by culture techniques does not help us describe complex, mostly anaerobic microbial communities in the human body, as most of the mammalian microbiota is not easily cultured in a laboratory, mainly owing to the lack of appropriate culture media (19). Furthermore, laboratory *in vitro* cultivation does not permit characterization of the biology of these organisms in their natural environment. Therefore, we utilized several 16S

rRNA-based approaches to answer questions about the interaction of the host and gut microbes in intestinal injury.

High-throughput technologies with next-generation sequencing enabling a deep characterization of the microbiota functions have been developed and implemented for the first time in the last few years (45). Next-generation sequencing techniques use beads, slides or solid surfaces to produce millions of sequences at once. A single run of the 454 Life Sciences pyrosequencing platform, which we utilized in our studies, can produce 1.2 million sequences in 8 hours (46). We used this sequencing technology in combination with advanced computational platforms and analytical techniques to characterize the role of microbial communities in human patients and animals with several forms of intestinal injury and inflammation. We then employed approaches integrating metagenomics, gnotobiology and microbiota transplantation to assess the function of complex microbial communities in the context of intestinal disorders, as well as that of individual constituent members of these assemblages.

An overall goal of this work was to generate data that can guide the design and implementation of diagnostic and therapeutic strategies that intentionally manipulate the human microbiota to optimize its performance in the context of an individual's physiology, and specifically when the host encounters threatening conditions presented by functional bowel disorders, spontaneous, immune-mediated intestinal inflammation, or radiation exposure.

REFERENCES

1. Camilleri M. Current and future pharmacological treatments for diarrhea-predominant irritable bowel syndrome. Expert Opin Pharmacother 2013; 14(9): 1151-60.

2. Tho LM, Glegg M, Paterson J, et al. Acute small bowel toxicity and preoperative chemoradiotherapy for rectal cancer: investigating dose-volume relationships and role for inverse planning. Int J Radiat Oncol Biol Phys 2006; 66: 505-513.

3. Allen PB, Peyrin-Biroulet L. Moving towards disease modification in inflammatory bowel disease therapy. Curr Opin Gastroenterol 2013; 29(4): 397-404.

4. Koloski NA, Talley NJ, Boyce PM. Epidemiology and health care seeking in the functional GI disorders: a population-based study. Am J Gastroenterol 2002; 97: 2290-9.

5. Shadad AK, Sullivan FJ, Martin JD. Egan LJ. Gastrointestinal radiation injury: Prevention and treatment. World J Gastroenterol 2013; 19(2): 199-208.

6. Molodecky NA, Soon IS, Rabi DM, et al. Increasing incidence and prevalence of the inflammatory bowel diseases with time, based on systematic review. Gastroenterology 2012; 142: 46-54.

7. Simren M, Svedlund J, Posserud I, et al. Health-related quality of life in patients attending a gastroenterology outpatient clinic: functional disorders versus organic diseases. Clin Gastroentrol Hepatol 2006; 4: 187-95.

8. Bismar MM, Sinicrope FA. Radiation enteritis. Curr Gastroenterol Rep 2002; 4: 361-365.

9. Peyrin-Biroulet L, Cieza A, Sandborn WJ, et al. Disability in inflammatory bowel diseases: developing ICF Core Sets for patients with inflammatory bowel diseases based on the International Classification of Functioning, Disability, and Health. Inflamm Bowel Dis 2010; 16: 15–22.

10. Hillila MT, Farkkila NJ, Farkkila MA. Societal costs for irritable bowel syndrome- a population based study. Scand J Gastroenterol 2010; 45: 582-91.

11. Gunnlaugsson A, Kjellen E, Nilsson P, et al. Dose-volume relationships between enteritis and irradiated bowel volumes during 5-fluorouracil and oxaliplatin based chemoradiotherapy in locally advanced rectal cancer. Acta Oncol 2007; 46: 937-944.

12. Kappelman M, Rifas-Shiman SL, Porter CQ, et al. Direct healthcare costs of Crohn's disease and ulcerative colitis in US children and adults. Gastroenterology 2008; 135: 1907-1913.

13. Simren M, Barbara G, Flint HJ, et al. Intestinal microbiota in functional bowel disorders: a Rome foundation report. Gut 2013; 62: 159-176.

14. Crawford PA, Gordon JI. Microbial regulation of intestinal radiosensitivity. Proc Natl Acad Sci U S A 2005; 102: 13254-13259.

15. Loh G, Blaut M. Role of commensal gut bacteria in inflammatory bowel diseases. Gut Microbes 2012; 3(6): 544-55.

16. Longstreth GF, Thompson WG, Chey WD, et al. Functional bowel disorders. Gastroenterology 2006; 130: 1480–91.

17. Wang J, Boerma M, Fu Q, Hauer-Jensen M. Significance of endothelial dysfunction in the pathogenesis of early and delayed radiation enteropathy. World J Gastroenterol 2007; 13: 3047-3055.

18. Sartor RB. Microbial influences in inflammatory bowel diseases. Gastroenterology 2008; 134 (2): 577-94.

19. Manichanh C, Borruel N, Casellas F, Guarner F. The gut microbiota in IBD. Nature Rev Gastroenterol Hepatol 2012; 9: 599-608.

20. Frank DN, Zhu W, Sartor RB, Li E. Investigating the biological and clinical significance of human dysbioses. Trends Microbiol 2011; 19(9): 427-34.

21. Qin J, Li R, Raes J, et al. A human gut microbial gene catalogue established by metagenomic sequencing. Nature 2010; 464: 59-65.

22. Backhed F, Ley RE, Sonnenburg JL, et al. Host-bacterial mutualism in the human intestine. Science 2005; 307: 1915-1920.

23. Eckburg PB, Bik EM, Bernstein CN, et al. Diversity of the human intestinal microbial flora. Science 2005; 308: 1635-1638.

24. Turnbaugh PJ, Ley RE, Hamady M, et al. The human microbiome project. Nature 2007; 804-810.

25. Frank DN, Pace NR. Gastrointestinal microbiology enters the metagenomics era. Curr Opin Gastroenterol 2008; 24: 4-10.

26. Metchnikoff II. The prolongation of life optimistic studies. The English translation edited by PC Mitchell. 1907.

27. Salminen S, Bouley C, Boutron-Ruault MC, et al. Functional food science and gastrointestinal physiology and function. Br J Nutr 1998; 80: S147-S171.

28. O'Hara AM, Shanahan F. The gut flora as a forgotten organ. EMBO Rep 2006; 7: 688-693.

29. Guarner F, Malagelada JR. Gut flora in health and disease. Lancet 2003; 361: 512-519.

30. Umesaki Y, Setoyama H, Matsumoto S, et al. Differential roles of segmented filamentous bacteria and clostridia in development of the intestinal immune system. Infect Immun 1999; 67: 3504-3511.

31. Cebra JJ. Influences of microbiota on intestinal immune system development. Am J Clin Nutr 1999; 69: 1046S-1051S.

32. Umesaki Y, Setoyama H. Structure of the intestinal flora responsible for development of the gut immune system in a rodent model. Microbes Infect 2000; 2: 1343-1351.

33. Eberl G, Lochner M. The development of intestinal lymphoid tissues at the interface of self and microbiota. Mucosal Immunol 2009; 2: 478-485.

34. Baarlen PV, Wells JM, Kleerebezem M. Regulation of intestinal homeostasis and immunity with probiotic *Lactobacilli.* Trends Immunol 2013; 34(5): 208-215.

35. Sokol H, Pigneur B, Watterlot L, et al. *Faecalibacterium prausnitzii* is an anti-inflammatory commensal bacterium identified by gut microbiota analysis of Crohn disease patients. Proc Natl Acad Sci 2008; 105: 16731-16736.

36. Blaser MJ, Kirschner D. The equilibria that allow bacterial persistence in human hosts. Nature 2007; 449: 843-849.

37. Flint HJ, Scott KP, Louis P, Duncan SH. The role of the gut microbiota in nutrition and health. Nat Rev Gastroenterol Hepatol 2012; 9: 577-589.

38. De Medina FS, Ortega-Gonzales M, Gonzales-Perez R, et al. Host-microbe interactions: the difficult yet peaceful coexistence of the microbiota and the intestinal mucosa. Br J Nutr 2013; 109: S12-S20.

39. Zoetnedal EG, Akkermans ADK, De Vos WM. Temperature gradient gel electrophoresis analysis of 16S rRNA from human fecal samples reveals stable and host-specific communities of active bacteria. Appl Environ Microbiol 1998; 64: 3854-3859.

40. Costello EK, Lauber CL, Hamady M, et al. Bacterial community variation in human body habitats across space and time. Science 2009; 326: 1694-1697.

41. Frank DN, St Amand Al, Feldman RA, et al. Molecular-phylogenetic characterization of microbial community imbalances in human inflammatory bowel diseases. Proc Natl Acad Sci 2007; 104: 13780-13785.

42. Ley RE, Turnbaugh PJ, Klein S, et al. Microbial ecology: human gut microbes associated with obesity. Nature 2006; 444: 1022-1023.

43. Qin J, Li Y, Cai Z, et al. A metagenome-wide association study of gut microbiota in type 2 diabetes. Nature 2012; 490: 55-58.

44. Vijay-Kumar M, Aitken JD, Carvalho FA, et al. Metabolic syndrome and altered gut microbiota in mice lacking Toll-like receptor 5. Science 2010; 328(5975): 228-31.

45. Gill SR, Pop M, Deboy RT, et al. Metagenomic analysis of the human distal gut microbiome. Science 2006; 312: 1355-1359.

46. Wu X, Berkow K, Frank DN, et al. Comparative analysis of microbiome measurement platforms using latent variable structural equation modeling. BMC Bioinformatics 2013; 14: 79.

CHAPTER 1: COMMENSAL BACTERIA, TRADITIONAL AND OPPORTUNISTIC PATHOGENS, DYSBIOSIS AND BACTERIAL KILLING IN INFLAMMATORY BOWEL DISEASES[1]

Introduction

Chronic idiopathic inflammatory bowel diseases (IBD), which affect 1.0–1.5 million Americans (1), are a heterogeneous group of disorders resulting from continuous enteric microbial antigenic stimulation of pathogenic T cell responses in individuals with genetic defects in mucosal barrier function, innate bacterial killing or immunoregulation (2). Altered microbial composition, defective clearance of bacteria and enhanced mucosal uptake in Crohn's disease and ulcerative colitis increase immune stimulation. Crohn's disease and ulcerative colitis preferentially occur in areas of highest intestinal bacterial concentrations and fecal flow sustains inflammation of Crohn's disease (3). Ciprofloxacin and metronidazole treat colonic Crohn's disease and experimental colitis in a number of rodent models (4). This review describes evidence of the roles of commensal bacteria in the pathogenesis of IBD in articles published from January 2007 to December 2008.

Defective bacterial killing in Crohn's disease

Pathophysiologic similarities between Crohn's disease and chronic granulomatous diseases associated with defective phagocyte function, polymorphisms of genes regulating clearance of intracellular pathogens and observed defects in innate antimicrobial function have led to the hypothesis that a subset of Crohn's disease is caused by defective clearance of commensal, opportunistic or pathogenic bacteria with subsequent initiation of compensatory

[1] This chapter previously appeared as an article in the journal *Current Opinion in Infectious Diseases*. The original citation is as follows: Packey CD, Sartor RB. Commensal bacteria, traditional and opportunistic pathogens, dysbiosis and bacterial killing in inflammatory bowel diseases. Curr Opin Infect Dis 2009; 22: 292-301.

antibacterial effector T cells that cause tissue damage (2, 5). Secretion of both α- and β-defensins is defective in Crohn's disease (6, 7), with decreased Paneth cell α-defensin production due to reduced expression of Tcf-4, a WNT signaling pathway transcription factor (8). The truncation mutation of NOD2, which is an intracellular receptor for the peptidoglycan component muramyl dipeptide, results in decreased ileal α-defensin production (6). Furthermore, NOD2-deficient mice exhibit decreased α-defensin defcr-4 (9), whereas deletion of the autophagy gene ATG16L1 or the endoplasmic reticulum stress protein XBP-1 results in Paneth cell morphologic changes and decreased expression of antimicrobial peptides (10,11). Crohn's disease is associated with genetic polymorphisms of at least two autophagy pathway components, ATG16L1 and IRGM, which, like NOD2 and NCF2, regulate intracellular bacterial killing (12–14). Decreased antimicrobial peptide secretion could lead to overgrowth, increased mucosal adherence and translocation of commensal bacteria, whereas defective clearance of invasive or phagocytosed bacteria promotes persistence of viable intracellular bacteria (Fig. 1.1). Both mechanisms could result in excessive antigenic stimulation of pathogenic Th1/Th17 cells, chronic granulomatous inflammation and susceptibility to infection by traditional and opportunistic pathogens.

Microbial pathogens

Comprehensive culture and molecular-based analyses of the microbiota of IBD patients fail to identify consistent enrichment of individual pathogenic species in IBD tissues. However, bacterial pathogens continue to reap attention because of similarities between Crohn's disease, ulcerative colitis and enteric infections and the hope of finding a cure analogous to *Helicobacter pylori* in peptic ulcers.

Mycobacterium avium subspecies *paratuberculosis*

Mycobacterium avium subspecies *paratuberculosis* (MAP) causes spontaneous granulomatous enterocolitis (Johne's disease) with diarrhea and wasting in ruminants, making this obligate intracellular pathogen a credible causative agent of Crohn's disease (15). After considerable investigation, the link between MAP and Crohn's disease remains neither substantiated nor invalidated. Many investigators continue to measure the MAP-specific insertion element IS900 DNA in the tissue and/or blood of IBD patients using polymerase chain reaction (PCR) with mixed results.

A study conducted at the University of Colorado reported no detectable MAP DNA in 190 tissue samples from Crohn's disease, ulcerative colitis and control patients (16). Baumgart *et al*. (17) similarly reported lack of detectable IS900 DNA in ileal Crohn's disease biopsies. Contradictory results were reported by Scanu *et al.* (18), who detected MAP DNA in 87% of Crohn's disease tissues and 15% of controls in a small cohort. Results are also inconsistent in PCR assays for MAP DNA in blood samples (20–22).

One recent blinded study offered an alternative method to PCR for identifying MAP in patients with Crohn's disease (25). Coded, paraffin-embedded surgical resections from Crohn's disease and control patients at two centers subjected to acid-fast staining and rRNA in-situ hybridization (ISH) for MAP were visualized with oil-immersion microscopy. Both methods provided positive results in 10/17 patients with Crohn's disease [59%, 95% confidence interval (CI) 36–78], contrasted with 5/35 control patients [odds ratio (OR) for Crohn's disease versus controls=8.6, P=0.002]. Agreement between the two methods was good, but the time-consuming ISH probes could not discriminate between mycobacterial subspecies.

Defective bacterial killing by innate immune cells could increase risk of infection by intracellular pathogens. Two recent studies showed no association between MAP and NOD2 mutations. No significant association was seen in New Zealand in patients with Crohn's disease for carriage of heterozygous or homozygous NOD2 mutations and MAP status (21), or between MAP serologies and NOD2 polymorphisms in a large, population-based study in Manitoba (26). A recent epidemiologic study also failed to support exposure to MAP by contaminated milk or water (27). Furthermore, consumption of pasteurized milk and fruit was associated with a reduced risk of Crohn's disease, whereas meat intake was associated with an increased risk. Finally, a well-designed, 2-year prospective trial of clarithromycin, rifabutin and ethambutol failed to show sustained clinical response in patients with Crohn's disease (28).

Recent studies possibly linking MAP to pathogenic mechanisms of Crohn's disease fuel the ongoing debate. Two hundred and thirty-five patients with Crohn's disease, ulcerative colitis, irritable bowel syndrome (IBS) and no known disease were tested for presence of MAP IS900 DNA and cytokine secretion in intestinal biopsy samples (23). Greater tumor necrosis factor levels correlated with the presence of MAP in patients with Crohn's disease ($P<0.05$). However, there was no correlation of MAP with interleukin (IL)-2, IL-12, IL-10 and interferon (IFN)-γ secretion. A separate study linked MAP to active Crohn's disease via IL-4 and IL-2 cytokine profiles in peripheral blood with no differences in IFN-γ or tumor necrosis factor levels (24).

Finally, MAP was recently reported to induce experimental colitis in gnotobiotic IL-$10^{-/-}$ mice (29). Germ-free IL-$10^{-/-}$ mice receiving a single oral dose of milk containing 104 colony-forming units (CFU) of live MAP obtained from a patient with Crohn's disease developed more severe and aggressively progressive colitis, had higher serum amyloid A, IFN-γ and tumor necrosis factor levels, and lost more weight than did IL-$10^{-/-}$ mice that received heat-killed MAP.

Despite continued suggestions of a link between MAP and IBD, it remains doubtful that MAP is the causative agent of most Crohn's disease patients, although infection of a subset of patients with intracellular killing defects caused by ATG16L1, IGRM or NCF4 needs to be investigated. Crohn's disease-related NOD2 polymorphisms do not appear to be risk factors for MAP infection.

Functional changes in *Escherichia coli*

Darfeuille-Michaud and colleagues (30, 31) reported that adherent/invasive *E. coli* (AIEC) that persist within macrophages and epithelial cells selectively colonize the ileum of patients with Crohn's disease. At least two separate groups have confirmed these observations. Baumgart *et al.* demonstrated AIEC in the ileum of patients with Crohn's disease, documented in-vivo mucosal adherence with fluorescent in-situ hybridization (FISH) and identified AIEC virulence factors common to uropathic *E. coli* strains and *E. coli* strains isolated from boxer dogs with spontaneous granulomatous colitis (17). In a separate study, *E. coli* comprised 99% of invasive bacterial isolates in mucosal biopsies of patients with Crohn's disease as opposed to 42% in patients with ulcerative colitis and 2% in normal controls (32). A prototypic AIEC strain, LF82, induced in-vitro granulomas using blood-derived mononuclear cells (33). Serum antibodies directed against *E. coli* outer membrane protein C (OmpC) are present in 37–55% of patients with Crohn's disease, in contrast to 5% or less of patients with ulcerative colitis and without IBD. High serum reactivity to *E. coli* OmpC is associated with severe Crohn's disease with longer disease duration, frequent disease progression, small bowel involvement and increased resections (34).

Mechanisms of epithelial adherence and invasion of AIEC are being elucidated. Studies utilizing isogenic mutants of LF82 that lack OmpC and other genes suggest that increased

expression of OmpC, particularly at high osmolarities reflecting the gastrointestinal tract, and/or induction of the δ^E regulatory pathway promote adherence and invasion of epithelial cells by LF82 independent of the transcriptional regulator OmpR (35).

Flagellin is necessary for LF82's ability to exacerbate dextran sulfate sodium (DSS)-induced murine colitis (36). Nonflagellated LF82 mutants behaved like the nonpathogenic *E. coli* strain K-12 in this model. An LF82 mutant lacking dsbA, a gene that encodes a periplasmic oxidoreductase that determines virulence for several pathogens, expressed neither flagella nor type 1 pili, and displayed decreased survival ability (37). In contrast, decreased epithelial adhesion and invasion of the LF82 OmpC and OmpR mutants were not associated with decreased expression of flagella and type 1 pili. In a separate study, *E. coli* 083:H1 was dependent upon flagellin for its adherent and invasive phenotype (38). Increased expression of carcinoembryonic antigen-related cell adhesion molecule 6 (CEACAM6), which acts as a receptor for AIEC, by ileal epithelial cells in active Crohn's disease may mediate increased mucosal adherence of AIEC (39). Increased CEACAM6 expression by cultured colonic epithelial cells after IFN-γ or tumor necrosis factor stimulation and after exposure to LF82 indicate that AIEC may promote its own colonization.

Monocytes from patients with Crohn's disease carrying homozygous or heterozygous NOD2 polymorphisms displayed reduced secretion of IL-1β, IL-6, and IL-10 to LF82 *in vitro* compared with monocytes from patients with Crohn's disease without NOD2 polymorphisms (40). TLR4 polymorphisms did not influence monocyte response. In preliminary studies, we showed that macrophages from NOD2-deficient mice display defective clearance of a murine AIEC strain with prolonged secretion of IL-12/23 p40 and tumor necrosis factor (41). These

findings demonstrate the importance of genetically programmed host immune responses to disease related bacteria in the pathogenesis of Crohn's disease.

Enteric pathogens as environmental triggers

A case–control study examining medical records of 3,019 US soldiers who developed IBD and 11,646 matched controls compared data using a conditional logistic regression model to determine that a single episode of infectious gastroenteritis increased the risk of IBD (OR 1.40, CI 1.19–1.66) (42). These results suggest that a self-limited enteric pathogen could trigger IBD, possibly by breaking the mucosal barrier and initiating an early inflammatory response in a genetically susceptible host with immunoregulatory abnormalities (2). *Clostridium difficile* can reactivate quiescent IBD (43) and induce acute experimental epithelial injury by Fas-mediated apoptosis (44). Likewise enterotoxigenic *Bacteroides fragilis* can induce experimental colitis and IL-17 production (45). A role for non-pylori *Helicobacter* in IBD pathogenesis is unlikely based on detection of species-specific serum antibodies in only 6/137 IBD patients (46).

Dysbiosis

Recent studies in rodents confirm that bacterial composition changes with colonic inflammation and/or infection (47). Use of molecular techniques is clarifying changes in the composition of the mucosally associated and fecal microbiota in patients with Crohn's disease and ulcerative colitis and vastly extending previous culture-based studies.

Examining DNA libraries of mucosal-associated microbiota, which may be more relevant than the fecal microbiota to the pathogenesis of IBD, reveals that patients with Crohn's disease and ulcerative colitis have decreased complexity of commensal bacteria (16). Most notably, members of the phyla Bacteroidetes and Firmicutes are decreased in Crohn's disease and ulcerative colitis. These organisms promote gastrointestinal health in multiple ways (59).

Reduced *Faecalibacterium prausnitzii*, a major member of the family Firmicutes, in patients with Crohn's disease (16, 50) was confirmed and associated with a higher risk of postresection recurrence of ileal Crohn's disease (49). In-vitro peripheral blood mononuclear cell stimulation by *F. prausnitzii* decreased IL-12 and IFN-γ production and stimulated secretion of IL-10. Oral administration of either live *F. prausnitzii* or its supernatant reduced the severity of trinitrobenzene sulfonic acid (TNBS) colitis and corrected the associated dysbiosis. In parallel, the abundance of *E. coli* is increased in IBD, particularly the B2+D phylogenetic group (17, 48). *E. coli* isolated from patients with Crohn's disease express uropathic-like virulence factors that are postulated to facilitate mucosal invasion (17). The number of mucosal *E. coli* in situ correlates with the severity of ileal disease and invasive *E. coli* are restricted to inflamed mucosa. Compositional changes of the microbiota (dysbiosis) in IBD subsets may contribute to disease severity, since abnormal microbiotas correlated with the occurrence of abscesses in patients with Crohn's disease, and IBD patients with dysbiosis underwent surgery at a younger age than those with normal microbiotas (16). Finally, fecal and mucosally associated microbial communities of patients with Crohn's disease and ulcerative colitis are consistently less diverse with increased temporal instability (16, 53–56).

Nonpathogenic bacteria can cause colitis in hosts with immunoregulatory and mucosal barrier deficits. When germ-free IL-$10^{-/-}$ and wild-type mice were inoculated with nonpathogenic *E. faecalis* and/or *E. coli*, dual-associated IL-$10^{-/-}$ (but not wild-type) mice developed aggressive Th1/Th17-mediated colitis within 3 weeks that progressed to severe pancolitis by 7 weeks (60). A separate study revealed that uptake of nonpathogenic *E. coli* strains K-12 and HB101 by specialized follicle-associated epithelial cells overlying Peyer's patches (the site of the earliest observable microscopic lesions of recurrent Crohn's disease), is increased in patients with

Crohn's disease, but not in patients with ulcerative colitis (61). Increased *E. coli* localized within dendritic cells of Crohn's disease mucosa correlated with augmented tissue release of tumor necrosis factor.

Metabolic products of the microbiota have important effects on mucosal epithelial cell and immune function (2). Butyrate and other short-chain fatty acids are the primary metabolic substrates of colonocytes, with rectal epithelial cells dependent on this fuel source, whereas hydrogen sulfide, nitric oxide and serine proteases produced by a subset of commensal microbiota can injure epithelial cells and matrix components (62). Hydrogen sulfide and nitric oxide block butyrate metabolism and could lead to a state of epithelial starvation relevant to the pathogenesis of ulcerative colitis.

Probiotics

Animal models and human studies suggest that therapeutically manipulating the balance between beneficial and detrimental intestinal bacterial species can influence health and disease (63). Use of probiotics (viable, nonpathogenic microorganisms that exert health benefits beyond basic nutrition), to shift this balance to favor protective species and treat IBD, has been extensively reviewed (63, 64, 65, 66, 67), yet the role for probiotics in treating Crohn's disease and ulcerative colitis remains undetermined because most trials are underpowered and therefore not definitive.

In a TNBS colitis model, oral *Lactobacillus acidophilus*, *Bifidobacterium lactis* and *Lactobacillus casei* reduced intestinal inflammation (68). *L. casei* had more modest protection than the other probiotic species, yet in a separate in-vitro study, live *L. casei* decreased tumor necrosis factor, IFN-γ, IL-2, IL-6, IL-8 and CXCL1 secretion by explanted Crohn's disease mucosa and counteracted the proinflammatory effects of commensal *E. coli* ATCC 35345 (69).

This and other studies emphasize host-specific responses to probiotics. Other probiotic species control aberrant immune responses in intestinal tissue. *Bifidobacterium bifidum* (BGN4) prevented colitis in a murine $CD4^+$ $CD45RB^{high}$ T cell transfer model (70). *Lactobacillus gasseri* expressing manganese superoxide dismutase ameliorated colitis in IL-$10^{-/-}$ mice, demonstrating the therapeutic potential of recombinant bacteria engineered to secrete biologically active molecules (71). Orally administered *Lactobacillus suntoryeus* HY7801 ameliorated TNBS-induced colitis, decreased colonic IL-1β, IL-6 and tumor necrosis factor expression and inhibited TLR4-linked NF-κB activation (72). *Bifidobacteria*-fermented milk enhanced IL-10 production in peripheral blood mononuclear cells from patients with ulcerative colitis and inhibited IL-8 secretion by intestinal epithelial cells (73). *Lactobacillus rhamnosus* GR-1 and *Lactobacillus reuteri* RC-14 fed in yogurt to IBD patients had peripheral blood anti-inflammatory effects. In an in-vitro study, *L. reuteri* potently suppressed human tumor necrosis factor production by lipopolysaccharide-activated monocytes and monocyte derived macrophages from children with Crohn's disease in a strain-dependent manner by inhibiting activation of mitogen activated protein kinase-regulated c-Jun and the transcription factor AP-1 (74).

Several groups have investigated the probiotic combination VSL#3 as a treatment for IBD based on its ability to maintain remission in relapsing pouchitis (75, 76). This combination of four live *Lactobacillus* strains, (*L. casei, L. bulgaricus, L. plantarium* and *L. acidophilus*), three live *Bifidobacterium* strains, (*B. longum, B. breve* and *B. infantis*), and one live *Streptococcus* strain, (*S. thermophilus*), dose-dependently ameliorated DSS-induced colitis in weanling rats (77). In a small (N=18) open-label study, VSL#3 induced remission in 56% of pediatric patients with mild to moderate ulcerative colitis. Six percent showed a response, and 39% had no response or did worse with treatment (78). Daily oral VSL#3 significantly reduced

the pouchitis disease activity index and expanded the number of mucosal regulatory T cells following colectomy with ileal pouch anal anastomosis (79). Two components of VSL#3, *B. longum* and *B. breve*, in combination with the prebiotic psyllium, were well tolerated at high doses and induced remission in 6/10 patients with Crohn's disease who had failed a regimen of aminosalicylates and prednisolone (80).

Similar to Sokol *et al*.'s (49) studies with *F. prausnitzii*, an Israeli group isolated and characterized a new putative protective bacterial species, *Enterococcus durans*, from the fecal microbiota of a healthy human vegetarian (81). In a DSS model of colitis, oral administration of *E. durans* significantly ameliorated colitis compared to controls and mice fed *Lactobacillus delbrueckii.* To properly note negative studies, oral administration of *Lactobacillus johnsonii* failed to prevent early postoperative endoscopic recurrence of Crohn's disease 12 weeks after ileo-cecal resection (82).

To date, probiotics appear to be more effective in preventing relapse of ulcerative colitis and pouchitis, with poor results in Crohn's disease. Examining *F. prausnitzii* in preventing postoperative recurrence of Crohn's disease will be quite interesting and could lay the foundation for targeted correction of dysbiotic microbiota in IBD. Use of prebiotics, which are poorly absorbed oligosaccharides that stimulate growth and metabolic activity of beneficial microbiota, could be a low-cost, nontoxic strategy to correct dysbiosis in IBD patients.

Conclusion and future directions

There remains no evidence that MAP is a causative agent in the pathogenesis of IBD. A more likely scenario involves specific *E. coli* strains and other species with virulence factors that allow them to adhere to and invade epithelial cells and persist within macrophages. These strains could be viewed as opportunistic pathogens in genetically susceptible hosts with innate killing,

mucosal barrier or immunoregulatory defects, with no disease induced in normal hosts. Identifying and then eliminating these strains, blocking expression of their virulence factors or altering their metabolism and identifying host susceptibility factors could be essential keys to treating IBD. Likewise, identifying changes in microbiota composition, gene expression and metabolic profiles in different IBD patient subsets using rapidly evolving molecular tools will provide important new insights into the pathogenesis and novel treatment of IBD using the example of *F. prausnitzii* (49). Meanwhile, using probiotics and prebiotics to enhance concentrations of beneficial species remains promising, although clinical trials lack statistical power due to small numbers. Treatments need to be individualized on the basis of compositional alterations in patient subsets. Understanding bacterial and host mutalistic interactions will determine success in this area.

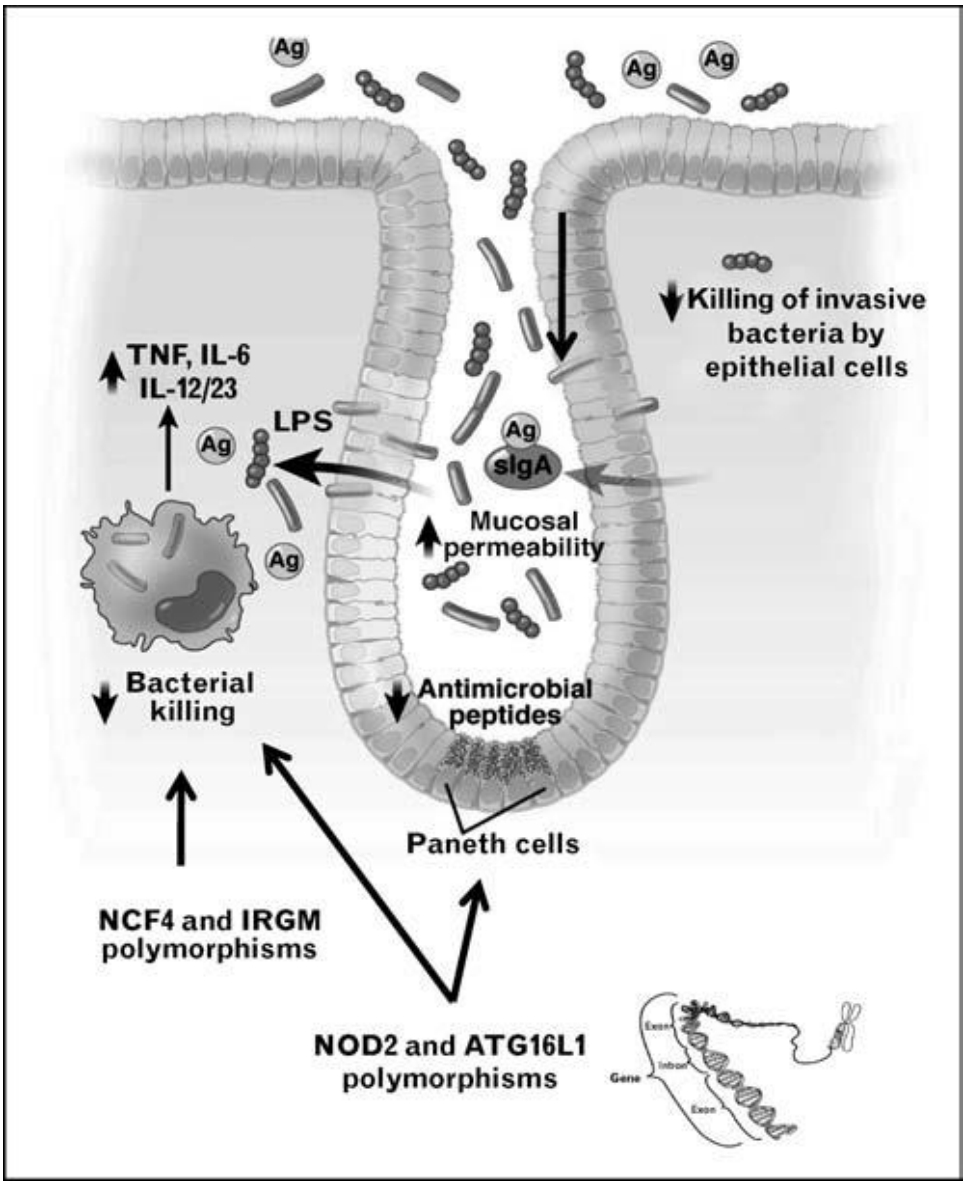

Figure 1.1. Defective containment of commensal bacteria in IBD.
Crohn's disease genes that affect bacterial killing result in defective containment of commensal bacteria. NOD2 polymorphisms result in defective α-defensin production and clearance of intracellular bacteria. Overgrowth of mucosal bacteria occurs with defective secretion of antimicrobial peptides (NOD2 and ATG16L1 polymorphisms) or secretory IgA. Inefficient killing of phagocytosed bacteria (NOD2, ATG16L1, NCF4 and IGRM polymorphisms) results in persistent intracellular bacteria and ineffective clearance of bacterial antigens. Increased mucosal permeability leads to overwhelming exposure of bacterial TLR ligands and antigens that activate pathogenic innate and T cell immune responses. Modified from (2) and used with permission of Elsevier Publishing Company.

REFERENCES

1. Kappelman M, Rifas-Shiman SL, Porter CQ, et al. Direct healthcare costs of Crohn's disease and ulcerative colitis in US children and adults. Gastroenterology 2008; 135: 1907–1913.

2. Sartor RB. Microbial influences in inflammatory bowel diseases. Gastroenterology 2008; 134: 577–594.

3. Winslet MC, Allan A, Poxon V, et al. Faecal diversion for Crohn's colitis: a model to study the role of the faecal stream in the inflammatory process. Gut 1994; 35: 236–242.

4. Kang SS, Bloom SM, Norian LA, et al. An antibiotic-responsive mouse model of fulminant ulcerative colitis. PLoS Medicine 2008; 5: e41.

5. Korzenik JR. Is Crohn's disease due to defective immunity? Gut 2007; 56: 2–5.

6. Wehkamp J, Salzman NH, Porter E, et al. Reduced Paneth cell alpha-defensins in ileal Crohn's disease. Proc Natl Acad Sci U S A 2005; 102: 18129–18134.

7. Fellermann K, Stange DE, Schaeffeler E, et al. A chromosome 8 gene-cluster polymorphism with low human beta-defensin 2 gene copy number predisposes to Crohn disease of the colon. Am J Hum Genet 2006; 79: 439–448.

8. Wehkamp J, Wang G, Kubler I, et al. The Paneth cell alpha-defensin deficiency of ileal Crohn's disease is linked to Wnt/Tcf-4. J Immunol 2007; 179: 3109–3118.

9. Kobayashi KS, Chamaillard M, Ogura Y, et al. NOD2-dependent regulation of innate and adaptive immunity in the intestinal tract. Science 2005; 307: 731–734.

10. Cadwell K, Liu JY, Brown SL, et al. A key role for autophagy and the autophagy gene ATG16L1 in mouse and human intestinal Paneth cells. Nature 2008; 456: 259–263.

11. Kaser A, Lee AH, Franke A, et al. XBP1 links ER stress to intestinal inflammation and confers genetic risk for human inflammatory bowel disease. Cell 2008; 134: 724–725.

12. Prescott NJ, Fisher SA, Franke A, et al. A nonsynonymous SNP in ATG16L1 predisposes to ileal Crohn's disease and is independent of CARD15 and IBD5. Gastroenterology 2007; 132: 1665–1671.

13. Rioux JD, Xavier RJ, Taylor KD, et al. Genome-wide association study identifies new susceptibility loci for Crohn disease and implicates autophagy in disease pathogenesis. Nat Genet 2007; 39: 596–604.

14. Barrett JC, Hansoul S, Nicolae DL, et al. Genome-wide association defines more than 30 distinct susceptibility loci for Crohn's disease. Nat Genet 2008; 40: 955–962.

15. Sartor RB. Does *Mycobacterium avium* subspecies *paratuberculosis* cause Crohn's disease? Gut 2005; 54:896–898.

16. Frank DN, St Amand AL, Feldman RA, et al. Molecular-phylogenetic characterization of microbial community imbalances in human inflammatory bowel diseases. Proc Natl Acad Sci U S A 2007; 104: 13780–13785.

17. Baumgart M, Dogan B, Rishniw M, et al. Culture independent analysis of ileal mucosa reveals a selective increase in invasive *Escherichia coli* of novel phylogeny relative to depletion of Clostridiales in Crohn's disease involving the ileum. ISME J 2007; 1: 403–418.

18. Scanu AM, Bull TJ, Cannas S, et al. *Mycobacterium avium* subspecies *paratuberculosis* infection in cases of irritable bowel syndrome and comparison with Crohn's disease and Johne's disease: common neural and immune pathogenicities. J Clin Microbiol 2007; 45: 3883–3890.

19. Toracchio S, El-Zimaity HM, Urmacher C, et al. *Mycobacterium avium* subspecies *paratuberculosis* and Crohn's disease granulomas. Scand J Gastroenterol 2008; 43: 1108–1111.

20. Singh AV, Singh SV, Makharia GK, et al. Presence and characterization of *Mycobacterium avium* subspecies *paratuberculosis* from clinical and suspected cases of Crohn's disease and in the healthy human population in India. Int J Infect Dis 2008; 12: 190–197.

21. Bentley RW, Keenan JI, Gearry RB, et al. Incidence of *Mycobacterium avium* subspecies *paratuberculosis* in a population-based cohort of patients with Crohn's disease and control subjects. Am J Gastroenterol 2008; 103: 1168–1172.

22. Juste RA, Elguezabal N, Garrido JM, et al. On the prevalence of *M. avium* subspecies *paratuberculosis* DNA in the blood of healthy individuals and patients with inflammatory bowel disease. PLoS ONE 2008; 3: e2537.

23. Clancy R, Ren Z, Turton J, et al. Molecular evidence for *Mycobacterium avium* subspecies *paratuberculosis* (MAP) in Crohn's disease correlates with enhanced TNF-alpha secretion. Dig Liver Dis 2007; 39: 445–451.

24. Ren Z, Turton J, Borody T, et al. Selective Th2 pattern of cytokine secretion in *Mycobacterium avium* subsp. *paratuberculosis* infected Crohn's disease. J Gastroenterol Hepatol 2008; 23: 310–314.

25. Jeyanathan M, Boutros-Tadros O, Radhi J, et al. Visualization of *Mycobacterium avium* in Crohn's tissue by oil-immersion microscopy. Microbes Infect 2007; 9: 1567–1573.

26. Bernstein CN, Wang MH, Sargent M, et al. Testing the interaction between NOD-2 status and serological response to *Mycobacterium paratuberculosis* in cases of inflammatory bowel disease. J Clin Microbiol 2007; 45: 968–971.

27. Abubakar I, Myhill DJ, Hart AR, et al. A case-control study of drinking water and dairy products in Crohn's Disease–further investigation of the possible role of *Mycobacterium avium paratuberculosis*. Am J Epidemiol 2007; 165: 776–783.

28. Selby W, Pavli P, Crotty B, et al. Two-year combination antibiotic therapy with clarithromycin, rifabutin, and clofazimine for Crohn's disease. Gastroenterology 2007; 132: 2313–2319.

29. Singh UP, Singh S, Singh R, et al. Influence of *Mycobacterium avium* subsp. *paratuberculosis* on colitis development and specific immune responses during disease. Infect Immun 2007; 8: 3722–3728.

30. Darfeuille-Michaud A, Boudeau J, Bulois P, et al. High prevalence of adherent-invasive *Escherichia coli* associated with ileal mucosa in Crohn's disease. Gastroenterology 2004; 127: 412–421.

31. Barnich N, Darfeuille-Michaud A. Adherent-invasive *Escherichia coli* and Crohn's disease. Curr Opin Gastroenterol 2007; 23: 16–20.

32. Sasaki M, Sitaraman SV, Babbin BA, et al. Invasive *Escherichia coli* are a feature of Crohn's disease. Lab Invest 2007; 87:1042–1054.

33. Meconi S, Vercellone A, Levillain F, et al. Adherent-invasive *Escherichia coli* isolated from Crohn's disease patients induce granulomas in vitro. Cell Microbiol 2007; 9: 1252–1261.

34. Mow WS, Vasiliauskas EA, Lin YC, et al. Association of antibody responses to microbial antigens and complications of small bowel Crohn's disease. Gastroenterology 2004; 126: 414–424.

35. Rolhion N, Carvalho FA, Darfeuille-Michaud A. OmpC and the δ^E pathway are involved in adhesion and invasion of the Crohn's disease-associated *Escherichia coli* strain LF82. Mol Microbiol 2007; 63: 1684–1700.

36. Carvalho FA, Barnich N, Sauvanet P, et al. Crohn's disease-associated *Escherichia coli* LF82 aggravates colitis in injured mouse colon via signaling by flagellin. Inflamm Bowel Dis 2008; 14: 1051–1060.

37. Bringer MA, Rolhion N, Glasser AL, Darfeuille-Michaud A. The oxidoreductase DsbA plays a key role in the ability of the Crohn's disease-associated adherent-invasive *Escherichia coli* strain LF82 to resist macrophage killing. J Bacteriol 2007; 189: 4860–4871.

38. Eaves-Pyles T, Allen CA, Taormina J, et al. *Escherichia coli* isolated from a Crohn's disease patient adhere, invade, and induce inflammatory responses in polarized intestinal epithelial cells. Int J Med Microbiol 2008; 298: 397–409.

39. Barnich N, Carvalho FA, Glasser AL, et al. CEACAM6 acts as a receptor for adherent-invasive *E. coli*, supporting ileal mucosa colonization in Crohn's disease. J Clin Invest 2007; 117: 1566–1574.

40. Peeters H, Bogaert S, Laukens D, et al. CARD15 variants determine a disturbed early response of monocytes to adherent-invasive *Escherichia coli* strain LF82 in Crohn's disease. Int J Immunogenet 2007; 34: 181–191.

41. Liu B, Schmitz JM, Holt LC, et al. Increased intracellular survival of *E. coli* NC101 within macrophages may contribute to its ability to induce colitis [abstract]. Gastroenterology.

42. Porter CK, Tribble DR, Aliaga PA, et al. Infectious gastroenteritis and risk of developing inflammatory bowel disease. Gastroenterology 2008; 135: 781–786.

43. Issa M, Vijayapal A, Graham MB, et al. Impact of *Clostridium difficile* on inflammatory bowel disease. Clin Gastroenterol Hepatol 2007; 5: 345–351.

44. Kim H, Rhee SH, Pothoulakis C, et al. Inflammation and apoptosis in *Clostridium difficile* enteritis is mediated by PGE(2) up-regulation of Fas ligand. Gastroenterology 2007; 133: 875–886.

45. Rabizadeh S, Rhee KJ, Wu S, et al. Enterotoxigenic *Bacteroides fragilis*: a potential instigator of colitis. Inflamm Bowel Dis 2007; 13: 1475–1483.

46. Veijola L, Nilsson I, Halme L, et al. Detection of *Helicobacter* species in chronic liver disease and chronic inflammatory bowel disease. Ann Med 2007; 39: 554–560.

47. Lupp C, Robertson ML, Wickham ME, et al. Host-mediated inflammation disrupts the intestinal microbiota and promotes the overgrowth of Enterobacteriaceae. Cell Host Microbe 2007; 2: 119–129.

48. Kotlowski R, Bernstein CN, Sepehri S, Krause DO. High prevalence of *Escherichia coli* belonging to the B2+D phylogenetic group in inflammatory bowel disease. Gut 2007; 56: 669–675.

49. Sokol H, Pigneur B, Watterlot L, et al. *Faecalibacterium prausnitzii* is an anti-inflammatory commensal bacterium identified by gut microbiota analysis of Crohn disease patients. Proc Natl Acad Sci U S A 2008; 105: 16731–16736.

50. Swidsinski A, Loening-Baucke V, Vaneechoutte M, Doerffel Y. Active Crohn's disease and ulcerative colitis can be specifically diagnosed and monitored based on the biostructure of the fecal flora. Inflamm Bowel Dis 2008; 14: 147–161.

51. Andoh A, Sakata S, Koizumi Y, et al. Terminal restriction fragment length polymorphism analysis of the diversity of fecal microbiota in patients with ulcerative colitis. Inflamm Bowel Dis 2007; 13: 955–962.

52. Takaishi H, Matsuki T, Nakazawa A, et al. Imbalance in intestinal microflora constitution could be involved in the pathogenesis of inflammatory bowel disease. Int J Med Microbiol 2008; 298: 463–472.

53. Dicksved J, Halfvarson J, Rosenquist M, et al. Molecular analysis of the gut microbiota of identical twins with Crohn's disease. ISME J 2008; 2: 716–727.

54. Nishikawa J, Kudo T, Sakata S, et al. Diversity of mucosa-associated microbiota in active and inactive ulcerative colitis. Scand J Gastroenterol 2008; 30: 1–7.

55. Ott SJ, Plamondon S, Hart A, et al. Dynamics of the mucosa-associated flora in ulcerative colitis patients during remission and clinical relapse. J Clin Microbiol 2008; 46: 3510–3513.

56. Martinez C, Antolin M, Santos J, et al. Unstable composition of the fecal microbiota in ulcerative colitis during clinical remission. Am J Gastroenterol 2008; 103: 643–648.

57. Zhang M, Liu B, Zhang Y, et al. Structural shifts of mucosa-associated *Lactobacilli* and *Clostridium leptum* subgroup in patients with ulcerative colitis. J Clin Microbiol 2007; 45: 496–500.

58. Vasquez N, Mangin I, Lepage P, et al. Patchy distribution of mucosal lesions in ileal Crohn's disease is not linked to differences in the dominant mucosa-associated bacteria: a study using fluorescence in situ hybridization and temporal temperature gradient gel electrophoresis. Inflamm Bowel Dis 2007; 13: 684–692.

59. Backhed F, Ley RE, Sonnenburg JL, et al. Host-bacterial mutualism in the human intestine. Science 2005; 307:1915–1920.

60. Kim SC, Tonkonogy SL, Karrasch T, et al. Dual-association of gnotobiotic IL-$10^{-/-}$ mice with 2 nonpathogenic commensal bacteria induces aggressive pancolitis. Inflamm Bowel Dis 2007; 13: 1457–1466.

61. Keita AV, Salim SY, Jiang T, et al. Increased uptake of nonpathogenic *E. coli* via the follicle-associated epithelium in longstanding ileal Crohn's disease. J Pathol 2008; 215: 135–144.

62. Roediger WE. Review article: nitric oxide from dysbiotic bacterial respiration of nitrate in the pathogenesis and as a target for therapy of ulcerative colitis. Aliment Pharmacol Ther 2008; 27: 531–541.

63. Sartor RB. Therapeutic manipulation of the enteric microflora in inflammatory bowel diseases: antibiotics, probiotics, and prebiotics. Gastroenterology 2004; 126: 1620–1633.

64. Boirivant M, Strober W. The mechanism of action of probiotics. Curr Opin Gastroenterol 2007; 23: 679–692.

65. Sheil B, Shanahan F, O'Mahony L. Probiotic effects on inflammatory bowel disease. J Nutr 2007; 137:S819–S824.

66. Hedin C, Whelan K, Lindsay JO. Evidence for the use of probiotics and prebiotics in inflammatory bowel disease: a review of clinical trials. Proc Nutr Soc 2007; 66: 307–315.

67. Isaacs K, Herfarth H. Role of probiotic therapy in IBD. Inflamm Bowel Dis 2008; 14: 1597–1605.

68. Peran L, Camuesco D, Comalada M, et al. A comparative study of the preventive effects exerted by three probiotics, *Bifidobacterium lactis*, *Lactobacillus casei* and *Lactobacillus acidophilus*, in the TNBS model of rat colitis. J Appl Microbiol 2007; 103: 836–844.

69. Llopis M, Antolin M, Carol M, et al. *Lactobacillus casei* downregulates commensals' inflammatory signals in Crohn's disease mucosa. Inflamm Bowel Dis 2009; 15: 275–283.

70. Kim N, Kunisawa J, Kweon MN, et al. Oral feeding of *Bifidobacterium bifidum* (BGN4) prevents CD4(+) CD45RB(high) T cell-mediated inflammatory bowel disease by inhibition of disordered T cell activation. Clin Immunol 2007; 123: 30–39.

71. Carroll IM, Andrus JM, Bruno-Barcena JM, et al. Anti-inflammatory properties of *Lactobacillus gasseri* expressing manganese superoxide dismutase using the interleukin 10-deficient mouse model of colitis. Am J Physiol Gastrointest Liver Physiol 2007; 293: G729–G738.

72. Lee JH, Lee B, Lee HS, et al. *Lactobacillus suntoryeus* inhibits proinflammatory cytokine expression and TLR-4-linked NF-κB activation in experimental colitis. Int J Colorectal Dis 2009; 24: 231–237.

73. Imaoka A, Shima T, Kato K, et al. Anti-inflammatory activity of probiotic *Bifidobacterium:* enhancement of IL-10 production in peripheral blood mononuclear cells from ulcerative colitis patients and inhibition of IL-8 secretion in HT-29 cells. World J Gastroenterol 2008; 14: 2511–2516.

74. Lin YP, Thibodeaux CH, Pena JA, et al. Probiotic *Lactobacillus reuteri* suppresses proinflammatory cytokines via c-Jun. Inflamm Bowel Dis 2008; 14: 1068–1083.

75. Gionchetti P, Rizzello F, Venturi A, et al. Oral bacteriotherapy as maintenance treatment in patients with chronic pouchitis: a double-blind, placebo-controlled trial. Gastroenterology 2000; 119: 305–309.

76. Gionchetti P, Rizzello F, Helwig U, et al. Prophylaxis of pouchitis onset with probiotic therapy: a double-blind, placebo-controlled trial. Gastroenterology 2003; 124: 1202–1209.

77. Fitzpatrick LR, Hertzog KL, Quatse AL, et al. Effects of the probiotic formulation VSL#3 on colitis in weanling rats. J Pediatr Gastroenterol Nutr 2007; 44: 561–570.

78. Huynh HQ, Debruyn J, Guan L, et al. Probiotic preparation VSL#3 induces remission in children with mild to moderate acute ulcerative colitis: a pilot study. Inflamm Bowel Dis 2009; 15(5): 760-8.

79. Pronio A, Montesani C, Butteroni C, et al. Probiotic administration in patients with ileal pouch-anal anastomosis for ulcerative colitis is associated with expansion of mucosal regulatory cells. Inflamm Bowel Dis 2008; 14: 662-668.

80. Fujimori S, Tatsuguchi A, Gudis K, et al. High dose antibiotic and prebiotic co-therapy for remission induction of active Crohn's disease. J Gastroenterol Hepatol 2007; 22: 1199–1204.

81. Raz I, Gollop N, Polak-Charcon S, Schwartz B. Isolation and characterization of new putative probiotic bacteria from human colonic flora. Br J Nutr 2007; 97: 725–734.

82. Van Gossum A, Dewit O, Louis E, et al. Multicenter randomized-controlled clinical trial of probiotics (*Lactobacillus johnsonii*, LA1) on early endoscopic recurrence of Crohn's disease after ileo-caecal resection. Inflamm Bowel Dis 2007; 13: 135–142.

CHAPTER 2: MICROBIAL INFLUENCES ON THE SMALL INTESTINAL RESPONSE TO RADIATION INJURY[2]

Introduction

The mammalian microbiome, as it relates to health and disease, has received increasing attention in medical research over the last decade. The human body is inhabited by at least 10 times more bacteria than the number of somatic and germline cells. The National Institutes of Health has funded the Human Microbiome Project (HMP) as a roadmap initiative to characterize the human microbiome in five body sites from healthy volunteers, including the gastrointestinal tract (1). Perhaps not coincidentally, an enhanced interest in probiotic bacteria (those which confer health benefits) has developed recently among both the scientific community and lay public. The majority of studies addressing pathogenic or beneficial microbial influences on gastrointestinal illnesses have focused on irritable bowel and the inflammatory bowel diseases. More recently, several lines of evidence have emerged that link the presence and composition of the luminal microbiota to the intestinal response to radiation. These include relative radiation resistance of germ-free mice, altered intestinal responses to radiation associated with colonization by commensal and probiotic bacterial species and recognition that stimulation of, or alteration in, innate immune system pathways modifies host responses to radiation. Radiation enteropathy remains a common complication for patients receiving abdominal or pelvic radiotherapy for cancer. Prophylactic or therapeutic strategies against radiation enteropathy are currently limited. However, as in other intestinal disorders, recent studies aimed at elucidating functions of the host–microbiome relationship in radiation injury have provided insight into both

[2] This chapter previously appeared as an article in the journal *Current Opinion in Gastroenterology.* The original citation is as follows: Packey CD, Ciorba MA. Microbial influences on the small intestinal response to radiation injury. Curr Opin Gastroenterol 2010; 26: 88-94.

disease pathophysiology and potential therapeutics. Our opinion will provide a background review on radiation-induced intestinal injury while examining in greater detail the data for microbial influences on this disease entity.

Radiation enteropathy in clinical medicine

Radiation therapy is used commonly for many forms of solid cancers including those that develop within the abdominal or pelvic cavities. A particular challenge that remains for the clinician is the lack of an available quantitative biomarker to measure the presence and degree of intestinal damage.

Scope and impact

More than 50% of patients with cancer receive radiation as a component of their treatment. The small intestine is rarely a primary target in radiotherapy, but by nature of its size and extent, it often receives exposure resulting in collateral damage. The rapidly proliferating mucosal lining of the small intestine is highly radiosensitive, and the resulting cell death leads to symptoms of malabsorption, including bloating, diarrhea and dehydration. Abdominal pain, anorexia, nausea and vomiting can also occur and are amplified by concurrent chemotherapy (2, 3). Symptoms adversely affect patient quality of life and can be severe enough to require hospitalization. The damaging effects related to small intestinal injury are a major reason for dose limitation and can force discontinuation of radiotherapy, impacting overall chances for cure of malignancy.

Patients typically experience symptoms from acute small intestinal injury after the first or second week of radiotherapy (4). The effect is dosage-dependent wherein low doses lead to mild and reversible disease and higher doses result in more severe and potentially irreversible damage. Thus, clinical regimens are usually designed to offer fractionated low-dosage (<2 Gy) therapy in

multiple sessions over the course of weeks. Extensive planning goes into treatment field design for radiation therapy to minimize the amount of small bowel which is exposed. Regardless, it is estimated that up to 70% or more of patients experience adverse gastrointestinal side effects by 3 weeks into therapy. Most of these acute symptoms subside by 2–6 weeks following completion of radiation therapy. Chronic severe complications of radiation enteropathy include dysmotility, strictures and fistulas, and occur in approximately 6% of patients 1 to 2 years after radiation therapy (5). Interestingly, both acute and chronic radiation therapy-related toxicities may be more severe in patients with pre-existing conditions of intestinal compromise or microbial dysbiosis such as those occurring in patients with inflammatory bowel diseases (6, 7).

Diagnosis

The diagnosis of acute radiation enteropathy is usually presumptively based on symptom type and time of onset. Basic laboratories, stool studies and abdominal imaging can be performed depending on symptom severity, but are often uninformative. Endoscopic biopsies are rarely used, although they may reveal histologic changes consistent with radiation damage. No specific biomarkers for radiation enteropathy are in common use; however, new potential serum or stool markers are being tested. Citrulline is a nitrogen-containing end product of small bowel enterocyte metabolism. Serum citrulline has been evaluated as a biomarker for functional enterocyte mass (8). In radiation enteropathy, testing of the feasibility and functionality of this biomarker in mice and in humans has revealed that it shows promise as a novel diagnostic test (9–11). Fecal calprotectin is another potential biomarker, which has been shown to significantly increase after pelvic radiation (11). However, as a neutrophil-derived protein, calprotectin is not small bowel-specific. Eosinophilic cationic protein levels (12) and C-reactive protein levels (13) have also been found to be increased in patients following pelvic irradiation, although not

consistently (11). It is possible that in the future, sequential evaluation of a cluster of markers will prove most informative for diagnosis and monitoring.

Pathophysiology of small bowel radiation injury

Acute radiation injury to the small intestine has been well-documented in animal models. When interpreting the literature, it is useful to recognize that whereas clinical medicine uses small fractionated doses of ionizing radiation, most animal studies evaluating mechanisms of disease use higher dose, single-exposure regimens, as would be encountered in accidental or warfare-associated ionizing radiation overexposure. Figure 1 (14–18, 19, 20–24, 25, 26, 27) summarizes several recent findings.

Epithelial and endothelial responses

Radiation-induced small intestinal injury is characterized by cell loss in the progenitor cell compartment (28) and a dose-dependent loss of barrier properties (29–31). Ionizing radiation causes a wide diversity of functional disorders in the small intestine, including altered motility (32, 33), disrupted absorption of carbohydrates (34), amino acids and bile acids (35), and a more thrombophilic endothelium due to the induction of inflammatory cell adhesion to the endothelium (36) and increased expression of endothelial von Willebrand factor (37).

It has traditionally been assumed that the radiation gastrointestinal syndrome that ensues with exposure to high doses of radiation or cumulative lower doses results from the direct killing of the rapidly proliferating epithelial stem cells, depletion of the differentiated parenchymal cells and subsequent loss of tissue function (38). However, vascular damage also ensues when the small intestine is exposed to ionizing radiation (39). A study (14) published in 2001 suggested that the radiation gastrointestinal syndrome is a direct consequence of an early (4-h) wave of apoptosis in the intestinal vascular endothelial cells. Recently, this assertion was challenged by

Schuller et al. (15) who exposed two groups of mice to an equivalent dose of total body irradiation (TBI), then directly targeted intestinal endothelial cells in one of the groups of mice with up to 27 Gy neutron beam irradiation and found no additional intestinal crypt stem cell loss or murine death related to the gastrointestinal syndrome.

Unanticipated overexposure to ionizing radiation

In clinical medicine, small fractionated doses of radiation are used. In mice exposure to doses of 8 Gy or higher leads to sterilization of individual small intestinal crypts, a process in which all of the actual and potential stem cells are inactivated. The survival of one or more clonogenic cells in a given crypt allows the regeneration of that crypt. Doses of 15 Gy and higher sterilize virtually all of the crypt stem cells, resulting in complete loss of the intestinal villi and death from the radiation gastrointestinal syndrome in 4–5 days (15). This syndrome is characterized by breaches in the intestinal mucosa, translocation of commensal intestinal bacteria and sepsis, and it is relevant in cases of bioterrorist attacks, nuclear accidents, medical errors and in appropriately fractionated dosing of therapeutic radiation to people whose tissues are exquisitely radiosensitive.

Linking the microbiota to the intestinal response to radiation

It had previously been observed that germ-free mice have improved survival as compared with colonized mice when exposed to equivalent doses of radiation (40). However, the impact of the intestinal microbiota on the pathogenesis of the radiation gastrointestinal syndrome was not understood until a more recent work by Crawford and Gordon (16). Here, hematopoietic rescue by bone marrow transplantation after lethal ionizing radiation was used to demonstrate that conventionally raised mice still exhibited earlier death than germ-free mice (16). Using Rag1 knockout mice, they also showed that mature lymphocytes are not required for the development

of lethal radiation enteropathy. Mechanistically, the investigation also suggested that increased expression of a fibrinogen/angiopoietin-like protein, fasting-induced adipose factor, which is normally suppressed by luminal microbiota, confers endothelial and lymphocyte radioresistance.

Recognition of commensal intestinal bacteria or their products by Toll-like receptors (TLRs) is necessary for the regulation of intestinal homeostasis (41). It is largely through binding to these receptors and the subsequent activation of the nuclear factor-kappa B (NF-κB) family of transcription factors that commensal bacteria have been shown to influence the small intestinal epithelial response to various forms of injury. Recent animal models have revealed that this is true for radiation-induced injury. Egan et al. (17) showed increased intestinal epithelial cell (IEC) apoptosis in mice with selected ablation of NF-κB signaling through IκB kinase, a common activation pathway for TLR signaling. This finding corresponded with increased expression and activation of the tumor suppressor p53. Mice in which the NF-κB p50 gene has been disrupted were shown to be more sensitive to TBI-induced lethality than are wild-type mice (18). These findings demonstrate the physiological importance of NF-κB activation in protection against radiation-induced death in the epithelium in vivo, and directly link intestinal commensal bacteria to the regulation of radiation-induced IEC apoptosis. Recent mouse knockout studies have revealed that bacterial products also activate signaling pathways other than the NF-κB pathway to protect IECs from radiation-induced apoptosis (19).

Both endogenous and exogenous sources of prostaglandins have been shown to confer protection to intestinal crypts that are exposed to radiation. In mice, parenterally administered lipopolysaccharide, a TLR4 ligand, increased endogenous intestinal prostaglandin production, thereby improving intestinal crypt survival after irradiation (20). Exogenous administration of a prostaglandin E2 (PGE2) analogue prior to radiation also increases the number of surviving

intestinal crypts. Several studies have demonstrated that the radioprotective effect of prostaglandins on the gut is a cyclooxygenase (COX)-1-dependent, COX-2-independent event. Irradiated COX-$1^{-/-}$ mice have increased crypt epithelial apoptosis, decreased clonogenic stem cell survival and diminished PGE2 synthesis as compared with wild-type littermates (21). Administration of indomethacin, which inhibits both COX-1 and COX-2, to a mouse prior to radiation increases radiation-induced IEC apoptosis and decreases intestinal crypt survival (22). However, selective COX-2 inhibitors have no effect on crypt survival; likewise COX-$2^{-/-}$ mice have a similar response to radiation to wild-type mice. So, the COX-1-dependent production of endogenous PGE2 appears to be an important downstream mediator of TLR signaling by which bacterial products promote IEC survival and proliferation in the response to radiation (23). The biologic effects of PGE2 have been shown to be mediated via AKT activation by the plasma membrane G-protein-coupled receptor EP2 (24), thereby preventing Bax translocation to the mitochondria (42).

Human polymorphisms and variations in microbiome

There are emerging, although not yet matured, data supporting the role of host and microbial genetic influences on the radiosensitivity of the small intestine. A recent study (43) identified a correlation between single nucleotide polymorphisms in mice and the amount of jejunal crypt cell apoptosis after 2.5 Gy TBI. Gene expression microarrays have also been used in attempts to predict the radiosensitivity of normal tissue (44).

An intriguing recent study (45) involving a small number of patients used DNA fingerprinting with 16S ribosomal RNA denaturing gradient gel electrophoresis (DGGE) to show different fecal microbial profiles in people receiving radiation who experienced diarrhea from those who received radiation and maintained normal stool consistency. They evaluated stool

before, during and after radiation, and proposed that a dysbiosis was linked to changes in bowel habits rather than the radiation exposure itself. Interestingly, the microbial profiles of individuals before receiving radiation clustered in three similarity sets that matched closely the control, the 'no diarrhea' and the 'diarrhea' groups, suggesting that the initial intestinal microbial composition of each individual could be a determinant for developing postirradiation diarrhea.

Current management principles

In cancer therapy, use of well-planned (46, 47), fractionated dose regimens with specific patient positioning remains key to minimizing symptoms of radiation enteropathy. Additionally, numerous pharmacologic therapies have been tested for reducing symptoms. Antispasmodic and antidiarrheal agents are effective for some patients. Cholestyramine has been shown to be effective in reducing bile salt-associated diarrhea, which can occur with radiation enteropathy (48). Amifostine, a broad-spectrum, free-radical scavenging cytoprotectant, is used as an adjuvant with treatment of some malignancies (49). Although the benefits of this drug are clear for xerostomia, its ability to prevent radiation enteropathy has not been proven and the side effect of hypotension has tempered interest in routine use.

Most current therapies for radiation enteropathy are initiated only after symptoms develop. As the percentage of patients who develop small bowel symptoms is high, widespread use of an effective prophylactic agent would likely be adopted if it became available. An ideal prophylactic radioprotectant for the small intestine would need to fulfill specific requirements including the possession of an ability to preserve or enhance the antitumor efficacy of radiation; the provision of wide-ranged normal tissue protection with a low-toxicity profile and the allowance of easy, safe and cost-effective administration.

Microbial manipulation in therapy or prevention

Development of small intestinal radioprotectants has primarily focused on antioxidants (50–54), modifiers of inflammation (55–57), growth factors (58–60) and regulators of IEC apoptosis (61, 62). Yet, recent evidence suggests that manipulation of the intestinal luminal microbiota or the administration of medications adapted from commensal or probiotic bacteria holds promise in providing prophylactic and possibly post-exposure enteric radioprotection.

Bacterial product-based therapies

Burdelya et al. (25, 63) recently evaluated a polypeptide drug derived from *Salmonella* flagellin that binds to TLR5 and activates NF-κB signaling. A single injection of this agent improved survival in mice exposed to radiation by limiting apoptosis and preserving cell proliferation in the epithelial crypts and lamina propria of the small intestine. However, protection was conferred only when mice were exposed to doses below those that universally cause the radiation gastrointestinal syndrome, and only if the agent was administered 15–60 min before exposure. In similar experiments using rhesus macaques, the investigators observed that the TLR5 agonist increased survival and had protective effects on bone marrow, although they did not provide data on the effect of the agonist on the gastrointestinal tract of the monkeys. Remarkably, this drug did not appear to decrease tumor radiosensitivity in the mouse model used. Hence, this TLR5 agonist is potentially useful as a prophylactic before therapeutic radiation, but may not be adequate as a treatment for the radiation gastrointestinal syndrome, as in the case of a nuclear accident or attack.

Probiotics

Probiotics are live microbial organisms, most often bacteria, which confer beneficial effects to the host when consumed. With increasing evidence suggesting that imbalance of the

intestinal microbiota may play a significant role in the pathogenesis of radiation enteropathy, probiotic bacteria are now attracting interest as potential radioprotectants. Single and multi-strain probiotic preparations have been evaluated in both animal models and humans over the last few decades. In rodents, *Lactobacillus* species have been shown to reduce radiation-induced small intestinal damage, Gram-negative bacteremia, endotoxemia and death (26, 64, 65). Primary endpoints were not achieved for probiotics in small trials in which humans underwent pelvic radiation for cancer; however, individuals receiving *Lactobacillus* spp. supplementation showed a trend toward having less severe symptoms (27, 66, 67). In the largest human trial (68) to date, patients taking the probiotic mixture VSL#3 experienced radiation-induced diarrhea less frequently than patients taking a placebo in a double-blind study involving almost 500 patients. Timing of probiotic administration, prophylactic versus therapeutic, respectively, may explain the more robust results identified in animal studies as compared with human trials. Early reports also suggest that soluble secreted factors from probiotic bacteria may be responsible for physiologic benefits observed in radiation (26) as in other injury models (69). As probiotic bacteria are inexpensive and would be predicted to offer extensive tissue protection with low toxicity, further investigation into their role as intestinal radioprotectants is warranted.

Antibiotics

Antibiotics have been considered for decades as a potential treatment option for radiation enteropathy (70). Researchers at the Armed Forces Radiobiology Research Institute used antibiotics in several radiation mouse models (71–73). Limitations to these studies included their focus on the activity of various antibiotics specifically against orally ingested pathogens, their use of bacterial translocation to the liver and mortality as primary readouts, and their evaluation of radiation doses that were not sufficient to cause the radiation gastrointestinal syndrome. In

their most recent review, this group summarized their findings and concluded that the potential use of several different antimicrobial agents from various classes may be effective for treating infection after exposure to radiation, but they do not identify a superior agent (74).

Intestinal commensal bacteria translocate across the intestinal mucosa and cause sepsis and early death in response to high doses of radiation. Yet, the aforementioned studies linking TLR binding by bacterial products to protection of the intestinal epithelium and the host against radiation-induced damage suggest that some commensal intestinal bacterial species provide protective functions in the response to radiation. Hence, an antibiotic that uniquely targets bacterial organisms that tend to translocate after exposure to radiation, while sparing bacterial species that are shown to be protective in the response of the intestinal epithelium and the host to radiation, may be optimal. This concept also lends support to the prophylactic and/or therapeutic potential of administrating both an antibiotic and a probiotic to people exposed to radiation.

Conclusion

Radiation injury to the small bowel remains an important clinical problem for which few therapeutic strategies exist. Several lines of evidence, which were reviewed here, suggest that dynamic interactions between the host's enteric microbiota and innate immune system modulate the intestinal response to radiation. Probiotics, antibiotics and bacterial-derived peptides and byproducts can modify radiation-induced injury and symptom severity. How to best harness the influence of these microbial symbionts remains to be determined. Future laboratory studies should be aimed at identifying specific prebiotic, probiotic, antibiotic or all regimens that optimize normal tissue radioresistance and tumoral radiosensitization. Bacterial-based compounds or secreted products will likely be an area of fruitful investigation. Clinical studies in this area should initially focus on clarifying how intestinal microbial compositions shift in

response to radiation. Using this knowledge, strain-specific probiotics could be administered to increase bacterial species that best confer host radioprotection. Likewise, antibiotic regimens could be developed that selectively target bacterial species that are found to proliferate, translocate and cause sepsis following exposure to radiation, while possessing minimal activity against the protective bacterial populations. Subsequent clinical studies should be aimed at determining the safety, efficacy and applicability of the developing therapeutic agents and regimens. Recent years have seen an explosive growth in knowledge associating the microbiome to human health; the prevention or treatment of small intestinal radiation injury should serve as a particularly productive target for future investigations in this area.

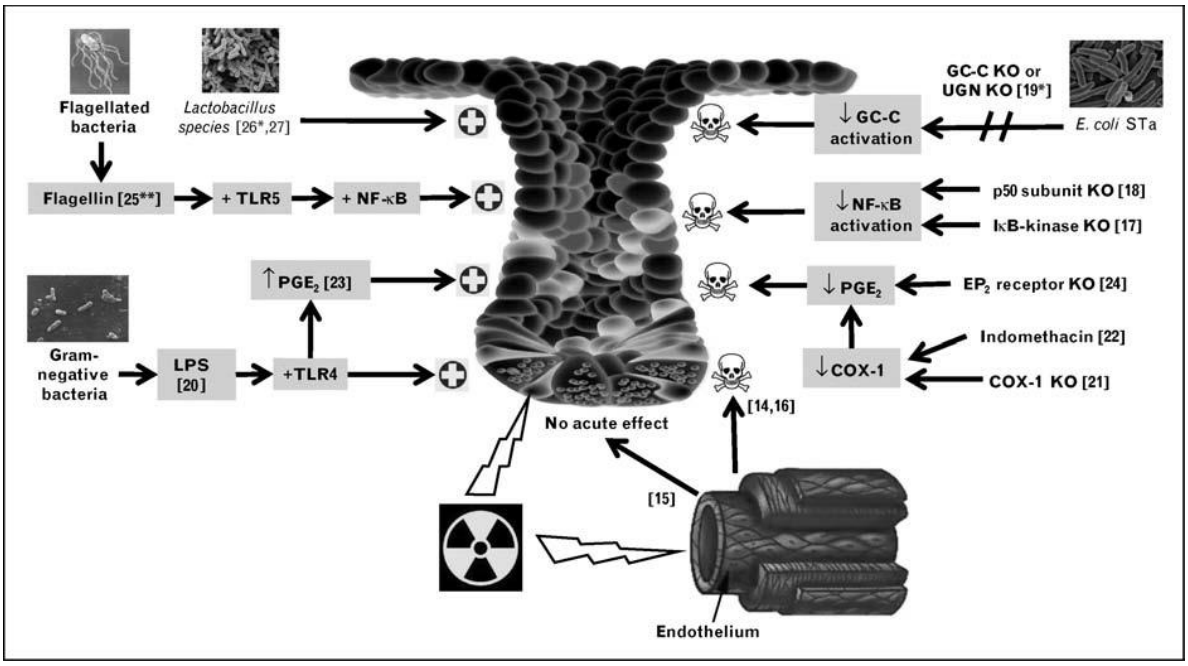

Figure 2.1. Modifiers of acute small intestinal radiation injury.
The small intestinal response to radiation is altered by signaling induced by luminal bacteria or bacterial-based products. Experimental models and human trials suggest *Lactobacillus* species or their soluble secreted proteins may protect intestinal crypts against damage from radiation exposure (26, 27). Flagellin, a TLR5 ligand that activates the NF-κB pathway, protected IECs from radiation-induced apoptosis and increased host survival when injected into mice before lethal doses of radiation (25). LPS, a TLR4 ligand found in the outer membrane of Gram-negative bacteria, increased endogenous intestinal prostaglandin production and intestinal crypt survival in mice exposed to 14 Gy when injected 2–24 h prior to exposure (20). Endogenous PGE2 decreases murine IEC apoptosis and increases post-radiation IEC proliferation (23). Conversely, blocking pathways that are activated by bacterial products has detrimental effects on the ability of IECs and crypts to survive radiation insults. The *E. coli* STa is a ligand for GC-C, an IEC transmembrane receptor. UGN is a peptide hormone that binds to and activates GC-C. Mice in which GC-C or UGN is knocked out have increased jejunal IEC apoptosis 3 h after 5-Gy radiation as compared with WT counterparts (19). Indomethacin blocks PGE_2 production by inhibiting COX-1 and COX-2, thereby increasing IEC apoptosis and intestinal crypt ablation (22). Similarly, irradiated COX-$1^{-/-}$ mice have diminished PGE_2 synthesis, leading to increased crypt epithelial apoptosis and decreased clonogenic stem cell survival (21). Irradiated EP_2 $receptor^{-/-}$ mice have decreased intestinal crypt survival and increase in IEC apoptosis (24). Blocking NF-κB activation by deleting the p50 subunit of the NF-κB complex (18) or the canonical NF-κB activation kinase (17) results in increased radiation-induced IEC apoptosis in mice. Although debate still exists as to the degree of importance of endothelial apoptosis in acute intestinal outcomes after high-dose radiation exposure (14, 15), endothelial apoptosis is lower in GF than SPF mice (16). COX, cyclooxygenase; *E. coli* STa, heat-stable enterotoxin of *Escherichia coli*; GC-C, guanylate cyclase C; IEC, intestinal epithelial cell; KO, knocked out; LPS, lipopolysaccharide; NF-kB, nuclear factor-kappaB; PGE_2, prostaglandin E_2; TLR, Toll-like receptor; UGN, uroguanylin. Red cross signifies attenuation of acute intestinal injury from radiation. Skull and crossbones signify contribution to acute intestinal injury from radiation.

REFERENCES

1. Peterson J. The NIH Human Microbiome Project. Genome Res 2009; 19: 2317–2323.

2. Gunnlaugsson A, Kjellen E, Nilsson P, et al. Dose–volume relationships between enteritis and irradiated bowel volumes during 5-fluorouracil and oxaliplatin based chemoradiotherapy in locally advanced rectal cancer. Acta Oncol 2007; 46: 937–944.

3. Tho LM, Glegg M, Paterson J, et al. Acute small bowel toxicity and preoperative chemoradiotherapy for rectal cancer: investigating dose-volume relationships and role for inverse planning. Int J Radiat Oncol Biol Phys 2006; 66: 505–513.

4. Bismar MM, Sinicrope FA. Radiation enteritis. Curr Gastroenterol Rep 2002; 4: 361–365.

5. Sher ME, Bauer J. Radiation-induced enteropathy. Am J Gastroenterol 1990; 85: 121–128.

6. Song DY, Lawrie WT, Abrams RA, et al. Acute and late radiotherapy toxicity in patients with inflammatory bowel disease. Int J Radiat Oncol Biol Phys 2001; 51: 455–459.

7. Willett CG, Ooi CJ, Zietman AL, et al. Acute and late toxicity of patients with inflammatory bowel disease undergoing irradiation for abdominal and pelvic neoplasms. Int J Radiat Oncol Biol Phys 2000; 46: 995–998.

8. Lutgens L, Lambin P. Biomarkers for radiation-induced small bowel epithelial damage: an emerging role for plasma citrulline. World J Gastroenterol 2007; 13: 3033–3042.

9. Lutgens LC, Deutz N, Granzier-Peeters M, et al. Plasma citrulline concentration: a surrogate end point for radiation-induced mucosal atrophy of the small bowel. A feasibility study in 23 patients. Int J Radiat Oncol Biol Phys 2004; 60: 275–285.

10. Lutgens LC, Deutz NE, Gueulette J, et al. Citrulline: a physiologic marker enabling quantitation and monitoring of epithelial radiation-induced small bowel damage. Int J Radiat Oncol Biol Phys 2003; 57: 1067–1074.

11. Wedlake L, McGough C, Hackett C, et al. Can biological markers act as noninvasive, sensitive indicators of radiation-induced effects in the gastrointestinal mucosa? Aliment Pharmacol Ther 2008; 27: 980–987.

12. Bowen JM, Newbold K, Blake P, et al. Do serum levels of eosinophil granule- derived protein change in patients undergoing pelvic radiotherapy? Clin Oncol (R Coll Radiol) 2005; 17: 382–384.

13. Cengiz M, Akbulut S, Atahan IL, Grigsby PW. Acute phase response during radiotherapy. Int J Radiat Oncol Biol Phys 2001; 49: 1093–1096.

14. Paris F, Fuks Z, Kang A, et al. Endothelial apoptosis as the primary lesion initiating intestinal radiation damage in mice. Science 2001; 293: 293–297.

15. Schuller BW, Binns PJ, Riley KJ, et al. Selective irradiation of the vascular endothelium has no effect on the survival of murine intestinal crypt stem cells. Proc Natl Acad Sci U S A 2006; 103: 3787–3792.

16. Crawford PA, Gordon JI. Microbial regulation of intestinal radiosensitivity. Proc Natl Acad Sci U S A 2005; 102: 13254–13259.

17. Egan LJ, Eckmann L, Greten FR, et al. IkappaB-kinase beta-dependent NF-kappaB activation provides radioprotection to the intestinal epithelium. Proc Natl Acad Sci U S A 2004; 101: 2452–2457.

18. Wang Y, Meng A, Lang H, et al. Activation of nuclear factor kappaB in vivo selectively protects the murine small intestine against ionizing radiation-induced damage. Cancer Res 2004; 64: 6240–6246.

19. Garin-Laflam MP, Steinbrecher KA, Rudolph JA, et al. Activation of guanylate cyclase C signaling pathway protects intestinal epithelial cells from acute radiation-induced apoptosis. Am J Physiol Gastrointest Liver Physiology 2009; 296: G740–G749.

20. Riehl T, Cohn S, Tessner T, et al. Lipopolysaccharide is radioprotective in the mouse intestine through a prostaglandin-mediated mechanism. Gastroenterology 2000; 118: 1106–1116.

21. Houchen CW, Stenson WF, Cohn SM. Disruption of cyclooxygenase-1 gene results in an impaired response to radiation injury. Am J Physiol Gastrointest Liver Physiol 2000; 279: G858–G865.

22. Cohn SM, Schloemann S, Tessner T, et al. Crypt stem cell survival in the mouse intestinal epithelium is regulated by prostaglandins synthesized through cyclooxygenase-1. J Clin Invest 1997; 99: 1367–1379.

23. Stenson WF. Prostaglandins and epithelial response to injury. Curr Opin Gastroenterology 2007; 23: 107–110.

24. Houchen CW, Sturmoski MA, Anant S, et al. Prosurvival and antiapoptotic effects of PGE2 in radiation injury are mediated by EP2 receptor in intestine. Am J Physiol Gastrointest Liver Physiology 2003; 284: G490–G498.

25. Burdelya LG, Krivokrysenko VI, Tallant TC, et al. An agonist of toll-like receptor 5 has radioprotective activity in mouse and primate models. Science 2008; 320: 226–230.

26. Ciorba MA, Stenson WF. Probiotic therapy in radiation-induced intestinal injury and repair. Ann N Y Acad Sci 2009; 1165: 190–194.

27. Osterlund P, Ruotsalainen T, Korpela R, et al. *Lactobacillus* supplementation for diarrhoea related to chemotherapy of colorectal cancer: a randomised study. Br J Cancer 2007; 97: 1028–1034.

28. Potten CS. A comprehensive study of the radiobiological response of the murine (BDF1) small intestine. Int J Radiat Biol 1990; 58: 925–973.

29. Dublineau I, Grison S, Grandcolas L, et al. Effects of chronic ^{137}Cs ingestion on barrier properties of jejunal epithelium in rats. J Toxicol Environ Health A 2007; 70: 810–819.

30. Guzman-Stein G, Bonsack M, Liberty J, Delaney JP. Abdominal radiation causes bacterial translocation. J Surg Res 1989; 46: 104–107.

31. Molla M, Gironella M, Miquel R, et al. Relative roles of ICAM-1 and VCAM-1 in the pathogenesis of experimental radiation-induced intestinal inflammation. Int J Radiat Oncol Biol Phys 2003; 57: 264–273.

32. Otterson MF. Effects of radiation upon gastrointestinal motility. World J Gastroenterol 2007; 13: 2684–2692.

33. Picard C, Wysocki J, Fioramonti J, Griffiths NM. Intestinal and colonic motor alterations associated with irradiation-induced diarrhoea in rats. Neurogastroenterol Motil 2001; 13: 19–26.

34. Overgaard J, Matsui M. Effect of radiation on glucose absorption in the mouse jejunum in vivo. Radiother Oncol 1990; 18: 71–77.

35. Thomson AB, Cheeseman CI, Walker K. Intestinal uptake of bile acids: effect of external abdominal irradiation. Int J RadiatOncol Biol Phys 1984; 10: 671–685.

36. Dunn MM, Drab EA, Rubin DB. Effects of irradiation on endothelial cell–polymorphonuclear leukocyte interactions. J Appl Physiol 1986; 60: 1932–1937.

37. van Kleef E, Verheij M, te Poele H, et al. In vitro and in vivo expression of endothelial von Willebrand factor and leukocyte accumulation after fractionated irradiation. Radiat Res 2000; 154: 375–381.

38. Potten CS. Radiation, the ideal cytotoxic agent for studying the cell biology of tissues such as the small intestine. Radiat Res 2004; 161: 123–136.

39. Wang J, Boerma M, Fu Q, Hauer-Jensen M. Significance of endothelial dysfunction in the pathogenesis of early and delayed radiation enteropathy. World J Gastroenterol 2007; 13: 3047–3055.

40. McLaughlin MM, Dacquisto MP, Jacobus DP, Horowitz RE. Effects of the germ free state on responses of mice to whole-body irradiation. Radiat Res 1964; 23: 333–349.

41. Rakoff-Nahoum S, Paglino J, Eslami-Varzaneh F, et al. Recognition of commensal microflora by toll-like receptors is required for intestinal homeostasis. Cell 2004; 118: 229–241.

42. Tessner TG, Muhale F, Riehl TE, et al. Prostaglandin E2 reduces radiation-induced epithelial apoptosis through a mechanism involving AKT activation and bax translocation. J Clin Invest 2004; 114: 1676–1685.

43. Iwata M, Iwakawa M, Noda S, et al. Correlation between single nucleotide polymorphisms and jejunal crypt cell apoptosis after whole body irradiation. Int J Radiat Biol 2007; 83: 181–186.

44. Kruse JJ, Stewart FA. Gene expression arrays as a tool to unravel mechanisms of normal tissue radiation injury and prediction of response. World J Gastroenterol 2007; 13: 2669–2674

45. Manichanh C, Varela E, Martinez C, et al. The gut microbiota predispose to the pathophysiology of acute postradiotherapy diarrhea. Am J Gastroenterol 2008; 103: 1754–1761.

46. Engels B, De Ridder M, Tournel K, et al. Preoperative helical tomotherapy and megavoltage computed tomography for rectal cancer: impact on the irradiated volume of small bowel. Int J Radiat Oncol Biol Phys 2009; 74: 1476–1480.

47. Fiorino C, Valdagni R, Rancati T, Sanguineti G. Dose-volume effects for normal tissues in external radiotherapy: pelvis. Radiother Oncol 2009; 93: 153–167.

48. Heusinkveld RS, Manning MR, Aristizabal SA. Control of radiation-induced diarrhea with cholestyramine. Int J Radiat Oncol Biol Phys 1978; 4: 687–690.

49. Weiss JF, Landauer MR. History and development of radiation-protective agents. Int J Radiat Biol 2009; 85: 539–573.

50. Guo HL, Wolfe D, Epperly MW, et al. Gene transfer of human manganese superoxide dismutase protects small intestinal villi from radiation injury. J Gastrointest Surg 2003; 7: 229–235.

51. HatonC, Francois A, Vandamme M, et al. Imbalance of the antioxidant network of mouse small intestinal mucosa after radiation exposure. Radiat Res 2007; 167: 445–453.

52. Huang EY, Wang FS, Lin IH, Yang KD. Aminoguanidine alleviates radiation-induced small-bowel damage through its antioxidant effect. Int J Radiat Oncol Biol Phys 2009; 74: 237–244.

53. Hussein MR, Abu-Dief EE, Kamel E, et al. Melatonin and roentgen irradiation-induced acute radiation enteritis in albino rats: an animal model. Cell Biol Int 2008; 32: 1353–1361.

54. Abbasoglu SD, Erbil Y, Eren T, et al. The effect of heme oxygenase-1 induction by octreotide on radiation enteritis. Peptides 2006; 27: 1570–1576.

55. Boerma M, Wang J, Burnett AF, et al. Local administration of interleukin-11 ameliorates intestinal radiation injury in rats. Cancer Res 2007; 67: 9501–9506.

56. Boerma M, Wang J, Richter KK, Hauer-Jensen M. Orazipone, a locally acting immunomodulator, ameliorates intestinal radiation injury: a preclinical study in a novel rat model. Int J Radiat Oncol Biol Phys 2006; 66: 552–559.

57. Kawashima R, Kawamura YI, Kato R, et al. IL-13 receptor alpha2 promotes epithelial cell regeneration from radiation-induced small intestinal injury in mice. Gastroenterology 2006; 131: 130–141.

58. Hagiwara A, Nakayama F, Motomura K, et al. Comparison of expression profiles of several fibroblast growth factor receptors in the mouse jejunum: suggestive evidence for a differential radioprotective effect among major FGF family members and the potency of FGF1. Radiat Res 2009; 172: 58–65.

59. Lee KK, Jo HJ, Hong JP, et al. Recombinant human epidermal growth factor accelerates recovery of mouse small intestinal mucosa after radiation damage. Int J Radiat Oncol Biol Phys 2008; 71: 1230–1235.

60. Potten CS, Booth D, Haley JD. Pretreatment with transforming growth factor beta-3 protects small intestinal stem cells against radiation damage in vivo. Br J Cancer 1997; 75: 1454–1459.

61. Haegebarth A, Perekatt AO, Bie W, et al. Induction of protein tyrosine kinase 6 in mouse intestinal crypt epithelial cells promotes DNA damage-induced apoptosis. Gastroenterology 2009; 137: 945–954.

62. Qiu W, Carson-Walter EB, Liu H, et al. PUMA regulates intestinal progenitor cell radiosensitivity and gastrointestinal syndrome. Cell Stem Cell 2008; 2: 576–583.

63. Abreu MT. Harnessing the power of bacteria to protect the gut. N Engl J Med 2008; 359: 756–759.

64. Demirer S, Aydintug S, Aslim B, et al. Effects of probiotics on radiation-induced intestinal injury in rats. Nutrition 2006; 22: 179–186.

65. Seal M, Naito Y, Barreto R, et al. Experimental radiotherapy-induced enteritis: a probiotic interventional study. J Dig Dis 2007; 8: 143–147.

66. Giralt J, Regadera JP, Verges R, et al. Effects of probiotic *Lactobacillus casei* DN-114 001 in prevention of radiation-induced diarrhea: results from multicenter, randomized, placebo-controlled nutritional trial. Int J Radiat Oncol Biol Phys 2008; 71: 1213–1219.

67. Urbancsek H, Kazar T, Mezes I, Neumann K. Results of a double-blind, randomized study to evaluate the efficacy and safety of antibiophilus in patients with radiation-induced diarrhoea. Eur J Gastroenterol Hepatol 2001; 13: 391–396.

68. Delia P, Sansotta G, Donato V, et al. Use of probiotics for prevention of radiation-induced diarrhea. World J Gastroenterol 2007; 13: 912–915.

69. Yan F, Cao H, Cover TL, et al. Soluble proteins produced by probiotic bacteria regulate intestinal epithelial cell survival and growth. Gastroenterology 2007; 132: 562–575.

70. Livstone EHT, Spiro H, Floch M. The gastrointestinal microflora of irradiated mice. II. Effect of oral antibiotic administration on the colonic flora and survival of adult mice. Yale J Biol Med 1970; 42: 448–454.

71. Brook I, Elliott TB, Ledney GD. Quinolone therapy of *Klebsiella pneumoniae* sepsis following irradiation: comparison of pefloxacin, ciprofloxacin, and ofloxacin. Radiat Res 1990; 122: 215–217.

72. Brook I, Tom SP, Ledney GD. Development of infection with *Streptococcus bovis* and *Aspergillus* sp. in irradiated mice after glycopeptide therapy. J Antimicrob Chemother 1993; 32: 705–713.

73. Brook I, Ledney GD. The treatment of irradiated mice with polymicrobial infection caused by *Bacteroides fragilis* and *Escherichia coli*. J Antimicrob Chemother 1994; 33: 243–252.

74. Brook I, Elliott TB, Ledney GD, et al. Management of postirradiation infection: lessons learned from animal models. Mil Med 2004; 169: 194–197.

CHAPTER 3: MOLECULAR ANALYSIS OF THE LUMINAL- AND MUCOSAL-ASSOCIATED INTESTINAL MICROBIOTA IN DIARRHEA-PREDOMINANT IRRITABLE BOWEL SYNDROME[3]

Introduction

Irritable bowel syndrome (IBS) is the most prevalent functional gastrointestinal (GI) disorder, affecting 10–20% of adults and adolescents (20). IBS can present as diarrhea-predominant IBS (D-IBS), constipation-predominant IBS, or mixed-bowel-habit IBS. These disorders are associated with a significantly reduced quality of life (17), psychological comorbidities (21), and a considerable economic burden (44). The lack of understanding of the factors associated with the pathogenesis of this complex group of disorders has resulted in limited effective treatment options for IBS patients. Recent studies have implicated new etiological factors in the pathogenesis of IBS, including alterations in the normal intestinal microbiota, genetic predeterminants, pathogenic bacterial infection, food sensitivity/allergy, altered enteric immune function, and intestinal inflammation (2, 30, 34).

The intestinal microbiota has been demonstrated to be important for normal GI motor and sensory functions (5, 14, 18, 34, 35), and alterations in the intestinal microbiota have been suggested as a possible etiological factor in the development of functional GI disorders, including IBS (34). Indeed, attempts to alter the composition of the intestinal microbiota using antibiotics, probiotics, or prebiotics have resulted in reduced IBS symptoms (8, 13, 27, 31–33, 35, 39, 43). Several studies have characterized a dysbiosis of the intestinal microbiota in patients with IBS. However, there is no consensus among these studies regarding the specific

[3] This chapter previously appeared as an article in the *American Journal of Physiology- Gastrointestinal and Liver Physiology*. The original citation is as follows: Carroll IM, Ringel-Kulka T, Keku TO, Chang YH, Packey CD, Sartor RB, Ringel Y. Molecular analysis of the luminal-and mucosal-associated intestinal microbiota in diarrhea-predominant irritable bowel syndrome. Am J Physiol Gastrointest Liver Physiol 2011; 301: G799-G807.

compositional changes of the intestinal microbiota associated with these disorders (4, 6, 9, 15, 16, 22, 23, 25, 26, 45). Identification of specific alterations in the intestinal bacterial groups that are associated with IBS symptoms is complicated by the heterogeneity of the disorders and the diversity of the intestinal microbiota (19). In addition, it is unclear whether symptoms of IBS are associated with compositional variation of microbial groups in the luminal and/or mucosal niches (49). Therefore, the possible association between IBS and the intestinal microbiota must be investigated in clinically relevant, well-defined subgroups of patients, and luminal and mucosal niches must be analyzed using techniques that explore the composition and diversity of these complex microbial communities. The present study used the molecular fingerprinting technique terminal-restriction fragment (T-RF) length polymorphism (T-RFLP) (7) to characterize and compare the microbiota in fecal and colonic mucosal samples obtained from a subgroup of D-IBS patients and healthy controls.

Materials and methods

Study population. We studied 16 patients that met the Rome III criteria for D-IBS and 21 healthy controls. Subjects were recruited from the general population of Chapel Hill, NC, with advertising and from the University of North Carolina (UNC) Hospitals outpatient clinics.

Inclusion criteria included subjects >18 yr of age and of any sex, race, or ethnicity. Healthy controls had no recurring GI symptoms. Subjects with a history of GI tract surgery other than appendectomy or cholecystectomy or a history of inflammatory bowel disease, celiac disease, lactose malabsorption, or any other diagnosis that could explain chronic or recurring bowel symptoms were excluded from the study. In addition, individuals were excluded if they had a history of treatment with antibiotics or anti-inflammatory agents, including aspirin or

nonsteroidal anti-inflammatory drugs (or steroids), or if they had intentionally consumed probiotics 2 mo prior to the study.

All subjects were evaluated by a physician to exclude an alternative diagnosis to IBS. The study was approved by the UNC Internal Review Board, and all subjects provided written consent prior to participation in the study.

Sample collection and preparation. Fresh stool samples were collected from all 37 subjects on site during a single study visit at UNC. Each fecal sample was immediately transferred on ice to the laboratory, where it was homogenized, divided into aliquots, and stored at -80°C for future DNA extraction and molecular microbiological analysis.

Colonic mucosal biopsies (n = 8 per patient) were collected from each subject at a single study visit during an unsedated flexible sigmoidoscopy. To avoid possible effects of colonic preparation on the composition and diversity of the intestinal microbiota, all biopsies were collected from unprepared colons (i.e., subjects did not undergo a bowel cleansing prior to the procedure). Cold forceps were used to take mucosal biopsy samples from the rectosigmoid colon. Taking biopsy samples from the rectosigmoid junction permits consistent collection of samples representative of the distal colon from all subjects and minimizes the discomfort associated with the procedure. Once removed from the colon, each biopsy sample was washed in 1 ml of sterile PBS to remove fecal material. The biopsy samples were then weighed, flash-frozen in liquid nitrogen, and stored at -80°C for further DNA extraction and molecular microbiological analysis.

Extraction of DNA. Bacterial DNA was extracted from one fecal and one mucosal sample from each of the subjects. DNA was isolated from 18 (7 D-IBS patients and 11 healthy controls) fecal and mucosal samples using a phenol-chloroform extraction method combined with physical

disruption of bacterial cells and a DNA clean-up kit (DNeasy blood and tissue extraction kit, Qiagen, Valencia, CA). Briefly, a 100-mg sample of frozen feces or a mucosal biopsy was suspended in 750 µl of sterile bacterial lysis buffer [200 mM NaCl, 100 mM Tris (pH 8.0), 20 mM EDTA, and 20 mg/ml lysozyme] and incubated at 37°C for 30 min. Then 40 µl of proteinase K (20 mg/ml) and 85 µl of 10% SDS were added to the mixture. After 30 min of incubation at 65°C, 300 mg of 0.1-mm zirconium beads (BioSpec Products, Bartlesville, OK) were added, and the mixture was homogenized in a bead beater (BioSpec Products, Bartlesville, OK) for 2 min. The homogenized mixture was cooled on ice and then centrifuged at 14,000 rpm for 5 min. The supernatant was transferred to a new 1.5-ml microfuge tube, and fecal DNA was further extracted by phenol-chloroform-isoamyl alcohol (25:24:1) and then by chloroform-isoamyl alcohol (24:1). After extraction, the supernatant was precipitated by absolute ethanol at -20°C for 1 h. The precipitated DNA was suspended in DNase-free H_2O and then cleaned using the DNeasy blood and tissue extraction kit (see above) according to the manufacturer's instructions. Additional fecal and mucosal DNA from 19 subjects (9 D-IBS patients and 10 healthy controls) was obtained from samples collected in a previous study (6). The study population, inclusion and exclusion criteria, and sample collection and handling procedures were identical in both studies.

T-RFLP PCR. A complex mixture of bacterial 16S rRNA genes was amplified by PCR from each intestinal DNA sample using fluorescently labeled universal primers [carboxyfluorescein (FAM)- labeled 5'-AGAGTTTGATCCTGGCTCAG-3' (forward primer 8F) and hexachlorocarboxyfluorescein (HEX)-labeled 5'-GGTTACCTTGTTACGACTT-3' (reverse primer 1492R)], as previously described (10, 40). PCR products were purified using a Qiagen PCR purification kit. PCR products of all fecal and mucosal samples were then digested with *Hha* I to generate T-RFs of varying sizes. All fecal samples were also digested separately with

Hae III or *Msp* I (mucosal samples were not digested with *Hae* III or *Msp* I because of a limited supply of DNA). As a result of polymorphisms in the variable regions of the 16S rRNA gene, T-RF size corresponds to different bacterial groups. T-RFs were separated by capillary electrophoresis on a genetic analyzer (model 3100, Applied Biosystems, Carlsbad, CA). GeneMapper software (Applied Biosystems) was used to determine the size (terminal fragment length in base pairs), height (fluorescence intensity), and abundance (peak width X height) of each T-RF. To attribute specific bacterial groups to T-RFs, we compared the fingerprints generated from each sample with a database containing T-RF data from known and unknown bacterial groups [Microbial Community Analysis (MiCA) database] (41).

Statistical analysis. T-RF size and abundance data from GeneMapper were compiled into a data matrix using Sequentix software (Sequentix, Klein Raden, Germany). These data were normalized (individual T-RF peak area as a proportion of total T-RF peak area within that sample), transformed by square root, and compiled into a Bray-Curtis similarity matrix using PRIMER version 6 software (Primer-E, Ivybridge, UK). T-RF data were then subjected to multivariate analysis, including hierarchical cluster analysis followed by analysis of similarity (ANOSIM). Using ANOSIM, we assessed the similarities between groups (D-IBS patients vs. healthy controls) and within groups. We computed the significance in PRIMER version 6 by permutation of group membership with 999 replicates. The test statistic *R*, which measures the strength of the results, ranges from -1 to 1: $R = 1$ signifies differences between groups, while $R = 0$ signifies that the groups are identical. The contribution of specific T-RFs to differences in bacterial composition between groups was assessed by similarity percentages (SIMPER). SIMPER results were used to generate pie charts of percent contribution of T-RFs within each group, after a 10% cutoff for low contributors. Biodiversity of each sample was measured by the

Shannon-Weiner diversity index, while differences in biodiversity between groups were assessed by a nonparametric Mann-Whitney test.

Results

Study population. A total of 37 subjects were investigated. All subjects provided a fecal and a colonic mucosal sample. The study population consisted of 75% females with a mean age of 36 yr. Demographics and body mass index were similar in the two study groups.

A total of 261 different *Hha* I-generated T-RFs, which represent different bacterial groups, were found in fecal and colonic mucosal samples from all subjects. *Hae* III and *Msp* I generated 252 and 284 T-RFs from fecal DNA samples, respectively. Thirty-six of the *Hha* I-generated T-RFs contributed ~90% of the total T-RFs found in all subjects (Fig. 3.1). The distribution of T-RFs differed between D-IBS patients and healthy controls and between intestinal niches. For example, 20 T-RFs found in fecal samples from healthy controls were not present in fecal samples from D-IBS patients. The abundance (peak width X height) of 5' FAM-187 and 3' HEX-402 in the feces was significantly altered between D-IBS patients and healthy controls. In addition, 3' HEX-400 was present in mucosal samples from healthy controls but not D-IBS patients, while 5' FAM-189 and 3' HEX-131 were found in mucosal samples from D-IBS patients but not healthy controls. These data demonstrate compositional differences in the fecal- and mucosal-associated microbiota between D-IBS patients and healthy controls. To attribute bacterial groups to these T-RFs, the MiCA database was queried (41). This database provided bacterial grouping (phylum, class, order, or family) for the majority of T-RFs that contribute to the composition of the fecal- and mucosal-associated microbiota in D-IBS patients and healthy controls. The majority of T-RFs represented several bacterial groups; however, comparison of bacterial groups identified by fecal T-RFs generated by three different enzymes [*Hha* I, *Hae* III,

and *Msp* I] revealed that the order Clostridiales and the family Planctomycetaceae were consistently associated with T-RFs that contributed 90% of fecal microbiota in healthy controls but not D-IBS patients.

Biodiversity of T-RFLP profiles. The Shannon-Weiner diversity index was used to determine the biodiversity (richness and evenness of T-RFs) of T-RFLP profiles from intestinal samples. A significant 1.2-fold decrease (2.7 + 0.65 for D-IBS patients and 3.3 + 0.86 for healthy controls, $P = 0.008$) in biodiversity was found in *Hha* I-generated T RFs from fecal samples from D-IBS patients compared with healthy controls (Fig. 3.2*B*). *Hae* III-generated T-RFs for 34 fecal samples [13 from D-IBS patients and 21 from healthy controls (3 samples from D-IBS patients failed to yield detectable T-RFs following digestion)] demonstrated a significant 1.06-fold decrease in biodiversity (3.47 + 0.37 for D-IBS patients and 3.67 + 0.60 for healthy controls, $P = 0.015$) in fecal samples from D-IBS patients compared with healthy controls. A 1.04-fold decrease in biodiversity in *Msp* I-generated T-RFs from D-IBS fecal samples failed to reach statistical significance (0.979 + 0.02 for D-IBS patients and 0.983 + 0.02 for healthy controls, $P = 0.296$). No significant differences were observed in biodiversity from mucosal samples between D-IBS patients and healthy controls (1.6 + 0.89 and 1.6 + 0.84, respectively, $P = 1$) using *Hha* I-generated T-RFs.

We also compared the biodiversity of fecal and mucosal niches within each group. We observed a significant increase in biodiversity in the fecal niche compared with the mucosal niche in both groups, with a 1.7-fold increase (2.7 + 0.65 for feces and 1.6 + 0.89 for mucosa, $P = 0.001$) in D-IBS patients and a 2.1-fold increase (3.3 + 0.86 for feces and 1.6 + 0.84 for mucosa, $P = 0.0001$) in healthy controls (Fig. 3.2, *C* and *D*).

Multivariate analysis of T-RFLP profiles. Nonmultidimensional scaling (nMDs) of T-RF profiles generated by *Hha* I-digested PCR products of samples obtained from all subjects (D-IBS patients and healthy controls) demonstrated that the community profiles in fecal and colonic mucosal niches are clearly distinct from one another (Fig. 3.3*A*). Hierarchal clustering analysis of T-RF profiles confirmed this observation (Fig. 3.3*B*). The degree of separation (as determined by *R* value, where $R = 1$ indicates complete separation between groups) between fecal and mucosal niches was more evident when these two niches were compared in healthy controls than in D-IBS patients, although both were statistically significant ($R = 0.41$, $P = 0.001$ in healthy controls; $R = 0.22$, $P = 0.001$ in D-IBS patients).

No distinct separation by nMDs or hierarchal clustering was observed between D-IBS patients and healthy controls from fecal or mucosal niches. T-RF profiles were also generated for fecal samples (13 from D-IBS patients and 21 from healthy controls) using *Hae* III or *Msp* I restriction enzymes (3 samples from D-IBS patients failed to yield detectable T-RFs following digestion). nMDs and hierarchal clustering of T-RFs generated by *Hae* III and *Msp* I did not detect a distinct separation between D-IBS patients and healthy controls from fecal samples ($R = -0.035$, $P = 0.687$ for *Hae* III; $R = -0.001$, $P = 0.470$ for *Msp* I).

Discussion

Several studies have investigated the composition of the intestinal microbiota in patients with IBS and healthy individuals (4, 9, 15, 16, 22, 23, 25, 26, 45). Although these studies demonstrated some differences between these two groups, the findings are not consistent. The majority of studies that characterized the intestinal microbiota in IBS patients investigated mixed populations of IBS patients (4, 42, 45) or focused on a single intestinal niche (4, 15, 16, 22, 23, 25, 42, 45, 46). Recent reports demonstrating compositional and diversity differences between

intestinal luminal- and mucosal associated microbiota in humans highlight the importance of characterizing enteric microorganisms in both niches when investigating the role of the microbiota in intestinal diseases (11, 29). Only two studies have investigated the intestinal microbiota of luminal and mucosal niches in patients with IBS (6, 9). In a recent study, using culture and quantitative real-time PCR (6), we investigated the intestinal microbiota in fecal and colonic mucosal samples from D-IBS patients and healthy controls. We found a significantly lower concentration of aerobic bacteria and a higher concentration of *Lactobacillus* species in fecal samples from D-IBS patients than in healthy controls. These two techniques identified no differences in the mucosal-associated microbiota between the groups. However, this study was limited to the analysis of a finite number of predetermined bacterial groups within the intestinal microbiota. Codling et al. (9) used denaturing gradient gel electrophoresis (an alternate fingerprinting technique to the method used in our current study) to investigate the intestinal microbiota in a mixed population of IBS patients. Similar to our findings, Codling et al. reported a greater variation of denaturing gradient gel electrophoresis profiles in fecal samples from healthy controls than IBS patients. However, in contrast to our findings, Codling et al. reported no differences in the variability between the fecal- and mucosal-associated microbiota in IBS patients. The discrepancy between the two studies may relate to the mixed population, preparation prior to mucosal sample collection, or inclusion of only nine IBS patients and no healthy controls for the mucosal analysis in the study of Codling et al. Thus our current study is the first to use a molecular fingerprinting technique in a comprehensive investigation of fecal and unprepared colonic mucosal samples from a large group of patients with a specific subtype of IBS (D-IBS) and healthy controls.

Analysis of the contribution of T-RFs to the composition of the intestinal microbiota demonstrated a considerable overlap in the predominant T-RFs within the fecal- and mucosal-associated microbiota in D-IBS patients and healthy controls. However, D-IBS fecal and mucosal samples contained T-RFs that were not present in healthy control samples, and vice versa. These findings demonstrate obvious compositional differences in specific bacterial groups (as represented by T-RFs) in the fecal- and mucosal-associated microbiota between D-IBS patients and healthy controls. On the basis of comparisons with the MiCA database, the majority of T-RFs for fecal and mucosal samples were associated with multiple bacterial groups. However, using three different restriction enzymes on our fecal samples, we were able to determine whether a bacterial group(s) was consistently represented by three different enzyme-generated T-RFs that contributed to the majority of the fecal microbiota. We found that the order Clostridiales and the family Planctomycetaceae were consistently represented by *Hha* I-, *Hae* III-, and *Msp* I-generated T-RFs that contributed 90% of the fecal microbiota in healthy controls but not D-IBS patients. Previous reports showed a reduction of *Clostridium coccoides* in IBS patients that is in line with our findings (23). Interestingly, a reduction in the order Clostridiales has also been reported in ileal Crohn's disease (47). The order Clostridiales encompasses many bacterial species, including the protective bacterium *Faecalibacterium prausnitzii*. It is therefore speculated that the absence of protective bacterial species from the order Clostridiales may be associated with D-IBS. A more sensitive molecular technique that classifies the intestinal microbiota at a species level will enable further investigation of this finding. The family Planctomycetaceae is a low-abundance member of the normal intestinal microbiota (1). The importance of our finding of reduced abundance of this bacterial group in D-IBS patients is

unclear, as the role of this group of organisms in the intestinal tract has not been investigated in depth.

Although we found compositional differences in the fecal microbiota between D-IBS patients and healthy controls with respect to specific T-RFs, we did not find a clear separation between these two groups with nMDs or hierarchal clustering. This suggests that the differences in composition of the microbiota between D-IBS patients and healthy controls are due to the relative abundances of specific bacterial groups that do not affect the overall composition of the intestinal microbiota. In support of this concept, it has been recently demonstrated that specific bacterial species (*Klebsiella pneumoniae* and *Proteus mirabilis*) that do not affect the overall composition of the intestinal microbiota independently drive colonic disease in the presence of the endogenous microbiota in a horizontally and vertically transmissible mouse model of ulcerative colitis (12).

Our study demonstrates a significantly lower level of fecal microbial biodiversity in patients with D-IBS compared with healthy controls. Additionally, our study demonstrates, for the first time, a significantly higher level of microbial biodiversity in fecal- than in mucosal-associated communities within D-IBS patients and healthy controls. The increase in biodiversity in fecal compared with mucosal samples is greater in the healthy controls than in D-IBS patients. This observation requires further investigation to determine whether the intestinal microbiota in D-IBS patients is distributed differently between the fecal and mucosal niches compared with the microbiota in a healthy intestine. The biodiversity in the human gut is a result of co-evolution between host and microbe (3) and has been shown to be stable over time in healthy individuals (48). Thus a departure from the normal biodiversity of the intestinal microbiota may reflect a disease state in the gut. For example, a reduction in enteric bacterial biodiversity has been

reported in inflammatory bowel diseases (24, 28, 37, 38). It can be speculated that a reduction in bacterial biodiversity allows for certain members of the intestinal microbiota to flourish and affect intestinal function, such as regulation of inflammation or motility, and therefore perpetuate GI symptoms.

Despite the meticulous efforts used in our study to preserve and characterize the microbiota from different intestinal niches, certain limitations were encountered. *1*) T-RFLP was unable to provide the resolution necessary to identify the bacterial species in the intestinal microbiota that are altered between D-IBS patients and healthy controls. We were able to assign a bacterial "phylum, class, order, or family" to most T-RFs. Although this level of characterization provides interesting insight into the intestinal microbiota associated with D-IBS patients, bacterial families encompass many bacterial genera and species. Thus, on the basis of these data sets, it is difficult to make definitive conclusions regarding the association of specific bacterial groups with D-IBS. *2*) It is important to remember that T-RFLP fingerprinting is limited to the analysis of only the predominant members (usually 30–50 T-RFs) of complex microbial communities (7). Not surprisingly then, our study found that 34 T-RFs contributed 90% of the fecal microbiota in healthy controls. Hence, it is possible that differences in less abundant bacteria were not detected by this technique. *3*) The biopsies analyzed in this study were taken during unprepared flexible sigmoidoscopy to avoid the effects of bowel cleansing agents on the intestinal microbiota. The biopsies were taken from the distal colon just above the rectosigmoid junction. This site was selected because it provides a clear anatomic point to enable consistent collection of mucosal samples and to minimize the discomfort of the subject. However, the microbiota of this colonic region may not be representative of the microbiota of the whole colon, and we did not collect biopsies from more proximal colonic regions.

In conclusion, we have demonstrated compositional and biodiversity differences in the intestinal microbiota between patients with D-IBS and healthy controls. Our study does not address whether these differences are an etiological cause or an effect of the disorder, but it does provide a rationale for further investigation of the role of the intestinal microbiota in the pathogenesis of IBS. Our findings emphasize the importance of investigating the fecal- and mucosal-associated microbiota in this disorder, as well as the need for techniques with higher resolution (e.g., high-throughput sequencing of the 16S rRNA gene), which may enable deeper characterization of the intestinal microbiota and identification of the specific bacterial groups that are altered in IBS.

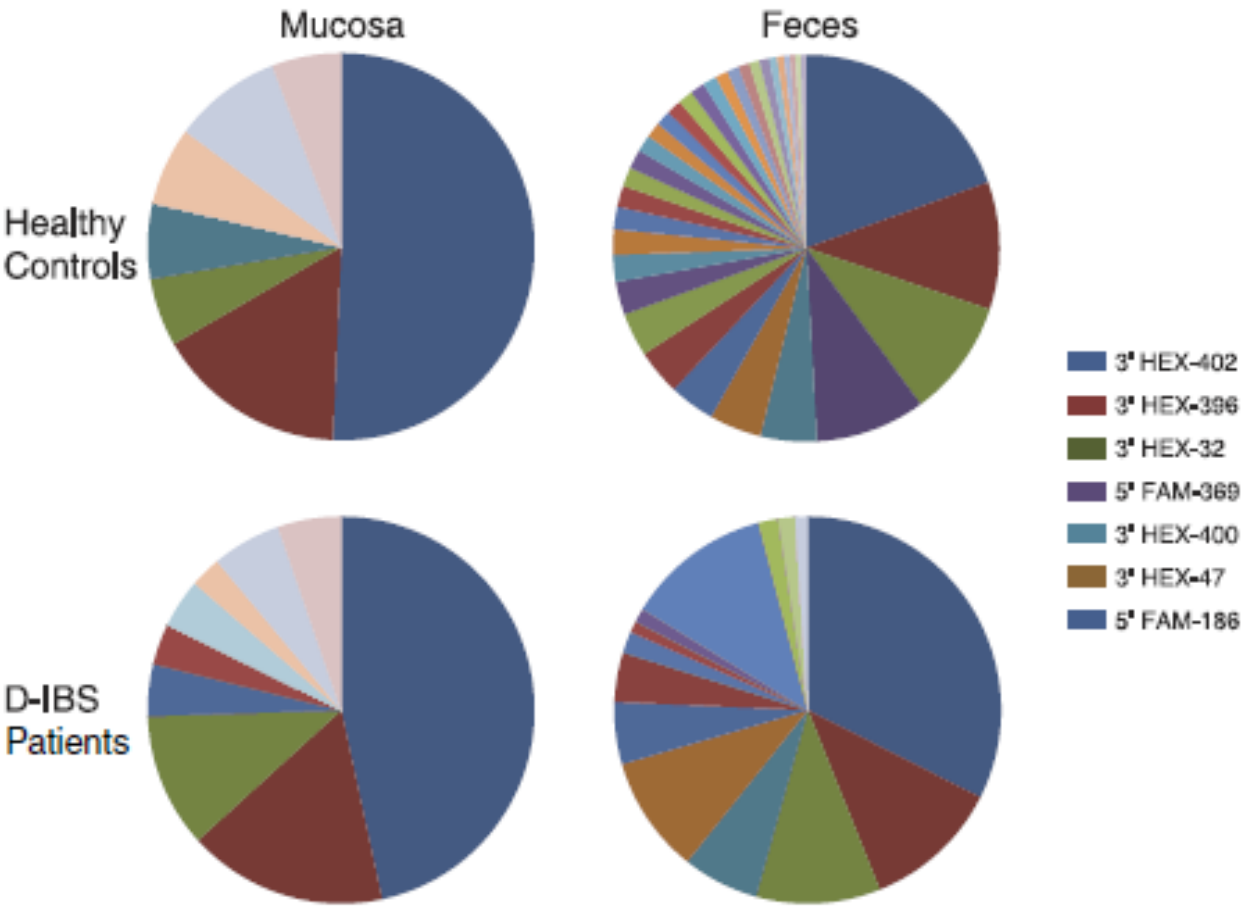

Figure. 3.1. Terminal-restriction fragment (T-RF) fingerprinting data displaying percent contribution of T-RFs within fecal and colonic mucosal samples from patients with diarrhea-predominant irritable bowel syndrome (D-IBS) and healthy controls.

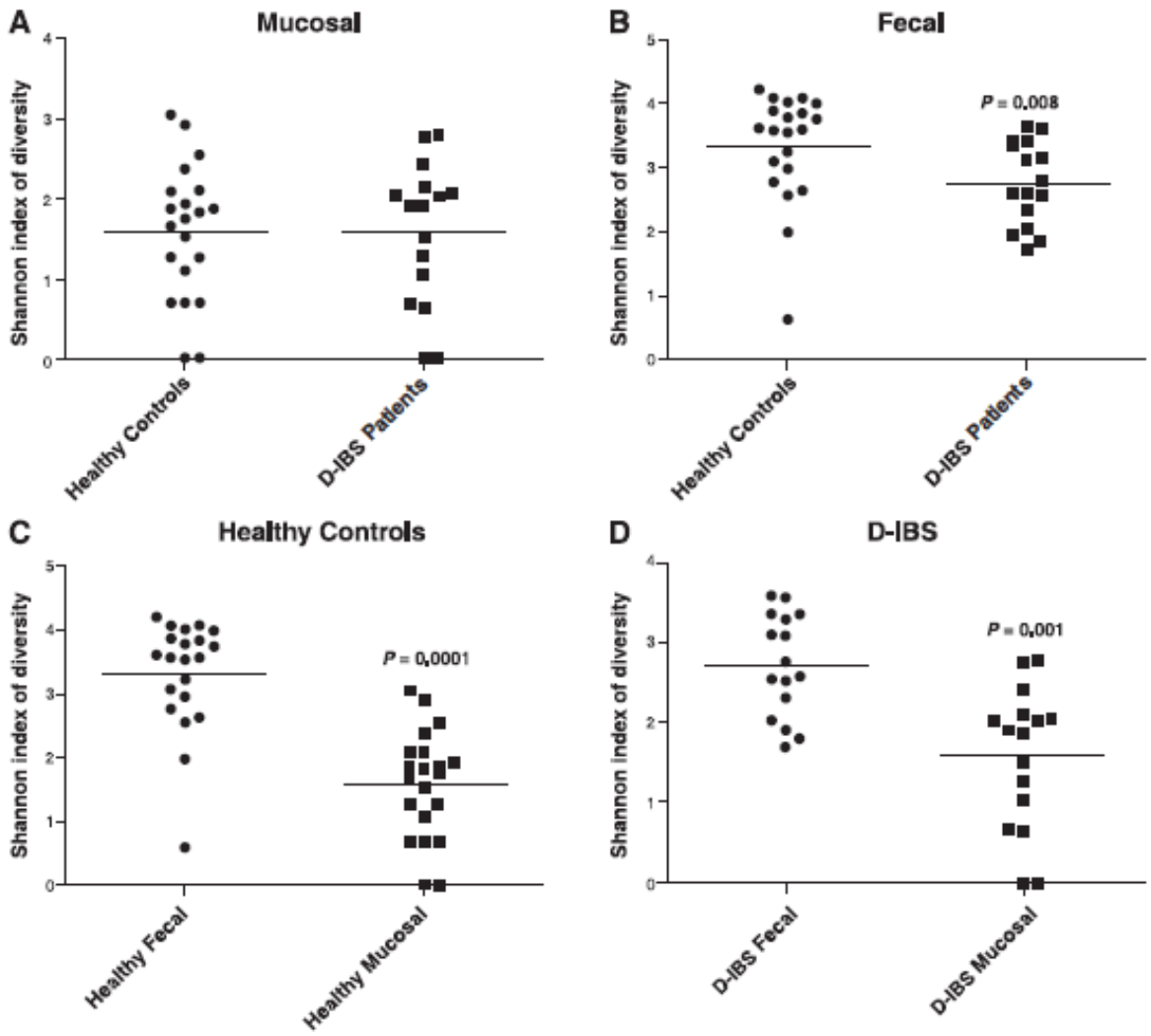

Figure. 3.2. Shannon-Weiner biodiversity index in mucosal samples from healthy controls and D-IBS patients (*A*), fecal samples from healthy controls and D-IBS patients (*B*; $P = 0.008$), fecal and mucosal samples from healthy controls (*C*; $P = 0.0001$), and fecal and mucosal samples from D-IBS patients (*D*; $P = 0.001$).

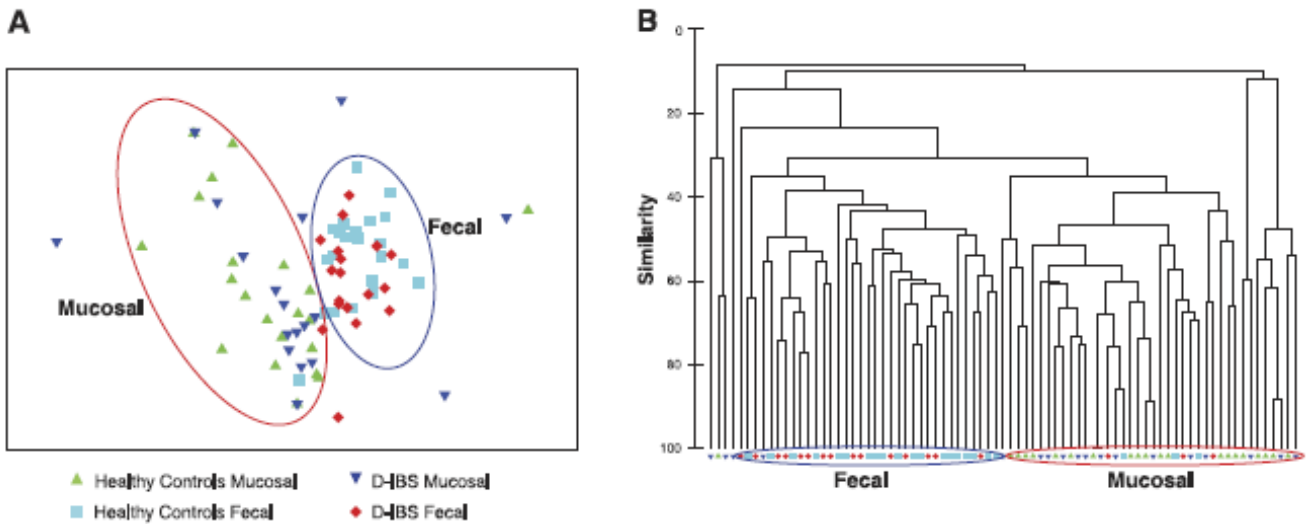

Figure. 3.3. *A*: non-multidimensional scaling analysis of T-RF profiles generated from fecal and mucosal samples from D-IBS patients and healthy controls. *B*: hierarchical cluster analysis of T-RF data from fecal and mucosal samples from D-IBS patients and healthy controls. Red and blue circles represent the majority of mucosal and fecal samples, respectively.

REFERENCES

1. Andersson AF, Lindberg M, Jakobsson H, et al. Comparative analysis of human gut microbiota by barcoded pyrosequencing. PLoS One 2008; 3: e2836.

2. Azpiroz F, Bouin M, Camilleri M, et al. Mechanisms of hypersensitivity in IBS and functional disorders. Neurogastroenterol Motil 2007; 19: 62–88.

3. Backhed F, Ley RE, Sonnenburg JL, et al. Host-bacterial mutualism in the human intestine. Science 2005; 307: 1915–1920.

4. Balsari A, Ceccarelli A, Dubini F, et al. The fecal microbial population in the irritable bowel syndrome. Microbiologica 1982; 5: 185–194.

5. Caenepeel P, Janssens J, Vantrappen G, et al. Interdigestive myoelectric complex in germ-free rats. Dig Dis Sci 1989; 34: 1180–1184.

6. Carroll IM, Chang YH, Park J, et al. Luminal- and mucosal-associated intestinal microbiota in patients with diarrhea-predominant irritable bowel syndrome. Gut Pathog 2010; 2: 19.

7. Carroll IM, Ringel-Kulka T, Ringel Y. Quantitating and identifying the organisms. In: Probiotics: A Clinical Guide, edited by Floch MH, Kim A. S. Thorofare, NJ: SLACK, 2009, p. 55–69.

8. Choi CH, Jo SY, Park HJ, et al. A randomized, double-blind, placebo-controlled multicenter trial of *Saccharomyces boulardii* in irritable bowel syndrome: effect on quality of life. J Clin Gastroenterol 2001; 45: 679–683.

9. Codling C, O'Mahony L, Shanahan F, et al. A molecular analysis of fecal and mucosal bacterial communities in irritable bowel syndrome. Dig Dis Sci 2009; 55: 392–397.

10. Dicksved J, Halfvarson J, Rosenquist M, et al. Molecular analysis of the gut microbiota of identical twins with Crohn's disease. ISME J 2008; 2: 716–727.

11. Durban A, Abellan JJ, Jimenez-Hernandez N, et al. Assessing gut microbial diversity from feces and rectal mucosa. Microb Ecol 2010; 61: 123–133.

12. Garrett WS, Gallini CA, Yatsunenko T, et al. Enterobacteriaceae act in concert with

the gut microbiota to induce spontaneous and maternally transmitted colitis. Cell Host Microbe 2010; 8: 292–300.

13. Guglielmetti S, Mora D, Gschwender M, Popp K. Randomised clinical trial: *Bifidobacterium bifidum* MIMBb75 significantly alleviates irritable bowel syndrome and improves quality of life—a double-blind, placebo controlled study. Aliment Pharmacol Ther 2011; 33: 1123–1132.

14. Husebye E, Hellstrom PM, Sundler F, et al. Influence of microbial species on small intestinal myoelectric activity and transit in germ-free rats. Am J Physiol Gastrointest Liver Physiol 2001; 280: G368–G380.

15. Kassinen A, Krogius-Kurikka L, Makivuokko H, et al. The fecal microbiota of irritable bowel syndrome patients differs significantly from that of healthy subjects. Gastroenterology 2007; 133: 24–33.

16. Krogius-Kurikka L, Lyra A, Malinen E, et al. Microbial community analysis reveals high level phylogenetic alterations in the overall gastrointestinal microbiota of diarrhoea-predominant irritable bowel syndrome sufferers. BMC Gastroenterol 2009; 9: 95.

17. Lea R, Whorwell PJ. Quality of life in irritable bowel syndrome. Pharmacoeconomics 2001; 19: 643–653.

18. Lesniewska V, Rowland I, Laerke HN, et al. Relationship between dietary-induced changes in intestinal commensal microflora and duodenojejunal myoelectric activity monitored by radiotelemetry in the rat in vivo. Exp Physiol 2006; 91: 229–237.

19. Ley RE, Hamady M, Lozupone C, et al. Evolution of mammals and their gut microbes. Science 2008; 320: 1647–1651.

20. Longstreth GF, Thompson WG, Chey WD, et al. Functional bowel disorders. Gastroenterology 2006; 130: 1480–1491.

21. Lydiard RB. Irritable bowel syndrome, anxiety, and depression: what are the links? J Clin Psychiatry 2001; 62 Suppl 8: 37–46.

22. Lyra A, Rinttila T, Nikkila J, et al. Diarrhoea-predominant irritable bowel syndrome distinguishable by 16S rRNA gene phylotype quantification. World J Gastroenterol 2009; 15: 5936–5945.

23. Malinen E, Rinttila T, Kajander K, et al. Analysis of the fecal microbiota of irritable bowel syndrome patients and healthy controls with real-time PCR. Am J Gastroenterol 2005; 100: 373–382.

24. Manichanh C, Rigottier-Gois L, Bonnaud E, et al. Reduced diversity of faecal microbiota in Crohn's disease revealed by a metagenomic approach. Gut 2006; 55: 205–211.

25. Matto J, Maunuksela L, Kajander K, et al. Composition and temporal stability of gastrointestinal microbiota in irritable bowel syndrome—a longitudinal study in IBS and control subjects. FEMS Immunol Med Microbiol 2005; 43: 213–222.

26. Maukonen J, Satokari R, Matto J, et al. Prevalence and temporal stability of selected clostridial groups in irritable bowel syndrome in relation to predominant faecal bacteria. J Med Microbiol 2006; 55: 625–633.

27. Moayyedi P, Ford AC, Talley NJ, et al. The efficacy of probiotics in the treatment of irritable bowel syndrome: a systematic review. Gut 2010; 59: 325–332.

28. Ott SJ, Musfeldt M, Wenderoth DF, et al. Reduction in diversity of the colonic mucosa associated bacterial microflora in patients with active inflammatory bowel disease. Gut 2004; 53: 685–693.

29. Ouwehand AC, Salminen S, Arvola T, et al. Microbiota composition of the intestinal mucosa: association with fecal microbiota? Microbiol Immunol 2004; 48: 497–500.

30. Park MI, Camilleri M. Is there a role of food allergy in irritable bowel syndrome and functional dyspepsia? A systematic review. Neurogastroenterol Motil 2006; 18: 595–607.

31. Parkes GC, Sanderson JD, Whelan K. Treating irritable bowel syndrome with probiotics: the evidence. Proc Nutr Soc 2010; 69: 187–194.

32. Pimentel M, Lembo A, Chey WD, et al. Rifaximin therapy for patients with irritable bowel syndrome without constipation. N Engl J Med 2011; 364: 22–32.

33. Pimentel M, Park S, Mirocha J, et al. The effect of a nonabsorbed oral antibiotic (rifaximin) on the symptoms of the irritable bowel syndrome: a randomized trial. Ann Intern Med 2006; 145: 557–563.

34. Ringel Y, Carroll IM. Alterations in the intestinal microbiota and functional bowel symptoms. Gastrointest Endosc Clin N Am 2009; 19: 141–150.

35. Ringel Y, Ringel-Kulka T, Maier D, et al. Probiotic bacteria: probiotic bacteria *Lactobacillus acidophilus* NCFM and *Bifidobacterium lactis* Bi-07 versus placebo for the symptoms of bloating in patients with functional bowel disorders—a double-blind study. J Clin Gastroenterol 2011; 45: 518–525.

37. Scanlan PD, Shanahan F, O'Mahony C, Marchesi JR. Culture-independent analyses of temporal variation of the dominant fecal microbiota and targeted bacterial subgroups in Crohn's disease. J Clin Microbiol 2006; 44: 3980–3988.

38. Seksik P, Rigottier-Gois L, Gramet G, et al. Alterations of the dominant faecal bacterial groups in patients with Crohn's disease of the colon. Gut 2003; 52: 237–242.

39. Sharara AI, Aoun E, Abdul-Baki H, et al. A randomized double-blind placebo-controlled trial of rifaximin in patients with abdominal bloating and flatulence. Am J Gastroenterol 2006; 101: 326–333.

40. Shen XJ, Rawls JF, Randall T, et al. Molecular characterization of mucosal adherent bacteria and associations with colorectal adenomas. Gut Microbes 2010; 1: 138–147.

41. Shyu C, Soule T, Bent SJ, et al. MiCA: a web-based tool for the analysis of microbial communities based on terminal-restriction fragment length polymorphisms of 16S and 18S rRNA genes. Microb Ecol 2007; 53: 562–570.

42. Si JM, Yu YC, Fan YJ, Chen SJ. Intestinal microecology and quality of life in irritable bowel syndrome patients. World J Gastroenterol 2004; 10: 1802–1805.

43. Sondergaard B, Olsson J, Ohlson K, et al. Effects of probiotic fermented milk on symptoms and intestinal flora in patients with irritable bowel syndrome: a randomized, placebo-controlled trial. Scand J Gastroenterol 2011; 46: 663–672.

44. Spiegel BM. The burden of IBS: looking at metrics. Curr Gastroenterol Rep 2009; 11: 265–269.

45. Swidsinski A, Weber J, Loening-Baucke V, et al. Spatial organization and composition of the mucosal flora in patients with inflammatory bowel disease. J Clin Microbiol 2005; 43: 3380–3389.

46. Tana C, Umesaki Y, Imaoka A, et al. Altered profiles of intestinal microbiota and organic acids may be the origin of symptoms in irritable bowel syndrome. Neurogastroenterol Motil 2009; 22: 512–519.

47. Willing BP, Dicksved J, Halfvarson J, et al. A pyrosequencing study in twins shows that gastrointestinal microbial profiles vary with inflammatory bowel disease phenotypes. Gastroenterology 2010; 139: 1844–1854.

48. Zoetendal EG, Akkermans AD, De Vos WM. Temperature gradient gel electrophoresis analysis of 16S rRNA from human fecal samples reveals stable and host-specific communities of active bacteria. Appl Environ Microbiol 1998; 64: 3854–3859.

49. Zoetendal EG, von Wright A, Vilpponen-Salmela T, et al. Mucosa-associated bacteria in the human gastrointestinal tract are uniformly distributed along the colon and differ from the community recovered from feces. Appl Environ Microbiol 2002; 68: 3401–3407.

CHAPTER 4: ALTERED ENTERIC MICROBIOTA ECOLOGY IN INTERLEUKIN 10-DEFICIENT MICE DURING DEVELOPMENT AND PROGRESSION OF INTESTINAL INFLAMMATION[4]

Introduction

Ulcerative colitis (UC) and Crohn's disease (CD), collectively known as inflammatory bowel diseases (IBD), are prevalent in the United States (US), affecting 1.4 million individuals (1), and are associated with reduced quality of life (2) and a heavy economic burden that is estimated to be $6.3 billion annually in the US (3). The chronic nature, high rate of recurrence and lack of safe and curative medical treatments for IBD underscore the need for alternate therapeutic approaches for these complex diseases. Although, the precise pathophysiology of IBD remains unclear, it is widely accepted that the pathogenesis of IBD involves dysregulated immune responses toward microbial and other luminal antigens in a genetically susceptible host (4-7). Environmental factors also play an important role in the initiation and reactivation of inflammation in IBD (4, 8). An altered composition of the intestinal microbiota (dysbiosis) has been reported for both UC and CD (9-11). However, this association is not as profound in recent pediatric studies (12, 13). Moreover, the primary versus secondary nature of an intestinal microbial dysbiosis in IBD remains unknown. Thus, more in depth characterization of sequential enteric microbial changes during early and later phases of the inflammatory process may enable the development of better therapeutic strategies for these diseases.

[4] This chapter previously appeared as an article in the journal *Gut Microbes*. The original citation is as follows: Packey CD, Maharshak N, Ellermann M, Manick S, Siddle JP, Huh EY, Plevy SE, Sartor RB, Carroll IM. Altered enteric microbiota ecology in interleukin 10-deficient mice during development and progression of intestinal inflammation. Gut Microbes 2013; 4(4): 316-324.

Among the various rodent models for IBD, interleukin-10 deficient (IL-$10^{-/-}$) mice are widely used for mechanistic studies investigating the pathogenesis of spontaneous, immune-mediated, chronic intestinal inflammation (14-16). IL-$10^{-/-}$ mice maintained in germ-free (GF) conditions do not develop intestinal inflammation. However, once colonized with conventional or specific pathogen-free (SPF) microbiota, IL-$10^{-/-}$ mice develop intestinal inflammation as early as one week following colonization with an SPF microbiota (17). Although alterations in the intestinal microbiota in subsets of IBD patients with established disease compared with healthy controls have been reported (9, 10, 18), early changes in the composition and diversity of this complex

microbial community at the onset of disease cannot be studied in the human intestinal tract, as it is impossible to predict who will develop disease (8, 19). Currently, little is known about the changes in composition and diversity of the enteric microbiota of IL-$10^{-/-}$ mice during the onset of intestinal inflammation. Molecular methods are effectively used to characterize the intestinal microbiota due to the limitations of culture-based methods. A study using 16S rRNA-based fingerprinting techniques (denaturing gradient gel electrophoresis [DGGE] and repetitive DNA element-based PCR) reported compositional changes in the intestinal microbiota in IL-$10^{-/-}$ mice over time (20, 21). However, due to the limitations in technology used for microbiota analysis, these studies provided limited data regarding the abundances of specific taxa and the diversity of the microbiota. Thus, we conducted the current study to characterize the intestinal microbiota of IL-$10^{-/-}$ mice during the progression of colitis in comparison with wild-type (WT) mice. We controlled for variations in the composition of the microbiota using previously GF IL-$10^{-/-}$ and WT mice colonized with a microbiota from the same donor. We also characterized

changes in diversity and composition of the intestinal microbiota in mice from two genetic backgrounds.

Results

16S rRNA gene sequences. The V1–3 regions of the 16S rRNA gene were amplified from all fecal DNA samples (n = 30). Following high throughput sequencing, four samples (three from week two of the IL-10$^{-/-}$ group and one from week one of the WT group) yielded sequence numbers that were too low (< 350 16S rRNA sequences per sample) to be included in our analyses. An average of 8,012 16S rRNA sequences per sample were obtained from the remaining 26 samples with the following ranges: WT week one (n = 4) 5647–10502 sequences; WT week two (n = 5) 6927–11490 sequences; IL-10$^{-/-}$ week one (n = 5) 1115–8116 sequences; IL-10$^{-/-}$ week two (n = 2) 9666–12789 sequences; IL-10$^{-/-}$ week three (n = 5) 6162–8467 sequences; IL-10$^{-/-}$ week four (n = 5) 1340–23189 sequences. To determine the numbers and abundances of different bacterial groups in each sample we used 97% similarity between 16S rRNA gene sequences as an indicator of a "species level" operational taxonomic unit (OTU). Using this procedure we found a total of 479 OTUs in our data set.

Intestinal microbial diversity decreases over time in formerly GF IL-10$^{-/-}$ mice. In our initial investigation we sought to characterize changes in diversity in the intestinal microbiota that arise over time in formerly GF WT and IL-10$^{-/-}$ mice. The microbiota was characterized in fecal samples collected weekly for two weeks in WT mice and for four weeks in IL-10$^{-/-}$ mice following association with an SPF microbiota. Based on IL-12p40 secretion from colonic tissue and composite histology scores, we found that WT mice did not develop significant inflammation whereas IL-10$^{-/-}$ mice developed moderate intestinal inflammation four weeks following association with an SPF microbiota (Fig. 4.1A and B).

We calculated UniFrac distances for all time points for each group. We found that average weighted and un-weighted UniFrac distances significantly increased ($p = 0.003$ and $p = 8.5 \times 10^{-5}$, respectively) over the two week observation period in the WT group (Fig. 4.2C). We investigated the weighted and un-weighted UniFrac distances of the microbiota in fecal samples obtained one, two, three and four weeks from formerly GF IL-$10^{-/-}$ mice following association with an SPF microbiota. We found a significant decrease in average weighted UniFrac distances at the three week ($p = 0.005$) and four week ($p = 0.005$) time points compared with the 1 week time point (Fig. 4.2A and B).

Intestinal microbial richness decreases over time in formerly GF IL-$10^{-/-}$ mice. We determined the richness of the intestinal microbiota in all groups using rarefaction analysis. A significant increase ($p = 0.004$) in the number of observed microbial species was found in WT mice two weeks following association with an SPF microbiota when compared with the one week time point (Fig. 4.3B). In contrast, a significant decrease in the number of observed microbial species was found in IL-$10^{-/-}$ mice three ($p = 0.02$) and four ($p = 0.009$) weeks following association with an SPF microbiota when compared with the one week time point (Fig. 4.3A).

Ecological succession of bacterial taxa in formerly GF IL-$10^{-/-}$ mice over time. In order to determine the dominant bacterial groups that are altered over time in WT and IL-$10^{-/-}$ mice following colonization with an SPF intestinal microbiota we summarized the bacterial taxa identified by our 16S rRNA sequences at the phylum level (Fig. 4.4). In WT mice we found no significant changes in bacterial phyla between one and two weeks post association with an SPF microbiota. In the IL-$10^{-/-}$ group we observed a significant decrease in the levels of

Bacteroidetes (20.06%–6.30%, false discovery rate [FDR] = 0.01) and Verrucomicrobia (0.74% 0.17%, FDR = 0.02) at three weeks compared with the one week time point. These changes were further reduced by four weeks: Bacteroidetes (20.06–9.5%, FDR = 0.003) and Verrucomicrobia (0.74%–0.09%, FDR = 0.02). At four weeks we observed a significant increase in the levels of Proteobacteria (0.17%–7.71%, FDR = 1.5×10^{-5}) and Tenericutes (39.21%–70.66%, FDR = 0.07) compared with the one week time point. In tandem, at four weeks we observed a decrease in the levels of Actinobacteria (1.27%–0.53%, FDR = 0.07) and Firmicutes (38.48%–11.46%, FDR = 0.03) compared with the one week time point. Additionally, we observed significant changes in the abundances of genus-level taxa over time in IL-$10^{-/-}$ mice (Table 4.1) and no significant changes in bacterial genera in WT mice over time.

***Escherichia coli* concentrations increase in formerly GF IL-$10^{-/-}$ mice over time.** Given that *E. coli* is a member of the Proteobacteria phylum and has been established as a pro-inflammatory microbe in the context of IBD (22), we used species-specific qPCR to determine the levels of this bacterial species in fecal samples from the IL-$10^{-/-}$ group of mice. We found that the levels of *E. coli* in the intestinal microbiota of IL-$10^{-/-}$ mice increased over time and became significantly higher at the four week time point when compared with the week one time point (Fig. 4.5). The stepwise increase of *E. coli* over time in the IL-$10^{-/-}$ group closely paralleled the increase in Proteobacteria in the same mice, confirming results by two different molecular methods (Fig. 4.5).

Alterations in the abundance of *E. coli* in formerly GF IL-$10^{-/-}$ mice over time are mirrored in SPF IL-$10^{-/-}$ mice. In order to determine whether inflammation associated alterations of specific taxa in formerly GF IL-$10^{-/-}$ mice are also altered in a gut that has developed naturally, we investigated the levels of *E. coli*, *Lactobacillus* species and *Akkermansia*

muciniphila in WT and IL-10$^{-/-}$ mice raised in an SPF environment. This group of IL-10$^{-/-}$ mice developed significant intestinal inflammation at 10 weeks of age compared with WT controls that did not develop inflammation (Fig. 4.1C and D). Similarly to formerly GF mice the abundance of *E. coli* was significantly higher in IL-10$^{-/-}$ mice at week ten compared with WT mice (Fig. 4.6A). *Akkermansia muciniphila* was significantly higher in IL-10$^{-/-}$ mice compared with WT mice at both eight and ten weeks (Fig. 4.6B). We did not observe any significant differences in the abundance of *Lactobacillus* species in IL-10$^{-/-}$ mice compared with WT mice at either time point (Fig. 4.6C).

Discussion

Based on the established association of the intestinal microbiota with IBD and the frequent use of the IL-10$^{-/-}$ mouse as a model of spontaneous, immune-mediated colonic inflammation, we characterized the diversity and composition of the intestinal microbiota in this mouse model during the progression of experimental colitis. Previous studies characterizing the intestinal microbiota of IL-10$^{-/-}$ mice focused on viable bacteria or used molecular techniques that characterize a limited number of bacterial taxa (20, 21). Our study used a current molecular technique that provided a comprehensive characterization of the changes in microbial composition and diversity in WT and IL-10$^{-/-}$ mice over time. Additionally, the use of formerly GF WT and IL-10$^{-/-}$ mice colonized with the same fecal microbiota provided a highly controlled environment to study these changes.

In our investigations we observed an increase in microbial richness (as determined by rarefaction of bacterial species) and diversity (as determined by UniFrac distances) in formerly GF WT mice two weeks following association with an SPF microbiota. This finding suggests that the intestinal microbiota in formerly GF WT mice may still be establishing a homeostatic

balance two weeks after colonization. UniFrac distances can be calculated in a weighted (relative abundance of taxa) or un-weighted (presence or absence of taxa) manner. Low average UniFrac distances indicate higher similarity in the composition of the microbiota within a group of samples, whereas high average UniFrac distances indicate more dissimilarity within a group of samples. We observed an increase in both weighted and un-weighted UniFrac distances two weeks post colonization in WT mice, suggesting that the rise in diversity values at this time point is due to an increase in both high and low abundance bacterial species. A limitation of our study is that we did not investigate the microbial composition and diversity of fecal samples in formerly GF WT mice at three and four weeks following conventionalization with an intestinal microbiota. Thus we cannot conclude whether the intestinal microbiota has reached equilibrium at this point. Interestingly, it has been reported that the microbial composition and diversity of cecal contents in formerly GF WT mice, from a different genetic background (C57BL/6), exhibited stability seven days post-inoculation (23).

We subsequently characterized the richness and diversity of the intestinal microbiota in formerly GF IL-10$^{-/-}$ mice up to four weeks following colonization with an SPF microbiota to investigate alterations in the intestinal microbiota during the progression of colitis. Indeed, we observed moderate inflammation at four weeks post colonization in IL-10$^{-/-}$ mice. A progressive decrease in weighted UniFrac distances was observed three and four weeks post colonization in comparison with one week values. In addition, the richness of the microbiota was significantly decreased in this cohort of mice at these later time points. Interestingly, we did not observe a significant decrease in un-weighted UniFrac distances at the three and four week time points compared with one week in IL-10$^{-/-}$ mice. These data suggest that the composition of newly introduced, complex microbial communities in formerly GF IL-10$^{-/-}$ mice becomes more alike

during the progression of colonic inflammation and that high abundance taxa are responsible for this change. In the absence of an established fecal marker indicative of intestinal inflammation we are unable to conclude whether the alterations in the richness and diversity of the enteric microbiota in IL-10$^{-/-}$ mice occur before, during or after the onset of colonic inflammation. In previous experiments we found that mild inflammation occurs in formerly GF IL-10$^{-/-}$ mice on a 129 SvEv background two weeks following microbial colonization (17).

Our current study shows that enteric microbial richness and diversity dramatically change at three weeks post association with an SPF microbiota. Thus, we speculate that decreases in enteric microbial richness and diversity in IL-10$^{-/-}$ mice occur after the onset of colonic inflammation in this mouse model. In tandem with altered enteric microbial richness and diversity in the intestinal microbiota of IL-10$^{-/-}$ mice over time, we observed changes in the relative abundances of specific bacterial phyla. Most notable was a step-wise increase in the levels of Proteobacteria that mirrored a significant increase of *E. coli* during the onset of colonic inflammation. Elevated Proteobacteria levels have been reported in UC and CD patients (9). Moreover, adherent invasive *E. coli* strains are associated with ileal CD (22, 24). A significant depletion in the concentrations of the Bacteroidetes and Firmicutes phyla were observed over time in IL-10$^{-/-}$ mice, which also reflects changes reported in the intestinal microbiota of human IBD (9, 10). Thus, our data demonstrate that the IL-10$^{-/-}$ mouse model of colitis exhibits alterations in specific members of the intestinal microbiota that parallel those of human IBD.

We also observed significant decreases in the levels of the Actinobacteria and Verrucomicrobia phylum, which have not been reported for human IBD and may be a consequence of enteric inflammation. It is interesting to note that *Bifidobacterium* species are encompassed within the Actinobacteria phylum and are considered probiotic microbes.

Alterations in the Verrucomicrobia phyla may be yet unreported components of a human IBD dysbiosis, or alternatively, they may be unique to this mouse model. However, it has been reported that *Akkermansia muciniphila* (a member of the Verrucomicrobia phylum) is depleted in the mucus of IBD patients (25). Indeed, in support of this finding, our 16S rRNA sequence data revealed a significant decrease in the *Akkermansia* genus in IL-10$^{-/-}$ mice over time. As bacterial richness and diversity decreased in IL-10$^{-/-}$ mice over time we observed a profound increase in the levels of the Tenericutes phylum. This phylum encompasses bacteria that lack a cell wall and are thus Gram negative. Tenericutes have been reported to be significantly elevated in fecal samples from colonic Crohn's disease patients but decreased in fecal samples from ileal Crohn's disease and ulcerative colitis patients (10). From our data set the dominant genus within the Tenericutes phylum is *Allobaculum*. However, although taxonomies were assigned to our 16S rRNA sequences using the Greengenes database (26), it is interesting to note that the RDP database (27) classifies the *Allobaculum* genus as belonging to the Firmicutes phylum, which would make the Firmicutes the dominant phylum in our data set. Nevertheless, it has been reported that the Greengenes database, which contains the largest and most diverse set of 16S rRNA sequences, is superior to other databases when classifying sequences at the phylum level, particularly with respect to the Tenericutes (28).

It has been reported that GF mice have abnormal mucosal and immunologic maturation resulting in increased morbidity in the oxazolone-induced mouse model of colitis when compared with SPF mice (29). Thus, we determined the abundances of specific bacterial groups in cohorts of WT and IL-10$^{-/-}$ mice that were raised with a normal intestinal microbiota. Even though the mice used were of a different genetic background (C57BL/6) to the mice used in our GF experiments we observed an increase in the abundance of *E. coli* in IL-10$^{-/-}$ mice compared

with WT mice, suggesting a strong association of this bacterial species with the development of intestinal inflammation in this mouse model over time. We also found that although abundances of *A. muciniphila* and *Lactobacillus* species appeared to decrease over time in IL-10$^{-/-}$ mice compared with WT mice, these decreases were not significant. Thus, it is possible that the alterations in the enteric microbiota during the development of intestinal inflammation that we observed in formerly GF IL-10$^{-/-}$ mice are influenced by host genetics and an abnormal gut physiology associated with GF mice.

Our data reports the changes in diversity and composition of the intestinal microbiota in the IL-10$^{-/-}$ mouse model of spontaneous, immune-mediated colitis over time. The reduction in diversity and most changes in specific bacterial taxa in the intestinal microbiota of this mouse model reflect the changes in this complex microbial community observed in human IBD patients. Thus, our study validates the use of this mouse model for studies relating to the intestinal microbiota and immune-mediated colonic inflammation. The progressive loss of diversity, of dominant commensal microbiota and expansion of Proteobacteria, notably *E. coli*, with increasing experimental inflammation suggests that dysbiosis is secondary to the immune response in this model. Despite the postulated secondary nature of the observed changes, the altered microbiota profiles may still be responsible for perpetuation and amplification of mucosal immune responses and inflammation, since we have documented enteric bacterial-specific TH1 and TH17 responses in this model (30).

Materials and Methods

Mice. Adult WT and IL-10$^{-/-}$ 129 SvEv mice were maintained in a GF state at the National Gnotobiotic Rodent Resource Center at UNC-Chapel Hill, NC, USA. One group of WT (n = 5) and one group of IL-10$^{-/-}$ (n = 5) mice were used in this study. Formerly GF mice were

inoculated with fecal slurry obtained from a common SPF WT 129 SvEv donor mouse via oral and rectal swabbing (see Fig. 4.7 for a schematic design of the study). Each experimental group (WT and IL-$10^{-/-}$) consisted of mice from the same litter that were housed in separate cages. Fresh fecal pellets were obtained weekly from all mice. All fecal pellets collected were flash frozen immediately in liquid nitrogen to retain the integrity of the fecal microbiota.

In order to translate our findings from GF animals to mice that were raised from birth with a normal microbiota, we investigated WT (n = 8) and IL-$10^{-/-}$ (n = 9) C57BL/6 mice housed in a specific pathogen-free (SPF) environment. Each experimental group (WT and IL-$10^{-/-}$) consisted of mice from the same litter that were housed in separate cages. Fecal samples were collected from all mice at eight and 10 weeks of age.

Assessment of intestinal inflammation. Sections of fixed (10% neutral buffered formalin) colons were embedded in paraffin and stained with hematoxylin and eosin. Using a well-validated scale (17, 31), the severity of inflammation was blindly assessed. Histological scores (0 to 4) were based on the degree of lamina propria and submucosal mononuclear cellular infiltration, crypt hyperplasia, goblet cell depletion and architectural distortion. A composite histology score was generated by the aggregate scores from the cecum and proximal and distal colon.

Colonic explant cultures were prepared as previously described (17). Briefly, colonic tissue was thoroughly irrigated with phosphate-buffered saline (PBS), shaken at room temperature in Roswell Park Memorial Institute medium (RPMI) containing 1% penicillin and streptomycin (GIBCO, Grand Island, NY) for 30 min at 280 rpm, cut into 1-mm fragments and weighed. Intestinal tissue fragments were then distributed (0.05 g per well) into 24-well plates and incubated in 1 mL of RPMI 1640 medium supplemented with 10% fetal bovine serum and

1% antibiotic/antimycotic (GIBCO) for 22 h at 37°C. Supernatants were collected and stored at −20°C before use for cytokine quantification. Commercially available monoclonal anti-mouse IL-12 p40 capture and detection reagents (BD Biosciences PharMingen, San Diego, CA) in an enzyme-linked immunosorbent assay (ELISA) were used to measure the levels of IL-12 p40 secreted constitutively in colonic explant cultures (17, 31). IL-12 p40 levels were measured in supernatants and compared with standard curves generated by using recombinant murine IL-12 p40.

Isolation of DNA. Bacterial DNA was isolated from all fecal pellets (n = 47) using a phenol/chloroform extraction method combined with physical disruption of bacterial cells and a DNA clean-up kit (Qiagen DNeasy® Blood and Tissue extraction kit) as previously described (32). Briefly, 100 mg of frozen feces were suspended in 750 μL of sterile bacterial lysis buffer (200 mM NaCl, 100 mM Tris [pH 8.0], 20 mM EDTA, 20 mg/mL lysozyme) and incubated at 37°C for 30 min. Next, 40 μL of proteinase K (20 mg/mL) and 85 μL of 10% SDS were added to the mixture and incubated at 65°C for 30 min. 300 mg of 0.1 mm zirconium beads (BioSpec Products) were then added and the mixture was homogenized in a bead beater (BioSpec Products) for 2 min. The homogenized mixture was cooled on ice and centrifuged at 14,000 rpm for 5 min. The supernatant was transferred to a new 1.5 ml microfuge tube and fecal DNA was further extracted by phenol/chloroform/iso-amyl alcohol (25:24:1) and chloroform/iso-amyl alcohol (24:1). Following extraction the supernatant was precipitated by absolute ethanol at −20°C for 1 h. The precipitated DNA was suspended in DNase free H2O and cleaned using the Qiagen DNeasy® Blood and Tissue extraction kit per the manufacturer's instructions.

454 pyro-sequencing of 16S rRNA genes. Bacterial community composition in isolated DNA samples was characterized by amplification of the V1–3 (forward, 8f: 5'-AGAGTTTGAT

CMTGGCTCAG-3'; reverse 518r: 5'-ATTACCGCGGCTGCTGG-3') variable regions of the 16S rRNA gene by polymerase chain reaction (PCR) as previously described (33). Forward primers were tagged with 10 bp unique barcode labels at the 5' end along with the adaptor sequence (5'-CCATCTCATCCCTGCGTGTC TCCGACTCAG-3') to allow multiple samples to be included in a single 454 Genome Sequencer (GS) FLX Titanium sequencing plate as previously described (34, 35). 16S rRNA PCR products were quantified, pooled and purified for the sequencing reaction. 454 GS FLX Titanium sequencing was performed on a 454 Life Sciences GS FLX machine (Roche, Florence, SC) at the Microbiome Core at UNC-Chapel Hill (http://www.med.unc.edu/microbiome).

Analysis of 16S rRNA sequences using the QIIME pipeline. 16S rRNA sequence data generated by the 454 GS FLX Titanium sequencer were processed by the quantitative insights into microbial ecology (QIIME) pipeline (36). Briefly, sequences that were less than 200 bp or greater than 1,000 bp in length, contained incorrect primer sequences or contained more than 1 ambiguous base were discarded. The remaining sequences were assigned to WT and IL-$10^{-/-}$ groups based on their unique nucleotide barcodes, including error-correction (34). Sequences were clustered into OTUs based on 97% sequence similarity (similar to species level) using BLAST (37) with the Greengenes reference database (38). α-diversity (diversity within samples) was determined with ten iterations at a maximal sequence depth where all samples could be included. β-diversity (diversity between groups of samples) was calculated using weighted and un-weighted UniFrac distances (39-41). UniFrac distances are a β-diversity measure that utilizes phylogenetic information to compare environmental samples (39, 40).

Quantitative real-time PCR (qPCR). qPCR assays were performed using the SYBR® Green PCR Master Mix (Applied Biosystems, Carlsbad, CA) with primers that amplify the genes

encoding 16S rRNA from *E. coli* (forward, 5'-GTTAATACCT TTGCTCATTG A-3'; reverse, 5'-ACCAGGGTAT CTAATCCTGT T-3'), *Lactobacillus* species (forward, 5'-AGCAGTAGGG AATCTTCCA-3'; reverse, 5'-CACCGCTACA CATGGAG-3'), *A. muciniphila* (forward, 5'-CAGCACGTGA AGGTGGGGAC-3'; reverse, 5'-CCTTGCGGTT GGCTTCAGAT-3') and all bacteria (forward, 5'-TGSTGCAYGG YTGTCGTCA-3'; reverse, 5'-ACGTCRTCCM CACCTTCCTC-3'). qPCR assays were conducted in 96-well plates on an Eppendorf Realplex^2 mastercycler thermocycler (Eppendorf, Hauppauge, NY). Each PCR was performed in a final volume of 25 μL and contained the following: 1× SYBR Green Master Mix, 0.5 μM of each primer and 10 ng of purified fecal DNA. PCR conditions were as follows: 10 min at 95°C, followed by 40 cycles of 95°C for 15 sec, 20 sec at 50°C and 72°C for 30 sec. Each plate included duplicate reactions per DNA sample, the appropriate set of standards and a "no template" negative control for each primer set. qPCR standards were generated by PCR amplification of target sequences from genomic DNA of an appropriate positive control strain. Analysis of melting curves confirmed that the fluorescence signal originated from specific PCR products and not from primer-dimers or other artifacts.

Statistical analyses. Bacterial taxon percentages and average UniFrac value data sets were assessed for normality using the D'Agostino and Pearson omnibus normality test. When a data set was identified as not having a normal distribution it was transformed by log (10, 42) and retested for normality. Normally distributed data sets were compared using a Student's t-test. All statistical comparisons were performed using GraphPad Prism software (v4.0a; Prism). We used taxon and phylogenetic-based analyses to compare 16S rRNA gene sequences within WT and IL-10$^{-/-}$ groups over time. Taxon-based: the means and standard deviations of abundances of bacterial Phyla were calculated and compared between all time-points for each group using the

Benjamini–Hochberg procedure (43) to correct for multiple corrections. A p value of less than 0.05 and a FDR less than 0.1 were considered significant. Phylogenetic-based: phylogenetic trees for WT and IL-$10^{-/-}$ groups were generated using the QIIME pipeline (36). Each tree was subjected to un-weighted and weighted UniFrac analyses (39, 40) through the QIIME pipeline. UniFrac distances represent the fraction of branch length that is shared by any two samples' communities in a phylogenetic tree built from 16S rRNA sequence data from all samples. Average UniFrac distances, which represent the similarity or dissimilarity of microbial communities within a group, were compared using a student's t test.

For qPCR assays, the percentage of *E. coli* was determined in all fecal samples ([copies 16S rRNA gene for *E. coli*/copies of 16S rRNA gene for all bacteria] × 100). The concentration of *E. coli* group was expressed as a "fold change" with respect to the concentration in the control group (WT) at week 1 after colonization. qPCR data were compared between groups using a non-parametric Mann-Whitney test. Similarly, the concentrations of IL-12p40 secreted by colonic tissue (pg/mL/mg of tissue) were compared between groups using a non-parametric Mann-Whitney test.

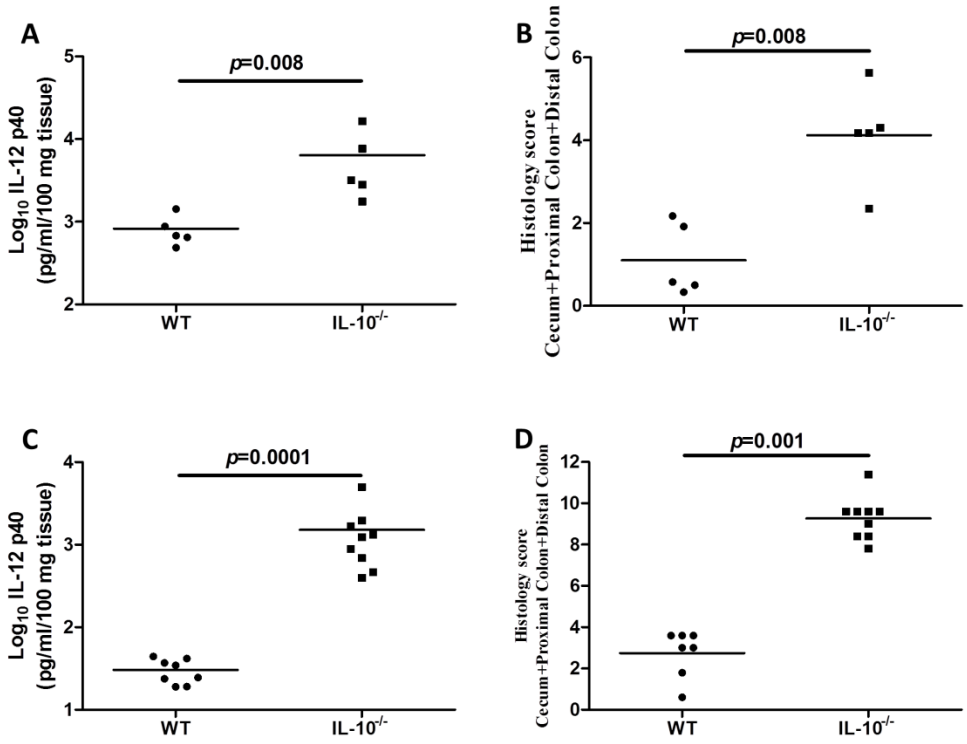

Figure 4.1. Inflammatory changes in the colons of formerly GF mice over time. Levels of IL-12 p40 secreted by colonic tissues from formerly GF WT and IL-10$^{-/-}$ mice (A) and SPF raised WT and IL-10$^{-/-}$ mice (C). The levels of IL-12 p40 in IL-10$^{-/-}$ mice are significantly higher compared with WT mice in both formerly GF ($p = 0.008$) and SPF ($p = 0.0001$) environments. Histological scores for formerly GF WT and IL-10$^{-/-}$ mice (B) and SPF WT ($n = 7$, as one tissue sample degraded during processing) and IL-10$^{-/-}$ mice (D). The degree of histological inflammation is significantly higher in IL-10$^{-/-}$ compared with WT mice in formerly GF ($p = 0.008$) and SPF ($p = 0.001$) environments.

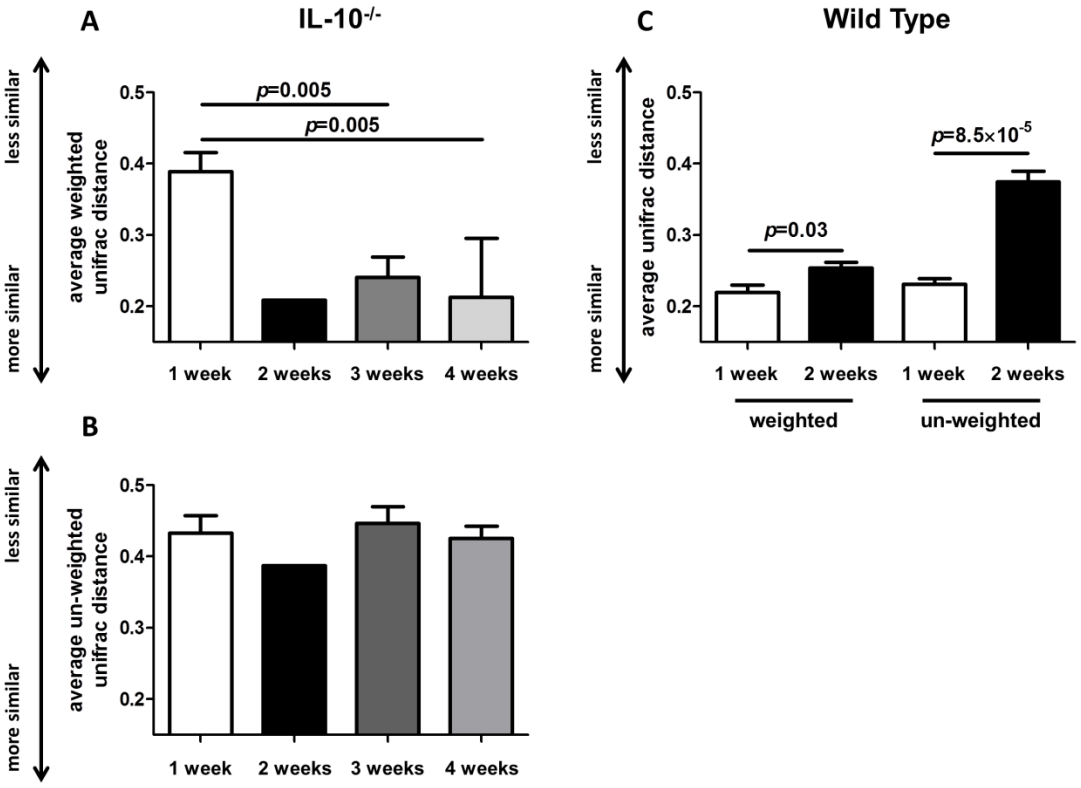

Figure 4.2. Changes in weighted and un-weighted average UniFrac distances in formerly GF wild type (WT) and IL-10$^{-/-}$ mice over time. (A) Average weighted UniFrac distances of the intestinal microbiota significantly decrease in IL-10$^{-/-}$ mice three and four weeks following colonization with a specific pathogen-free (SPF) microbiota. (B) Average un-weighted UniFrac distances of the intestinal microbiota do not significantly alter in the IL-10$^{-/-}$ mice following colonization with an SPF microbiota. (C) Average weighted and un-weighted UniFrac distances significantly increase in WT mice between one and two weeks following colonization with an SPF microbiota.

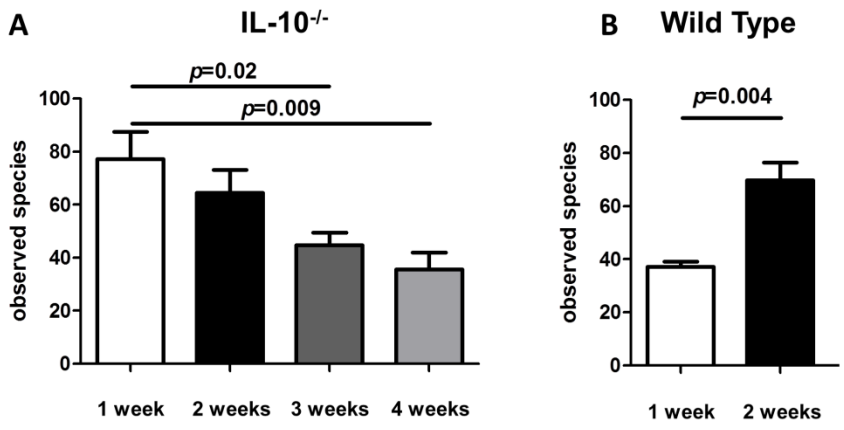

Figure 4.3. Microbial richness of 16S rRNA data. (A) The number of observed bacterial species in formerly GF IL-$10^{-/-}$ mice decreases between one and four weeks following colonization with an SPF microbiota. (B) The number of observed bacterial species in formerly GF WT mice significantly increases between one and two weeks following colonization with an SPF microbiota.

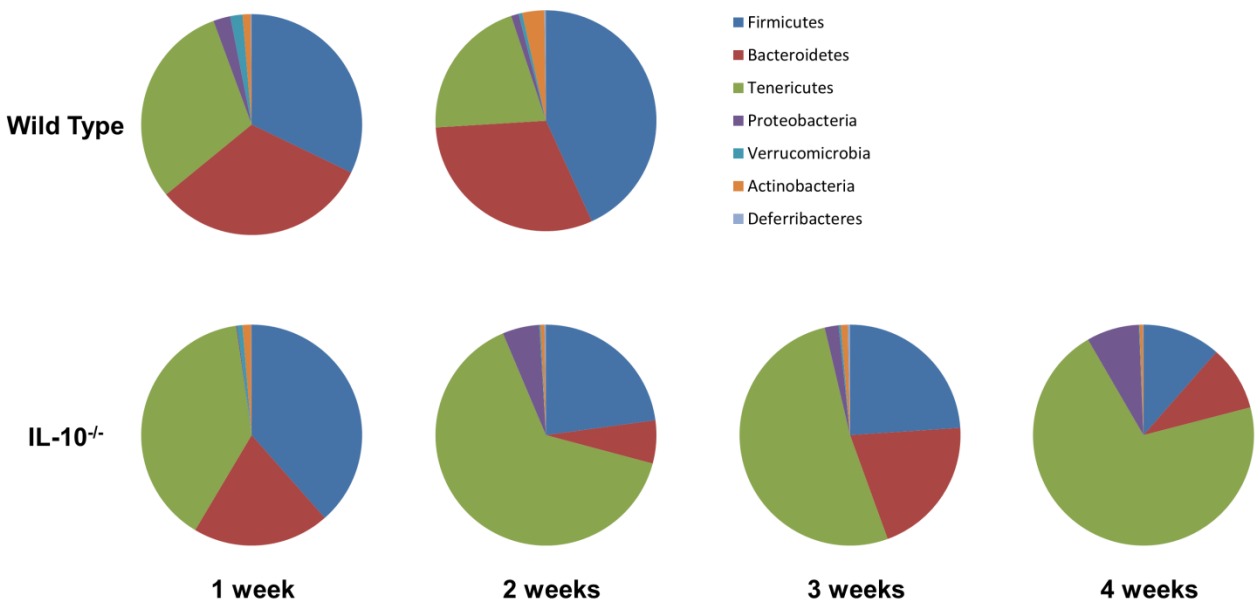

Figure 4.4. Bacterial taxa alterations over time in formerly GF WT and IL10$^{-/-}$ mice.

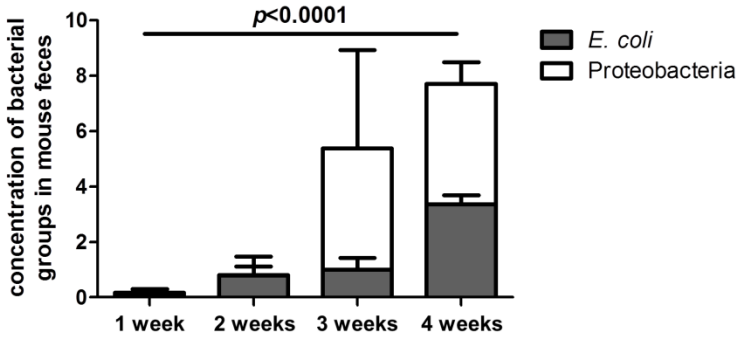

Figure 4.5. Change in levels of Proteobacteria and *Escherichia coli* in formerly GF IL-$10^{-/-}$ mice over time. Proteobacteria are expressed as the percentage of total 16S rRNA sequences. *E. coli* are expressed as fold increase with respect to baseline (WT at week 1). *The levels of Proteobacteria and *E. coli* are significantly higher at week 4 post colonization compared with week 1 (*E. coli*, p = 0.0001; Proteobacteria, FDR = 1.5×10^{-5}).

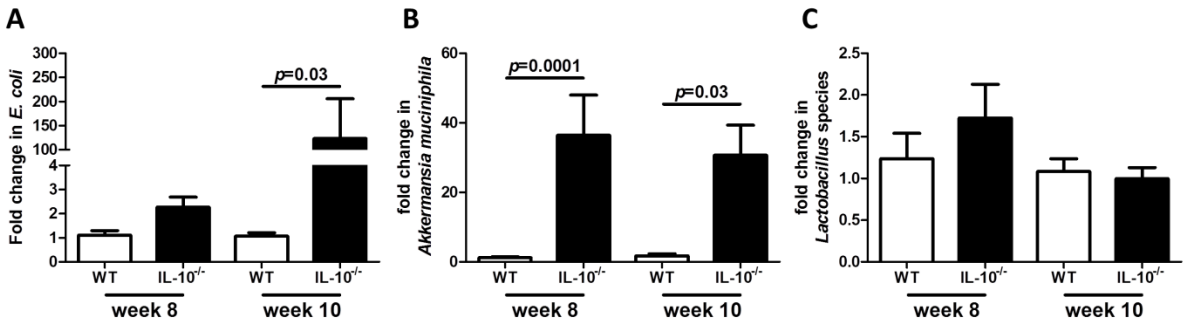

Figure 4.6. Change in levels of *E. coli* (A), *Akkermansia muciniphila* (B) and *Lactobacillus* species (C) in SPF WT and IL-10$^{-/-}$ mice over time.

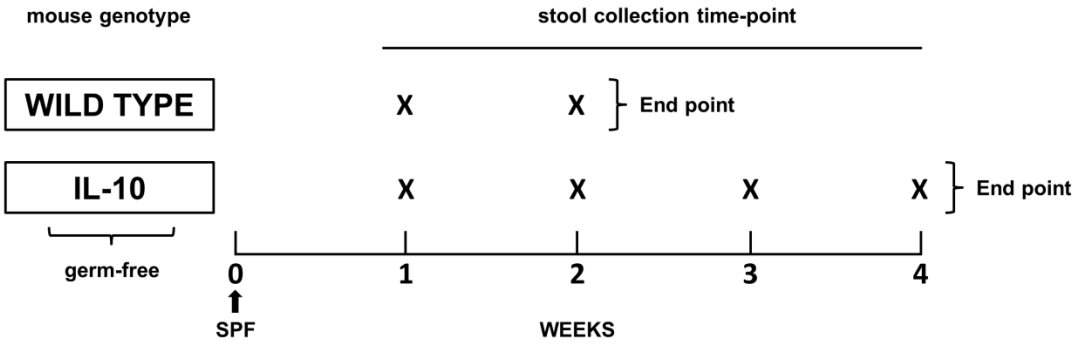

Figure 4.7. Schematic outline of experimental design. Adult WT and IL-$10^{-/-}$ 129 SvEv GF mice were inoculated with an SPF microbiota from a single donor (black arrow). Fresh fecal pellets were obtained from the WT group (n = 5) at 1 and 2 weeks following SPF inoculation. Fecal pellets were obtained from the IL-$10^{-/-}$ group (n = 5) at 1, 2, 3 and 4 weeks following association with an SPF intestinal microbiota.

Taxon	% week 1	% week 3	% week 4	*p*	FDR
Coprobacillus	0.86	0.06		0.004	0.07
Akkermansia	0.75	0.17		0.007	0.06
Lactobacillus	1.20	12.83		0.008	0.05
Staphylococcus	0.50	0.00		0.020	0.10
Parabacteroides	9.15	4.05		0.023	0.10
Raoultella	0.00		0.08	0.002	0.03
Akkermansia	0.75		0.09	0.003	0.02
Clostridium	0.02		0.00	0.006	0.04
Enterobacter	0.10		5.14	0.009	0.04
Oscillospira	0.83		0.04	0.010	0.04

Table 4.1. Changes in the abundances of genus-level taxa over time in formerly GF IL-10$^{-/-}$ mice
*False discovery rate (FDR) < 0.1 = statistically significant.

REFERENCES

1. Xavier RJ, Podolsky DK. Unravelling the pathogenesis of inflammatory bowel disease. Nature 2007; 448: 427-34.

2. Cohen RD. The quality of life in patients with Crohn's disease. Aliment Pharmacol Ther 2002; 16: 1603-9.

3. Kappelman MD, Rifas-Shiman SL, Porter CQ, et al. Direct health care costs of Crohn's disease and ulcerative colitis in US children and adults. Gastroenterology 2008; 135: 1907-13.

4. Packey CD, Sartor RB. Interplay of commensal and pathogenic bacteria, genetic mutations, and immunoregulatory defects in the pathogenesis of inflammatory bowel diseases. J Intern Med 2008; 263: 597-606.

5. Packey CD, Sartor RB. Commensal bacteria, traditional and opportunistic pathogens, dysbiosis and bacterial killing in inflammatory bowel diseases. Curr Opin Infect Dis 2009; 22: 292-301.

6. Albenberg LG, Lewis JD, Wu GD. Food and the gut microbiota in inflammatory bowel diseases: a critical connection. Curr Opin Gastroenterol 2012; 28: 314-20.

7. Shanahan F. The microbiota in inflammatory bowel disease: friend, bystander, and sometime-villain. Nutr Rev 2012; 70(Suppl 1): S31-7.

8. Sartor RB. Microbial influences in inflammatory bowel diseases. Gastroenterology 2008; 134: 577-94.

9. Frank DN, St Amand AL, Feldman RA, et al. Molecular-phylogenetic characterization of microbial community imbalances in human inflammatory bowel diseases. Proc Natl Acad Sci U S A 2007; 104: 13780-5.

10. Willing BP, Dicksved J, Halfvarson J, et al. A pyrosequencing study in twins shows that gastrointestinal microbial profiles vary with inflammatory bowel disease phenotypes. Gastroenterology 2010; 139: 1844-54.

11. Gophna U, Sommerfeld K, Gophna S, et al. Differences between tissue-associated intestinal microfloras of patients with Crohn's disease and ulcerative colitis. J Clin Microbiol 2006; 44: 4136-41.

12. Kellermayer R, Mir SA, Nagy-Szakal D, et al. Microbiota separation and C-reactive protein elevation in treatment-naïve pediatric granulomatous Crohn disease. J Pediatr Gastroenterol Nutr 2012; 55: 243-50.

13. Hansen R, Russell RK, Reiff C, et al. Microbiota of de-novo pediatric IBD: increased *Faecalibacterium prausnitzii* and reduced bacterial diversity in Crohn's but not in ulcerative colitis. Am J Gastroenterol 2012; 107: 1913-22.

14. Büchler G, Wos-Oxley ML, Smoczek A, et al. Strain-specific colitis susceptibility in IL10-deficient mice depends on complex gut microbiota-host interactions. Inflamm Bowel Dis 2012; 18: 943-54.

15. Barnett MP, McNabb WC, Cookson AL, et al. Changes in colon gene expression associated with increased colon inflammation in interleukin-10 gene-deficient mice inoculated with *Enterococcus* species. BMC Immunol 2010; 11: 39.

16. Hansen JJ, Holt L, Sartor RB. Gene expression patterns in experimental colitis in IL-10-deficient mice. Inflamm Bowel Dis 2009; 15: 890-9.

17. Sellon RK, Tonkonogy S, Schultz M, et al. Resident enteric bacteria are necessary for development of spontaneous colitis and immune system activation in interleukin-10-deficient mice. Infect Immun 1998; 66: 5224-31.

18. Sokol H, Pigneur B, Watterlot L, et al. *Faecalibacterium prausnitzii* is an anti-inflammatory commensal bacterium identified by gut microbiota analysis of Crohn disease patients. Proc Natl Acad Sci U S A 2008; 105: 16731-6.

19. Garrett WS, Gordon JI, Glimcher LH. Homeostasis and inflammation in the intestine. Cell 2010; 140: 859-70.

20. Bibiloni R, Simon MA, Albright C, et al. Analysis of the large bowel microbiota of colitic mice using PCR/DGGE. Lett Appl Microbiol 2005; 41: 45-51.

21. Peña JA, Li SY, Wilson PH, et al. Genotypic and phenotypic studies of murine intestinal lactobacilli: species differences in mice with and without colitis. Appl Environ Microbiol 2004; 70: 558-68.

22. Darfeuille-Michaud A, Boudeau J, Bulois P, et al. High prevalence of adherent-invasive *Escherichia coli* associated with ileal mucosa in Crohn's disease. Gastroenterology 2004; 127: 412-21.

23. Gillilland MG 3rd, Erb-Downward JR, Bassis CM, et al. Ecological succession of bacterial communities during conventionalization of germ-free mice. Appl Environ Microbiol 2012; 78: 2359-66.

24. Wine E, Ossa JC, Gray-Owen SD, Sherman PM. Adherent-invasive *Escherichia coli*, strain LF82 disrupts apical junctional complexes in polarized epithelia. BMC Microbiol 2009; 9: 180.

25. Png CW, Lindén SK, Gilshenan KS, et al. Mucolytic bacteria with increased prevalence in IBD mucosa augment in vitro utilization of mucin by other bacteria. Am J Gastroenterol 2010; 105: 2420-8.

26. DeSantis TZ, Hugenholtz P, Larsen N, et al. Greengenes, a chimera-checked 16S rRNA gene database and workbench compatible with ARB. Appl Environ Microbiol 2006; 72: 5069-72.

27. Cole JR, Chai B, Farris RJ, et al. The ribosomal database project (RDP-II): introducing myRDP space and quality controlled public data. Nucleic Acids Res 2007; 35(Database issue): D169-72.

28. Werner JJ, Koren O, Hugenholtz P, et al. Impact of training sets on classification of high-throughput bacterial 16s rRNA gene surveys. ISME J 2012; 6: 94-103.

29. Olszak T, An D, Zeissig S, et al. Microbial exposure during early life has persistent effects on natural killer T cell function. Science 2012; 336: 489-93.

30. Kim SC, Tonkonogy SL, Albright CA, et al. Variable phenotypes of enterocolitis in interleukin 10-deficient mice monoassociated with two different commensal bacteria. Gastroenterology 2005; 128: 891-906.

31. Veltkamp C, Tonkonogy SL, De Jong YP, et al. Continuous stimulation by normal luminal bacteria is essential for the development and perpetuation of colitis in Tg(epsilon26) mice. Gastroenterology 2001; 120: 900-13.

32. Gulati AS, Shanahan MT, Arthur JC, et al. Mouse background strain profoundly influences Paneth cell function and intestinal microbial composition. PLoS One 2012; 7: e32403.

33. Carroll IM, Ringel-Kulka T, Siddle JP, Ringel Y. Alterations in composition and diversity of the intestinal microbiota in patients with diarrhea-predominant irritable bowel syndrome. Neurogastroenterol Motil 2012; 24: 521-30.

34. Hamady M, Walker JJ, Harris JK, et al. Error-correcting barcoded primers for pyrosequencing hundreds of samples in multiplex. Nat Methods 2008; 5: 235-7.

35. Fierer N, Hamady M, Lauber CL, Knight R. The influence of sex, handedness, and washing on the diversity of hand surface bacteria. Proc Natl Acad Sci U S A 2008; 105: 17994-9.

36. Caporaso JG, Kuczynski J, Stombaugh J, et al. QIIME allows analysis of high-throughput community sequencing data. Nat Methods 2010; 7: 335-6.

37. Altschul SF, Gish W, Miller W, et al. Basic local alignment search tool. J Mol Biol 1990; 215: 403-10.

38. McDonald D, Price MN, Goodrich J, et al. An improved Greengenes taxonomy with explicit ranks for ecological and evolutionary analyses of bacteria and archaea. ISME J 2012; 6: 610-8.

39. Lozupone C, Knight R. UniFrac: a new phylogenetic method for comparing microbial communities. Appl Environ Microbiol 2005; 71: 8228-35.

40. Lozupone C, Lladser ME, Knights D, et al. UniFrac: an effective distance metric for microbial community comparison. ISME J 2011; 5: 169-72.

41. Lozupone CA, Hamady M, Kelley ST, Knight R. Quantitative and qualitative beta diversity measures lead to different insights into factors that structure microbial communities. Appl Environ Microbiol 2007; 73: 1576-85.

42. Ramette A. Multivariate analyses in microbial ecology. FEMS Microbiol Ecol 2007; 62: 142-60.

43. Benjamini Y, Drai D, Elmer G, et al. Controlling the false discovery rate in behavior genetics research. Behav Brain Res 2001; 125: 279-84.

CHAPTER 5: MOLECULAR DETECTION OF BACTERIAL CONTAMINATION IN GNOTOBIOTIC RODENT UNITS[5]

Introduction

The role of the indigenous microbiota in human health and disease has received a great deal of attention in the last decade. Gnotobiotic (from the Greek roots *gnotos* "known" and *bios* "life") rodents, reared under germ-free (GF) conditions, with or without subsequent exposure during postnatal life or adulthood to single or combinations of microbial species, provide an excellent system for controlling microbial community composition and housing conditions. Gnotobiology has greatly facilitated our understanding of the contribution of commensal bacteria to host developmental, physiologic and pathophysiologic processes (1). It has revealed some of the operating principles that underlie host-microbial and microbial-microbial relationships, including the discoveries that commensal bacteria affect the structure of mucosal surfaces and contribute to the development, organization and function of the immune system (2-5).

It is now known that individual bacterial members of the commensal microbiota (6-8) have the potential to carry out striking immunomodulatory functions. Perhaps not unsurprisingly then, the microbiota also heavily contributes to inflammatory (9-13), autoimmune (14), metabolic (11, 15, 16), neoplastic (17), functional (18-20) and treatment-induced (21, 22) disorders.

[5] This chapter previously appeared as an article in the journal *Gut Microbes*. The original citation is as follows: Packey CD, Shanahan MT, Manick S, Bower MA, Ellermann M, Tonkonogy SL, Carroll IM, Sartor RB. Molecular detection of bacterial contamination in gnotobiotic rodent units. Gut Microbes 2013; 4(5): 361-370.

GF rodents, which possess no bacteria, yeast, molds, parasites or viruses, except retroviruses, are the foundation of gnotobiology, and provide a critical approach for characterizing the properties of the human gut microbiota. GF animals are derived by sterile Caesarian section or embryo transfer and maintained in sterile isolators. These animals can be selectively inoculated with various microbial species, either singly (monoassociation) or in combination, to study their effects on the host. Once colonized, these rodents must be maintained in barrier intact isolators with positive pressure filtered air and sterilized bedding, food and water to avoid contamination with bacteria, as occurs rapidly in rodents maintained in conventional filter top cages. Maintaining these animals requires compulsively maintained sterile technique, with periodic monitoring for contamination.

The accuracy and reproducibility of gnotobiotic experimental results depend on maintaining precise microbial conditions within each isolator with exclusion of undesired external organisms. This is achieved with double-sided entry ports, sleeved gloves, a continuous flow of filtered air and complete sterilization of all materials entering the isolator. However, this unique system is highly labor intensive and vulnerable to contamination. Any interruption in air flow, incomplete sterilization of food, water or bedding, (due to an undetected autoclave malfunction, for example), or breach in the integrity of the isolator walls, entry ports, filters, sleeves or gloves that are used to manipulate the animals will jeopardize isolator sterility.

Hence, screening of gnotobiotic units for contamination must be performed on a routine basis. The traditional approach to screening relies on aerobic and anaerobic bacterial and fungal culturing with or without Gram staining (23-26). However, these methods have considerable limitations. First, many bacteria in the mammalian gut microbiota are not easily cultured in a laboratory, mainly owing to the lack of appropriate culture media (27). Second, identifying

contaminating organisms can be quite tedious and difficult by culture techniques. Finally, the interpretation of fecal Gram stains, which is often complicated by the presence of distracters such as dietary vegetable fibers, fecal matter and dead bacteria present in autoclaved or irradiated chow, can be extremely challenging even to experienced observers.

Consequently, we have optimized molecular polymerase chain reaction (PCR)-based techniques for the specific purpose of screening for and identifying bacterial contamination of gnotobiotic animals with maximal sensitivity and specificity. 16S ribosomal RNA (rRNA) sequencing has been utilized to survey bacterial species within the microbiota and the potential for using 16S rRNA PCR to verify GF status was recently mentioned in the literature for the first time (28). However, the methods to carry out 16S rRNA PCR and quantitative PCR (qPCR) screening of gnotobiotic isolators for contamination have not been described to date.

In this study, we outline techniques, programs and conditions that we optimized for screening gnotobiotic isolators for contamination utilizing PCR and qPCR assays with templates of murine fecal DNA and universal 16S rRNA primers that detect a broad range of bacterial species, as well as molecular sequencing of the 16S rRNA amplicons to identify contaminating bacterial species. Our PCR protocol is able to detect contamination in GF animals, but not in animals that have been deliberately colonized with selected microorganisms, as amplification of the 16S rRNA gene results in one band when the PCR products are run on a polyacrylamide gel.

Therefore, to screen selectively colonized animals for bacterial contamination, we utilized Random Amplification of Polymorphic DNA (RAPD) PCR. It has been suggested that with meticulous optimization of DNA concentrations, PCR conditions and reagents, RAPD PCR can be a reliable, sensitive and reproducible assay to generate high quality genomic DNA

profiles from various bacterial strains (29). Recently, RAPD PCR has been used to profile and discriminate different strains of *Staphylococcus aureus* (30), *Bacillus cereus* (31), *Klebsiella pneumoniae* (32), *Lactobacillus paraplantarum* (33), and *Enterococcus* species (30). However, there are only a few reports of RAPD PCR being conducted on bacteria isolated from fecal samples (35), with two studies reporting the typing of *Bacillus subtilis* (36) and *Lactobacillus* species (37) from the human gastrointestinal (GI) tract using RAPD PCR.

Here we describe our application of RAPD PCR, in addition to more classic PCR methods to evaluate the gnotobiotic and GF status respectively of our experimental rodents. Gnotobiotic facilities may use these techniques to screen isolators for bacterial contamination at their own institutions, as we currently do at the National Gnotobiotic Rodent Resource Center (NGRRC) at UNC-Chapel Hill (UNC).

Results

Spectrophotometry. Following isolation of DNA from rodent fecal samples, total fecal DNA concentrations were measured using spectrophotometry (Fig. 5.1). While there were significant differences between DNA concentrations in putative GF fecal samples and spontaneously contaminated ex-GF fecal samples ($p=0.0002$), an overlap in DNA concentrations between these two groups rendered spectrophotometry insufficient for sterility screening. Differences between fecal DNA concentrations from putative GF and monoassociated or SPF mice were also statistically significant ($p<0.0001$), and we did not see any overlap with DNA concentrations obtained from GF mouse feces. When the DNA extraction protocol was run with water and no sample, DNA concentrations were between 2-7 ng/µl.

Detection of bacterial contamination of GF animals using 16S rRNA PCR. DNA isolated from GF, gnotobiotic and SPF fecal samples served as templates in PCR assays amplifying the 16S rRNA gene. We blindly screened samples obtained from nine isolators at the NGRRC with PCR. The PCR results after gel electrophoresis revealed contamination in an isolator previously thought to be GF, (Fig. 5.2A, isolator 200; lane marked with a "C" for "contaminated"), because cultures and Gram stains of fecal samples derived from mice in this isolator did not reveal the contamination. The prominent PCR band from the fecal sample DNA from the contaminated isolator was about the same size and at least as dense as those from the positive control mice that were dual-associated with *E. coli* NC101 and *E. faecalis* OG1RF, (Fig. 5.2A, isolator 158; lane marked "D" for "dual-associated"), or from mice colonized with specific pathogen-free (SPF) bacteria. The seven remaining fecal DNA samples collected from mice housed in putative GF isolators did not reveal 16S rRNA amplification (Fig. 5.2A, isolators 124, 136, 166, 168, 180, 186 and 198; lanes marked by asterisks for GF), and Gram stain and cultures of feces from animals in these isolators likewise revealed no bacterial growth. It should be noted that there is a larger, much less intense band from isolator #200 as well, although we are unsure of its origin. We speculate that it could be random amplification of bacterial or mammalian DNA. We did not see this second amplicon from any other samples shown in Figure 2 or in any samples not shown in this manuscript.

We then blindly screened 10 additional NGRRC isolators using PCR, and included samples in our assay from isolators 124 and 180 that had previously been shown with PCR to be GF, in order to show that our screening results were reproducible, and also to serve as negative controls. Fecal DNA samples derived from mice housed in four gnotobiotic isolators produced detectable amplicons using the 16S rRNA PCR assay, including two isolators that contained

experimentally monoassociated mice, (Fig. 5.2B, isolators 106 and 112; lanes marked “M” for “mono-associated”) and two ex-GF isolators that had been recently determined to be contaminated by traditional culture and Gram staining (Fig. 5.2B, isolators 100 and 196; lanes marked “C” for “contaminated”). The eight remaining fecal DNA samples collected from mice housed in putative GF isolators did not reveal visually detectable 16S rRNA amplification (Fig. 5.2B, isolators 102, 124, 134, 180, 182, 190, 194 and 202; lanes marked by asterisks for GF), and Gram stain and cultures of feces from mice in these isolators verified the lack of presence of bacteria in these animals.

Next, we blindly screened 14 mouse and two rat isolators at the Gnotobiotic Animal Core (GAC) at North Carolina State University (NCSU). Using 16S rRNA PCR, we confirmed the GF status of 15 of these isolators, (Fig. 5.2C, mouse isolators 1-3 and 5-14, and rat isolators 1-2; lanes marked by asterisks for GF), as well as the contaminated status of a known spontaneously contaminated ex-GF isolator (Fig. 5.2C, mouse isolator 4; lane marked by “C” for “contamination”). Cultures of fecal samples taken from mice in these isolators provided the same results as PCR.

qPCR quantitation of bacterial levels in experimental mice. To validate our PCR assay, we also used a qPCR assay to determine levels of bacteria in NGRRC and GAC gnotobiotic fecal samples by quantifying copies of the 16S rRNA gene per microgram of fecal DNA. We found that the 16S rRNA gene was not amplified to detectable levels in the 30 GF fecal samples that were also screened with PCR (Fig. 5.3). Meanwhile, spontaneously contaminated ex-GF samples identified by PCR, (from isolators #200, #100, and #196 from UNC and isolator #4 at NC State), SPF samples (5 samples included in PCR screening plus 5 additional samples), and selectively colonized samples (samples from dual-associated isolator

#158 and monoassociated isolators #106 and #112 at UNC shown in PCR gels, along with a sample from a fourth monoassociated isolator at UNC not screened with PCR) contained 10^7-10^8 copies of the 16S rRNA gene per microgram of fecal DNA (Fig. 5.3).

Melting curves from qPCR assays provide valuable information about the specificity of the qPCR assay. Melting curves from our qPCR assays revealed that true amplification of the 16S rRNA gene occurred at melting temperatures of 83° to 87°C (Fig. 5.4; panels b, c, d). No melting curve from GF samples is seen at these melting temperatures (Fig. 5.4; panel a). Finally, the two peaks seen in the melting curves of dual-associated fecal DNA samples (Fig. 5.4; panel c) most likely represent the individual melting curves of the 16S rRNA PCR products of DNA from the two organisms that were deliberately introduced to GF mice, *E. coli* NC101 and *E. faecalis* OG1RF. While melting curves provide information about qPCR assay specificity, they are not a reliable method to determine the number of OTUs colonizing an animal.

Chow PCR. To address the possibility that dead bacteria from autoclaved or irradiated chow may pass through the GI tract of GF animals and cause false positives when screening these animals for bacterial contamination using 16S rRNA PCR of fecal DNA, we sought to determine whether or not bacterial DNA that may or may not be present in food sources might be detectable by PCR. We tested several types of chow used in various NGRRC isolators using PCR. We did not detect the 16S rRNA gene from these samples with PCR (Fig. 5.5A) or qPCR (Fig. 5.5B) assays.

Identification of contaminating bacterial species by 16S rRNA sequencing. The bacterial species contaminating GF mice were identified by sequencing 16S rRNA gene PCR products. We were able to identify *Staphylococcus lentus* as the organism contaminating

formerly GF isolator 4 at NC State, and *Paenibacillus glucanolyticus* as the organism contaminating formerly GF isolator 100 at UNC. We also identified what may be the aerobic Gram positive rod *Bacillus simplex* as the contaminant in ex-GF isolator 196, which is included in Figure 2B, and in isolator 184, which was not included in our molecular screening. However, the % identity for these two sequences were only 94% and 95%, and coupled with the fact that one of the sequences is relatively short, we are unable to identify this particular organism with a high degree of confidence. By base pair (bp) match length, we refer to the number of bases that are shared between the sequence from the given DNA sample and the known 16S rRNA sequence of a bacterial species of note. Though weight of fecal samples and DNA concentrations are normalized and the DNA extractions are performed the same way each time with the same reagents, volumes, storage procedures, etc. we frequently see slight differences in read lengths that are probably related to the protocol and the quality of the DNA that remains at the end of purification. This explains the slightly different bp match lengths and % identity that we see for the two samples that are both presumed to be *B. simplex.* Monoassociated mice were confirmed to be colonized with *E. coli* and no contaminating organisms.

Detection of bacterial contamination in selectively colonized animals using RAPD PCR. RAPD fingerprinting revealed unique, reproducible fingerprints for DNA isolated from pure cultures of several strains of *E. coli,* as well as from several *Lactobacillus* species, *Pseudomonas* species and *Staphylococcus* species, *Klebsiella pneumoniae, Listeria monocytogenes,* and *Salmonella typhimurium* (not shown). Unique RAPD fingerprints of DNA isolated from pure cultures of *E. coli* NC101, *E. coli* K12, *E. faecalis* OG1RF, and *Bacteroides vulgatus* exhibited a high degree of similarity to fingerprints of fecal DNA from rodents monoassociated with each of these bacterial strains (Fig. 5.6A). Inoculation of *E. coli* NC101

monoassociated mice with *E. faecalis* OG1RF (and vice versa) was easily determined using this fingerprinting technique. The RAPD PCR profile of DNA isolated from *E. coli* NC101/*E. faecalis* OG1RF dual-associated mice was similar to that of DNA isolated from 50/50 and 75/25 mixtures of pure cultures of *E. coli* NC101 and *E. faecalis* OG1RF (Fig. 5.6B). The 7 bacterial strains belonging to the **si**mplified **hu**manized **mi**crobiota (SIHUMI) cocktail demonstrated unique fingerprints. Each of these fingerprints was clearly identifiable when up to 4 constituent strains were mixed. RAPD PCR fingerprints of mixtures of *E. coli* LF82, *R. gnavus* ATCC 29149, *E. faecalis* OG1RF and *B. longum* ATCC 15707 are shown in Figure 5.7.

Discussion

The current primary methods of screening at most gnotobiotic facilities are culture and Gram staining, and while the advantages of these methods are that they are fairly inexpensive and they provide instantaneous results in the case of Gram staining, more objective and sensitive molecular methods of detecting gnotobiotic contamination are needed. In this study, we describe methods to isolate DNA from fecal samples of gnotobiotic rodents and screen for contamination using PCR and qPCR assays. The strategies we have developed use PCR assays with universal 16S rRNA primers as an initial screen for gnotobiotic contamination and 16S rRNA qPCR as a means to confirm contamination by determining fecal bacterial concentrations in gnotobiotic animals. We have optimized conditions for these PCR and qPCR assays, including 10 ng DNA loading used in conjunction with 25-cycle PCR assays. Importantly, DNA isolated from chow did not amplify with these conditions nor did documented GF feces show positive results.

Using 16S rRNA PCR product sequencing, we identified an organism that may be *Bacillus simplex* contaminating two isolators previously judged to be GF. These discordant results illustrate the insensitivity and difficulty in interpretation of traditional culture and Gram stain screening methods. We validated our PCR method by blindly identifying *E. coli* that had been deliberately introduced into ex-GF isolators to monoassociate mice and also by identifying bacterial species in two isolators determined by Gram stain and/or culture results to be contaminated. Identifying contaminating species can be useful in determining the source of contamination, potentially preventing future breaches in sterility, and in investigating the biological effects or pathogenicity of a contaminating bacterial species. For example, we postulate that contamination in GAC isolator 4 by *Staphylococcus lentus*, a common skin organism, arose from a leak in a glove, while the contamination by spore formers *B. simplex* and *Paenibacillus glucanolyticus* originated from an autoclave malfunction. If multiple, unknown contaminants exist in a previously germ-free or selectively colonized isolator, cloning and sequencing of animal fecal DNA should be carried out to determine the identity of the contaminating microbes.

RAPD PCR can also assist in the more difficult detection of contamination in selectively colonized isolators. Detection of contamination in GF isolators is relatively straightforward with our proposed PCR and qPCR techniques. However, our study reveals that in mice colonized with one or two bacterial species, the microorganism(s) reach densities in the GI tract approaching that of the complex microbiota in SPF mice. Therefore, quantifying levels of fecal bacteria alone is not sufficient to determine whether or not contamination of a selectively colonized isolator has occurred. However, we have shown that RAPD PCR can be used to screen selectively colonized animals for contamination. RAPD PCR gels showing DNA from several bacterial species can be

quite complex and difficult to interpret, but we are confident that based on careful scrutiny, one can discriminate between at least 4 bacterial strains that are mixed together based on their unique RAPD fingerprints.

The advantages of using these molecular techniques compared to traditional culture and Gram stain approaches used to screen for contamination are many, including increased sensitivity in detecting anaerobic or uncultivable contaminants and more objective results that do not depend on Gram stain interpretation. These techniques also provide a definitive determination of the presence or absence of contamination, thereby preventing use of contaminated animals in scientific studies with subsequent wasted resources and results that cannot be interpreted. Finally, these methods permit the identification of contaminating bacterial species. The major disadvantages of these molecular methods are that they do not provide instantaneous results and they are performed at an increased cost compared to traditional, non-molecular methods. Because of these limitations, we recommend the continued use of Gram staining and culturing for frequent, first-line screening in gnotobiotic facilities. However, in the case of un-interpretable or inconsistent results, in a situation of high suspicion of contamination despite negative results with traditional techniques, or perhaps before conducting large or lengthy experiments, we recommend using these PCR, qPCR and RAPD PCR techniques to definitively determine the presence or absence of contamination in gnotobiotic units (Fig. 5.8).

We are currently using the PCR assay described herein at the NGRRC at UNC to routinely screen gnotobiotic isolators for contamination, with increased sensitivity and specificity compared to Gram staining and culturing performed concurrently. We screen stable breeding isolators at NGRRC every 2-4 weeks with Gram stain and culture, and slightly less frequently with PCR. However, as a general rule, the more an isolator is being used, the greater

the risk of bacterial contamination, and hence the greater the frequency of both traditional and molecular screening should be. When active investigations are ongoing, ports are being opened, animals, food, water or bedding are being imported, or agents are being injected, PCR screening should be performed. In addition, it should be kept in mind that some mucosally-associated intestinal bacteria are not shed continuously in feces, with resultant insensitive monitoring of feces for bacterial contamination. Thus, sampling frequency absolutely plays an important role in detecting contamination, whether conventional or molecular techniques are utilized for screening.

While most microorganisms in the intestine are bacteria, members of Eukarya and Archaea are also present (38). Abundant and diverse fungi have been identified in the murine intestine (39), and 0.8% of 536,112 unique genes identified in a metagenomic analysis of fecal samples taken from 124 healthy Europeans were archaeal (40). Our bacterial-specific 16S rRNA primers screened only for bacterial contamination. It may be possible to screen for eukaryotic microorganisms as well, however. Recently, methods were described for detecting fungi in complex microbial communities using specialized DNA extraction techniques and qPCR (41). Primer pairs that amplify rRNA from Archaea have also been described (42), but this is beyond the scope of this study.

In summary, we describe PCR techniques and conditions using universal 16S rRNA primers to screen for bacterial contamination of GF animals. qPCR assays with the same primers can be used to determine bacterial concentrations in respective GF animal fecal samples. Sequencing of 16S rRNA PCR products can be used to identify contaminating bacterial species to potentially determine the source of a GF contamination, or to investigate the biological effects or pathogenicity of a contaminating species. We have developed an optimal RAPD protocol that

can serve as a highly sensitive and reproducible method to screen selectively colonized gnotobiotic animals for contamination that does not require the use of specialized or expensive equipment. Finally, we suggest a cost-effective strategy to screen gnotobiotic animals for contamination by a combination of traditional and molecular methods.

Materials and methods

Experimental design (Fig. 5.9). Fresh fecal pellets were collected from rodents housed in GF, spontaneously contaminated ex-GF, and selectively colonized isolators at the NGRRC at UNC and the GAC of the Center for Gastrointestinal Biology and Diseases (CGIBD) at NCSU, and SPF rooms. The respective colonization status of each sample was not revealed to the investigator performing the analyses until after completion of the testing. Samples from all known contaminated isolators were purposefully included in the study. DNA was isolated from fecal samples and used as templates for 16S rRNA PCR and qPCR assays. Selected 16S rRNA PCR products were sequenced to identify contaminating bacterial species.

Extraction of DNA from fecal samples. DNA was extracted from fecal samples using a phenol/chloroform extraction method combined with physical disruption of bacterial cells and a DNA clean-up kit (Qiagen DNeasy Blood and Tissue Kit). Briefly, fresh fecal pellets were collected from mice and rats. Stool was weighed, normalized to 200 mg per sample, suspended in 750 µl of sterile bacterial lysis buffer (200 mM NaCl, 100 mM Tris [pH 8.0], 20 mM EDTA, 20 mg/ml lysozyme) and incubated at 37°C for 30 minutes. Next, 85 µl of 10% sodium dodecyl sulfate (Gibco) and 40 µl of 20 mg/ml proteinase K (Qiagen) were added to the mixture, which was then incubated at 65°C for 30 minutes. 300 mg of 0.1 mm zirconium beads (BioSpec Products) were added and the mixture was homogenized in a bead beater (BioSpec Products) for

two minutes. The homogenized mixture was cooled on ice and then centrifuged at 14,000 rpm for five minutes at 4°C. The supernatant was transferred to a new 1.5 ml microfuge tube and fecal DNA was further extracted by phenol/chloroform/iso-amyl alcohol and chloroform/iso-amyl alcohol, as described. Following extraction, the supernatant was precipitated by ethanol at -20°C for one hour. Precipitated DNA was suspended in DNase-free H_2O and then cleaned using the Qiagen DNeasy Blood and Tissue Kit per the manufacturer's instructions. Purified fecal DNA was eluted in 50 µl volumes. The concentration of each DNA extract was determined by spectrophotometric measurement using a Nanodrop 1000 spectrophotometer (Thermo Fisher Scientific).

Chow was removed from several gnotobiotic isolators, placed in sterile plastic bags, crushed with a hammer, weighed and normalized to approximately 200 mg per sample. DNA was then extracted using the above methods.

PCR amplification. 10 ng fecal/chow DNA templates in conjunction with the following PCR conditions resulted in optimal specificity and sensitivity: 95°C for 5 minutes, then 25 cycles of 95°C for 30 seconds, 52°C for 30 seconds, and 72°C for 45 seconds. These cycles were followed by 72°C for seven minutes. Reactions were carried out in a final volume of 25 µl containing 1 µl of DNA template, 1.5 µl $MgCl_2$, 1 µl of each primer, 2.5 U Taq polymerase (Invitrogen), 80 µM each of dATP, dCTP, dGTP and dTTP in 10 mM Tris/HCl buffer (pH 8.3), 50 mM KCl and 0.001% (w/v) gelatin. "Universal" primers were used to amplify the genes encoding 16S rRNA from all bacterial groups: Forward primer, UniF (5'-GTGSTGCAYGGYTGTCGTCA-3') and reverse primer, UniR (5'-ACGTCRTCCMCACCTTCCTC-3') (18). These Universal primer sequences are complementary to highly conserved sequences within the *E. coli* 16S rRNA gene, which is 1542

nucleotides. UniF is complementary to nucleotides 1047 through 1067, while UniR is complementary to nucleotides 1174 through 1194. Amplicons generated using these primers are 147 base pairs. PCR assays were performed in a GeneAmp PCR system 9700 thermocycler (Applied Biosystems) under various conditions to optimize results. Reaction products were stored at 4°C. Amplified products were separated on a 1% (m/v) agarose (Invitrogen) gel in Tris/acetate/EDTA buffer (40 mM Tris/acetate, 1 mM EDTA, pH 8.0) containing 0.5 μg 1% ethidium bromide. PCR products were then visualized under UV light.

qPCR assays. qPCR assays were performed using universal primers that amplify the genes encoding 16S rRNA from all bacterial groups (see above) to quantitate copies of the 16S rRNA gene per μg of fecal DNA. qPCR assays were conducted in 96-well plates on a Realplex Mastercycler thermocycler (Eppendorf) Each qPCR assay was carried out in a final volume of 12 μl and contained: 6 μl SYBR Green qPCR Master Mix (Qiagen), 0.5 μl of each primer and 1 μl of DNA template. qPCR conditions were as follows: 95°C for ten minutes, followed by 40 cycles of 95°C for 15 seconds, 60°C for 20 seconds, and 72°C for one minute. Each plate included triplicate reactions per DNA sample and the appropriate set of standards. qPCR standards were generated by PCR amplification of the purified target 16S rRNA genes from a positive control *Escherichia coli* NC101 strain used in our monoassociation studies (43). Melting curve analysis of PCR product amplification was conducted following each assay to confirm that each fluorescence signal originated from specific PCR products and not from primer-dimers or other artifacts. All qPCR plates included a "no template" negative control for each primer set.

Bacterial identification by 16S rRNA gene sequencing. We identified contaminating bacterial species by sequencing the 16S rRNA PCR products obtained from positive reactions using primers that amplify the genes encoding 16S rRNA from all bacterial groups to generate longer products for sequencing, 8F (5'-AGAGTTTGATCCTGGCTCAG-3') and 1391R (5'-GACGGGCGGTGWGTRCA-3') (18). After purifying the resulting 16S rRNA PCR products with a Qiagen clean-up kit, the products were sequenced by the UNC Automated DNA Sequencing Facility using Sanger sequencing, and the results were cross-referenced with The National Center for Biotechnology Information (NCBI) Reference Sequence (RefSeq) database (44).

RAPD PCR assays. We used a single random oligonucleotide 3H primer (5'-AAGCTTGATTGCCC-3') and optimized RAPD PCR conditions. RAPD PCR reactions were carried out in a final volume of 25 μL containing 10 ng of DNA template, 2 U of Taq Polymerase (Invitrogen, Carlsbad, CA), 1.5 μL $MgCl_2$ (50 mM), 2.5 μL primer (20 μM) and 2 μL dNTPs (Promega, 10 mM). The PCR reactions were carried out in a GeneAmp PCR system 9700 thermocycler (Applied Biosystems, Foster City, CA) using the following conditions: 95°C for 5 minutes, 36 cycles of 95°C for 1 minute, 36°C for 1 minute and 72°C for 2 minutes followed by one cycle of 72°C for 7 minutes for completion of DNA extension. PCR products were stored at 4°C. Finally, 10 μL of each amplified product was separated on a 2% (w/v) agarose (Invitrogen, Carlsbad, CA) gel in Tris/acetate/EDTA buffer (40 mM Tris/acetate, 1 mM EDTA, pH 8.0) containing 0.5 μg 1% ethidium bromide. The products were then visualized under UV light.

We generated fingerprints from cultures of 30 relevant bacterial strains. To test applicability to gnotobiotic screening, we conducted RAPD PCR assays on DNA isolated from cultures of defined intestinal bacterial species as well as fecal samples of mice monoassociated with the same respective bacterial strains. We performed RAPD PCR on fecal DNA from monoassociated mice before and after inoculation with a second bacterium. Finally, we tested RAPD PCR's ability to discern between combinations of the 7 members of the SIHUMI cocktail, *E. coli* LF82, *Ruminococcus gnavus* ATCC 29149, *Enterococcus faecalis* OG1RF, *Bifidobacterium longum* ATCC 15707, *Faecalibacterium prausnitzii* A2-165, *Lactobacillus plantarum* WCFS1, and *Bacteroides vulgatus* ATCC 8482.

REFERENCES

1. Packey CD, Sartor RB. Commensal bacteria, traditional and opportunistic pathogens, dysbiosis and bacterial killing in inflammatory bowel diseases. Curr Opin Infect Dis 2009; 22: 292-301.

2. Ivanov II, Frutos Rde L, Manel N, et al. Specific microbiota direct the differentiation of IL-17-producing T-helper cells in the mucosa of the small intestine. Cell Host Microbe 2008; 4(4): 337-49.

3. Ferreira RB, Gill N, Willing BP, et al. The intestinal microbiota plays a role in *Salmonella*-induced colitis independent of pathogen colonization. PLoS ONE 2011; 6: e20338.

4. Willing BP, Vacharaksa A, Croxen M, et al. Altering host resistance to infections through microbial transplantation. PLoS ONE 2011; 6: e26988.

5. Reeves AE, Theriot CM, Bergin IL, et al. The interplay between microbiome dynamics and pathogen dynamics in a murine model of *Clostridium difficile* infection. Gut Microbes 2011; 2: 145-148.

6. Ivanov II, Atarashi K, Manel N, et al. Induction of intestinal Th17 cells by segmented filamentous bacteria. Cell 2009; 139(3): 485-98.

7. Atarashi K, Tanoue T, Shima T, et al. Induction of colonic regulatory T cells by indigenous *Clostridium* species. Science 2011; 331(6015): 337-41.

8. Round JL, Lee SM, Li J, et al. The Toll-like receptor 2 pathway establishes colonization by a commensal of the human microbiota. Science 2011; 332(6032): 974-7.

9. Sartor RB. Microbial influences in inflammatory bowel diseases. Gastroenterology 2008; 134: 577-594.

10. Sartor RB. Genetics and environmental interactions shape the intestinal microbiome to promote inflammatory bowel disease versus mucosal homeostasis. Gastroenterology 2010; 139: 1816-1833.

11. Greenblum S, Turnbaugh PJ, Borenstein E. Metagenomic systems biology of the human gut microbiome reveals topological shifts associated with obesity and inflammatory bowel disease. Proc Natl Acad Sci U S A 2012; 109: 594-599.

12. Wang Z, Klipfell E, Bennett BJ, et al. Gut flora metabolism of phosphatidylcholine promotes cardiovascular disease. Nature 2011; 472(7341): 57-63.

13. Devkota S, Wang Y, Musch MW, et al. Dietary-fat-induced taurocholic acid promotes pathobiont expansion and colitis in $Il10^{-/-}$ mice. Nature 2012; 487(7405): 104-8.

14. Giongo A, Gano KA, Crabb DB, et al. Toward defining the autoimmune microbiome for type 1 diabetes. ISME J 2011; 5: 82-91.

15. Zupancic ML, Cantarel BL, Liu Z, et al. Analysis of the gut microbiota in the old order Amish and its relation to the metabolic syndrome. PLoS ONE 2012; 7: e43052.

16. Turnbaugh PJ, Hamady M, Yatsunenko T, et al. A core gut microbiome in obese and lean twins. Nature 2009; 457: 480-484.

17. Wallace BD, Wang H, Lane KT, et al. Alleviating cancer drug toxicity by inhibiting a bacterial enzyme. Science 2010; 330: 831-835.

18. Carroll IM, Ringel-Kulka T, Keku TO, et al. Molecular analysis of the luminal- and mucosal-associated intestinal microbiota in diarrhea-predominant irritable bowel syndrome. Am J Physiol Gastrointest Liver Physiol 2011; 301(5): G799-807.

19. Ringel Y, Carroll IM. Alterations in the intestinal microbiota and functional bowel symptoms. Gastrointest Endosc Clin N Am 2009; 19: 141-150.

20. Carroll IM, Ringel-Kulka T, Siddle JP, Ringel Y. Alterations in composition and diversity of the intestinal microbiota in patients with diarrhea-predominant irritable bowel syndrome. Neurogastroenterol Motil 2012; 24: 521-530, e248.

21. Packey CD, Ciorba MA. Microbial influences on the small intestinal response to radiation injury. Curr Opin Gastroenterol 2010; 26(2): 88-94.

22. Crawford PA, Gordon JI. Microbial regulation of intestinal radiosensitivity. Proc Natl Acad Sci U S A 2005; 102: 13254-13259.

23. Nishino R, Mikami K, Takahashi H, et al. Commensal microbiota modulate murine behaviors in a strictly contamination-free environment confirmed by culture-based methods. Neurogastroenterol Motil 2013; 25(6): 521-8.

24. Asano Y, Hiramoto T, Nishino R, et al. Critical role of gut microbiota in the production of biologically active, free catecholamines in the gut lumen of mice. Am J Physiol Gastroenterol Liver Hepatol 2012; 303(11): G1288-95.

25. Fagundes CT, Amaral FA, Vieira AT, et al. Transient TLR activation restores inflammatory response and ability to control pulmonary bacterial infection in germfree mice. J Immunol 2012; 188(3): 1411-20.

26. Patwa LG, Fan TJ, Tchaptchet S, et al. Chronic intestinal inflammation induces stress-response genes in commensal *Escherichia coli*. Gastroenterology 2011; 141(5): 1842-51.

27. Manichanh C, Borruel N, Casellas F, Guarner F. The gut microbiota in IBD. Nature Rev Gastroenterol Hepatol 2012; 9: 599-608.

28. Faith JJ, Rey FE, O'Donnell D, et al. Creating and characterizing communities of human gut microbes in gnotobiotic mice. ISME J 2010; 4(9): 1094-8.

29. Atienzar FA, Jha AN. The random amplified polymorphic DNA (RAPD) assay and related techniques applied to genotoxicity and carcinogenesis studies: A critical review. Mutat Res 2006; 613: 76-102.

30. Gutierrez D, Delgado S, Vazquez-Sanchez D, et al. Incidence of *Staphyloccus aureus* and analysis of associated bacterial communities on food industry surfaces. Appl Environ Microbiol 2012; 78: 8547-8554.

31. Kuwana R, Imamura D, Takamatsu H, Watabe K. Discrimination of the *Bacillus cereus* group members by pattern analysis of random amplified polymorphic DNA-PCR. Biocontrol Sci 2012; 17: 83-86.

32. Ashayeri-Panah M, Eftekhar F, Feizabadi MM. Development of an optimized random amplified polymorphic DNA protocol for fingerprinting of *Klebsiella pneumoniae.* Lett Appl Microbiol 2012; 54: 272-279.

33. Saito S, Kobayashi M, Kimoto-Nira H, et al. Intraspecies discrimination of *Lactobacillus paraplantarum* by PCR. FEMS Microbiol Lett 2011; 316: 70-76.

34. Martin B, Corominas L, Garriga M, Aymerich T. Identification and tracing of *Enterococcus* spp. by RAPD-PCR in traditional fermented sausages and meat environment. J Appl Microbiol 2008; 106: 66-77.

35. Martin V, Maldonado-Barragan A, Moles L, et al. Sharing of bacterial strains between breast milk and infant feces. J Hum Lact 2012; 28: 36-44.

36. Hong HA, Khaneja R, Tam NMK, et al. *Bacillus subtilis* isolated from the human gastrointestinal tract. Res Microbiol 2009; 160: 134-143.

37. Ahlroos T, Tynkkynen S. Quantitative strain-specific detection of *Lactobacillus rhamnosus* GG in human faecal samples by real-time PCR. J Appl Microbiol 2009; 106: 506-514.

38. Samuel BS, Gordon JI. A humanized gnotobiotic mouse model of host-archaeal-bacterial mutualism. Proc Natl Acad Sci U S A 2006; 103: 10011-10016.

39. Scupham AJ, Presky LL, Wei B, et al. Abundant and diverse fungal microbiota in the murine intestine. Appl Environ Microbiol 2006; 72: 793-801.

40. Virgin HW, Todd JA. Metagenomics and personalized medicine. Cell 2011; 147: 44-56.

41. Iliev ID, Funari VA, Taylor KD, et al. Interactions between commensal fungi and the C-type lectin receptor Dectin-1 influence colitis. Science 2012; 336(6086): 1314-7.

42. Chachkhiani M, Dabert P, Abzianidze T, et al. 16S rDNA characterisation of bacterial and archaeal communities during start-up of anaerobic thermophilic digestion of cattle manure. Bioresource Technol 2004; 93: 227-232.

43. Kim SC, Tonkonogy SL, Albright CA, et al. Variable phenotypes of enterocolitis in interleukin 10-deficient mice monoassociated with two different commensal bacteria. Gastroenterology 2005; 128: 891-906.

44. Pruitt KD, Tatusova T, Brown GR, Maglott DR. NCBI Reference Sequences (RefSeq): current status, new features and genome annotation policy. Nucleic Acids Res 2012; 40: D130–D135.

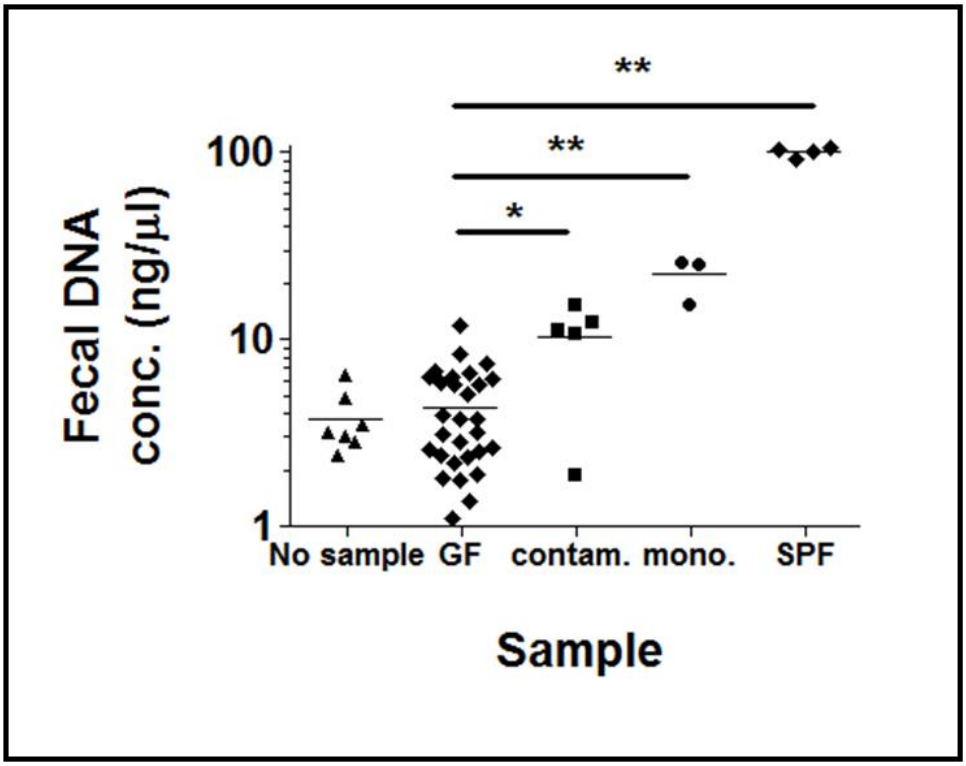

Figure 5.1. Fecal DNA concentrations as measured by spectrophotometry. The fecal DNA concentrations in putative germ-free (GF) rodents, represented by diamonds in the second lane from the left, are significantly different from fecal DNA concentrations in spontaneously contaminated ex-GF rodents (squares; middle lane). However, there was slight overlap in the respective fecal DNA concentrations between these two groups. This rendered spectrophotometry insufficient as a screening tool for bacterial GF contamination. Differences in fecal DNA concentrations between putative GF and monoassociated (circles; second from right) and specific pathogen-free (SPF) (diamonds; far right) mice were also significant. No sample=DNA extraction protocol run without sample present; contam.=spontaneously contaminated, ex-GF; mono.=monoassociated; *p=0.0002; **p=0.0001.

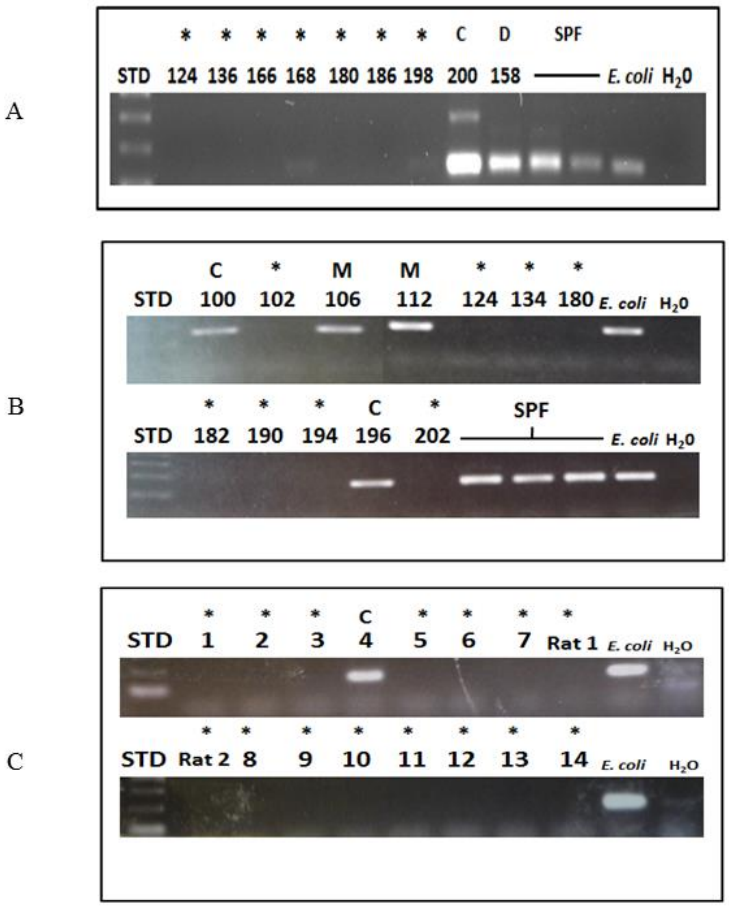

Figure 5.2. Agarose gel electrophoresis of PCR products of DNA isolated from rodent feces. (A): 8 National Gnotobiotic Rodent Resource Center (NGRRC) isolators that were thought to be GF were screened with 16S ribosomal RNA (rRNA) polymerase chain reaction (PCR) of mouse fecal DNA. Bacterial contamination was detected in isolator 200. Dual-associated mouse fecal DNA from isolator 158, SPF mouse fecal DNA and *Escherichia coli* genomic DNA served as positive controls for these PCR assays. (B): 12 NGRRC gnotobiotic isolators were blindly screened with 16S rRNA PCR of mouse fecal DNA. Fecal DNA isolated from mice from four isolators amplified: Fecal DNA from mice in isolators 106 and 112, which were subsequently revealed to be monoassociated, and fecal DNA from mice in isolators 100 and 196, which were ex-GF isolators that had been recently determined to be spontaneously contaminated. SPF mouse fecal DNA and *E. coli* genomic DNA served as positive controls for these PCR assays. (C): 14 mouse (lanes marked 1-14) and two rat (lanes marked Rat1 and Rat2) isolators at the Gnotobiotic Animal Core (GAC) of the Center for Gastrointestinal Biology and Disease (CGIBD) at North Carolina State University were blindly screened with 16S rRNA PCR of rodent fecal DNA. The GF status of 15 of these isolators was confirmed, as was the recently-contaminated status of ex-GF isolator #4. *E. coli* genomic DNA served as positive controls for these PCR assays. STD=100 base pair ladder; *=GF; C=spontaneously contaminated ex-GF; D=dual-associated; *E. coli=E. coli* genomic DNA; H20=water negative control template; M=monoassociated.

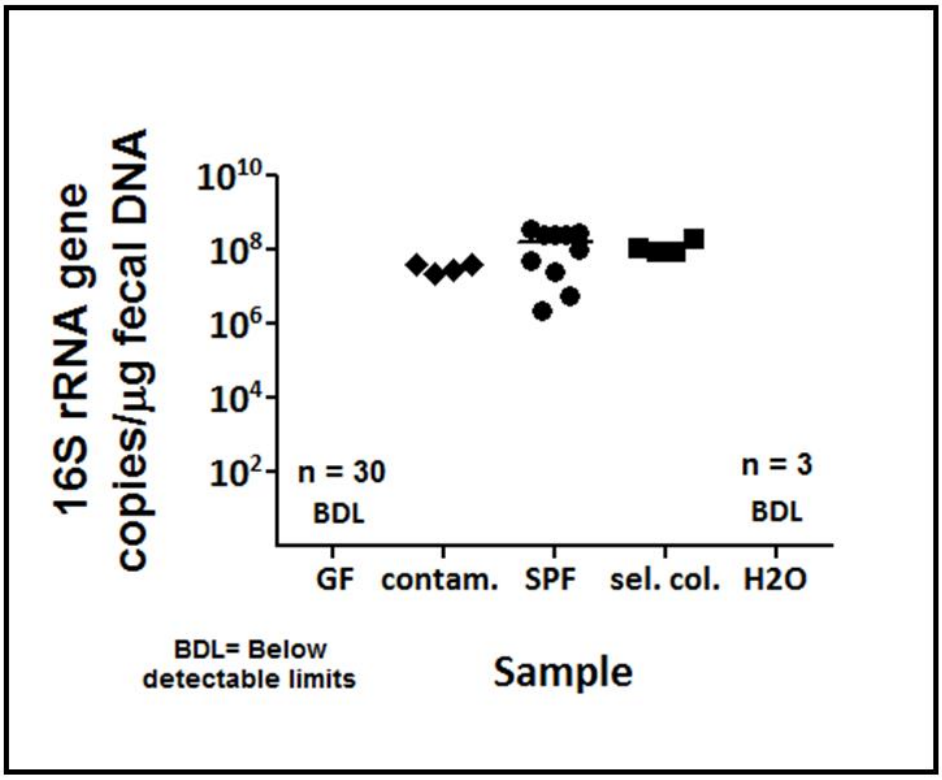

Figure 5.3. Bacterial levels in gnotobiotic rodent fecal samples determined by qPCR. Quantitative PCR (qPCR) assays were utilized to determine bacterial levels in gnotobiotic fecal samples by quantitating copies of the 16S rRNA gene per microgram of fecal DNA. The 16S rRNA gene was not amplified to detectable levels in GF mice (n=30). There were on the order of 10^{7}-10^{8} copies of the 16S rRNA gene per microgram of fecal DNA in spontaneously contaminated ex-GF mice (n=4), SPF mice (n=10), and selectively colonized mice (n=4). BDL=below detectable limits; contam.=contaminated ex-GF; sel. col.=selectively colonized; H20=water negative control template.

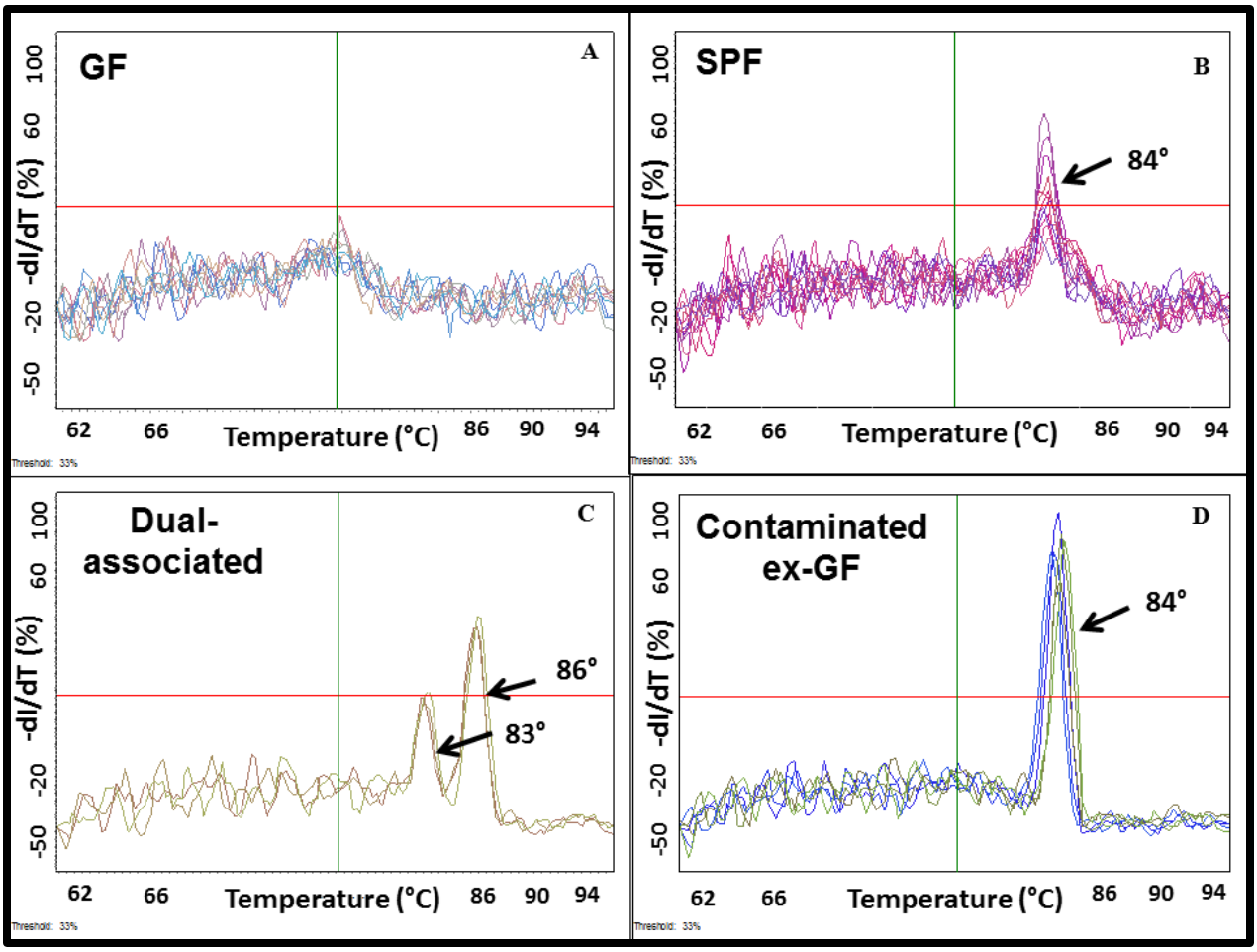

Figure 5.4. 16S rRNA qPCR melting curves from gnotobiotic and SPF mouse fecal DNA. Melting curves from qPCR assays reveal that true amplification of the 16S rRNA gene occurs at melting temperatures of 83° to 87°C (B-D). No amplification from GF mouse fecal DNA is seen at these melting temperatures (A).

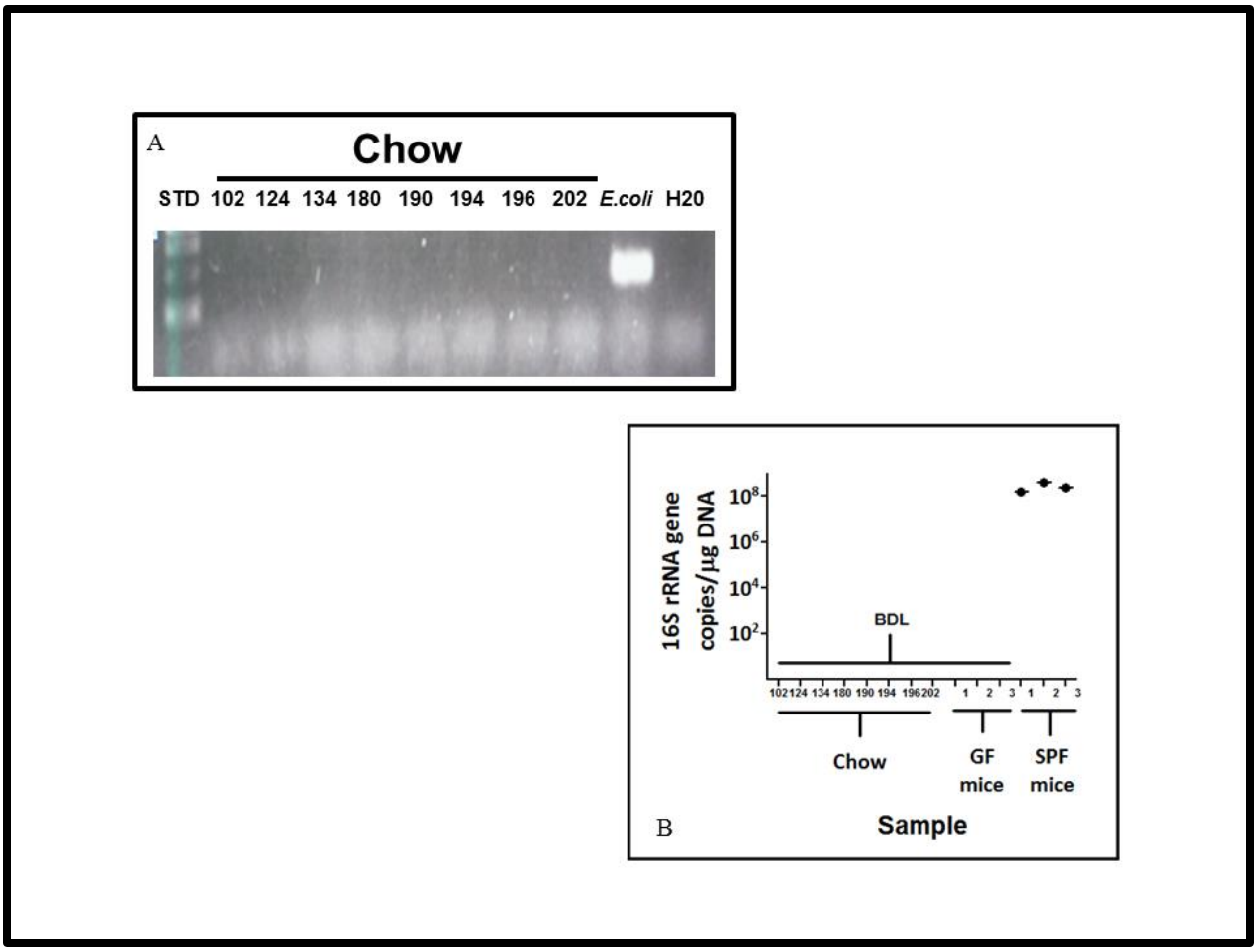

Figure 5.5. PCR and qPCR screening of animal chow for bacterial DNA. DNA was isolated from several types of chow used in various NGRRC isolators, and there was no detectable amplification from these samples with 16S rRNA PCR (A) or qPCR (B). *E. coli* genomic DNA served as a positive control for the PCR assay.

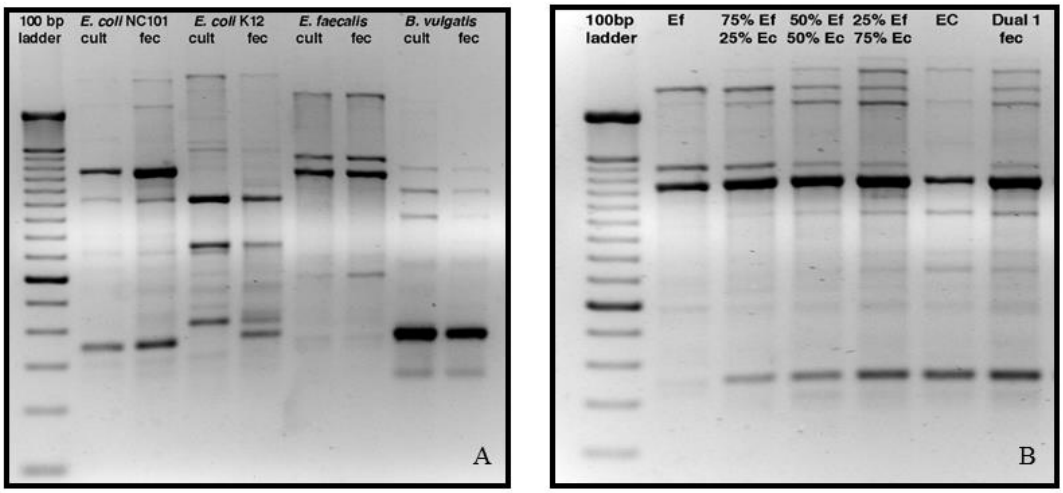

Figure 5.6. Distinguishing different individual bacterial strains by RAPD PCR fingerprints. (A) Unique rapid amplification of polymorphic DNA (RAPD) fingerprints of DNA isolated from pure cultures of *E. coli* NC101, *E. coli* K12, *Enterococcus faecalis* OG1RF, and *Bacteroides vulgatus* exhibited a high degree of similarity to fingerprints of fecal DNA from rodents monoassociated with each of these bacterial strains. (B) Inoculation of *E. coli* NC101 monoassociated mice with *E. faecalis* OG1RF (and vice versa) was easily determined using RAPD PCR. The 2nd lane from the left shows RAPD PCR products from DNA isolated from pure culture of *E. faecalis.* The second lane from the right shows RAPD PCR products from DNA isolated from pure culture of *E. coli.* Lanes 3, 4 and 5 show mixtures of RAPD PCR products of *E. faecalis* and *E. coli* pure culture DNA. The 50/50 mixture of *E. faecalis* and *E. coli* DNA RAPD PCR products in lane 4 matches the fingerprint of DNA isolated from *E. faecalis/E. coli* dual-associated mice, shown in the far right lane. Lanes 3 and 5 show RAPD PCR profiles of DNA isolated from 75/25 mixtures of *E. faecalis/E. coli* and *E. coli/E. faecalis*, respectively. Cult=pure culture DNA; fec=fecal DNA; Ef=*Enteroccous faecalis* pure culture DNA*;* Ec=*E. coli* pure culture DNA.

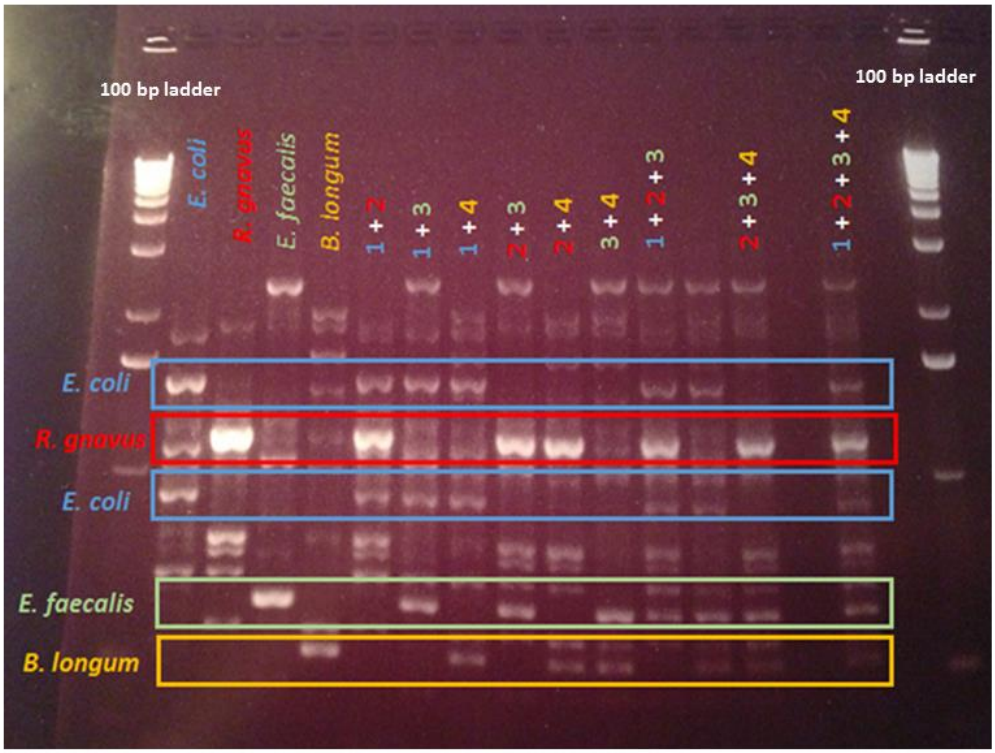

Figure 5.7. Distinguishing different bacterial strains in complex microbial communities using RAPD PCR. The 7 bacterial strains belonging to the SIHUMI cocktail demonstrated unique fingerprints. Each of these fingerprints was clearly identifiable when up to 4 constituent strains were mixed. From left to right after the ladder on the left side, *E. coli* (blue), *Ruminococcus gnavus* (red), *E. faecalis* (green) and *Bifidobacterium longum* (orange) are shown, followed by combinations of two, three or four of the respective strains. Unique bands for each bacterium are highlighted by appropriately colored boxes, including two bands that are unique to *E. coli.*

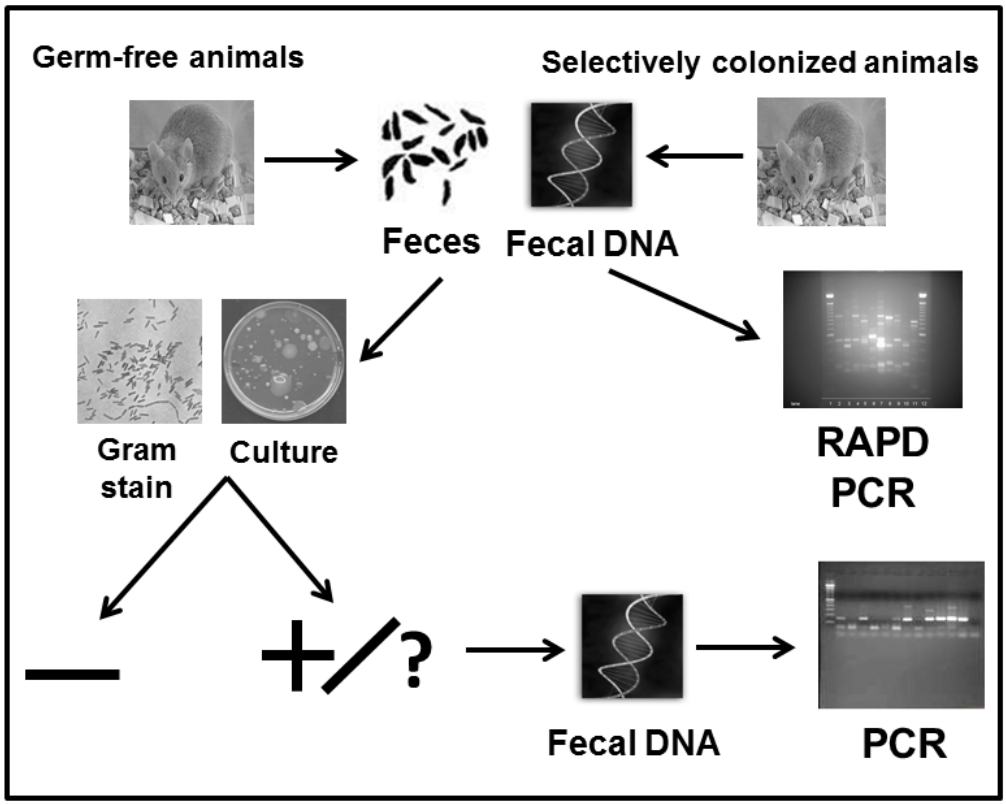

Figure 5.8. Gnotobiotic unit contamination screening algorithm. The continued use of inexpensive Gram staining and culturing for weekly detection of bacterial contamination of GF animals is recommended. However, when Gram stain or culture results are difficult to interpret or inconsistent, isolator portals are opened, a compromise in a glove, sleeve, or isolator wall occurs, an autoclave malfunction is diagnosed, or a large scale experiment is planned, it is recommended that these PCR and qPCR techniques be used to definitively determine the presence or absence of contamination in GF units. RAPD PCR can be used to screen selectively colonized animals for contamination.

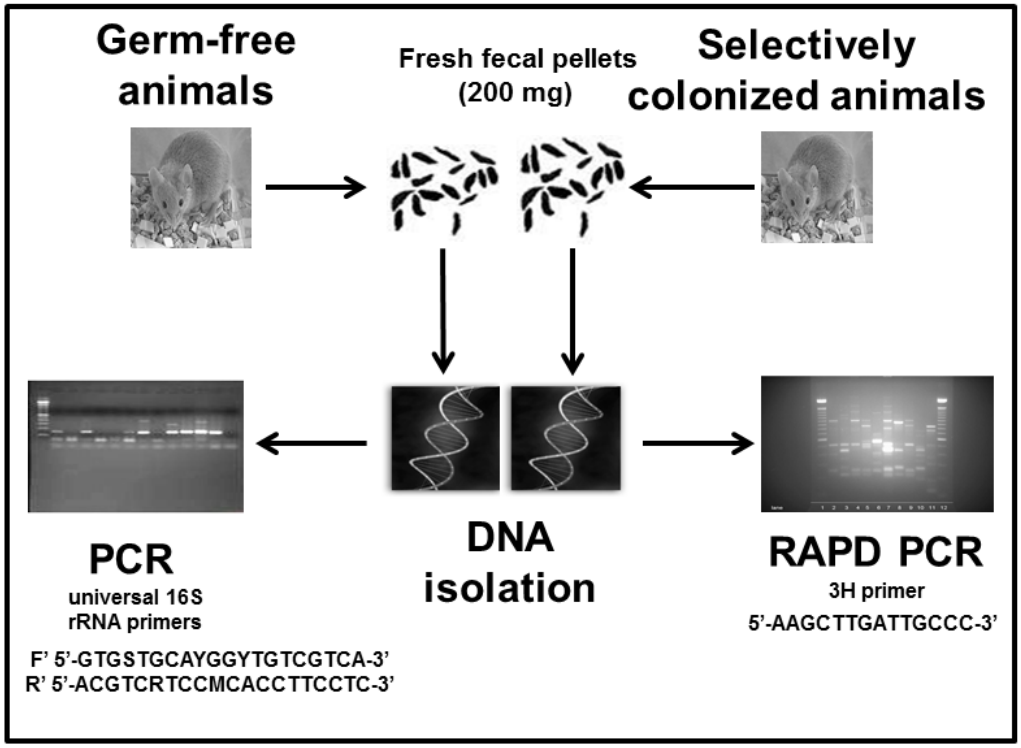

Figure 5.9. Experimental design. DNA was isolated from GF rodent fecal samples and used as templates for PCR assays using universal bacterial 16S rRNA primers. DNA was similarly isolated from selectively colonized rodent fecal samples and used as templates for RAPD PCR assays.

CHAPTER 6: RECIPROCAL HOST-MICROBIAL INTERACTIONS MEDIATE THE RADIATION GASTROINTESTINAL SYNDROME[6]

Introduction

"Radiation gastrointestinal (GI) syndrome", characterized by epithelial apoptosis with breaches in the small intestinal and colonic mucosa, translocation of commensal intestinal bacteria and sepsis, can ensue following nuclear power plant accident, terrorist attack, space exploration, medical error, or appropriately fractionated dosing of therapeutic radiation in people whose tissues are radiosensitive (1). 70% of all cancer patients receive radiation as a component of their disease treatment, and radiotherapy plays a central role in 25% of all cancer cures (2). However, 80% of patients who receive therapeutic radiation experience side effects associated with acute radiation enteropathy, and 10-21% experience severe acute intestinal toxicity necessitating cessation of treatment (1). Concomitant chemotherapy can improve survival, but increases intestinal toxicity risk. The rapidly proliferating mucosal lining of the intestinal tract is highly radiosensitive, and epithelial cell apoptosis results in abdominal pain, nausea, vomiting and diarrhea. Yet, the pathophysiology of the radiation GI syndrome is poorly understood, few therapeutic strategies exist, and there is no FDA-approved treatment (1).

The human intestinal mucosa constantly contacts a complex microbial community or "microbiota" that contains up to 100 trillion (10^{14}) microorganisms belonging to more than 1,000 "species-level" phylotypes (3). Most of these phylotypes are bacteria belonging to just a few

[6] This chapter is part of the following manuscript currently being prepared for submission: Packey CD, Maharshak N, Shanahan MT, Jobin C, Keku TO, Plevy SE, Carroll IM, Sartor RB. Reciprocal host-microbial interactions mediate the radiation gastrointestinal syndrome.

phyla (4). The commensal gut microbiota provides many crucial functions to the host, including influencing the development and maintenance of a healthy immune system (5). While the composition of the adult intestinal microbiota is relatively stable, it undergoes dynamic changes in response to certain environmental factors (6). Dysbiosis, the deviation of a microbial community from its normal state, may be associated with functional changes in the host that predispose to disease development (7). Changes in the composition of the enteric microbiota have been associated with a number of diseases including inflammatory bowel diseases (IBD), diabetes mellitus, obesity, asthma, and allergic, cardiovascular and neurologic disorders (8).

To date, studies exploring the pathogenesis of radiation intestinal injury have predominantly focused on responses of the host intestinal epithelium (9), endothelium (10), or both (11). The role of the microbiota has received considerably less attention. However, host intestinal radiation responses have been linked to bacterial component-stimulated innate signaling pathways (12, 13). Investigations that clarify how intestinal microbial populations impact radiation enteropathy are badly needed (1), as results can direct studies to identify antibiotics, probiotics, prebiotics and bacterial-derived peptides and byproducts that improve normal tissue radioresistance. We used gnotobiotic mice to demonstrate that commensal microbiota facilitate intestinal epithelial cell (IEC) homeostatic mechanisms early in the radiation response, but later contribute to the pathogenesis of the radiation GI syndrome. We subsequently employed several molecular 16S ribosomal RNA (rRNA)-based techniques to characterize the kinetics of a profound radiation-induced dysbiosis in mucosal and luminal communities in several regions of the small intestine and colon, and to show that these microbiota compositional shifts were largely independent of inflammation and dietary changes. Cecal content transplantation and selective colonization experiments in germ-free recipients

demonstrated that intestinal dysbiosis and *Escherichia coli* directly impact the host response to radiation. Finally, we showed that commonly used probiotic and antibiotic treatments confer protection from the radiation GI syndrome by inducing small intestinal antimicrobial peptides (AMPs) and/or promoting eubiosis.

Results

The enteric microbiota are necessary for early death from the radiation GI syndrome, yet contribute to homeostatic intestinal epithelial cell radiation responses. Germ-free (GF) mice had lower clinical scores and prolonged survival compared to specific pathogen-free (SPF) mice following exposure to 15 Gy (Fig. 6.1a). 15 Gy is the radiation dose that universally causes the GI syndrome in mice bred and housed in our facilities (Supplementary Fig. 6.1a, b). To assess the contribution of the microbiota to host IEC radiation responses, we exposed GF and SPF mice to 15 Gy total body irradiation and compared the number of apoptotic and proliferating IECs in jejunal and cecal crypts at 0, 6, and 24 hours after irradiation. These time points were selected based on our time course studies evaluating radiation-induced IEC apoptosis (Supplementary Fig. 6.1c, d) and proliferation (Supplementary Fig. 6.1e) in SPF mice.

SPF mice showed fewer apoptotic IECs than GF mice, in the jejunum (Fig. 6.1b) and in cecal crypts (Fig. 6.1c), at 6 hours post 15 Gy, as assessed histologically. Bromodeoxyuridine (BrdU) immunohistochemistry (IHC) revealed that SPF mice also had more robust IEC proliferative responses than GF mice at 6 hours after radiation, both in the jejunum (Fig. 6.1d) and cecum (Supplementary Fig. 6.1f).

Radiation induces profound intestinal dysbiosis. To test the hypothesis that radiation induces a dysbiosis of the commensal microbiota that could contribute to the pathogenesis of the

radiation GI syndrome, we determined mucosal and luminal bacterial composition at three different locations of the small intestine and colon of untreated or radiation-exposed mice using 16S rRNA-based 454 pyrosequencing. First, we calculated and compared average weighted and unweighted UniFrac distances. A global analysis of complex bacterial communities from the mucosa of the small intestine and colon of healthy control mice and mice exposed to radiation indicated that radiation profoundly affected intestinal bacterial community structure (Fig. 6.2a). Separate clustering between bacterial communities in healthy control mice and mice exposed to radiation was seen in the jejunum mucosa, cecum mucosa, cecum lumen, and distal colon mucosa (Fig. 6.2c, d, e, f; Supplementary Fig. 6.2a). Comparison of average UniFrac distances, or β-diversity, showed a significant increase in mice exposed to radiation compared to unexposed mice, in the small intestine, cecum and distal colon (Fig. 6.2b), indicating that the microbiota of irradiated mice are more dissimilar to each other. Hierarchial clustering on operational taxonomic units (OTUs) revealed that samples clustered separately based on exposure to radiation or lack thereof, in the jejunum mucosa, cecum mucosa, cecum lumen, and distal colon mucosa (Supplementary Fig. 6.2b). Fecal bacterial communities from mice exposed to radiation also clustered separately from those of healthy control mice by terminal-restriction fragment length polymorphism (T-RFLP) analysis (Supplementary Fig. 6.2c), a complementary fingerprinting method. Finally, we assessed bacterial richness, or α-diversity, by OTU rarefaction and found that richness was higher after radiation in the cecum mucosa, cecum lumen and distal colon mucosa and lower in the jejunum mucosa (Supplementary Fig. 6.2d). Increases in both β-diversity and α-diversity after radiation implicate that the intestinal microbiota are more variable in evenness and composition among irradiated mice. Collectively, these results demonstrate that

a profound intestinal dysbiosis ensued in the small intestine and colon of mice following radiation exposure.

Radiation exposure results in decreased abundance of intestinal Firmicutes and increased Proteobacteria concentrations. To evaluate the effect of radiation on the abundance of specific members of the gut microbiota, we utilized deep sequencing and quantitative PCR (qPCR) to determine the number of different bacterial groups in each intestinal sample by using 3% dissimilarity between 16S rRNA gene sequences as an indicator of a "species level" OTU. The abundance of key intestinal bacterial taxa, ranging from phylum to species and identified by 16S rRNA V1-V3 region OTU sequence alignments, differed between healthy control mice and mice exposed to radiation. At the phylum level, radiation exposure significantly increased levels of intestinal Proteobacteria, with concomitant decreases in members of Firmicutes (Fig. 6.3a, Supplementary Fig. 6.3a, b, c). Intestinal *Escherichia coli*, a representative Proteobacteria member, increased following radiation, as shown by qPCR (Fig. 6.3b) and 454 pyrosequencing (data not shown). In contrast, members of the *Lactobacillus* genus were decreased in the small intestine and colon following radiation, as shown by 454 pyrosequencing (Fig. 6.3c) and confirmed by qPCR (Fig. 6.3d). The majority of *Lactobacillus* species in the C57BL/6 mouse gut were *Lactobacillus reuteri*; this species was almost eradicated 5 days following radiation exposure (Fig. 6.3e). Importantly, we showed that radiation-induced shifts in key intestinal bacterial groups, including *E. coli* and *Lactobacillus* species, occur within the first 24 hours, days before maximal epithelial injury and sepsis ensue (Supplementary Fig. 6.3d). In addition, radiation suppresses appetite. Therefore, we showed that dysbiosis following radiation is largely independent of reduced dietary intake by describing significant shifts in members of the commensal microbiota 48 hours after radiation but negligible shifts in *E. coli* (Supplementary

Fig. 6.3e) and *Lactobacillus* species (Supplementary Fig. 6.3f) in cage-mate littermates 48 hours after initiation of severe dietary restriction.

The intestinal microbiota composition directly impacts clinical responses to radiation. After determining that radiation induces an intestinal dysbiosis, we sought to establish whether these compositional changes in the microbiota are primary events that drive the radiation GI syndrome. Recent studies have shown that colitis (14) and susceptibility to chemical-induced colitis (15) can be transmitted with transfer of microbiota alone. To investigate whether changes in the gut microbiota are a cause or consequence of the radiation GI syndrome, we transplanted freshly obtained 1) post-irradiation cecal contents or 2) healthy control cecal contents into GF recipient mice to preserve the complex composition of the transferred organisms. In these studies, any gut microbial dysbiosis present in the host would be transferred to the recipient (14). The transplanted post-irradiation microbiota conferred accelerated onset of radiation-induced morbidity and mortality compared to transplanted microbiota from healthy control mice (Fig. 6.4a). This suggests that altered gut microbiota observed in mice exposed to irradiation contribute to the development of the radiation GI syndrome. When this experiment was repeated with SPF recipient mice, we observed similar results (data not shown). Next, we compared radiation responses of GF mice selectively colonized with selected species that are increased following radiation. *E. coli* mono-associated mice had increased morbidity and accelerated mortality compared to GF mice after 15 Gy; *Enterococcus faecalis* mono-associated mice exhibited intermediate susceptibility to the GI syndrome (Fig. 6.4b). These results indicate that individual constituents of the intestinal microbiota differentially contribute to the pathogenesis of the radiation GI syndrome.

The antibiotic ciprofloxacin promotes eubiosis and mitigates the radiation GI syndrome. Because antibiotics modulate microbiota composition, we tested the ability of several clinically-relevant antibiotics and antibiotic combinations to alter the radiation phenotype. One of the tested antibiotics, the fluoroquinolone ciprofloxacin (cipro), mitigated radiation intestinal injury, prolonged survival (Fig. 6.5a), and prevented radiation-induced dysbiosis in the small intestine and colon (Fig. 6.5b). Cipro attenuated radiation-induced increases in Proteobacteria and decreases in Firmicutes (Fig. 6.5c). Proliferation of intestinal *E. coli* following radiation was prevented by cipro administration (Fig. 6.5d, e), as were other alterations in the microbiota composition. Cipro also prevented increases in microbial diversity in the cecum and colon (data not shown).

The probiotic VSL#3 induces antimicrobial peptide expression and confers protection from the radiation GI syndrome. Combination probiotic VSL#3 treatment reduced the incidence and severity of radiation-induced diarrhea in one double-blind, placebo-controlled trial (16). Therefore, we tested efficacy of protection and mechanisms by which VSL#3 may confer radioprotection using our mouse model. Administration of VSL#3 significantly reduced the severity of colitis in mice exposed to lethal irradiation (Fig. 6.6a) and prolonged survival (Fig. 6.6b). Radiation reduced jejunal and ileal expression of α-defensins, small intestinal Paneth cell-specific AMPs, both at the mRNA (Fig. 6.6c) and protein (Fig. 6.6d, Supplementary Fig. 6.4) levels. This may be related to excessive radiation-induced apoptosis in the crypt cell positions of the Paneth cells in the small intestine (Supplementary Fig. 6.5). VSL#3 induced α-defensin expression in the jejunum and ileum (Fig. 6.6e), and also promoted eubiosis (Supplementary Fig. 6.6a, b, c).

Discussion

Our study shows the presence of a pathogenetically important enteric dysbiosis in the radiation GI syndrome and demonstrates that commensal bacteria have both protective and deleterious roles in this condition. Protective roles include attenuation of apoptosis and enhancement of proliferative responses of IECs in the first 6-24 hours after radiation exposure, which augment previous observations that the microbiota protect against acute dextran sodium sulfate (DSS) and radiation-induced intestinal injury through toll-like receptor (TLR) and NF-κB-mediated pathways (13, 17, 18). Commensal microbiota subsequently contribute to later onset radiation-induced mortality through sepsis, consistent with observations by Crawford and Gordon (19).

Radiation-induced alterations in the small intestinal and colonic microbiota mimic those seen in IBD (Supplementary Table 6.1), as demonstrated by high throughput sequencing and validated by qPCR. Both inflammation (20) and diet (21) can alter the composition of the intestinal microbiota. We show that radiation induces dysbiosis within the first 24 hours after exposure, days before inflammation ensues histologically or as measured by intestinal secretion of inflammatory cytokines, and the dysbiosis is independent of reduced dietary intake, which can occur following radiation exposure secondary to appetite suppression.

Numerous reports submit that perturbing the gut ecosystem results in dynamic changes in which species that are well adapted to changed environment (22) or perturbation in general (23) flourish. We identify three species within the Proteobacteria phylum that have been associated with IBD, *E. coli, Klebsiella pneumoniae* (24), and *Pseudomonas fluorescens* (25), that bloom in the intestine following radiation. Our selective colonization experiments demonstrate that

commensal *E. coli* directly impact the host radiation phenotype, more so than an *E. faecalis* strain. This is important since specific bacterial subsets can selectively induce experimental colitis in mice, whereas other subsets do not (26), and individual commensal bacteria can cause intestinal inflammation in an age- and site-specific manner (27).

The ratio of pathogenic to protective enteric species is considered an important determinant of intestinal inflammation versus homeostasis. We demonstrated that not only does radiation exposure enrich Proteobacteria species, but also leads to diminished levels of *Lactobacillus reuteri* and *Bifidobacterium* species, bacteria that possess established anti-inflammatory properties in the gut and are decreased in human IBD (28, 29). Within the Firmicutes phylum, members of the *Clostridium coccoides* subgroup were also significantly decreased following radiation. These colonic regulatory T cell-inducing bacteria (30) are also less abundant in IBD patients than in healthy subjects (31). It has been proposed that loss of *Faecalibacterium prausnitzii*, a Firmicute whose low abundance is linked to postoperative relapse of Crohn's disease (32), is an important determinant of intestinal disease activity, but levels of this bacterium were not altered in irradiated mice.

Three known "autobionts," commensal bacteria that directly influence host immune cell homeostasis or function (5), were among the most significantly altered intestinal species following radiation. *Bacteroides fragilis*, a species that expresses a protective membrane polysaccharide that stimulates IL-10-producing Foxp3+ regulatory T cells (33) and that is increased in IBD patients (34), was more prevalent following radiation. Conversely, bacteria that induce regulatory T cell (*C. coccoides*) (30) and Th17 cell (SFB) (35) differentiation were decreased. Finally, we describe both increased bacterial β-diversity (diversity between groups) and α-diversity (diversity within a group), in the cecum and colon following radiation. Increased

vaginal bacterial diversity has been associated with disease in that location (36), although decreased diversity of commensal microbiota typically accompanies active IBD (31). Understanding microbial diversity is important because high species diversity can enhance ecosystem functioning (37), although higher diversity does not always have this effect (38). Increased bacterial diversity following radiation could be part of host and/or microbial compensatory responses.

Our cecal content transplantation to gnotobiotic animals demonstrated that dysbiotic microbiota predisposes mice to accelerated death from the radiation GI syndrome. Importantly, our data verify that the radiation GI syndrome is caused by bacteria found in healthy hosts. These results may facilitate the ability to predict radiation induced-injury based on microbiota composition, and provide a rationale for restoring normal microbiota with specific interventions to prevent injury or reestablish health in patients receiving therapeutic radiation or in people accidentally exposed to radiation. While transplantation of feces from normal subjects treats *Clostridium difficile* infection (39) and may treat radiation enteropathy based on our data, we identified an antibiotic, ciprofloxacin, and a combination probiotic, VSL#3, that mitigate the radiation GI syndrome in mice by promoting eubiosis, precluding the need for intestinal content transplantation. We propose that VSL#3 promotes eubiosis and protects the host from the radiation GI syndrome by stimulating expression of α-defensins, Paneth cell-produced AMPs that are impaired in IBD (40). Since other AMPs promote the spatial segregation of the intestinal microbiota (41), α-defensins could regulate microbiota composition and protect against mucosal bacterial translocation.

The presence of major microbial clustering patterns at body sites including the GI tract (42) provides new ways to classify disease risk based on microbiota composition. Substantial

progress has been made in developing the tools for inquiry and in defining overarching concepts, but studying model animal systems with strong phenotypes is essential to advance this field (8). We have identified qualitative and quantitative kinetic changes in specific bacterial components of the gut microbiota following radiation in biologically-important mucosal and luminal compartments along the longitudinal axis of the small intestine and colon. This comprehensive spatial and temporal information will help guide region-specific clinical trials and inform personalized medicine (42) based on individual microbial profiles. Our species-level characterization of the intestinal bacterial communities following radiation facilitates future studies using techniques such as metagenomic sequencing and metabolomics that will describe the functional diversity in these communities.

There is an immediate need to develop easily administered radioprotectants or mitigators with few side effects for first responders at nuclear accidents (43) and for astronauts on long-term space missions. Development of intestinal radioprotectants has primarily focused on antioxidants (44), modifiers of inflammation (45), growth factors (46), and regulators of IEC apoptosis (47), and has generated very modest results to date. Our results indicate that selectively manipulating the intestinal luminal and/or mucosal microbiota holds promise for preventing and treating radiation intestinal injury in humans. Our mouse model avoids limitations of human investigations by standardizing the diet during sampling and accessing microbiota in proximal intestinal regions. This approach can identify tractable therapeutic manipulations for countermeasures against accidental or therapeutic radiation exposure. These results may also have important implications for cancer therapy by limiting healthy tissue toxicity, thereby improving radiation efficacy and survival rates as well as potentially impacting radiation sequelae such as fibrosis, ulcerations, fistulas, obstruction or perforation. However, death from

radiation is complicated, involving failure of multiple organs (43), so optimal radiation countermeasures will require combined approaches, including ones that target the intestinal microbiota.

Materials and Methods

Animals and Animal Care. *Conventionally raised specific pathogen-free (SPF) mice:* Wild-type (WT) mice on a C57BL/6 (B6) background were purchased from Jackson Laboratories (Bar Harbor, Maine), bred for multiple generations and maintained in microisolator cages (five mice per cage) in the same temperature and light-controlled SPF room at the University of North Carolina-Chapel Hill (UNC), matched for gender, and used for experiments at 8 to 12 weeks of age. Mice were negative for all *Helicobacter* species. To avoid confounding cage effects on microbiota composition and diversity, we selected mice from multiple litters that were housed in separate cages.

Germ-free (GF) mice: WT B6 mice originally derived in sterile conditions by embryo transfer were maintained in GF conditions at the National Gnotobiotic Rodent Resource Center at UNC. Isolator contamination absence was confirmed by Gram stain, aerobic/anaerobic fecal cultures and 16S rRNA (16S) PCR. All mouse experiments were approved by the UNC Institutional Animal Care and Use Committee.

Radiation Gastrointestinal Syndrome Model. Non-anesthetized mice were exposed to a single dose of external beam total body irradiation (TBI) using XRad320 x-ray machine (Precision X-Ray, North Branford, CT; Filter: 4 mm Cu; 47 cm; 320 kV/s, 12.5 mA; 1.0 Gy/min). 4 mice were irradiated at a time in a pie cage (Braintree Scientific, Braintree, MA). For gnotobiotic experiments, a pie cage with an autoclaved filter top (Braintree Scientific) was used

to maintain sterility. Daily water consumption was measured, and clinical scores (0-12) were given daily for the duration of experiments, consisting of 0-4 each for weight loss, stool consistency and GI bleeding. Upon experiment termination, tissues were dissected for analysis. Survival was calculated by the Kaplan-Meier method.

Histology and Immunohistochemistry. Animals were euthanized and the entire jejunum and cecum were harvested, cut longitudinally, washed, formalin-fixed for 24 hours, paraffin-embedded, cut and stained with hematoxylin and eosin (H&E) or bromodeoxyuridine (BrdU) using a standard protocol after heat-mediated antigen retrieval. (Mice were injected intraperitoneally with 120 mg/kg BrdU [Sigma-Aldrich, St. Louis, MO] 2 hours before death.) IEC apoptosis and proliferation were quantitated on a cell positional basis by light microscopic analysis of 50 half-crypts/mouse (48), using H&E and BrdU IHC, respectively. All crypts chosen were >20 cells in height, with cell position 1 located at the crypt base. Scoring was performed by 2 blinded investigators, including a pathologist.

Bacterial Composition Analyses. *Extraction of Genomic DNA and Bacterial 16S rRNA Amplification*: Bacterial genomic DNA was isolated from feces, intestinal mucosa and luminal contents using a phenol-chloroform extraction method combined with physical disruption of bacterial cells and a DNA clean-up kit (DNeasy blood and tissue extraction kit, Qiagen, Valencia, CA), as previously described (57). DNA was quantitated using a Nanodrop 2000c spectrophotometer (Thermo/Fisher Scientific, Waltham, MA) and used to PCR amplify the V1-V3 (forward, 8F: 5'-AGAGTTTGATCMTGGCTCAG-3'; reverse 518R: 5'-ATTACCGCGGCTGCTGG-3') hypervariable regions of the 16S gene. Forward primers were tagged with unique 10 base pair barcode labels at the 5' end along with the adaptor sequence (5'-CCATCTCATCCCTGCGTGTCTCCGACTCAG-3') to allow multiple samples to be included

in a single plate as previously described (49, 50). 16S PCR products were quantified, pooled, and purified for sequencing.

454 FLX Sequencing and Taxonomic Analysis: Sequencing was performed on a 454 Life Sciences Genome Sequencer FLX machine (Roche, Florence, SC) at the UNC Microbiome Core (http://www.med.unc.edu/microbiome). 16S sequence data was processed by the quantitative insights into microbial ecology (QIIME) pipeline (51). Briefly, sequences were assessed for quality and those that were <200 or >1000 base pairs in length or that contained incorrect primer sequences or more than one ambiguous base were discarded. Remaining sequences were assigned to groups based on their unique nucleotide barcodes, including error correction (49). Sequences were clustered into operational taxonomic units (OTUs) based on 97% sequence similarity (similar to species level) using BLAST (52) with the Greengenes reference database (53).

We used taxon and phylogenetic-based analyses to compare 16S gene sequences. Taxon-based: The means and standard deviations of abundances of bacterial groups (phylum, class, order, family, and genus) were calculated and compared between groups of mice. α-diversity was assessed and rarefaction curves were generated for each experimental group that measured the distribution of bacterial taxa richness. β-diversity used unweighted and weighted UniFrac distances (54-56) to generate principal coordinate plots for each sample that visualized the similarities or dissimilarities between sample groups. Phylogenetic-based: Phylogenetic trees were generated with QIIME (51) by subjecting data to weighted and unweighted UniFrac analysis. UniFrac distances represent the branch length fraction that is shared by any two sample communities in a phylogenetic tree built from 16S sequence data from all samples (54-56).

UniFrac distances were compiled into matrices and average UniFac distances were calculated for each group and compared using a Student's *t*-test.

16S rRNA Gene Quantitative Polymerase Chain Reaction: All assays were performed in 96 well plates (Eppendorf, Hauppauge, NY) with appropriate standards, duplicate/triplicate reactions per sample and "no template" negative controls on an Eppendorf Realplex^2 mastercycler thermocycler using SYBR Green PCR master mix (Applied Biosystems/Life Technologies, Grand Island, NY). Each PCR was carried out in a final volume of 25 µl. Standards were generated by PCR amplification of target sequences from appropriate positive control strain genomic DNA. Standard curves were generated for each bacterial group and used to enumerate copy number in individual samples utilizing appropriate bacterial primer sequences (Supplementary Table 6.2). Fold change was calculated using the ΔΔCt method relative to universal 16S.

Terminal-Restriction Fragment Length Polymorphism: The 16S gene was PCR amplified using fluorescently labeled universal primers, as previously described (57). Purified products were digested with *Hae* III, (and separately with Msp I), to generate terminal-restriction fragments (T-RFs) that were separated by capillary electrophoresis on a genetic analyzer (model 3100; Applied Biosystems). T-RF size and abundance data were generated using GeneMapper software (Applied Biosystems), compiled into a matrix (Sequentix, Germany), standardized and compiled into a Bray-Curtis similarity matrix using PRIMER version 6 software (Primer-E, Ivybridge, UK), as previously described (57). Data were subjected to hierarchical cluster analysis followed by analysis of similarity (ANOSIM), multidimensional scaling plots were constructed to illustrate similarity/dissimilarity, and biodiversity of each sample was measured by Shannon-

Weiner diversity index. Student's *t*-tests assessed differences in richness or diversity between groups.

Microbiota Transplantation, Selective Colonization, Antibiotic and Probiotic Treatment Experiments. *Cecal Content Transplantation:* Cecal contents were pooled from 8-12 SPF WT B6 mice on day #5 after 15 Gy, and from age- and gender-matched untreated littermates. Cecal extracts were suspended in 8 ml phosphate buffered saline and administered to GF WT B6 mice (n=3-4 mice/group) orally, via rectal swab, in water, on food, and in bedding (2 ml per cage of 4 mice, including 200 µl orally). 72 hours after transplantation, mice were exposed to 10 Gy while sterility was maintained and then returned to cages. The experiment was repeated with the same two donor microbiota groups and recipient SPF WT B6 mice (n=5 mice/group), with microbiota transfer performed similarly 1 hour after 11 Gy.

Selective Colonization: Mice were maintained in sterile cages as GF or mono-associated with the nonpathogenic murine *Escherichia coli* NC101 (27) or *Enterococcus faecalis* OG1RF strains by swabbing the snout, fur and anus with 1 X 10^9 colony-forming units of overnight bacterial culture (n=5 mice/group). 24 hours after inoculation, mice were exposed to 15 Gy and returned to cages for observation.

Antibiotic and Probiotic Treatment of Mice: Mice were treated with various antibiotics (Sigma-Aldrich, St. Louis, MO) dissolved in drinking water, starting one hour after radiation: ciprofloxacin, metronidazole, ciprofloxacin/metronidazole, rifaximin, trimethoprim and sulfamethoxazole or neomycin sulfate (n=8 mice/group). 50 mg/kg/d of each antibiotic were administered in initial experiments; 25 and 12.5 mg/kg/d were given in subsequent experiments with similar results. In a separate experiment, mice received VSL#3 delivered in drinking water (30 mg in 100 ml) for one week prior to radiation. VSL#3 sachets contained 900 billion viable

lyophilized bacteria consisting of four strains of *Lactobacillus* species, (*L. casei, L. plantarum, L. acidophilus,* and *L. delbrueckii* subsp. *bulgaricus*), three strains of *Bifidobacterium* species, (*B. longum, B. breve,* and *B. infantis*), and *Streptococcus salivarius* subsp. *thermophilus*.

Quantitative Real-Time Reverse-Transcription Polymerase Chain Reaction

Antimicrobial Peptide Analysis. Quantitative RT-PCR was performed using TaqMan or SYBR Green assays (Applied Biosystems) per manufacturer's instructions, as previously described (58). β-actin was used as an internal control, and ΔΔCt values were calculated to obtain fold changes relative to the healthy control group.

Acid Urea-Polyacrylamide Gel Electrophoresis. Jejunum and ileum tissue protein was extracted using acetonitrile, trifluoroacetic acid and acetic acid, and analyzed by acid urea-polyacrylamide gel electrophoresis (AU-PAGE), as previously described (58). Extracts were analyzed alongside a sample of recombinant α-defensin 4 (rDefa4), and resolved proteins were visualized utilizing Coomassie Brilliant Blue staining.

Statistical Analyses. Analyses were performed using the GraphPad Prism 5 software (GraphPad, La Jolla, CA). Means of normally distributed data were compared using one-way analysis of variance (ANOVA), followed by Tukey's multiple comparison testing and 2-tailed, unpaired Student's *t*-tests. When data was not normally distributed, the Kruskal-Wallis test was utilized to compare means, followed by Dunn's multiple comparison testing and 2-tailed Mann-Whitney tests. Data are expressed as mean ± SEM. Statistical significance was defined as $p<0.05$. In point plots, horizontal lines indicate means.

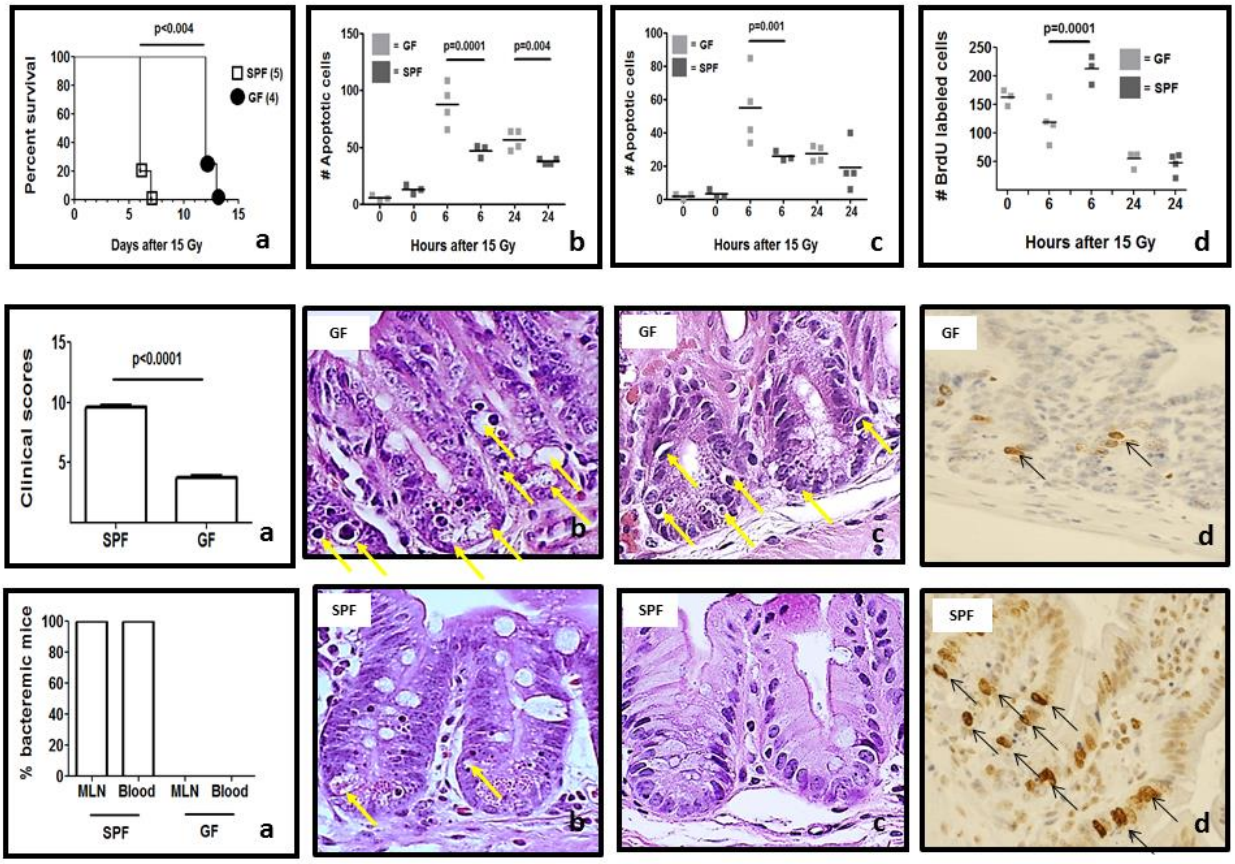

Figure 6.1. The enteric microbiota is necessary for the early death of mice from the "radiation GI syndrome", yet it exerts protective effects on intestinal epithelial cells in response to radiation. (a) Survival (top), clinical colitis scores at day 5 (middle) and percent of positive blood cultures at day 5 (bottom) of GF (n=4) and SPF mice (n=5) treated with 15 Gy. (b) Representative H&E-stained jejunum sections from GF (middle) and SPF (bottom) mice at 6 hours after 15 Gy. Yellow arrows point to apoptotic cells. Quantitation per mouse (50 half crypts) is shown (top). (c) Representative H&E-stained cecum sections from GF (middle) and SPF (bottom) mice at 6 hours after 15 Gy. Yellow arrows point to apoptotic cells. Quantitative comparison (50 half crypts per mouse) is shown (top). (d) Representative bromodeoxyuridine (BrdU) immunohistochemistry on jejunum sections from GF (middle) and SPF (bottom) mice at 6 hours after 15 Gy. Proliferating cells are visible (brown cells with black arrows). Quantitative comparison (50 half crypts per mouse) is shown (top). Magnification for all sections shown is 60X. GF=germ-free; SPF=specific pathogen-free; MLN=mesenteric lymph node; BrdU=bromodeoxyuridine.

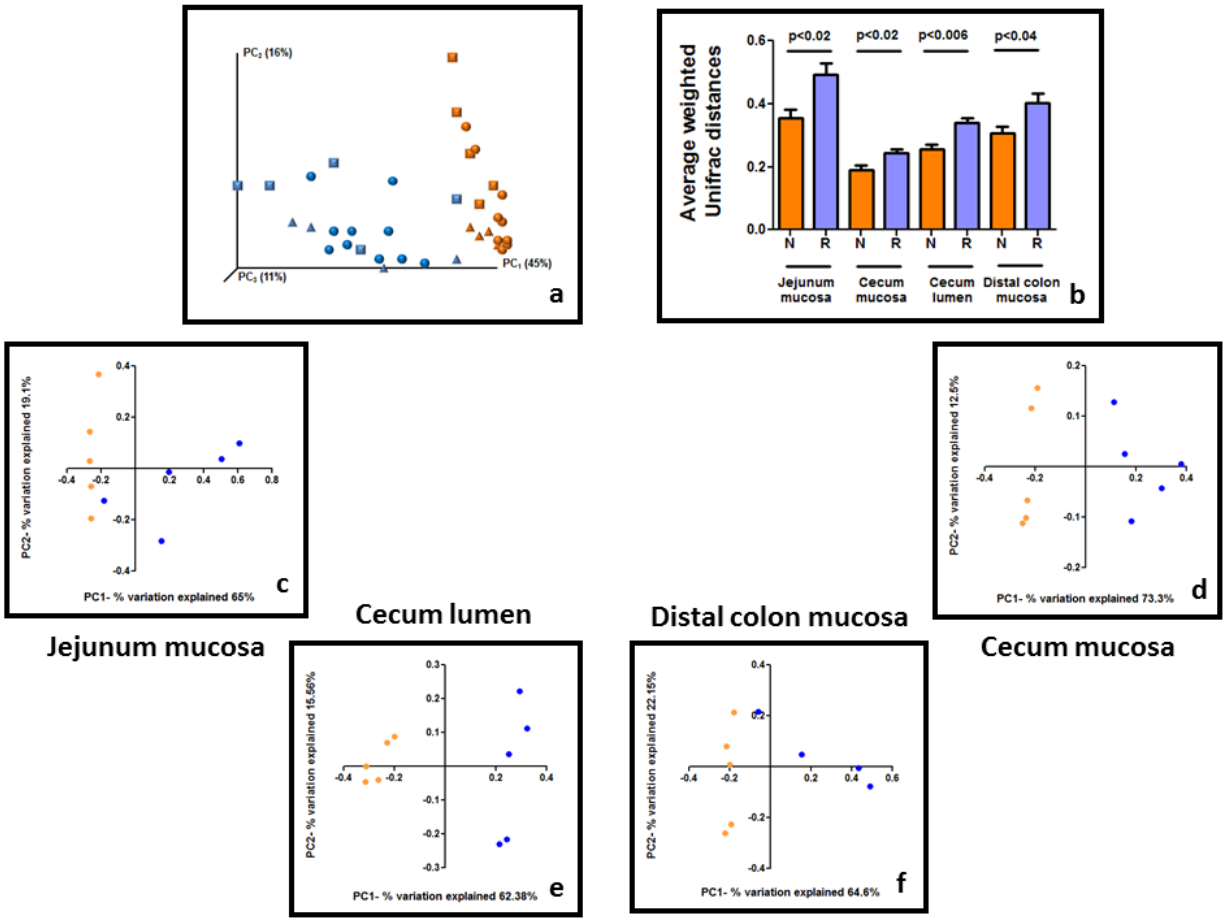

Figure 6.2. Radiation induces an intestinal dysbiosis. (a) Principal coordinates analysis of weighted UniFrac distances of 16S rRNA sequences demonstrating clustering according to radiation exposure. Symbols represent individual mucosal bacterial communities obtained from healthy control mice (orange) and mice exposed to irradiation (blue), in the jejunum (squares), cecum (circles), and the distal colon (triangles). (b) A significant increase in average UniFrac distances, or β-diversity, was shown in mice exposed to radiation when compared to healthy control mice. N= "No radiation" healthy control; R= Radiation. Multidimensional scaling reveals separate clustering of bacterial communities based on radiation exposure in the jejunum mucosa (c), cecum mucosa (d), cecum lumen (e) and distal colon mucosa (f). Symbols represent individual intestinal bacterial communities obtained from healthy control mice (orange) and mice exposed to irradiation (blue).

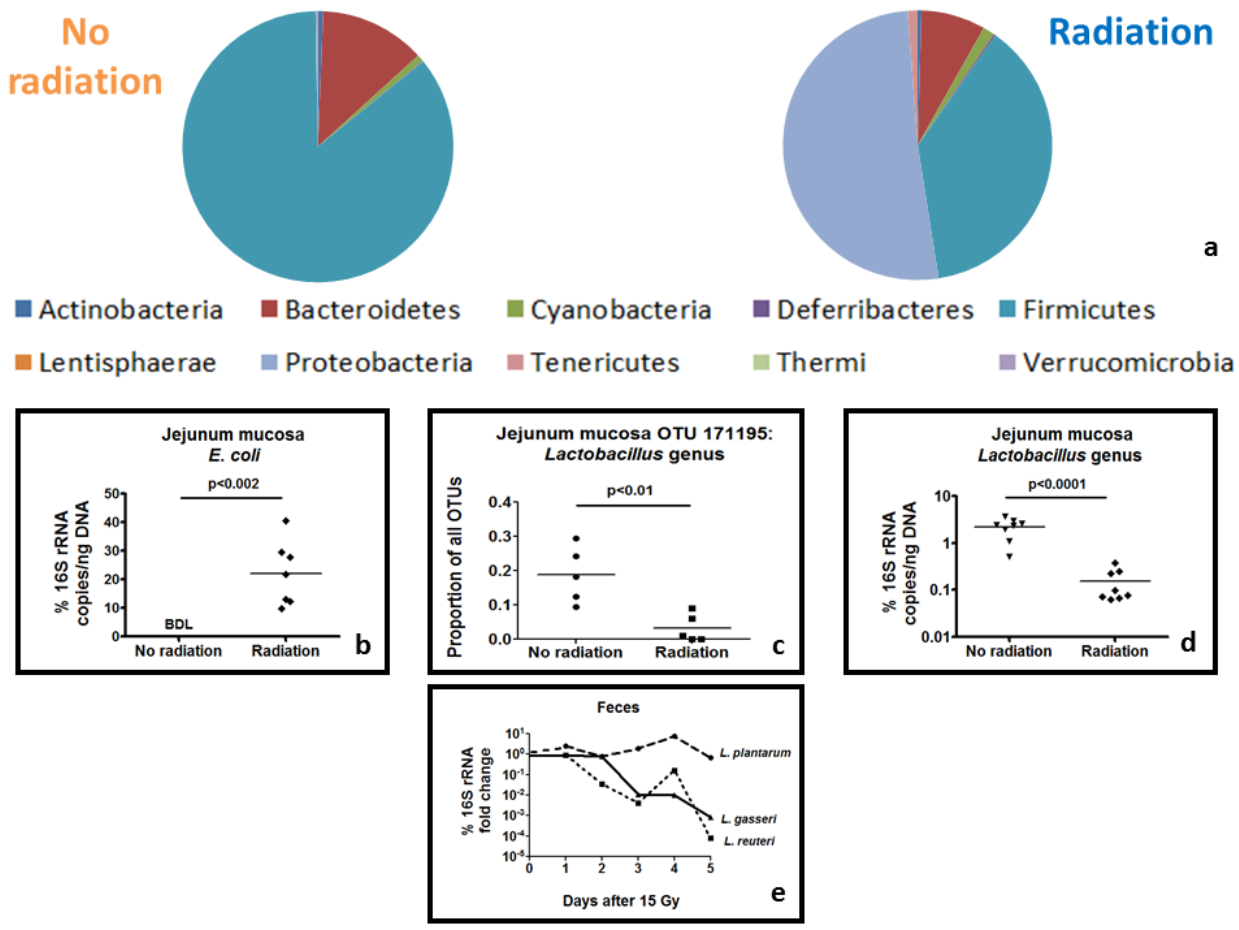

Figure 6.3. Transitions in gut bacterial populations associated with radiation exposure. (a) Average abundances of bacterial phlya in the jejunum mucosa of healthy control mice (left) and mice exposed to radiation (right). Radiation exposure results in an increase in intestinal Proteobacteria and a decrease in Firmicutes ($p<0.007$). (b) Concentrations of Proteobacteria phylum member *E. coli* were determined in healthy control mice and mice exposed to radiation using quantitative PCR (qPCR) of the 16S rRNA gene. Within the Firmicutes phylum, radiation specifically reduces *Lactobacillus* spp., as shown by 16S rRNA 454 pyrosequencing (c) and qPCR (d), and *Lactobacillus reuteri* comprise most of the *Lactobacillus* species and are almost eradicated after radiation (e). Copy number is normalized to total 16S in (b), (d), and (e).

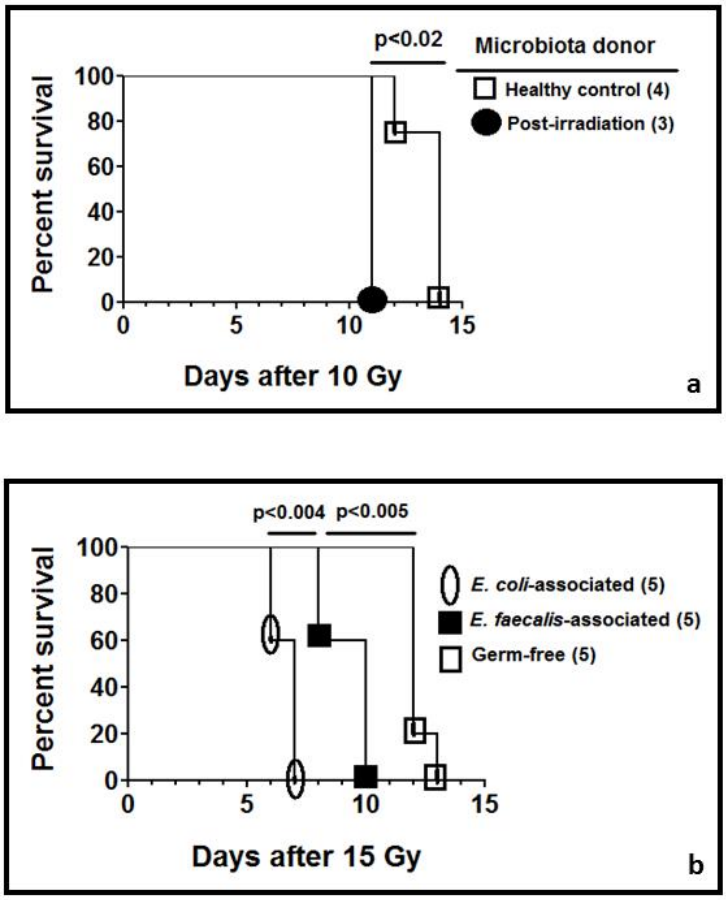

Figure 6.4. The intestinal microbiota directly impacts the host response to radiation. (a) In cecal transplantation experiments, mice receiving post-irradiation microbiota had increased morbidity and accelerated mortality after radiation compared to mice receiving healthy control microbiota ($p<0.02$). (b) *Escherichia coli* mono-associated mice had increased morbidity and accelerated mortality after 15 Gy compared to *Enterococcus faecalis* mono-associated mice and GF mice.

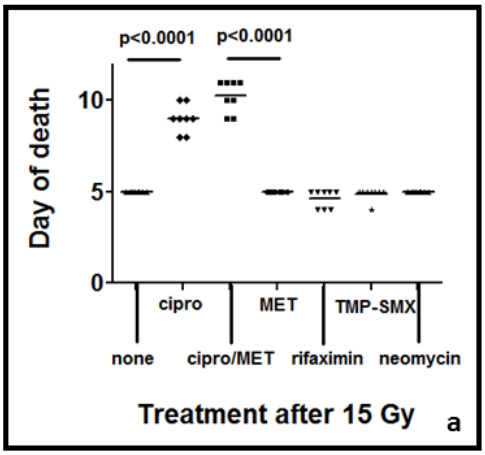

Jejunum mucosa | Cecum mucosa | Cecum lumen | Distal colon mucosa

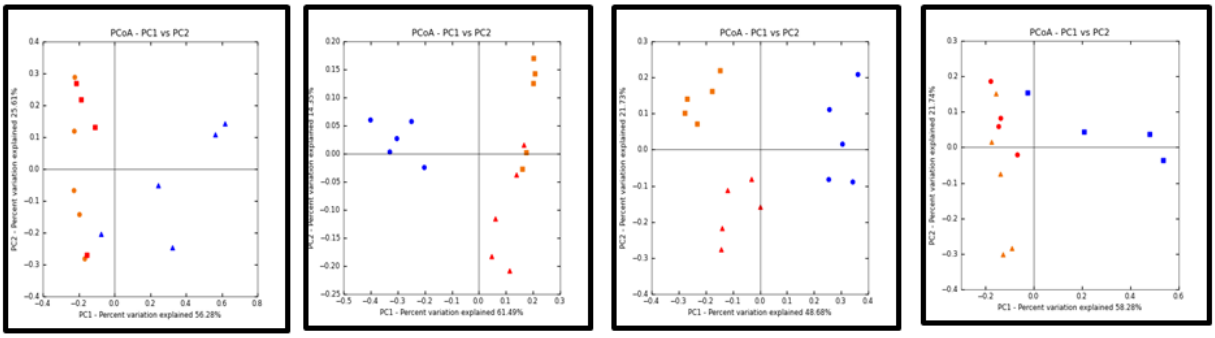

p=0.006 | p=0.001 | p=0.001 | p=0.003

b

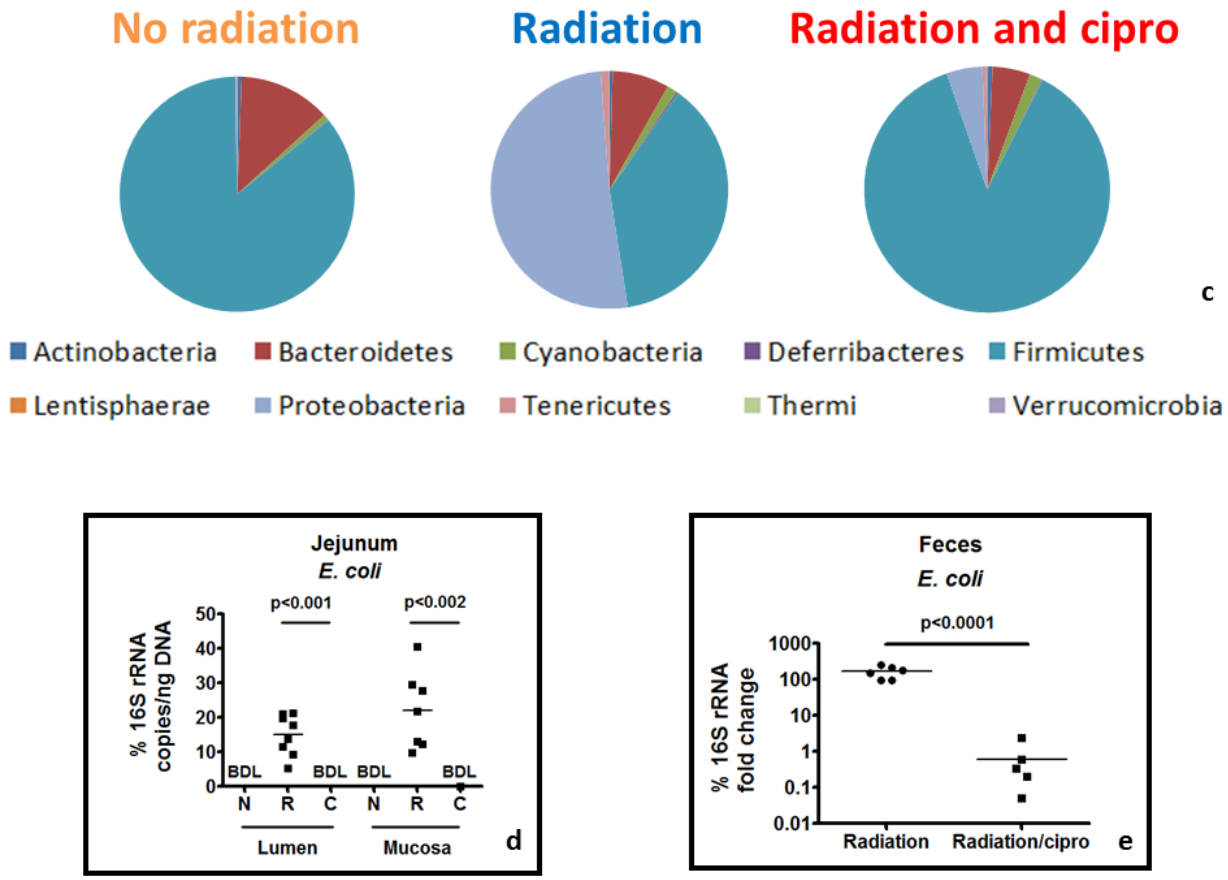

Figure 6.5. Radiation-induced dysbiosis and the GI syndrome are mitigated by ciprofloxacin. Ciprofloxacin rescues mice from the GI syndrome (a). cipro=ciprofloxacin; MET=metronidazole; TMP-SMX=trimethoprim-sulfamethoxazole. (b) Principal coordinates analysis of weighted UniFrac distances between bacterial communities determined from 16S rRNA genes. Symbols represent individual intestinal bacterial communities obtained from healthy control mice (orange), mice exposed to irradiation (blue), and mice exposed to irradiation and treated with ciprofloxacin (red). (c) Average abundances of bacterial phlya in the jejunum mucosa of healthy control mice (left), irradiated mice (middle), and irradiated mice treated with ciprofloxacin (right). Radiation exposure results in a decrease in Firmicutes ($p<0.0001$) and an increase in Proteobacteria ($p=0.05$), and these shifts are largely prevented by ciprofloxacin ($p<0.003$). (d) Administration of ciprofloxacin prevents radiation-induced proliferation of *E. coli* species in the jejunum, both in the lumen and the mucosa. N=No radiation; R=Radiation; C=radiation/Cipro; BDL=below detectable limits. (e) Ciprofloxacin also prevents expansion of fecal *E. coli* populations after radiation. Copy number is normalized to total 16S rRNA copies in (d) and (e).

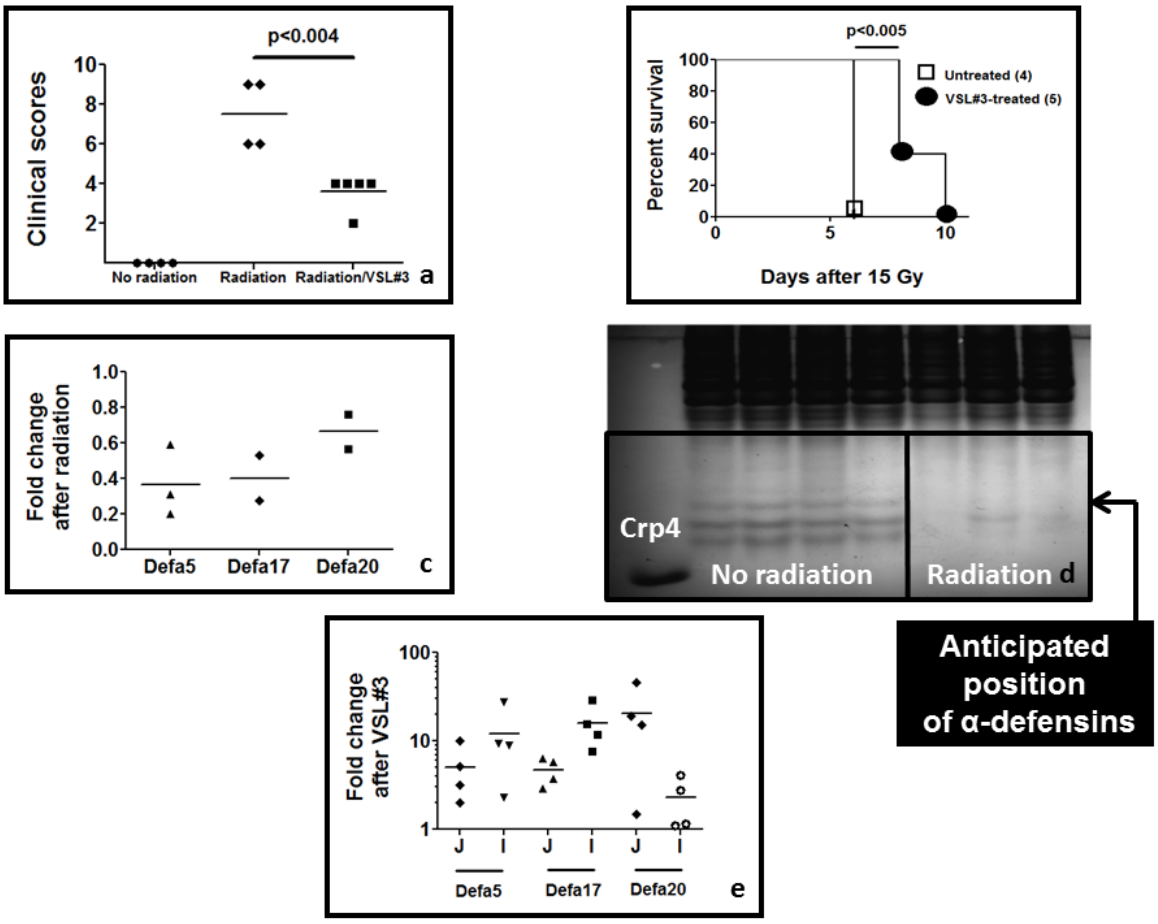

Figure 6.6. Radiation GI syndrome is prevented by administration of the probiotic VSL#3. VSL#3 abated clinical colitis scores in irradiated mice as measured at day 5 (a) and prolonged survival after lethal irradiation (b). (c) Radiation lessened α-defensin mRNA expression in the jejunum on day 3 after radiation. Defa5 ($p<0.002$), Defa17 ($p<0.002$) and Defa20 ($p<0.006$) transcript levels are shown. Copy numbers are normalized to β-actin, and fold change is relative to the healthy control group. (d) Acid urea polyacrylamide gel electrophoresis demonstrates peptide expression patterns of α-defensin isoforms in the ileum of healthy control mice and mice exposed to radiation. The first lane is recombinant Defa4 control (Crp4), and each additional lane represents protein extracts from an individual mouse. (e) VSL#3 induces small intestinal α-defensin mRNA expression. Defa5, Defa17 and Defa20 transcripts were measured using quantitative RT-PCR of jejunum and distal ileum RNA extracts from untreated and VSL#3-treated mice. Copy numbers are normalized to β-actin, and fold change is relative to the untreated group. J=Jejunum; I=Ileum.

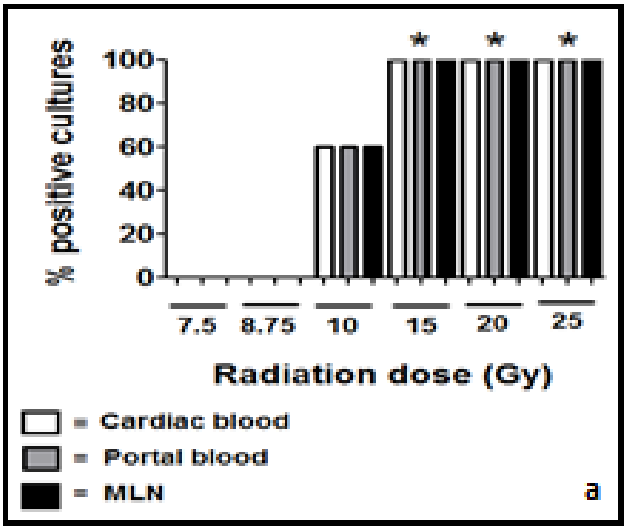
% positive cultures
100
80
60
40
20
0
*
*
*
7.5
8.75
10
15
20
25
Radiation dose (Gy)
= Cardiac blood
= Portal blood
= MLN
a

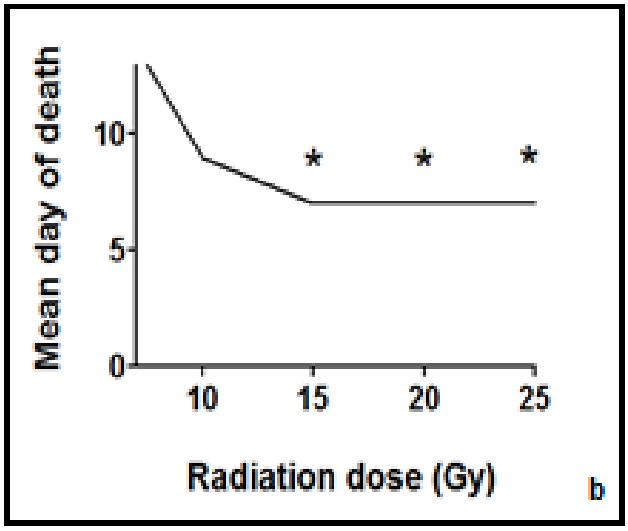
Mean day of death
10
5
0
*
*
*
10
15
20
25
Radiation dose (Gy)
b

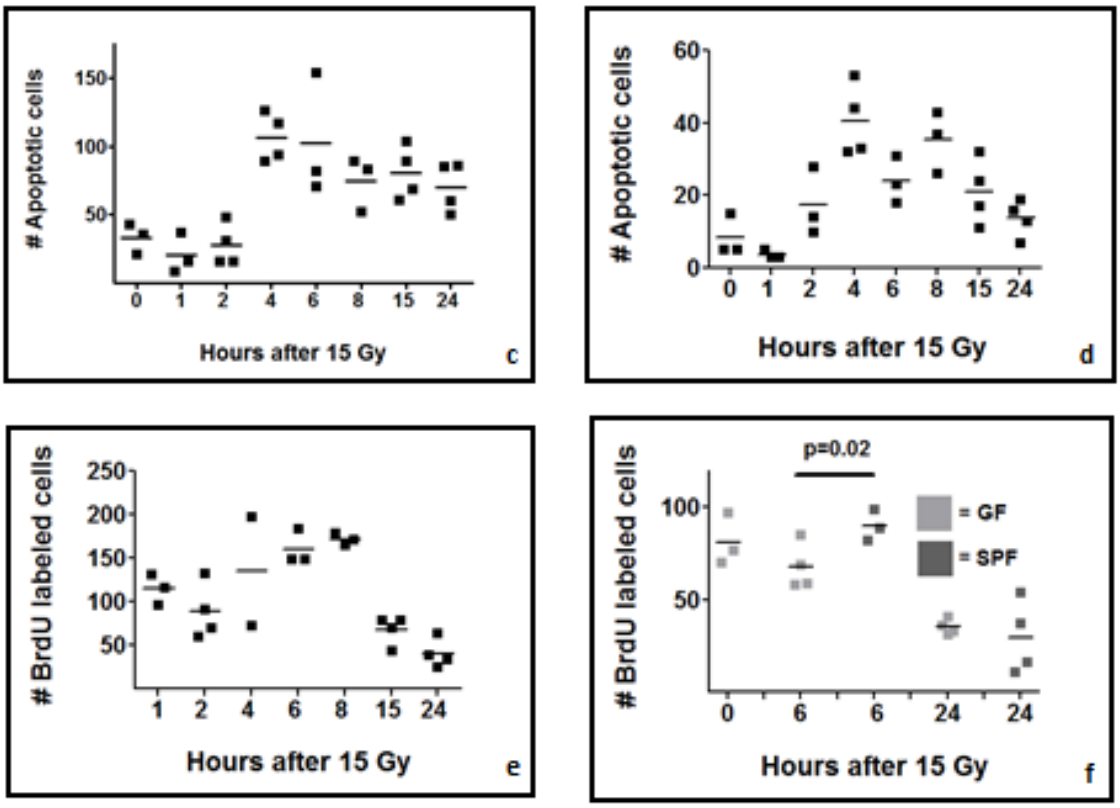

Supplementary Figure 6.1. (a) Results of aerobic cultures of cardiac blood, portal blood and mesenteric lymph nodes harvested from mice at day 5 after exposure to a range of radiation doses (n= 5 mice/group). (b) Mortality in mice exposed to 10-25 Gy total body irradiation (n=8 mice/group). *=radiation dose causing GI syndrome in all mice. Quantitation of apoptotic cells per SPF mouse (50 half crypts or 25 whole crypts) in the jejujum (c) and cecum (d) of mice 0-24 hours after 15 Gy. (e) Quantitation of BrdU-labelled cells per SPF mouse (50 half crypts or 25 whole crypts) in the jejunum after 15 Gy. (f) Quantitation of BrdU-labelled cells per 50 half crypts in the cecum of GF and SPF mice 0, 6, and 24 hours after 15 Gy.

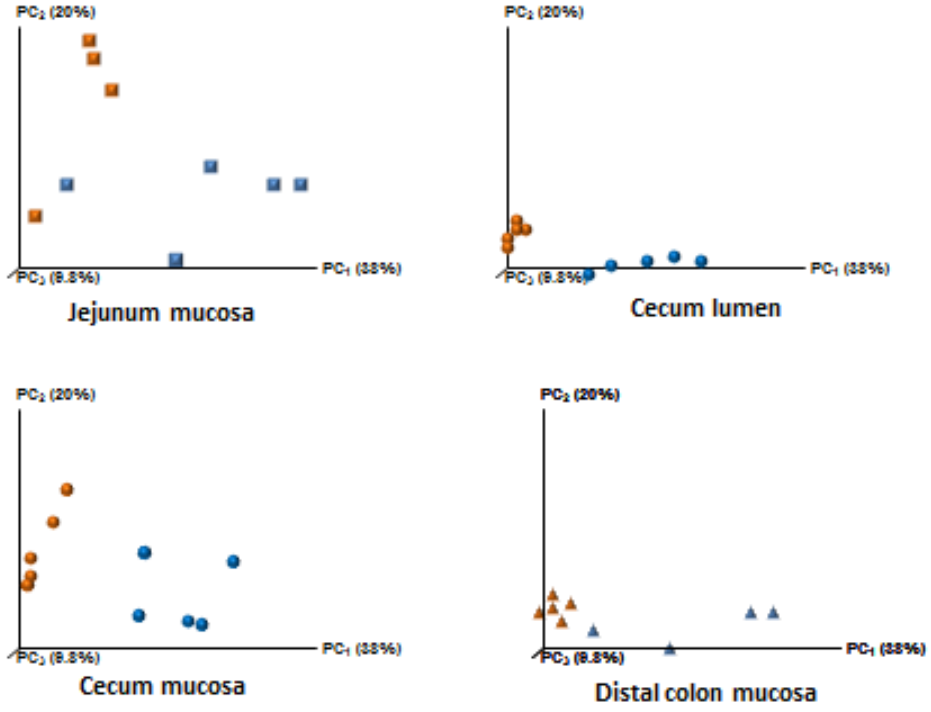

Supplementary Fig. 6.2A. Principal coordinates analysis of weighted UniFrac distances between bacterial communities determined from 16S rRNA genes. Symbols represent individual intestinal communities obtained from healthy control mice (orange) and mice exposed to irradiation (blue).

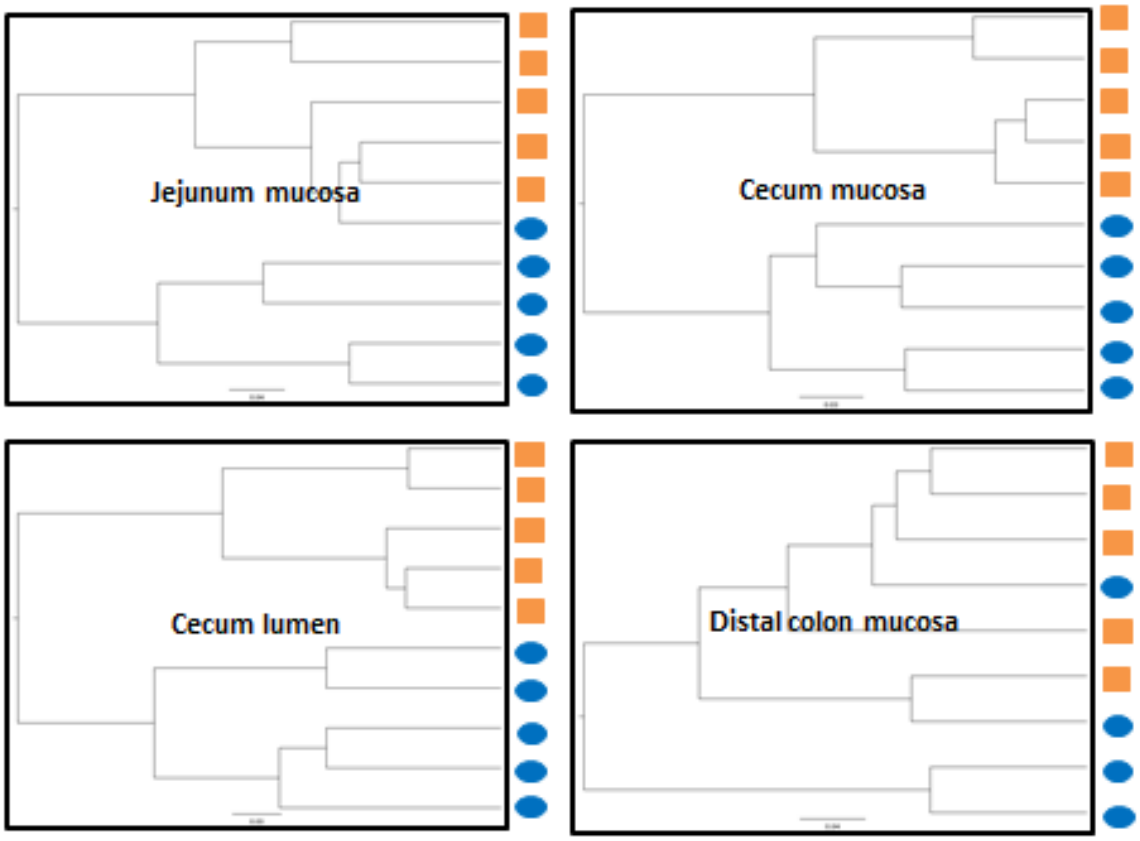

Supplementary Figure 6.2B. Hierarchial clustering of intestinal microbiota samples based on OTUs at 97% sequence similarity. Samples from healthy control mice (orange squares), and mice exposed to irradiation (blue circles) are shown.

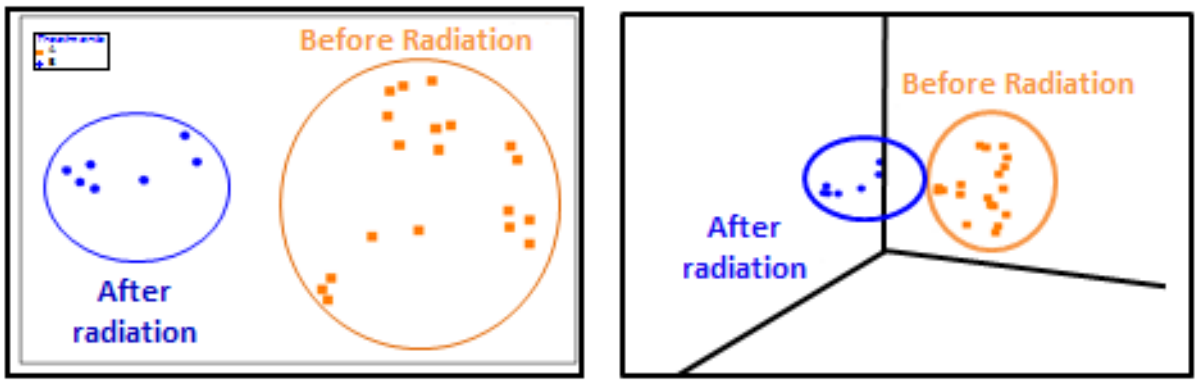

Supplementary Figure 6.2C. T-RFs derived from fecal bacterial communities of the same mice before (orange) and after (blue) exposure to radiation were used to generate nonmetric multidimensional scaling plots in two (left) and three (right) dimensions. The communities were statistically dissimilar before and after radiation based on ANOSIM analysis ($p<0.05$).

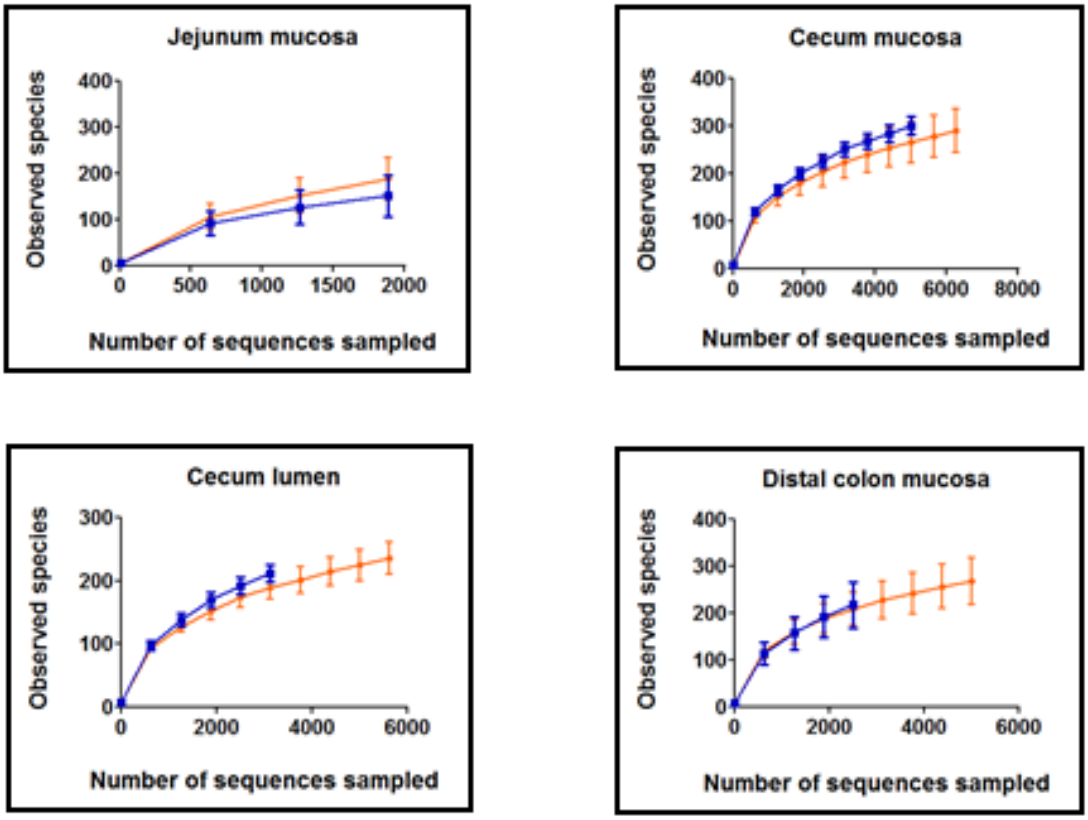

Supplementary Figure 6.2D: Rarefaction curves of intestinal bacterial communities from healthy control mice (orange) and mice exposed to radiation (blue). Curves are based on α-diversity within sample groups for the V1-V3 16S rRNA region.

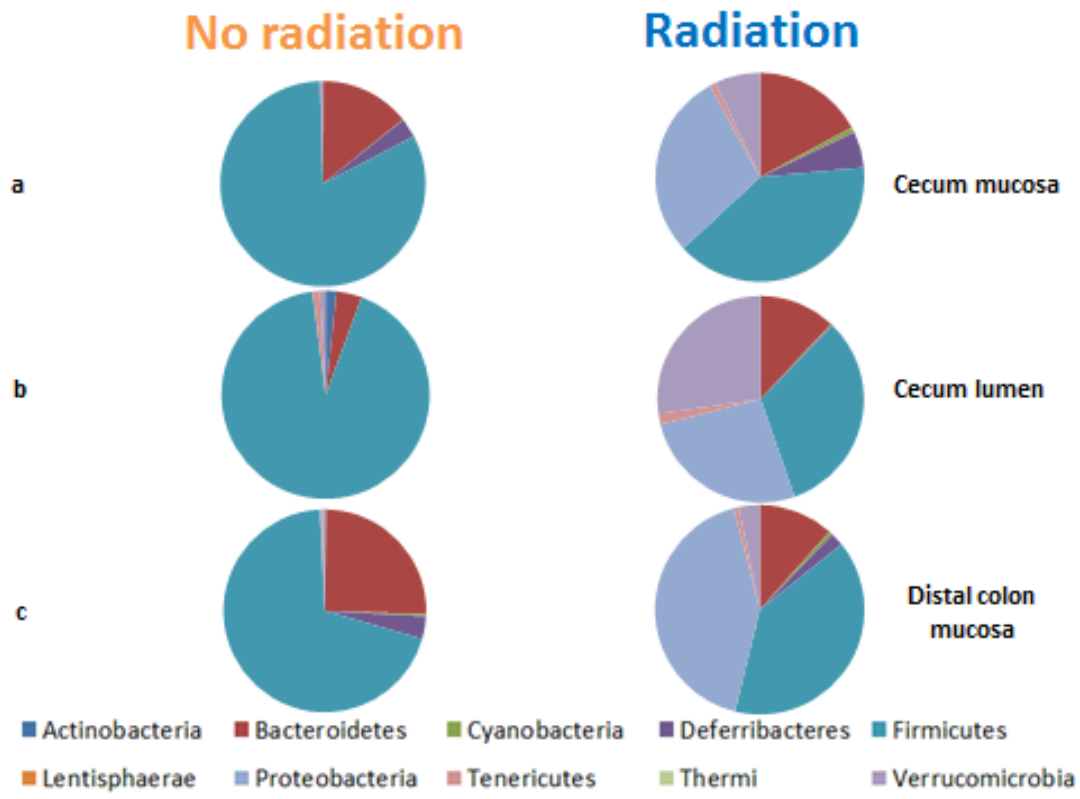

Supplementary Figure 6.3: Average abundances of bacterial phlya in healthy control mice (left) and mice exposed to radiation (right). Radiation exposure results in a decrease in Firmicutes and an increase in Proteobacteria and Verrucomicrobia, in the cecum mucosa (a), cecum lumen (b), and distal colon mucosa (c).

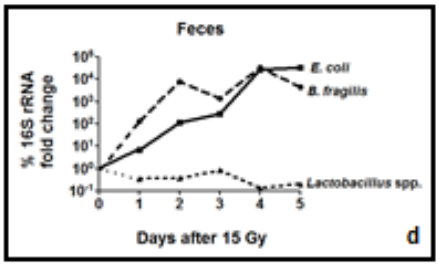

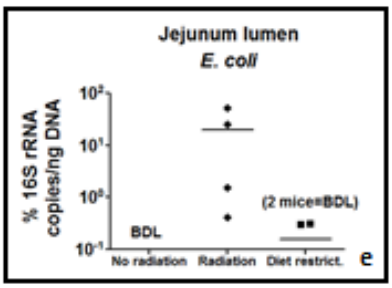

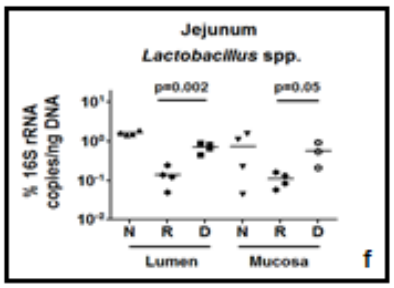

Supplementary Figure 6.3. (d) Intestinal dysbiosis begins by 24 hours after radiation and progresses thereafter (n=4 mice). Copy number is normalized to total 16S. (e, f) Intestinal dybiosis following radiation is not due to changes in dietary intake. (e) *E. coli* were increased from below detectable limits in healthy mice to an average of 20% of all bacteria in the jejunum lumen at 48 hours after radiation. In contrast, after 48 hours of severe dietary restriction, two mice still had below detectable limits of *E. coli*, while in two mice only 0.3% of all bacteria were *E. coli*. BDL=below detectable limits; Diet restrict.=diet restricted. (f) There were significant differences between contractions of *Lactobacillus* spp. populations in the jejunum at 48 hours after radiation, compared to minimal decreases of these species after 48 hours of severe dietary restriction.

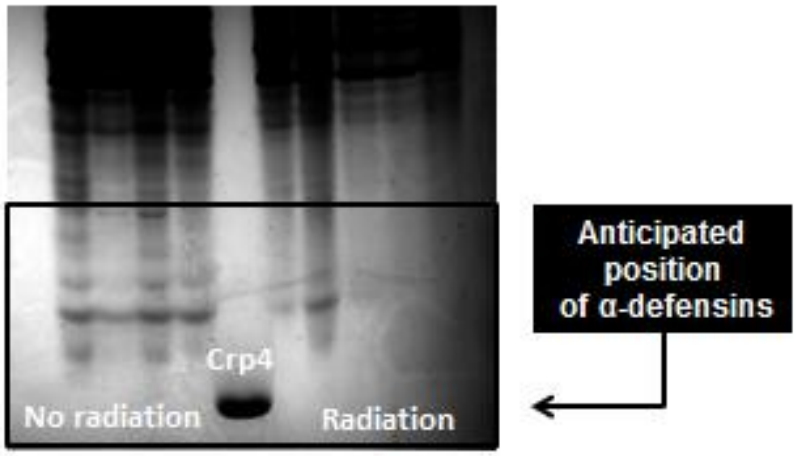

Supplementary Figure 6.4. Acid urea polyacrylamide gel electrophoresis demonstrates peptide expression patterns of α-defensin isoforms in the jejunum of healthy control mice and mice exposed to radiation. The 5th lane is recombinant Defa4 control, and each additional lane represents protein extracts from an individual mouse.

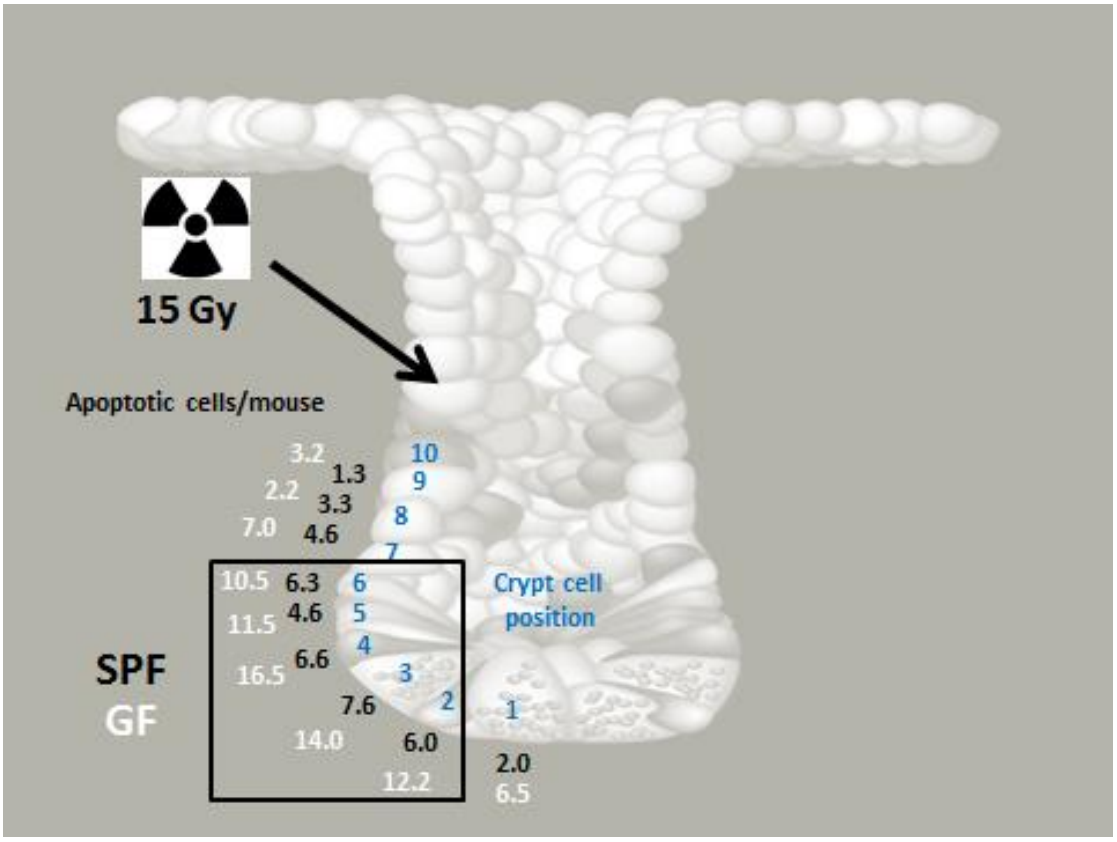

Supplementary Figure 6.5. Radiation induces apoptosis in the small intestinal crypt region of the Paneth cells, which produce and secrete the antimicrobial α-defensins. Shown are the number of apoptotic cells per 50 half crypts in the jejunum at each respective cell position, both in germ-free (white) and specific pathogen-free (black) mice, at 6 hours after 15 Gy.

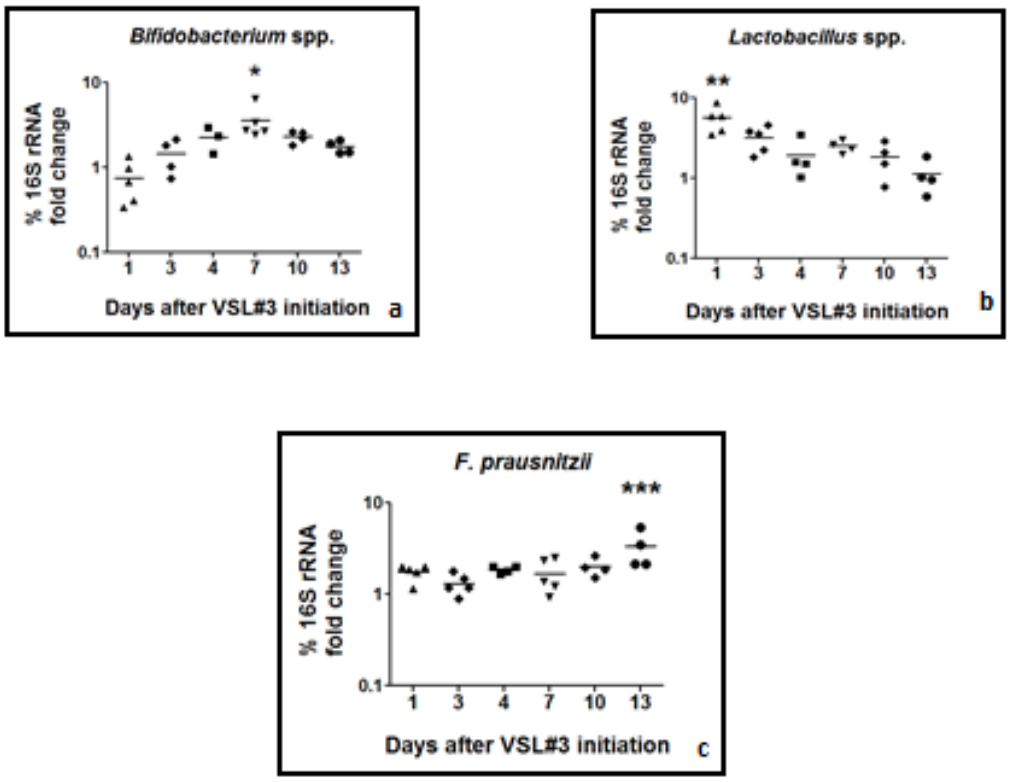

Supplementary Figure 6.6. Quantitation of putative protective fecal bacterial species after administration of VSL#3. Copy number is normalized to total 16S. *Bifidobacterium* species (a), *Lactobacillus* species (b) and *Faecalibacterium prausnitzii* (c) are shown. *p<0.007 compared to day 0. **p<0.005 compared to day 0. *** p<0.03 compared to day 0.

Bacteria	Fold change after radiation	p value
Escherichia coli	**+ 14811**	**<0.0001**
Bacteroides fragilis	**+ 1749**	**<0.003**
Klebsiella pneumonia	**+ 1600**	**<0.02**
Enterococcus faecalis	**+ 110**	**<0.009**
Pseudomonas fluorescens	**+ 5**	**<0.0001**
Clostridium coccoides	**- 24**	**0.007**
***Lactobacillus* spp.**	**- 35**	**0.0003**
***Bifidobacterium* spp.**	**- 54**	**0.005**

Supplementary Table 6.1. Radiation-induced shifts in clinically-relevant bacterial groups are very similar to those seen in human inflammatory bowel diseases.

Primer	Forward primer	Reverse primer
Universal	**5'-GTGSTGCAYGGYTGTCGTCA-3'**	**5'-ACGTCRTCCMCACCTTCCTC-3'**
***Lactobacillus* spp.**	**5′-AGCAGTAGGGAATCTCCA-3′**	**5′-CACCGCTACACATGGAG-3′**
***Bifidobacterium* spp.**	**5′-GGGTGGTAATGCCGGATG-3'**	**5′-CACCGCTACACATGGAG-3′**
Faecalibacterium prausnitzii	**5′-GATGGCCTCGCGTCCGATTAG-3′**	**5′-CCGAAGACCTTCTTCCTCC-3′**
Escherichia coli	**5′-GTTAATACCTTTGCTCATTGA-3′**	**5′-ACCAGGGTATCTAATCCTGTT-3′**
***Bacteriodes* spp.**	**5'-ATAGCCTTTCGAAAGRAAGAT-3'**	**5'-CCAGTATCAACTGCAATTTTA-3'**
***Clostridium* spp.**	**5'-CGGTACCTGACTAAGAAGC-3'**	**5'-AGTTTYATTCTTGCGAACG-3'**

Supplementary Table 6.2. Primer sequences utilized to assess bacterial populations with quantitative PCR.

REFERENCES

1. Packey CD, Ciorba MA. Microbial influences on the small intestinal response to radiation injury. Curr Opin Gastroenterol 2010; 26: 88-94.

2. Shadad AK, Sullivan FJ, Martin JD, Egan LJ. Gastrointestinal radiation injury: prevention and treatment. World J Gastroenterol 2013; 19(2): 199-208.

3. Claesson MJ, O'Sullivan O, Wang Q, et al. Comparative analysis of pyrosequencing and a phylogenetic microarray for exploring microbial community structures in the human distal intestine. PLoS One 2009; 4(8): e6669.

4. Lozupone CA, Stombaugh JI, Gordon JI, et al. Diversity, stability and resilience of the human gut microbiota. Nature 2012; 489: 220-230.

5. Ivanov II, Honda K. Intestinal commensal microbes as immune modulators. Cell Host and Microbe 2012; 12: 496-508.

6. Kau AL, Ahern PP, Griffin NW, et al. Human nutrition, the gut microbiome and the immune system. Nature 2011; 474: 327-336.

7. Blumberg R, Powrie F. Microbiota, disease, and back to health: A metastable journey. Sci Transl Med 2012; 4(137): 1-9.

8. Cho I, Blaser MJ. The human microbiome: At the interface of health and disease. Nat Rev Genet 2012; 13: 260-270.

9. Kawashima R, Kawamura YI, Kato R, et al. IL-13 receptor α2 promotes epithelial cell regeneration from radiation-induced small intestinal injury in mice. Gastroenterology 2006; 131: 130-141.

10. Paris F, Fuks Z, Kang A, et al. Endothelial apoptosis as the primary lesion initiating intestinal radiation damage in mice. Science 2001; 293: 293-297.

11. Kirsch DG, Santiago PM, di Tomaso E, et al. p53 controls radiation-induced gastrointestinal syndrome in mice independent of apoptosis. Science 2010; 327(5965): 593-6.

12. Riehl T, Cohn S, Tessner T, et al. Lipopolysaccharide is radioprotective in the mouse intestine through a prostaglandin-mediated mechanism. Gastroenterology 2000; 118: 1106-1116.

13. Burdelya LG, Krivokrysenko VI, Tallant TC, et al. An agonist of toll-like receptor 5 has radioprotective activity in mouse and primate models. Science 2008; 320: 226-230.

14. Garrett WS, Gallini CA, Yatsunenko T, et al. Enterobacteriaceae act in concert with the gut microbiota to induce spontaneous and maternally transmitted colitis. Cell Host Microbe 2010; 8: 292-300.

15. Elinav E, Strowig T, Kau AL, et al. NLRP6 inflammasome regulates colonic microbial ecology and risk for colitis. Cell 2011; 145: 745-757.

16. Delia P, Sansotta G, Donato V, et al. Use of probiotics for prevention of radiation-induced diarrhea. World J Gastroenterol 2007; 13(6): 912-5.

17. Rakoff-Nahoum S, Paglino J, Eslami-Varzaneh F, et al. Recognition of commensal microflora by Toll-like receptors is required for intestinal homeostasis. Cell 2004; 118: 229-241.

18. Egan LJ, Eckmann L, Greten FR, et al. IκB-kinaseβ-dependent NF-κB activation provides radioprotection to the intestinal epithelium. Proc Natl Acad Sci U S A 2004; 101(8): 2452-7.

19. Crawford PA, Gordon JI. Microbial regulation of intestinal radiosensitivity. Proc Natl Acad Sci U S A 2005; 102: 13254-13259.

20. Lupp C, Robertson ML, Wickham ME, et al. Host-mediated inflammation disrupts the intestinal microbiota and promotes the overgrowth of Enterobacteriaceae. Cell Host Microbe 2007; 2: 119-129.

21. Wu GD, Chen J, Hoffmann C, et al. Linking long-term dietary patterns with gut microbial enterotypes. Science 2011; 334(6052): 105-8.

22. Winter SE, Thiennimitr P, Winter MG, et al. Gut inflammation provides a respiratory electron acceptor for Salmonella. Nature 2010; 467: 426-429.

23. Lozupone C, Faust K, Raes J, et al. Identifying genomic and metabolic features that can underlie early successional and opportunistic lifestyles of human gut symbionts. Genome Res 2012; 22: 1974-84.

24. Gutiérrez A, Frances R, Amoros A, et al. Cytokine association with bacterial DNA in serum of patients with inflammatory bowel disease. Inflamm Bowel Dis 2009; 15(4): 508-14.

25. Wei B, Huang T, Dalwadi H, et al. *Pseudomonas fluorescens* encodes the Crohn's disease-associated I2 sequence and T-cell superantigen. Infect Immun 2002; 70(12): 6567-75.

26. Bloom SM, Bijanki VN, Nava GM, et al. Commensal *Bacteroides* species induce colitis in host-genotype-specific fashion in a mouse model of inflammatory bowel disease. Cell Host and Microbe 2011; 9: 390-403.

27. Kim SC, Tonkonogy SL, Albright CA, et al. Variable phenotypes of enterocolitis in interleukin 10-deficient mice monoassociated with two different commensal bacteria. Gastroenterology 2005; 128: 891-906.

28. Mondot S, Kang S, Furet JP, et al. Highlighting new phylogenetic specificities of Crohn's disease microbiota. Inflamm Bowel Dis 2010; 17: 185-192.

29. Verma R, Verma AK, Ahuja V, Paul J. Real-time analysis of mucosal flora in patients with inflammatory bowel disease in India. J Clin Microbiol 2010; (11): 4279-82.

30. Atarashi K, Tanoue T, Shima T, et al. Induction of colonic regulatory T cells by indigenous *Clostridium* species. Science 2011; 331: 337-341.

31. Frank DN, St Amand AL, Feldman RA, et al. Molecular phylogenetic characterization of microbial community imbalances in human inflammatory bowel diseases. Proc Natl Acad Sci U S A 2007; 104: 13780-85.

32. Sokol H, Pigneur B, Watterlot L, et al. *Faecalibacterium prausnitzii* is an anti-inflammatory commensal bacterium identified by gut microbiota analysis of Crohn disease patients. Proc Natl Acad Sci U S A 2008; 105: 16731-16736.

33. Round JL, Mazmanian SK. Inducible Foxp3+ regulatory T-cell development by a commensal bacterium of the intestinal microbiota. Proc Natl Acad Sci U S A 2010; 107: 12204-12209.

34. Kang S, Denman SE, Morrison M, et al. Dysbiosis of fecal microbiota in Crohn's disease patients as revealed by a custom phylogenetic microarray. Inflamm Bowel Dis 2010; 16(12): 2034-42.

35. Ivanov II, Atarashi K, Manel N, et al. Induction of intestinal Th17 cells by segmented filamentous bacteria. Cell 2009; 139: 485-498.

36. Srinivasan S, Hoffman NG, Morgan MT, et al. Bacterial communities in women with bacterial vaginosis: high resolution phylogenetic analyses reveal relationships of microbiota to clinical criteria. PLoS One 2012; 7(6): e37818.

37. Cardinale BJ, Palmer MA, Collins SL. Species diversity enhances ecosystem functioning through interspecific facilitation. Nature 2002; 415: 426-429.

38. Ives AR, Carpenter SR. Stability and diversity of ecosystems. Science 2007; 317: 58-62.

39. Mattila E, Uusitalo-Seppälä R, Wuorela M, et al. Fecal transplantation, through colonoscopy, is effective therapy for recurrent *Clostridium difficile* infection. Gastroenterology 2012; 142: 490-496.

40. Bevins CL, Stange EF, Wehkamp J. Decreased Paneth cell defensin expression in ileal Crohn's disease is independent of inflammation, but linked to the NOD2 1007fs genotype. Gut 2009; 58(6): 882-3.

41. Vaishnava S, Yamamoto M, Severson KM, et al. The antibacterial lectin RegIIIγ promotes the spatial segregation of microbiota and host in the intestine. Science 2011; 334: 255-258.

42. Arumugam M, Raes J, Pelletier E, et al. Enterotypes of the human gut microbiome. Nature 2011; 473(7346): 174-80.

43. Bhattacharjee Y. Devastation in Japan. Candidate radiation drugs inch forward. Science 2011; 331(6024): 1505.

44. Huang EY, Wang FS, Lin IH, Yang KD. Aminoguanidine alleviates radiation induced small bowel damage through its antioxidant effect. Int J Radiat Oncol Biol Phys 2009; 74: 237-244.

45. Boerma M, Wang J, Burnett AF, et al. Local administration of interleukin-11 ameliorates intestinal radiation injury in rats. Cancer Res 2007; 67: 9501-9506.

46. Hagiwara A, Nakayama F, Motomura K, et al. Comparison of expression profiles of several fibroblast growth factor receptors in the mouse jejunum: suggestive evidence for a differential radioprotective effect among major FGF family members and the potency of FGF1. Radiat Res 2009; 172: 58-65.

47. Qiu W, Carson-Walter EB, Liu H, et al. PUMA regulates intestinal progenitor cell radiosensitivity and gastrointestinal syndrome. Cell Stem Cell 2008; 2: 576-583.

48. Pritchard DM, Potten CS, Korsmeyer SJ, et al. Damage-induced apoptosis in intestinal epithelia from bcl-2-null and bax-null mice: investigations of the mechanistic determinants of epithelial apoptosis in vivo. Oncogene 1999; 18: 7287-93.

49. Hamady M, Walker JJ, Harris JK, et al. Error-correcting bar-coded primers for pyrosequencing hundreds of samples in multiplex. Nat Methods 2008; 5: 235-7.

50. Fierer N, Hamady M, Lauber CL, Knight R. The influence of sex, handedness, and washing on the diversity of hand surface bacteria. Proc Natl Acad Sci U S A 2008; 105: 17994-9.

51. Caporaso JG, Kuczynski J, Stombaugh J, et al. QIIME allows analysis of high-throughput community sequencing data. Nat Methods 2010; 7: 335-6.

52. Altschul SF, Gish W, Miller W, et al. Basic local alignment search tool. J Mol Biol 1990; 215: 403-10.

53. McDonald D, Price MN, Goodrich J, et al. An improved Greengenes taxonomy with explicit ranks for ecological and evolutionary analyses of bacteria and archaea. ISME J 2012; 6: 610-8.

54. Lozupone C, Knight R. UniFrac: a new phylogenetic method for comparing microbial communities. Appl Environ Microbiol 2005; 71: 8228–35.

55. Lozupone CA, Hamady M, Kelley ST, Knight R. Quantitative and qualitative beta diversity measures lead to different insights into factors that structure microbial communities. Appl Environ Microbiol 2007; 73: 1576–85.

56. Lozupone C, Lladser ME, Knights D, et al. UniFrac: an effective distance metric for microbial community comparison. ISME J 2011; 5: 169–72.

57. Carroll IM, Ringel-Kulka T, Keku TO, et al. Molecular analysis of the luminal- and mucosal-associated intestinal microbiota in diarrhea-predominant irritable bowel syndrome. Am J Physiol Gastrointest Liver Physiol 2011; 301: G799-807.

58. Shanahan MT, Carroll IM, Grossniklaus E, et al. Mouse Paneth cell antimicrobial function is independent of Nod2. Gut 2013.

CHAPTER 7: CIPROFLOXACIN PREVENTS THE RADIATION-INDUCED GASTROINTESTINAL SYNDROME BY INHIBITING ENTERIC DYSBIOSIS[7]

Introduction

Radiation-induced gastrointestinal syndrome (RIGS) remains the major limitation for delivering tumoricidal radiation doses for treatment of abdominal and pelvic malignancies (1). Interest surged in the development of medical countermeasures for radiological/nuclear, biological and chemical threats after the 2001 terrorist attacks in the United States and further intensified after explosions at Japan's nuclear power plant in 2011 (2). At higher radiation doses, the mortality rate of RIGS exceeds that of the hematopoietic syndrome (3-5). Yet, beyond the utility of potassium iodide in preventing thyroid cancer, there are no proven drugs to ward off the devastating health effects of a large radiation exposure (2).

The pathophysiological mechanisms of RIGS involve loss of clonogenic crypt cells, depopulation of intestinal villi, mucosal denudation and host death (6-8). Rapid proliferation of intestinal epithelial cells (IECs) makes the enteric mucosa particularly susceptible to damage following exposure to genotoxic stressors such as radiation. Thus, maintenance of intestinal mucosal homeostasis is critical to combating RIGS. Most studies to date have focused on the elucidation of radiation effects on the host epithelium or endothelium (1, 9-13) and/or the mechanisms by which growth factors, cytokines or other molecules may inhibit IEC cycling to promote radioresistance (14-16), enhance IEC proliferation subsequent to insult to facilitate recovery (13, 16-21), or prevent radiation-induced endothelial cell death (9, 22-27). Extensive

[7] This chapter is part of the following manuscript currently being prepared for submission: Packey CD, Maharshak N, Bowen R, Miller PL, Plevy SE, Keku TO, Shanahan MT, Jobin C, Carroll IM, Sartor RB. Ciprofloxacin prevents the radiation-induced gastrointestinal syndrome by inhibiting enteric dysbiosis.

experimental studies in these areas have enhanced our knowledge of radiation biology. However, translational research using these agents in various RIGS scenarios, such as prophylactic adjuncts in radiotherapy or post-exposure treatments for potential victims of radiation accidents, has been largely non-existent (5).

The radiosensitive human intestinal mucosa is in intimate contact with bacteria that outnumber the host somatic and germline cells by at least 10 times (1). These bacteria provide critical contributions to intestinal mucosal homeostasis. Gnotobiotic experiments have demonstrated that the commensal microbiota are necessary for the pathogenesis of RIGS (28); however, their exact role is poorly understood. Cellular signaling through toll-like receptors (TLRs) and other pathogen-associated molecular pattern (PAMP) recognition molecules plays a key role in the dynamic interactions between the host's enteric microbiota and innate immune system (29-31). It is thus unsurprising that bacterial-derived molecules that activate TLRs (32-35) or downstream transcription factors (36, 37) may possess radioprotective properties.

There are currently no U.S. Food and Drug Administration (FDA)-approved agents for the mitigation of the gastrointestinal (GI) consequences of therapeutic, accidental or intentional radiation exposure. Following a radiation disaster or act of terrorism, the goal would be to provide a potent frontline therapy that increases the chance for survival for exposed individuals. Ideally, this therapy would be easy to administer and have minimal deleterious side effects. We hypothesized that radiation might induce a clinically-important intestinal dysbiosis, and that an antibiotic with appropriate activity might prevent RIGS by inhibiting development of this dysbiosis. In the studies presented here, we compared the efficacy of several clinically relevant, FDA-approved antibiotics in treating RIGS in mice, and we identified one antibiotic, ciprofloxacin (cipro), which rescued mice from RIGS. We showed with clinical scoring,

enzyme-linked immunosorbent assays (ELISA) and high definition endoscopy that cipro prevented radiation-induced colitis. We demonstrated with high-throughput deep sequencing that cipro also inhibited the development of a profound dysbiosis that ensued in both biologically important mucosal and luminal bacterial communities in the small intestine and colon following radiation exposure. Finally, we utilized a gnotobiotic cecal content transplantation mouse model to demonstrate that modulation of the intestinal microbiota by cipro directly impacts host morbidity and mortality following irradiation.

Materials and methods

Radiation-Induced Gastrointestinal Syndrome (RIGS) Mouse Model. *Specific pathogen-free (SPF) mice.* All mice used were wild-type (WT) mice on a C57BL/6 (B6) background, purchased from Jackson Laboratories (Bar Harbor, Maine), bred for multiple generations and maintained in individually-ventilated microisolator cages (five mice per cage) in the same animal room at the University of North Carolina-Chapel Hill (UNC), and used for experiments at 8 to 12 weeks of age. In all experiments, mice were matched for gender, as gender-based genetic differences have been reported in B6 mice that may explain sexual dimorphism in IEC apoptotic responses to radiation (38). Mice in the colony were negative for all *Helicobacter* species. We used B6 mice because mice of this genetic background experience RIGS similar to that seen in humans, with translocation of bacteria to the blood, sepsis and early death, while other mouse strains do not (39). To avoid confounding cage effects on the composition and diversity of the intestinal microbiota, each experimental group was comprised of mice from multiple litters that were housed in separate cages. All animals were maintained under a 12-hour light/dark cycle in a temperature-controlled SPF facility and had free access to water and standard laboratory mouse chow unless otherwise specified.

Germ-free (GF) mice. All mice used were WT mice on a B6 background, and were maintained in GF conditions at the National Gnotobiotic Rodent Resource Center at UNC. Absence of isolator contamination was confirmed by Gram stain, fecal culture on Brain Heart Infusion agar with 10% sheep blood ([blood BHI]; Becton Dickinson, Sparks, MD) under aerobic and anaerobic conditions, and 16S ribosomal RNA (rRNA) PCR. All mouse experiments were approved by the UNC Institutional Animal Care and Use Committee.

Irradiation of mice. Mice that were not anesthetized received total body irradiation (TBI), with exposure to a single dose of 15 Gy external beam irradiation using an XRad320 x-ray machine (Precision X-Ray, North Branford, CT; Filter: 4 mm Cu; 47 cm; 320 kV/s, 12.5 mA; 1.0 Gy/min). 15 Gy TBI was used for all experiments except cecal content transplantation experiments, as this dose causes RIGS in 100% of our SPF B6 mice, consistent with previous reports (9, 25, 40). Although many past reports have suggested otherwise, recent evidence supports our findings that 15 Gy TBI universally causes RIGS in SPF B6 mice, while doses of 14 Gy and less do not (1, 26, 40). SPF mice were irradiated in a mouse irradiation pie cage (Braintree Scientific, Braintree, MA) that is divided to provide 12 ventilated restraints. Only 4 mice were irradiated simultaneously to facilitate the placement of all mice in the middle of the radiation field away from the periphery. For gnotobiotic experiments, a mouse irradiation pie cage with an autoclaved filter top (Braintree Scientific) was used to maintain sterility. Quality assessment experiments were performed regularly to confirm that dose and energy output remained within range. Experiments were separately performed with a ^{137}Cs source and an additional x-ray machine, with similar results.

Health status monitoring, survival of mice after irradiation and evaluation of animal death causes. Well-being of all animals was inspected daily from the initiation of treatment to

the end of the study. Daily water consumption was measured, and clinical colitis scores of 0-12 were given daily for the duration of the experiments, consisting of GI bleeding (0-4), stool consistency (0-4) and weight loss (0-4). GI bleeding was assessed by sampling for the presence of blood in the stool using a Hemoccult immunochemical fecal occult blood test (Beckman Coulter, Brea, CA). Upon termination of the experiment, mice were killed by CO_2 inhalation and cervical dislocation, and tissues were dissected for further analysis. To assess for bacteremia, blood was aseptically aspirated directly from the heart under a laminar flow hood. 0.5 mL cardiac blood per mouse was plated onto two blood BHI agar plates. One plate was incubated aerobically for 48 hours and the other was incubated anaerobically for 4 days, at which point plates were assessed for bacterial growth. Actuarial survival was calculated by the Kaplan-Meier method and statistical significance of survival differences were calculated by the Mantel log-rank test. Causes of death were evaluated by autopsies.

Antibiotic treatment of mice. B6 mice were treated with the following antibiotics (Sigma-Aldrich, St. Louis, MO) dissolved in their drinking water, starting one hour after radiation exposure, unless otherwise noted: ciprofloxacin, metronidazole, ciprofloxacin/metronidazole, rifaximin, trimethoprim and sulfamethoxazole and neomycin sulfate (n=8 mice/group). Experiments were conducted with administration of 50 mg/kg/day of each antibiotic, and then repeated at 25 mg/kg/day and 12.5 mg/kg/day with similar results. Daily fluid intake was recorded.

Enzyme-linked immunosorbent assays. Colon cultures were generated for assessing cytokine levels. Briefly, entire colons were cut longitudinally, gently washed in phosphate-buffered saline (PBS) to remove contents, and vigorously shaken for 30 minutes in RPMI-1640 medium (Sigma-Aldrich). Colons were then thoroughly blotted, weighed, divided into 100 mg

segments, placed in 24-well Corning Costar cell culture plates (Sigma-Aldrich) in duplicate or triplicate, as the amount of tissue permitted, cut into 0.5 to 1.0 cm pieces, and cultured in 1 mL/well of RPMI-1640 medium supplemented with 50 mg/mL gentamicin, 100 mg/mL streptomycin, and 0.25 mg/mL fungizone (antibiotic/antimycotic; Life Technologies [Gibco], Grand Island, NY). Cultures were incubated at 37° for 20 hours and then centrifuged, and supernatants were collected and stored at −80°C for ELISA**.** IL-12p40 and IL-1β concentrations were determined by sandwich ELISA, according to the manufacturer's instructions (BD Biosciences, San Jose, CA). Concentrations of cytokines were established in triplicate culture supernatants by comparison with standard curves generated using the appropriate recombinant cytokine.

Endoscopic investigation. The presence or absence of colon inflammation was evaluated in situ by mini-endoscopy (Karl Storz Veterinary Endoscopy, Goleta, CA). Mice were anesthetized with isoflurane (Minrad, Orchard Park, NY). If fecal matter obstructed visualization, colons were flushed with 1X PBS. After air inflation, the colonoscopy allowed for the real-time evaluation of 3–4 cm of colon from the anus to the splenic flexure. All colonoscopic procedures were digitally recorded. Endoscopy was performed on healthy control mice (n=2), mice exposed to radiation (day 5; n=3), and mice exposed to radiation and administered cipro (day 5; n=3).

Antibiograms. Antibiograms were performed on bacteria cultured from the blood of untreated, irradiated using the Kirby-Bauer disk diffusion sensitivity testing method. Paper discs impregnated with antibiotics were dropped in different zones of the culture on blood BHI agar plates. The diameters of the areas of bacterial lysis in millimeters, which can be converted to

μg/mL minimum inhibitory concentrations (MIC) using known linear regression curves, were recorded.

Crypt Regeneration Assay. Healthy control mice, irradiated mice and cipro-treated, irradiated mice were killed and the entire small intestine was harvested, cut longitudinally, gently washed with 1X PBS to remove contents, splayed out on 1.5 mm Whatman blotting paper (GE Healthcare, Little Chalfont, United Kingdom), and fixed in 10% phosphate-buffered formalin (Fisher Scientific, Pittsburgh, PA) for 24 hours. Fixed tissue was then rinsed in 1X PBS repeatedly, manipulated into Swiss roll conformation to maximize tissue surface area to score, embedded in paraffin and stained with hematoxylin and eosin (H&E). Scoring was performed blindly and the percentages of regenerating crypts per mouse and per group were determined according to a modification of established criteria (6, 41). Criteria for a surviving/regenerating crypt were 10 or more chromophilic, tightly packed cells, each with a prominent nucleus and little cytoplasm. Non-viable crypts contained no cells, or were sparsely populated by enlarged cells with prominent eosinophilic cytoplasm. Only regions that were oriented correctly and did not contain Peyer's patches were scored, as Peyer's patches influence both the number of crypts in a given circumference and the ability of a crypt to survive insult.

Bacterial Composition Analyses. *Genomic DNA extraction and 16S rRNA amplification*: Intestinal tissue and luminal samples were snap frozen on dry ice and stored at -80°C. 250 mg of frozen samples were suspended in sterile bacterial lysis buffer (200 mM NaCl, 100 mM Tris [pH 8.0], 20 mM EDTA, 20 mg/mL lysozyme [Sigma-Aldrich]) and incubated at 37°C for 30 minutes. Next, 40 μl of proteinase K (20 mg/mL; Qiagen, Valencia, CA) and 85 μl of 10% SDS were added to the mixture and incubated at 65°C for 30 minutes. 300 mg of 0.1 mm zirconium beads (BioSpec Products, Bartlesville, OK) were then added and the mixture was

homogenized in a bead beater (BioSpec Products) for 2 minutes. The homogenized mixture was cooled on ice and then centrifuged at 14,000 g for 5 minutes. The supernatant was transferred to a new 1.5 mL microfuge tube and DNA was further extracted by phenol/chloroform/iso-amyl alcohol [25:24:1 (v/v); Acros/Fisher Scientific] and then chloroform/iso-amyl alcohol [24:1 (v/v); Acros]. Following extraction, the supernatant was ethanol precipitated at -20°C for one hour. Precipitated DNA was suspended in DNase free H_20, cleaned using the Qiagen DNeasy Blood and Tissue extraction kit per manufacturer's instructions, quantified using a Nanodrop 2000c spectrophotometer (Fisher Scientific [Thermo]), and used to PCR amplify the V1-V3 (forward primer, 8F: 5'-AGAGTTTGATCMTGGCTCAG-3'; reverse primer, 518R: 5'-ATTACCGCGGCTGCTGG-3') hypervariable regions of the 16S rRNA gene. Forward primers were tagged with unique 10 base pair barcode labels at the 5' end along with the adaptor sequence (5'-CCATCTCATCCCTGCGTGTCTCCGACTCAG-3') to allow multiple samples to be included in a single plate as previously described (42, 43). 16S rRNA PCR products were quantified, pooled, and purified for the sequencing reaction.

454 pyrosequencing and analysis. Sequencing was performed on a 454 Life Sciences Genome Sequencer FLX machine (Roche, Florence, SC) at the UNC Microbiome core (http://www.med.unc.edu/microbiome). 16S rRNA sequence data was processed by the Quantitative Insights Into Microbial Ecology (QIIME) pipeline (44). Briefly, sequences were checked for quality and sequences that were less than 200 or greater than 1000 base pairs in length, that contained incorrect primer sequences, or that contained more than one ambiguous base were discarded. The remaining sequences were assigned to groups based on their unique nucleotide barcodes, including error correction (42). Sequences were clustered into operational taxonomic units (OTUs) based on sequence similarity at 97% sequence similarity (similar to

species level) using UC-LUST. A representative sequence for each OTU was chosen for downstream analysis based on the most abundant sequence from each OTU. PyNAST was used to align sequences with a minimum length of 150 base pairs and a minimum of 75% identity. OTUs were assigned to a taxonomy using the Ribosomal Database Project (RDP) Naive Bayes classifier. The RDP classifies a 16S rRNA sequence based on Bergey's manual of determinative bacteriology. A bacterial group was designated as unclassified if the 16S rRNA gene sequence from an organism did not show significant homology to any known classified bacterium in the RDP. β-diversity (diversity between groups of samples) was used to generate principal coordinate plots for each sample using unweighted and weighted UniFrac distances. β-diversity measurements were combined with each group to produce visualizations (principal coordinate analysis [PCoA]) that allow the composition of the intestinal microbiota of the groups to be characterized. PCoA plots were used to visualize the similarities or dissimilarities of variables that best represent the pair-wise distances between sample groups. We used taxon and phylogenetic-based analyses to compare 16S rRNA gene sequences. Taxon-based: The means and standard deviations of abundances of bacterial groups (phylum, class, order, family, and genus) were calculated and compared between groups of mice. Phylogenetic-based: Phylogenetic trees were generated using the QIIME pipeline. Each tree was subjected to weighted and unweighted UniFrac analysis. UniFrac distances represent the fraction of branch length that is shared by any two sample communities in a phylogenetic tree built from 16S rRNA sequence data from all samples. "Weighted" UniFrac analysis refers to microbiota community differences between sample groups due to differences in relative taxon abundance, whereas "unweighted" UniFrac analysis refers to microbiota community differences between sample groups based on the presence or absence of taxa. Weighted and unweighted UniFrac distances were compiled into

matrices and average UniFac distances were calculated for each group and compared using Student's *t*-test.

16S rRNA qPCR. All assays were performed in 96 well plates (Eppendorf, Hauppauge, NY) with appropriate standards, duplicate/triplicate reactions per sample and "no template" negative controls on an Eppendorf Realplex^2 mastercycler thermocycler. Each reaction was carried out in a final volume of 25 µl containing 1X SYBR Green (Life Technologies [Applied Biosystems]), 0.5 µM of each primer, and 10 ng of purified DNA. PCR conditions were as follows: 10 minutes at 95°C, followed by 40 cycles of 95°C for 15 seconds, 20 seconds at 50°C, and 72°C for 1 minute. Melting curves were assessed to confirm that the fluorescence signal originated from specific PCR products and not from primer dimers or other artifacts. Standards were generated by PCR amplification of target sequences from genomic DNA of an appropriate positive control strain. Standard curves were generated for each bacterial group and used to enumerate copy number in individual samples using appropriate bacterial primer sequences: Universal primers, 5'-GTGSTGCAYGGYTGTCGTCA-3' (forward primer) and 5'-ACGTCRTCCMCACCTTCCTC-3' (reverse primer); *E. coli* primers, 5′-GTTAATACCTTTGCTCATTGA-3′ (forward primer) and 5′-ACCAGGGTATCTAATCCTGTT-3′ (reverse primer); *Lactobacillus* genus primers, 5′-AGCAGTAGGGAATCTCCA-3′ (forward primer) and 5′-CACCGCTACACATGGAG-3′ (reverse primer); *Bifidobacterium* genus primers, 5′-GGGTGGTAATGCCGGATG-3' (forward primer) and 5′-CACCGCTACACATGGAG-3′ (reverse primer); and *Faecalibacterium prausnitzii* primers, 5′-GATGGCCTCGCGTCCGATTAG-3′ (forward primer) and 5′-CCGAAGACCTTCTTCCTCC-3′ (reverse primer). Fold change was calculated using the ΔΔCt method relative to universal 16S rRNA.

Terminal-Restriction Fragment Length Polymorphism (T-RFLP). The 16S rRNA gene was amplified by PCR using fluorescently labeled universal primers (carboxyfluorescein [FAM]-labeled 5'-AGAGTTTGATCCTGGCTCAG-3' [forward primer 8F] and hexachlorocarboxyfluorescein [HEX]-labeled 5'-GGTTACCTTGTTACGACTT-3' [reverse primer 1492R]). PCR products were purified using a Qiagen PCR purification kit and digested with Hha1 to generate terminal-restriction fragments (T-RFs) of varying sizes. All samples were also digested separately with Msp1. T-RFs were separated by capillary electrophoresis on a genetic analyzer (model 3100; Life Technologies [Applied Biosystems]). GeneMapper software (Life Technologies [Applied Biosystems]) was used to determine the size (T-RF length in base pairs), height (fluorescence intensity), and abundance (peak width X height) of each T-RF. T-RF size and abundance data from GeneMapper were compiled into a data matrix using Sequentix software (Sequentix, Germany).

Microbiota transplantation experiments. Cecal contents were pooled from 1) 12 SPF WT B6 mice on day #5 after 15 Gy, 2) 12 age- and gender-matched, non-irradiated littermates, and 3) 12 age- and gender-matched, non-irradiated littermates treated with cipro for 7 days. Cecal extracts were suspended in 8 mL PBS and administered to GF recipient WT B6 mice (n = 3-4 mice/group) orally, via rectal swab, in water, on food, and in bedding (2 mL per cage of 4 mice, including 200 ul orally). Transplanted mice were maintained in sterile cages and monitored daily for GI bleeding, diarrhea and weight loss. 72 hours after transplantation, mice were exposed to 10 Gy TBI while sterility was maintained, and then returned to cages for health status monitoring, continued clinical colitis scoring, and actuarial survival calculation.

Statistical analyses. *16S rRNA qPCR analysis.* These analyses and others were performed using the GraphPad Prism 5 software (GraphPad, La Jolla, CA). Means of normally

distributed data were compared using one-way analysis of variance (ANOVA), followed by Tukey's multiple comparison testing and 2-tailed, unpaired Student's *t*-test. When data was not normally distributed, the Kruskal-Wallis test was utilized to compare means, followed by Dunn's multiple comparison testing and 2-tailed Mann-Whitney tests. Data are expressed as mean ± SEM. Statistical significance was defined as $p<0.05$. In point plots, horizontal lines indicate means.

T-RFLP analysis. All T-RF data were standardized (individual T-RF peak height as a proportion of total T-RF peak heights within that sample), transformed by square root, and compiled into a Bray-Curtis similarity matrix using PRIMER version 6 software (Primer-E, Ivybridge, UK). To test for differences in global community composition, T-RF data were subjected to hierarchical cluster analysis followed by analysis of similarity (ANOSIM). Multidimensional scaling plots were constructed to illustrate similarity/dissimilarity. Biodiversity of each sample was measured by Shannon-Weiner diversity index while differences in richness or diversity between treatment groups were assessed by Student's *t* test.

Results

Ciprofloxacin prevents the radiation-induced gastrointestinal syndrome in mice. Given recent evidence that commensal enteric bacteria play an important role in RIGS, we investigated the efficacy of several clinically-relevant antibiotics in treating RIGS in mice. We studied several antibiotics that are commonly used clinically to treat diarrheal illnesses and intra-abdominal infections, including ciprofloxacin (cipro), metronidazole (met), rifaximin (rifax), trimethoprim-sulfamethoxazole (TMP-SMX) and neomycin (neo). We found that only one antibiotic, cipro, prevented the development of RIGS when administered continuously in drinking water starting one hour after radiation exposure. This was the case when 50 mg/kg/day

of each antibiotic was delivered, as well as when 25 or 12.5 mg/kg/day of each antibiotic was administered. Following radiation, clinical colitis scores were significantly lower in mice receiving cipro or the combination of cipro/met compared to mice exposed to equivalent doses of irradiation and receiving the same dose of other antibiotics (Figure 7.1A; $p<0.0001$). Cipro, but not other antibiotics, prevented radiation-induced GI bleeding (Figure 7.1B; $p<0.0001$) and diarrhea (Figure 7.1C; $p<0.0001$). Cipro's protection appeared to be primarily in the gut, as weight loss after radiation exposure was unaffected by cipro (Figure 7.1D). Gut-derived sepsis is a critical component of RIGS pathogenesis, and cipro also prevented the development of bacteremia following radiation (Figure 7.1E). Untreated mice exposed to 15 Gy died on days 5-7 post-irradiation, which is consistent with B6 mouse radiation mortality data in the literature (9, 25, 40). In contrast, mice treated with cipro after 15 Gy died on days 8-12 post-irradiation, which is improved survival compared to that achieved in previous studies with administration of growth factors or cytokines before lethal irradiation (17, 18, 22-25). Upon necropsy at days 8-12 post-irradiation, mice treated with cipro were found to have gross GI bleeding and, in some cases, intra-abdominal bleeding (Figure 7.1F), likely contributing to death as part of thrombocytopenia and the hematopoietic syndrome that ensue in the absence of a lethal RIGS. No gross GI bleeding or intra-abdominal bleeding was observed in untreated mice exposed to 15 Gy or in mice exposed to 15 Gy and treated with antibiotics other than cipro. These mice underwent necropsy 5-7 days after radiation.

Ciprofloxacin prevents radiation-induced colitis. We used several methods to demonstrate that radiation causes inflammation in the colon in mice. First, we showed that colonic weight, which is a non-specific marker of inflammation, is significantly increased in mice following radiation (Figure 7.2A; $p<0.04$). Second, colonic secretion of pro-inflammatory

cytokines IL-12p40 (Figure 7.2B; $p<0.0001$) and IL-1β (Figure 7.2C; $p<0.04$) is increased following radiation, as measured by ELISA. Finally, high definition endoscopy revealed erythema and loss of the vascular appearance of the colon in mice exposed to radiation, findings consistent with mild to moderate inflammation (Figure 7.2D). Cipro administration prevented radiation-induced colitis, as assessed by colonic weight (Figure 7.2A; $p<0.002$), colonic secretion of IL-12p40 (Figure 7.2B; $p<0.002$) and IL-1β (Figure 7.2C; $p<0.02$), and mouse endoscopy (Figure 7.2D).

Ciprofloxacin has strong bactericidal activity against microbes that translocate to the blood following radiation exposure. Gut-derived sepsis is believed to be a critical component of the pathogenesis of RIGS. We examined the ability of several clinically-relevant antibiotics to kill bacteria that translocate to the blood in mice exposed to lethal doses of irradiation. Cipro had 100% bactericidal activity against 16 randomly chosen isolates cultured from the cardiac blood of untreated, irradiated mice, while other antibiotics demonstrated 20-67% bactericidal activity against the same isolates (Figure 7.3A). The mean zones of inhibition, which were converted to Minimum Inhibitory Concentrations (MICs), were determined for each antibiotic against each bacterial isolate. Cipro demonstrated a mean zone of inhibition of 11.3 mm, while the mean zone of inhibition of other antibiotics ranged from 0.9-7.6 mm (Figure 7.3B).

Events ensuing in the first 24 hours after radiation exposure critically impact host morbidity and mortality. Because radiation exposure can occur unexpectedly in the case of a nuclear reactor meltdown or nuclear terrorist attack, we set out to determine how soon cipro must be administered following radiation exposure to obtain protection from RIGS. We exposed mice to 15 Gy TBI, administered cipro continuously in drinking water starting at 0, 1, 12, and 24

hours after exposure, and found that significant protection was conferred from RIGS only if cipro was started by 12 hours after radiation exposure (Figure 7.4A). Furthermore, only one dose of cipro administered directly by mouth 1 hour after radiation was sufficient to confer protection. In fact, untreated, irradiated cage mates of mice receiving one oral dose of cipro experienced prolonged survival similar to that of their cipro-treated cage mates (Figure 7.4B). IEC apoptotic and proliferative responses to radiation, which determine the ultimate fate of intestinal crypts, peak within the first 4-8 hours following exposure, then quickly return to near-baseline levels. And cipro administration preserved small intestinal and colonic crypts in mice after lethal irradiation (Figure 7.4C-D). Cumulatively, these data suggest that there are events in the first 24 hours after radiation exposure that critically impact host morbidity and mortality.

Ciprofloxacin prevents radiation-induced shifts in the overall composition of the intestinal microbiota that begin within the first 24 hours. We identified an intestinal dysbiosis that ensues within 24 hours of radiation exposure. Principal coordinate analysis (Figure 7.5A) and hierachial clustering (Figure 7.5B) of intestinal bacterial communities generated by QIIME analysis of 16S rRNA-based 454 pyrosequencing data revealed that a dysbiosis occurs after radiation in the small intestine and colon, in both biologically-important mucosal and luminal bacterial communities. Cipro largely prevents these radiation-incited shifts in the composition of the microbiota in the jejunum mucosa, cecum lumen, cecum mucosa and distal colon mucosa (Figure 7.5A-B). Multidimensional scaling plots generated with a second technique, T-RFLP, confirmed that cipro alters the radiation-impelled intestinal dysbiosis (Figure 7.5C). T-RFLP also suggested that reductions in intestinal bacterial richness initiated by radiation were partly prevented by cipro administration (Figure 7.5D). Another measure of the diversity of a complex bacterial community is β-diversity, or the diversity between groups. We assessed intestinal

bacterial β-diversity by calculating average weighted UniFrac distances of microbial communities generated by QIIME, and we found that cipro prevented increases in β-diversity actuated by radiation in the cecum lumen ($p=0.0001$), cecum mucosa ($p=0.05$) and distal colon mucosa ($p<0.003$) (Figure 7.5E).

Ciprofloxacin largely prevents alterations in predominant intestinal bacterial phyla following radiation exposure. To evaluate the effect of cipro on the abundance of groups within the gut microbiota following radiation, we determined the number of different bacterial groups in each sample by using 3% dissimilarity between 16S rRNA gene sequences as an indicator of a "species level" OTU. The abundances of different bacterial taxa ranging from phylum to species, identified by 16S rRNA V1-V3 region OTU sequence alignments, were found to differ between untreated mice exposed to radiation and mice exposed to radiation and administered cipro. At the phylum level, radiation exposure resulted in significant decreases in levels of enteric Firmicutes, with concomitant increases in Proteobacteria members. Cipro administration largely prevented these alterations in phylum level intestinal bacterial community composition (Figure 7.6).

Ciprofloxacin inhibits changes in concentrations of important intestinal bacterial groups caused by radiation. 454 pyrosequencing revealed increases in intestinal populations of the Proteobacteria phylum following radiation that were prevented by cipro administration. To determine what members of this phylum were increased by radiation, we used 16S rRNA qPCR and bacterial species specific primers. *E. coli*, *Pseudomonas flourescens* and *Klebsiella pneumoniae*, all members of the Gamma Proteobacteria class within the Proteobacteria phylum, were increased in the gut following radiation, and cipro largely prevented these increases (Figure 7.7A). Conversely, *Lactobacillus* species, (members of the Firmicutes phylum that was identified by deep sequencing as decreasing in the small intestine and colon following radiation), were

reduced by radiation, but cipro administration largely preserved these enteric bacterial populations (Figure 7B). Deep sequencing and qPCR revealed that *Bacteroides* species increased after radiation in the cecum mucosa, but not when cipro was administered starting one hour after radiation exposure (Supplementary Figure 7.1).

Effects of ciprofloxacin on the intestinal microbiota directly impact host morbidity and mortality following radiation. To address the question of whether or not the effects of cipro on radiation-induced dysbiosis impact host morbidity and mortality following radiation, we performed cecal content transplantation experiments. We harvested cecal contents from 3 groups of mice and transplanted them into GF recipient mice that were maintained in sterile cages. The 3 donor groups were: 1) healthy mice 2) mice exposed to radiation 3) mice treated with cipro. After a 72 hour post-transplantation equilibration period, all 3 groups of mice were exposed to an equivalent dose of radiation. We found that mice transplanted with microbiota from cipro-treated mice had significantly prolonged survival after exposure to a lethal dose of irradiation compared to mice receiving normal microbiota or post-irradiation microbiota (Figure 7.8; $p<0.02$).

Discussion

Ionizing radiation is widely used in medicine for treating cancers, in industrial radiographic devices, and in generating electrical power in nuclear reactors. Gamma rays and x-rays easily penetrate body tissues and injure internal organs. Recent world events have reminded us that use of nuclear power is not without risk. While nuclear power is clean and sustainable, it can cause considerable loss of human health and life. Even with the most stringent measures, the risk of radiation exposure cannot be eradicated. Many agents have been investigated as potential mitigators of radiation intestinal injury in humans, with negative or very modest results, including growth factors (21), cytokines (13, 45), prostaglandins (46, 47), vitamins (48-50), and

thiols (51). Almost all studies that claim efficacy of agents against radiation intestinal injury investigated radiation doses that do not consistently cause RIGS (13, 20, 21, 33, 35, 45, 49, 50, 52-59) or did not show protection with post-radiation exposure administration (20, 21, 27, 32, 35, 45, 49, 50, 52, 55, 57-59). Some investigators have anesthetized mice before delivering experimental radiation (14, 20, 33, 56, 60), despite the fact that anesthetics can have unpredictable effects on radiosensitivity.

Antibiotics have been considered for decades as a potential treatment option for radiation enteropathy (1, 61). Yet, the last serious attention that antibiotics received as potential intestinal radioprotectors was in the 1990's when investigators at the Armed Forces Radiobiology Research Institute studied the efficacy of antibiotics in several radiation mouse models (62-64). These studies were limited by their focus on activity of antibiotics against orally ingested pathogens, their use of hepatic bacterial translocation and mortality as primary readouts, and their evaluation of radiation doses that do not cause RIGS. In a 2004 review, these authors concluded that they were not able to identify an antibiotic that was most effective among those studied (65).

Here, we report that the mean survival of mice exposed to 15 Gy is approximately 10 days when they are administered the antibiotic ciprofloxacin, and cipro is effective when administered between 1-12 hours after exposure. In comparison, three of the most noteworthy previous studies reported genetic or pharmacologic protection of a total of 54 mice from radiation doses of 15-16 Gy, with a mean survival of 8.2 days in treated mice (9, 23, 25). In addition, the evaluation of intestinal radioprotection in mice should be multiparametric (25), and we employed an intestinal crypt regeneration assay, Kaplan-Meier dose survival analysis, and autopsy evaluation of every experimental animal at the time of death. In addition, we did not

anesthetize animals prior to radiation in order to avoid the potential impact of these drugs on intestinal radiosensitivity.

Humans undergoing radiation therapy for abdominal or pelvic malignancy receive lower, fractionated doses of radiation. While our studies focused on single doses of radiation, it is possible that cipro may also confer intestinal radioprotection from similar total doses that are fractionated therapeutically. If this is the case, quality of life of cancer patients undergoing radiation treatment may be improved by cipro's reduction of adverse side effects including diarrhea and by cipro's contribution to the maintenance of intestinal mucosal integrity. This may allow for radiation dose escalation and, hence, improved cancer cure rates. By preserving the intestinal mucosa, cipro may also prevent the development of fibrosis and potentially life-threatening fibrosis-related sequelae months to years after radiation treatment or exposure. It is important to note that we did not study the effect of cipro on tumor radiosensitivity. These are fruitful areas for future investigations.

This study raises the possibility of using oral cipro as a radioprotective agent in man and provides insight into the timing and mechanism of cipro-mediated protection from RIGS. In an era of increased risk for radiological accident and terrorism, medical contingency plans and preparedness are crucial to saving lives. Effective radiomitigators are key to the success of preparedness. Yet, there are no FDA-approved agents to mitigate the lethal effects of RIGS. Our findings suggest that cipro may serve as an intervention that mitigates death from RIGS through its prevention of profound enteric dysbiosis. Ciprofloxacin is an approved oral drug, available in the market and thus may be easier to be developed as a medical countermeasure for RIGS in humans. The single, oral, low dose of cipro required for its radiomitigation effects underscores its potency, safety, ease of administration, and low expense. Oral delivery provides a quick route

of administration in the event of a nuclear disaster without the need for specialized personnel. In addition, cipro can be used in combination with agents that have been approved as treatments for the radiation hematopoietic syndrome, such as granulocyte-colony stimulating factor (G-CSF) (66). Given its favorable safety and expense profile as an FDA-approved generic antibiotic, cipro could be rapidly and cheaply disseminated to all individuals in the vicinity of a radiological event, even in the absence of knowledge of actual level of radiation exposure. As such ciprofloxacin fulfills a mandate of the United States Department of Health and Human Services Public Health Emergency Medical Countermeasures Enterprise, a national security measure designed to protect the American public from the use of weapons of mass destruction, consistent with the goals of the President's Biodefense for the 21st Century and National Strategy for Medical Countermeasures against Weapons of Mass Destruction directives.

REFERENCES

1. Packey CD, Ciorba MA. Microbial influences on the small intestinal response to radiation injury. Curr Opin Gastroenterol 2010; 26: 88-94.

2. Bhattacharjee Y. Devastation in Japan. Candidate radiation drugs inch forward. Science 2011; 331(6024): 1505.

3. Waselenko JK, MacVittie TJ, Blakely WF, et al. Medical management of the acute radiation syndrome: recommendations of the Strategic National Stockpile Radiation Working Group. Ann Intern Med 2004; 140: 1037-1051.

4. Wolbarst AB, Wiley AL, Nemhauser JB, et al. Medical response to a major radiologic emergency: a primer for medical and public health practitioners. Radiology 2010; 254: 660-677.

5. Weiss JF, Landauer MR. History and development of radiation-protective agents. Int J Radiat Biol 2009; 85: 539-573.

6. Withers HR, Elkind MM. Radiosensitivity and fractionation response of crypt cells of mouse jejunum. Radiat Res 1969; 38: 598-613.

7. Withers HR. Regeneration of intestinal mucosa after irradiation. Cancer 1971; 28: 75-81.

8. Potten CS. A comprehensive study of the radiobiological response of the murine (BDF1) small intestine. Int J Radiat Biol 1990; 58: 925-973.

9. Ch'ang HJ, Maj JG, Paris F, et al. ATM regulates target switching to escalating doses of radiation in the intestines. Nat Med 2005; 11: 484-490.

10. Brown M. What causes the radiation gastrointestinal syndrome?: Overview. Int J Radiation Oncology Biol Phys 2008; 70: 799-803.

11. Kirsch DG, Santiago PM, di Tomaso E, et al. p53 controls radiation-induced gastrointestinal syndrome in mice independent of apoptosis. Science 2010; 327(5965): 593-6.

12. Schuller BW, Binns PJ, Riley KJ, et al. Selective irradiation of the vascular endothelium has no effect on the survival of murine intestinal crypt stem cells. Proc Natl Acad Sci USA 2006; 103: 3787-3792.

13. Kawashima R, Kawamura YI, Kato R, et al. IL-13 receptor α2 promotes epithelial cell regeneration from radiation-induced small intestinal injury in mice. Gastroenterology 2006; 131: 130-141.

14. Booth D, Haley JD, Bruskin AM, Potten CS. Transforming growth factor-B3 protects murine small intestinal crypt stem cells and animal survival after irradiation, possibly by reducing stem-cell cycling. Int J Cancer 2000; 86: 53-59.

15. Gudkov AV, Komarova EA. Radioprotection: smart games with death. J Clin Invest 2010; 120: 2270-2273.

16. Qiu W, Carson-Walter EB, Liu H, et al. PUMA regulates intestinal progenitor cell radiosensitivity and gastrointestinal syndrome. Cell Stem Cell 2008; 2: 576-583.

17. Booth D, Potten CS. Protection against mucosal injury by growth factors and cytokines. J Natl Cancer Inst Monogr 2001; pp 16-20.

18. Khan WB, Shui C, Ning S, Knox SJ. Enhancement of murine intestinal stem cell survival after irradiation by keratinocyte growth factor. Radiat Res 1997; 148: 248-253.

19. Zhang L, Sun W, Wang J, et al. Mitigation effect of an FGF-2 peptide on acute gastrointestinal syndrome after high-dose ionizing radiation. Int J Radiat Oncol Biol Phys 2010; 77: 261-268.

20. Bhanja P, Saha S, Kabarriti R, et al. Protective role of R-spondin1, an intestinal stem cell growth factor, against radiation-induced gastrointestinal syndrome in mice. PLoS ONE 2009; 4: e8014.

21. Farrell CL, Bready JV, Rex KL, et al. Keratinocyte growth factor protects mice from chemotherapy and radiation-induced gastrointestinal injury and mortality. Cancer Res 1998; 58: 933-939.

22. Okunieff P, Mester M, Wang J, et al. In vivo radioprotective effects of angiogenic growth factors on the small bowel of C3H mice. Radiat Res 1998; 150: 204-211.

23. Paris F, Fuks Z, Kang A, et al. Endothelial apoptosis as the primary lesion initiating intestinal radiation damage in mice. Science 2001; 293: 293-297.

24. Maj JG, Paris F, Haimovitz-Friedman A, et al. Microvascular function regulates intestinal crypt response to radiation. Cancer Res 2003; 63: 4338-4341.

25. Rotolo JA, Maj JG, Feldman R, et al. Bax and Bak do not exhibit functional redundancy in mediating radiation-induced endothelial apoptosis in the intestinal mucosa. Int J Radiat Oncol Biol Phys 2008; 70: 804-815.

26. Rotolo J, Stancevic B, Zhang J, et al. Anti-ceramide antibody prevents the radiation gastrointestinal syndrome in mice. J Clin Invest 2012; 122: 1786-1790.

27. Bonnaud S, Niaudet, Legoux F, et al. Sphingosine-1-phosphate activates the AKT pathway to protect small intestines from radiation-induced endothelial apoptosis. Cancer Res. 2010; 70(23): 9905-15.

28. Crawford PA, Gordon JI. Microbial regulation of intestinal radiosensitivity. Proc Natl Acad Sci USA 2005; 102(37): 13254-9.

29. Stenson WF. Toll-like receptors and intestinal epithelial repair. Curr Opin Gastroenterol 2008; 24: 103-107.

30. Rakoff-Nahoun S, Paglino J, Eslami-Varzaneh F, et al. Recognition of commensal microflora by toll-like receptors is required for intestinal homeostasis. Cell 2004; 118: 229-241.

31. Rachmilewitz D, Katakura K, Karmeli F, et al. Toll-like receptor 9 signaling mediates the anti-inflammatory effects of probiotics in murine experimental colitis. Gastroenterology 2004; 126: 520-528.

32. Burdelya LG, Krivokrysenko VI, Tallant TC, et al. An agonist of toll-like receptor 5 has radioprotective activity in mouse and primate models. Science 2008; 320: 226-30.

33. Saha S, Bhanja P, Liu L, et al. TLR9 agonist protects mice from radiation-induced gastrointestinal syndrome. PLoS ONE 2012; 7: e29357.

34. Riehl, Cohn S, Tessner T, et al. Lipopolysaccharide is radioprotective in the mouse intestine through a prostaglandin-mediated mechanism. Gastroenterology 2000; 118: 1106-16.

35. Jones RM, Sloane VM, Wu H, et al. Flagellin administration protects gut mucosal tissue from irradiation-induced apoptosis via MKP-7 activity. Gut 2011; 60: 648-57.

36. Egan LJ, Eckmann L, Greten FR, et al. IκB-kinaseβ-dependent NF-κB activation provides radioprotection to the intestinal epithelium. Proc Natl Acad Sci U S A 2004; 101: 2452-2457.

37. Wang Y, Meng A, Lang H, et al. Activation of nuclear factor kappa B *in vivo* selectively protects the murine small intestine against ionizing radiation-induced damage. Cancer Res 2004; 64: 6240-6246.

38. Weil MM, Xia C, Xia X, et al. A chromosome 15 quantitative trait locus controls levels of radiation-induced jejunal crypt cell apoptosis in mice. Genomics 2001; 72: 73-77.

39. Duran-Struuck R, Hartigan A,Clouthier SG, et al. Differential susceptibility of C57BL/6NCr and B6.Cg-Ptprc^{a} mice to commensal bacteria after whole body irradiation in translational bone marrow transplant studies. J Transl Med 2008; 6: 10.

40. Rotolo JA, Kolesnick R, Fuks Z. Timing of lethality from gastrointestinal syndrome in mice revisited. Int J Radiat Oncol Biol Phys 2009; 73: 6-8.

41. Withers HR, Elkind MM. Microcolony survival assay for cells of mouse intestinal mucosa exposed to radiation. Int J Radiat Biol Relat Stud Phys Chem Med 1970; 17(3): 261-267.

42. Hamady M, Walker JJ, Harris JK, et al. Error-correcting bar-coded primers for pyrosequencing hundreds of samples in multiplex. Nat Methods 2008; 5: 235-7.

43. Fierer N, Hamady M, Lauber CL, et al. The influence of sex, handedness, and washing on the diversity of hand surface bacteria. Proc Natl Acad Sci U S A 2008; 105: 17994-9.

44. Caporaso JG, Kuczynski J, Stombaugh J, et al. QIIME allows analysis of high-throughput community sequencing data. Nat Methods 2010; 7: 335-6.

45. Potten CS. Protection of the small intestinal clonogenic stem cells from radiation-induced damage by pretreatment with interleukin 11 also increases murine survival time. Stem Cells 1996; 14: 452-459.

46. Hanson WR. Radiation protection of murine intestine by WR-2721, 16, 16-dimethyl prostaglandin E2, and the combination of both agents. Radiat Res 1987; 111: 361-373.

47. Houchen CW, Sturmoski MA, Anant S, et al. Prosurvival and antiapoptotic effects of PGE2 in radiation injury are mediated by EP2 receptor in intestine. Am J Physiol-Gastrointest Liver Physiol 2003; 284: G490-498.

48. Empey LR, Papp JD, Jewell LD, Fedorak RN. Mucosal protective effects of vitamin E and misoprostol during acute radiation-induced enteritis in rats. Digest Dis Sci 1992; 37: 205-214.

49. Yamamoto T, Kinoshita M, Shinomiya N, et al. Pretreatment with ascorbic acid prevents lethal gastrointestinal syndrome in mice receiving a massive amount of radiation. J Radiat Res 2010; 51: 145-156.

50. Berbee M, Qiang F, Boerma M, et al. γ-tocotrienol ameliorates intestinal radiation injury and reduces vascular oxidative stress after total-body irradiation by an HMG-CoA reductase-dependent mechanism. Radiat Res 2009; 171(5): 596-605.

51. Yuhas JM, Storer JB. Chemoprotection against three modes of radiation death in the mouse. Int J Radiat Biol Relat Stud Phys Chem Med 1969; 15: 233-237.

52. Ciorba MA, Riehl TE, Rao MS, et al. *Lactobacillus* probiotic protects intestinal epithelium from radiation injury in a TLR-2/cyclo-oxygenase-2-dependent manner. Gut 2011; 61: 829-838.

53. Basile LA, Ellefson D, Gluzman-Poltorak Z, et al. HemaMax^{TM}, a recombinant human interleukin-12, is a potent mitigator of acute radiation injury in mice and non-human primates. PLoS ONE 2012; 7: e30434.

54. Chen BJ, Deoliveira D, Spasojevic I, et al. Growth hormone mitigates against lethal irradiation and enhances hematologic and immune recovery in mice and nonhuman primates. PLoS ONE 2010; 5: e11056.

55. Garin-Laflam MP, Steinbrecher KA, Rudolph JA, et al. Activation of guanylate cyclase C signaling pathway protects intestinal epithelial cells from acute radiation-induced apoptosis. Am J Physiol Gastrointest Liver Physiol 2009; 296: G740-749.

56. Ajakaiye MA, Jacob A, Wu R, et al. Recombinant human MFG-E8 attenuates intestinal injury and mortality in severe whole body irradiation in rats. PLoS ONE 2012; 7: e46540.

57. Wang J, Boerma M, Fu Q, et al. Simvastatin ameliorates radiation enteropathy development after localized, fractionated irradiation by a protein C-independent mechanism. Int J Radiat Oncol 2007; 68: 1483-1490.

58. Hussein MR, Abu-Dief EE, Kamel E, et al. Melatonin and roentgen irradiation-induced acute radiation enteritis in Albino rats: An animal model. Cell Biol Int 2008; 32: 1353-1361.

59. Pamujula S, Kishore V, Rider B, et al. Radioprotection in mice following oral administration of WR-1065/PLGA nanoparticles. Int J Radiat Biol 2008; 84: 900-908.

60. Booth C, Tudor G, Tudor J, et al. Acute gastrointestinal syndrome in high-dose irradiated mice. Health Phys 2012; 103(4): 383-99.

61. Livstone EHT, Spiro H, Floch M. The gastrointestinal microflora of irradiated mice. II. Effect of oral antibiotic administration on the colonic flora and survival of adult mice. Yale J Biol Med 1970; 42: 448-454.

62. Brook I, Elliot TB, Ledney GD. Quinolone therapy of *Klebsiella pneumoniae* sepsis following irradiation: comparison of pefloxacin, ciprofloxacin, and ofloxacin. Radiat Res 1990; 122: 215-217.

63. Brook I, Tom SP, Ledney GD. Development of infection with *Streptococcus bovis* and *Aspergillus* sp. in irradiated mice after glycopeptide therapy. J Antimicrob Chemother 1993; 32: 705-713.

64. Brook I, Ledney GD. The treatment of irradiated mice with polymicrobial infection caused by *Bacteroides fragilis* and *Escherichia coli.* J Antimicrob Chemother 1994; 33: 243-252.

65. Brook I, Elliott TB, Ledney GD, et al. Management of postirradiation infection: lessons learned from animal models. Mil Med 2004; 169: 194-197.

66. Tanikawa S, Nose M, Akoi Y, et al. Effects of recombinant human granulocyte colony stimulating factor on the hematologic recovery and survival of irradiated mice. Blood 1990; 76: 445-449.

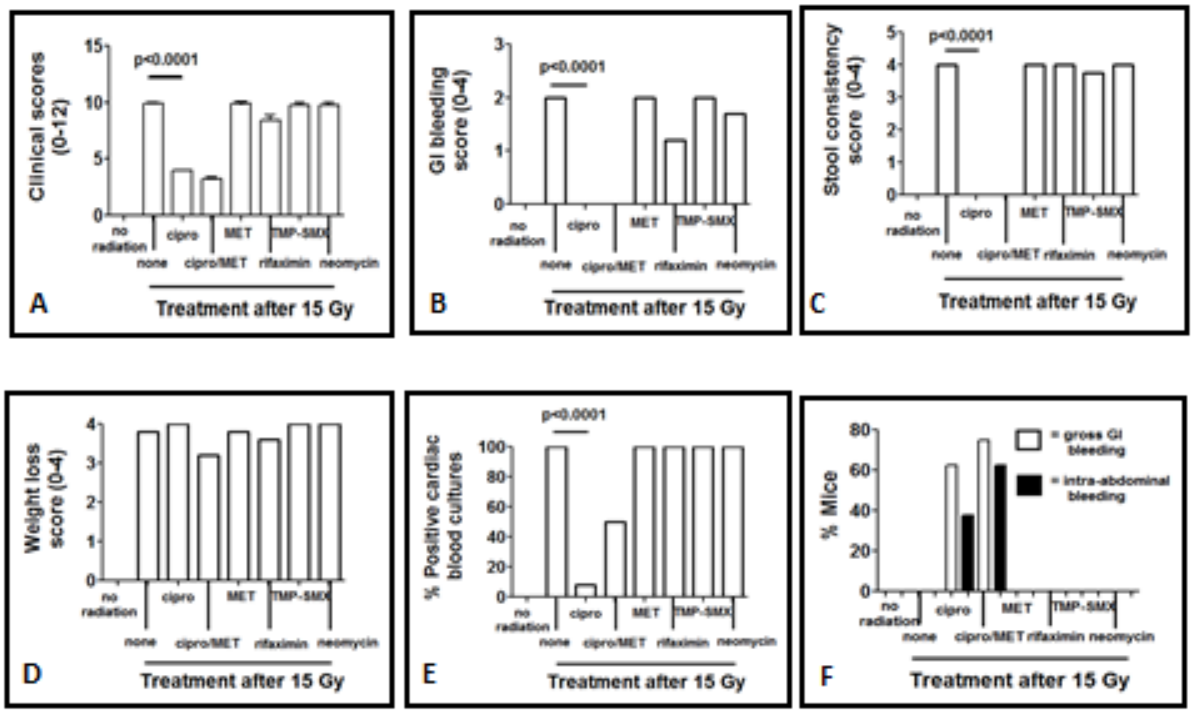

Figure 7.1. Ciprofloxacin (cipro) prevents radiation gastrointestinal syndrome (RIGS). (A) Antibiotics were administered to mice in drinking water, starting one hr after 15 Gy TBI (n=8 mice/group). Clinical colitis scores at day 5 after radiation are shown. Mean clinical colitis scores for untreated, irradiated mice and irradiated mice treated with metronidazole (MET), rifaximin (RIF), trimethoprim-sulfamethoxazole (TMP) or neomycin (NEO) were 8.4-9.9. Mean clinical colitis scores for irradiated mice receiving cipro or cipro/MET were 4.0 and 3.2, respectively. (B) Untreated mice and mice treated with MET, RIF, TMP or NEO after radiation have guaiac positive stools 5 days after radiation, while irradiated mice treated with cipro or cipro/MET have no evidence of GI bleeding. (C) Untreated mice and mice treated with MET, RIF, TMP or NEO after radiation have loose stools 5 days after radiation, while irradiated mice treated with cipro or cipro/MET have normal stools. (D) Cipro had no effect on weight loss following radiation exposure. (E) Radiation exposure results in bacteremia. Cipro reduced the percentage of irradiated mice with positive blood cultures from 100% to 8%. (F) Mice treated with cipro or cipro/MET after radiation live 5-9 days longer than untreated mice or mice treated with other antibiotics. At necropsy, 62.5% of mice treated with cipro after radiation are found to have gross blood in their intestinal contents, while 75% of mice treated with cipro/MET after radiation have gross GI bleeding. Irradiated mice that are untreated or treated with other antibiotics die of presumed sepsis and have no evidence of GI bleeding. 37% of irradiated mice treated with cipro and 62.5% of mice treated with cipro/MET have intra-abdominal bleeding at necropsy, while untreated, irradiated mice and irradiated mice treated with other antibiotics have no intra-abdominal bleeding. cipro=ciprofloxacin; MET=metronidazole; TMP-SMX=trimethoprim-sulfamethoxazole; GI=gastrointestinal.

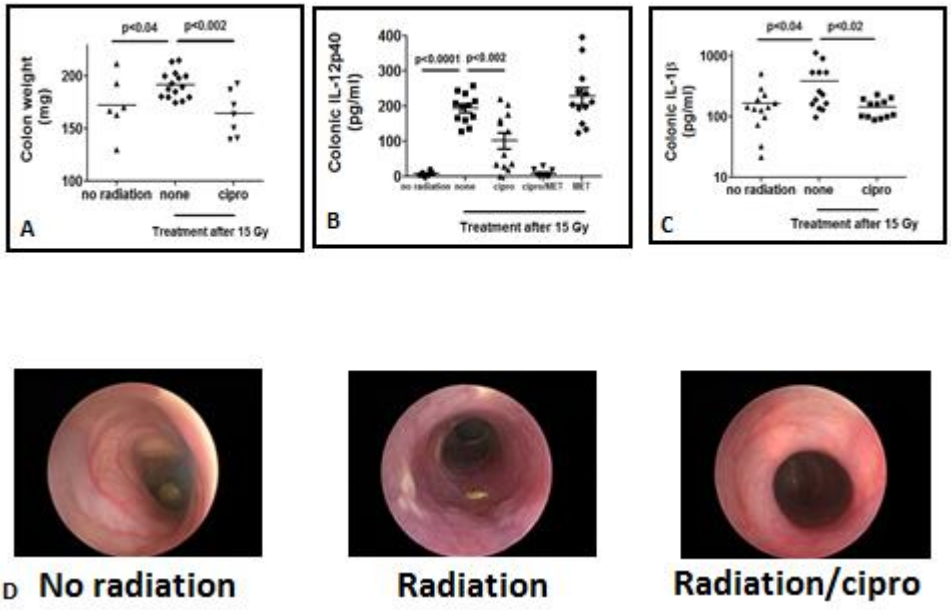

Figure 7.2. Ciprofloxacin prevents radiation-induced colitis. (A) Colon weight, a non-specific marker of inflammation, is increased in untreated mice on day 5 after radiation, but not in irradiated mice treated with cipro ($p<0.002$). (B) Radiation results in significant secretion of the pro-inflammatory, Th-1-mediated cytokine interleukin-12p40 (IL-12p40) by *ex vivo* colonic tissue explants at 5 days after exposure, as measured by ELISA. Cipro and cipro/MET administration after radiation reduce colonic IL-12p40 secretion, but MET alone does not. (C) Colonic tissue secretion of pro-inflammatory, Th-1-mediated cytokine IL-1β is also increased at 18 hours after radiation exposure, and cipro administration prevents this increased secretion. (D) High-resolution endoscopy revealed evidence of mild to moderate colonic injury 5 days after radiation (middle; n=3), while cipro-treated, irradiated mice have colonic mucosa (right; n=3) that is similar in appearance to that of a healthy mouse (left; n=2).

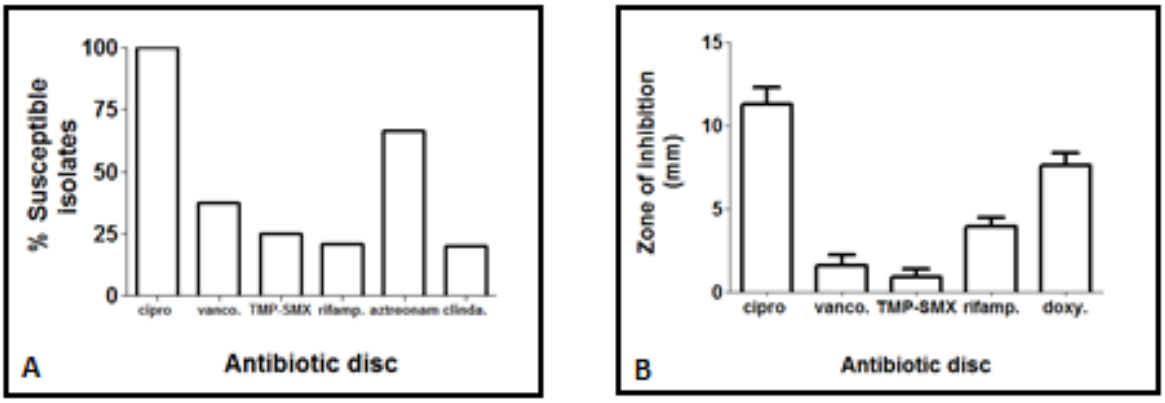

Figure 7.3. Cipro has strong bactericidal activity against microbes that translocate to the blood following radiation exposure. Antibiograms of bacteria cultured from the blood of untreated mice after 15 Gy using the Kirby-Bauer disk diffusion sensitivity testing method. (A) 100% of isolates (n=16) were susceptible to killing by cipro, compared to 67% susceptibility to aztreonam (n=15), 37% to vancomycin (n=16), 25% to trimethoprim-sulfamethoxazole (n=16), 21% to rifampin (n=16), and 20% to clindamycin (n=15). The mean zone of inhibition of bacterial growth was 11.3 mm with cipro, compared to 1.6 mm with vancomycin, 0.9 mm with trimethoprim-sulfamethoxazole, and 3.9 mm with rifampin. Cipro=ciprofloxacin; vanco=vancomycin; TMP-SMX=trimethoprim-sulfamethoxazole; rifamp=rifampin; clinda=clindamcyin; doxy=doxycycline.

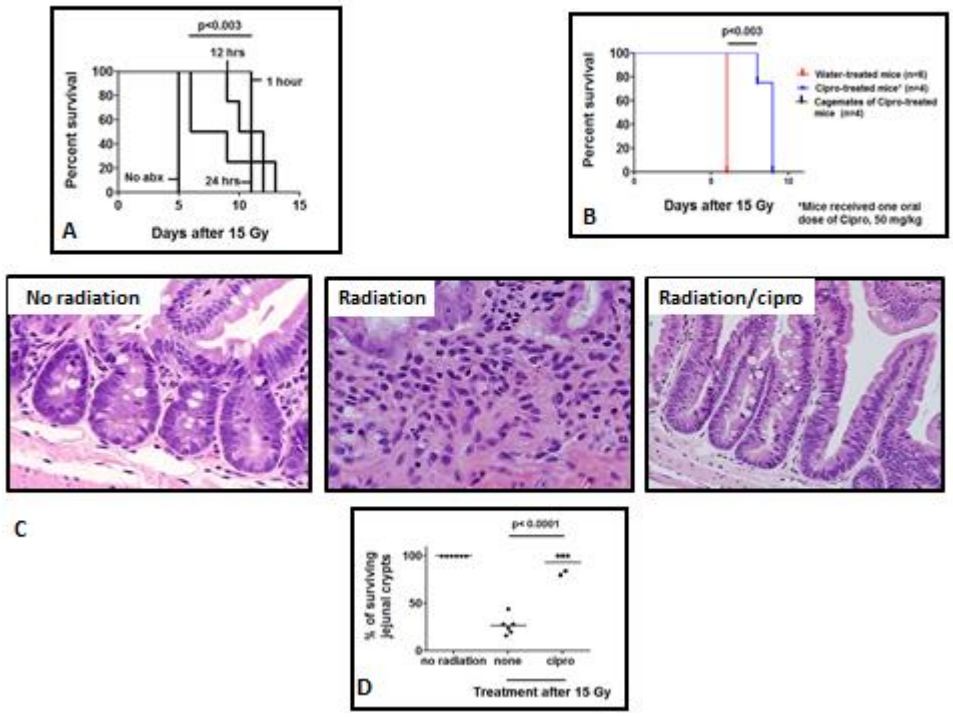

Figure 7.4. Events ensuing in the first 24 hours after radiation exposure are critical to host morbidity and mortality. (A) Delaying cipro treatment until 24 hours after radiation exposure results in mortality similar to that seen in untreated, irradiated mice, even when cipro is administered continuously in drinking water. Median survival after 15 Gy is 5 days without intervention. Median survival after 15 Gy is 11.5 days when cipro is administered continuously starting one hour after radiation exposure. However, median survival after 15 Gy is only 6 days when cipro is administered continuously starting at 24 hours after radiation exposure. n=4 mice per group. (B) Just one dose of cipro, 50 mg/kg administered orally by pipette one hour after radiation, prolongs survival in mice and in their untreated, irradiated cage mates ($p<0.003$). (C) Representative histology (n=6) from paraffin-embedded mid-jejunal sections of healthy mice (left), mice exposed to radiation (middle), and mice exposed to radiation and treated with cipro starting one hour after exposure (right). Magnification 20X. Hematoxylin and eosin staining demonstrates loss of intestinal crypt architecture following radiation, compared to preservation of crypt and villus structure with cipro administration. Crypt regeneration assay quantitates crypt preservation by cipro following lethal irradiation (D; $p<0.0001$), and this is seen as early as 24 hours after radiation exposure.

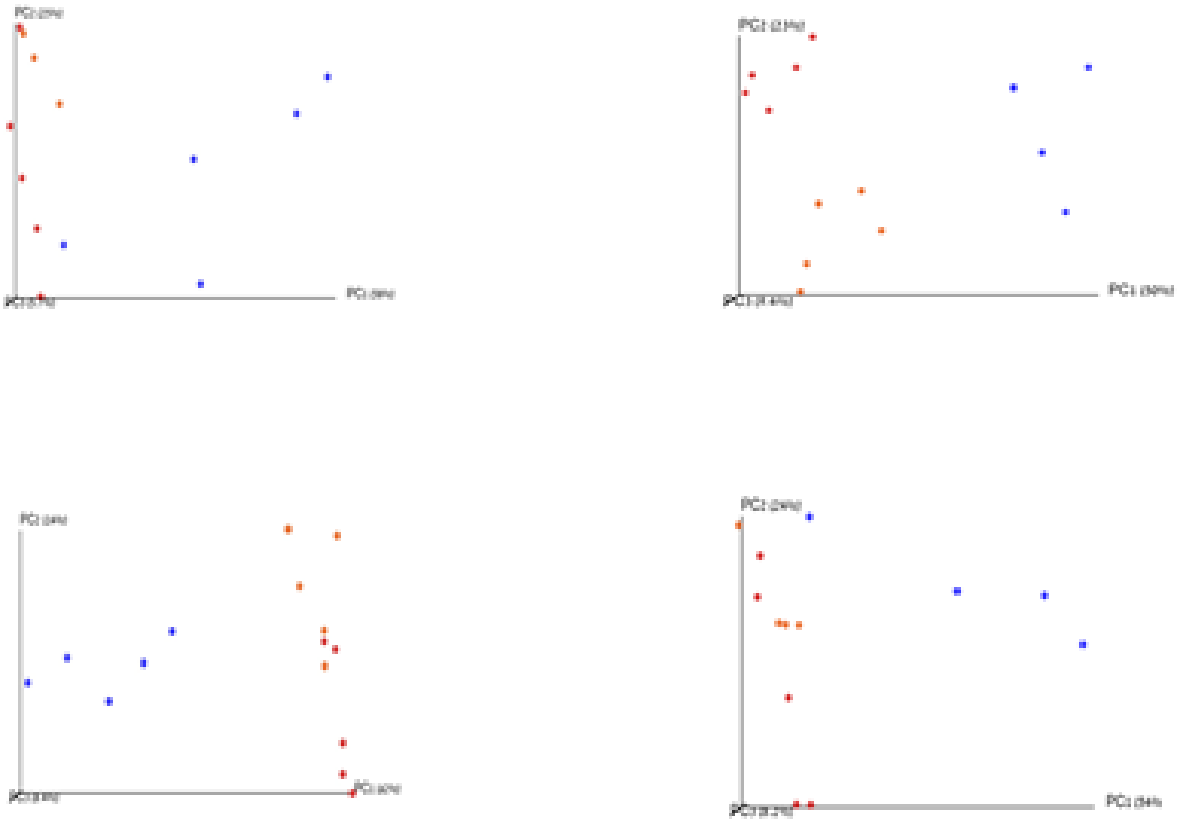

Figure 7.5. Ciprofloxacin inhibits development of radiation-induced intestinal dysbiosis. (A) Principal coordinates analysis (PCoA) of weighted UniFrac distances of 16S rRNA sequences. Symbols represent individual intestinal mucosal bacterial communities obtained from healthy control mice (orange), mice exposed to irradiation (blue), and mice exposed to radiation and treated with ciprofloxacin (red). Shown are communities from the jejunum mucosa (top left), cecum lumen (top right), cecum mucosa (bottom left), and distal colon mucosa (bottom right).

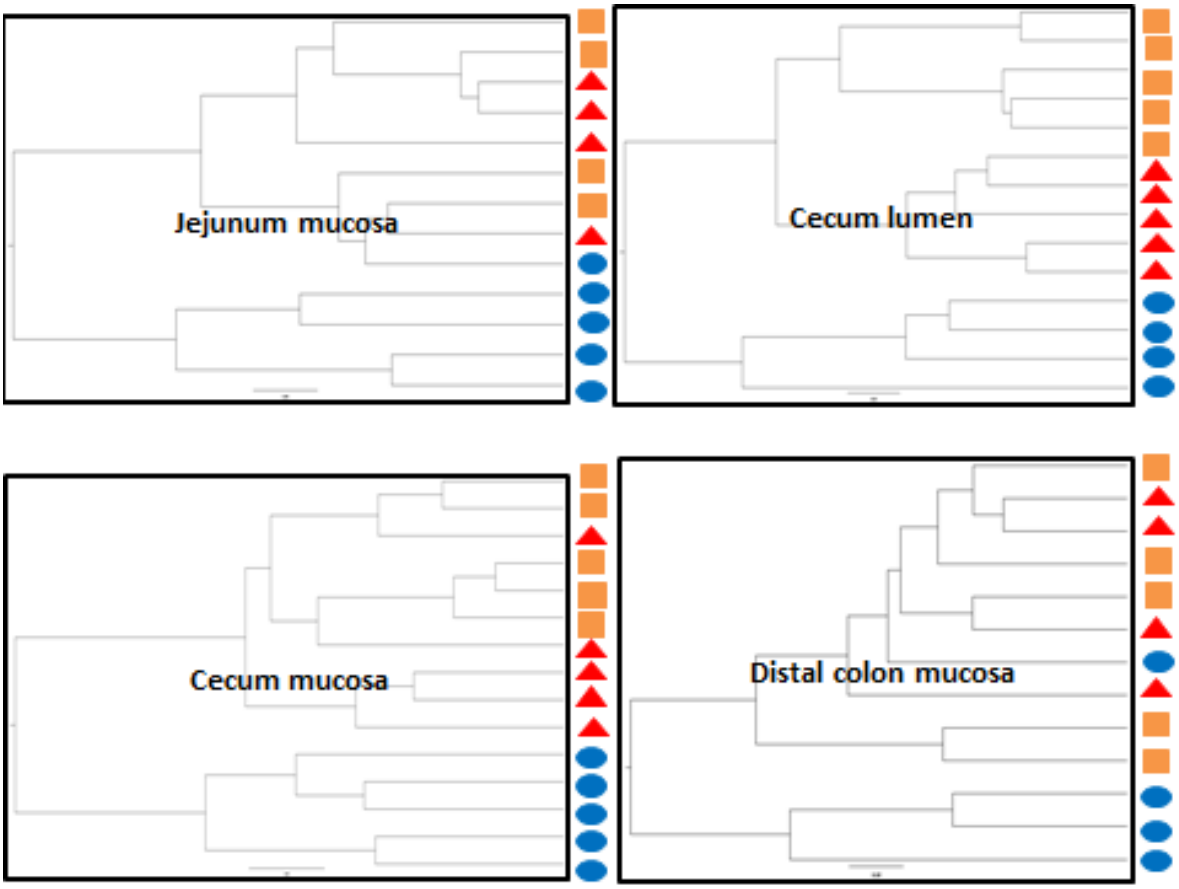

Figure 7.5. (B) Hierarchial clustering of intestinal microbiota samples based on OTUs at 97% sequence similarity. Samples from healthy control mice (orange squares), mice exposed to irradiation (blue circles) and mice exposed to irradiation and treated with cipro (red triangles) are shown. Jejunum mucosa (top left), cecum lumen (top right), cecum mucosa (bottom left) and distal colon mucosa (bottom right) are shown.

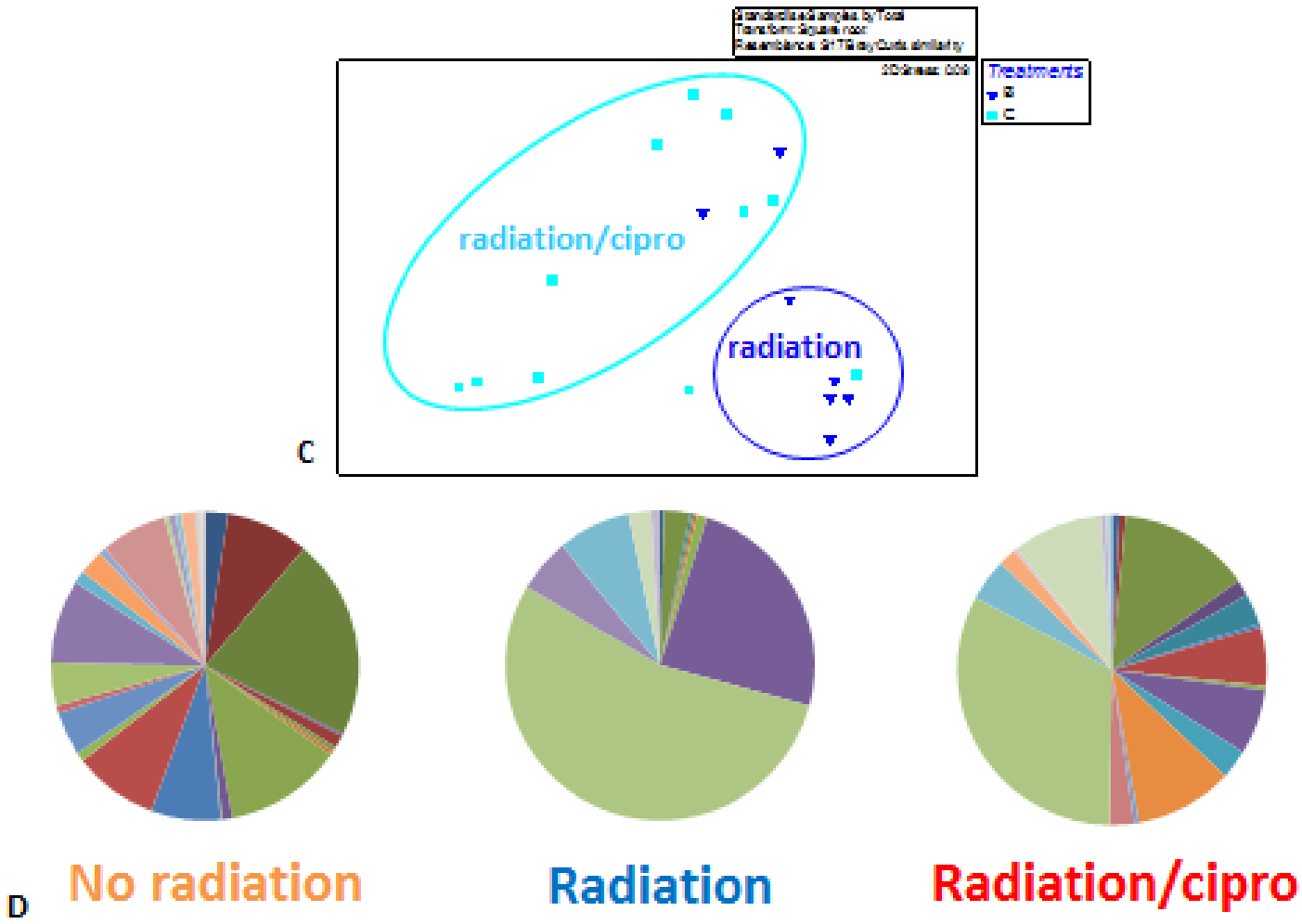

Figure 7.5. (C) Cipro alters radiation-induced shifts in the composition of the intestinal microbiota. T-RFs derived from fecal bacterial communities of mice exposed to radiation (dark blue) and mice exposed to irradiation and treated with cipro (light blue) were used to generate nonmetric multidimensional scaling plots. The communities in mice exposed to radiation and those exposed to irradiation and treated with cipro were statistically dissimilar based on ANOSIM analysis ($p<0.05$; n = 8-16 mice/group). (D) Cipro administration attenuates the reduction in fecal T-RFs seen after radiation exposure.

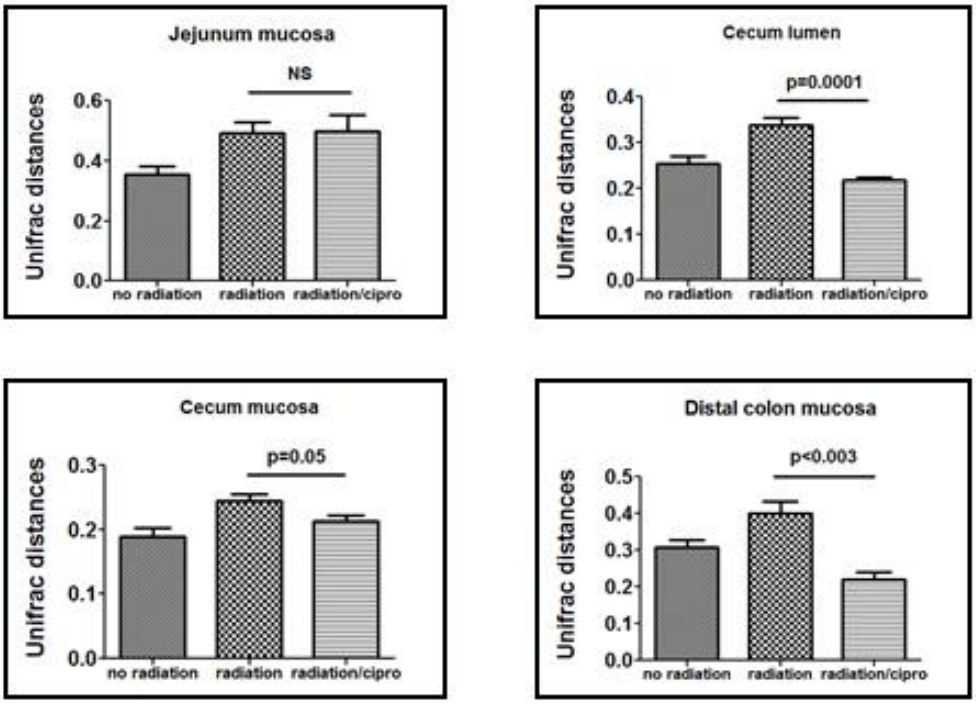

Figure 7.5. (E) Average weighted UniFrac distances of microbial communities from healthy control mice (left), irradiated mice (middle), and irradiated mice treated with ciprofloxacin (right). Jejunum mucosa (top left), cecum lumen (top right), cecum mucosa (bottom left) and distal colon mucosa (bottom right) are shown.

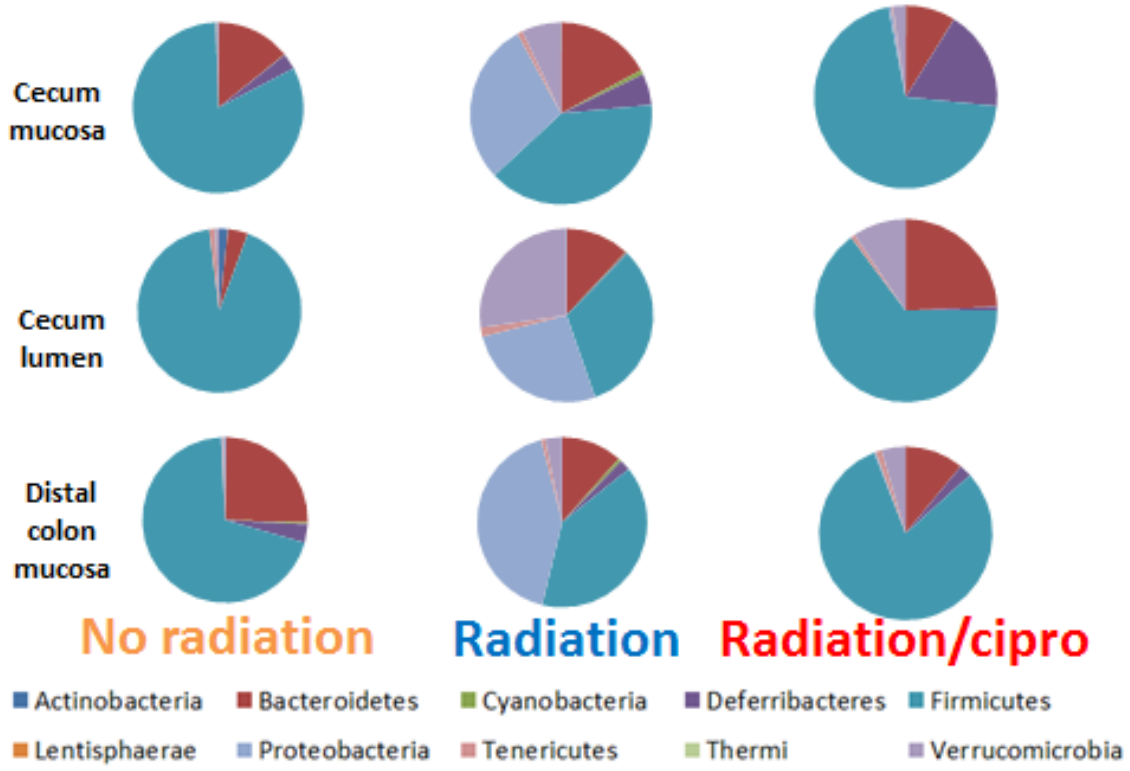

Figure 7.6. Cipro largely prevents alterations in predominant intestinal bacterial phyla following radiation exposure. Average abundances of bacterial phlya in the intestine of healthy mice (left), mice exposed to irradiation (middle), and mice exposed to irradiation and treated with ciprofloxacin (right). Cecum mucosa (top), cecum lumen (middle) and distal colon (bottom) are shown. Radiation exposure results in a decrease in Firmicutes and an increase in Proteobacteria, and these shifts are largely prevented by administration of ciprofloxacin.

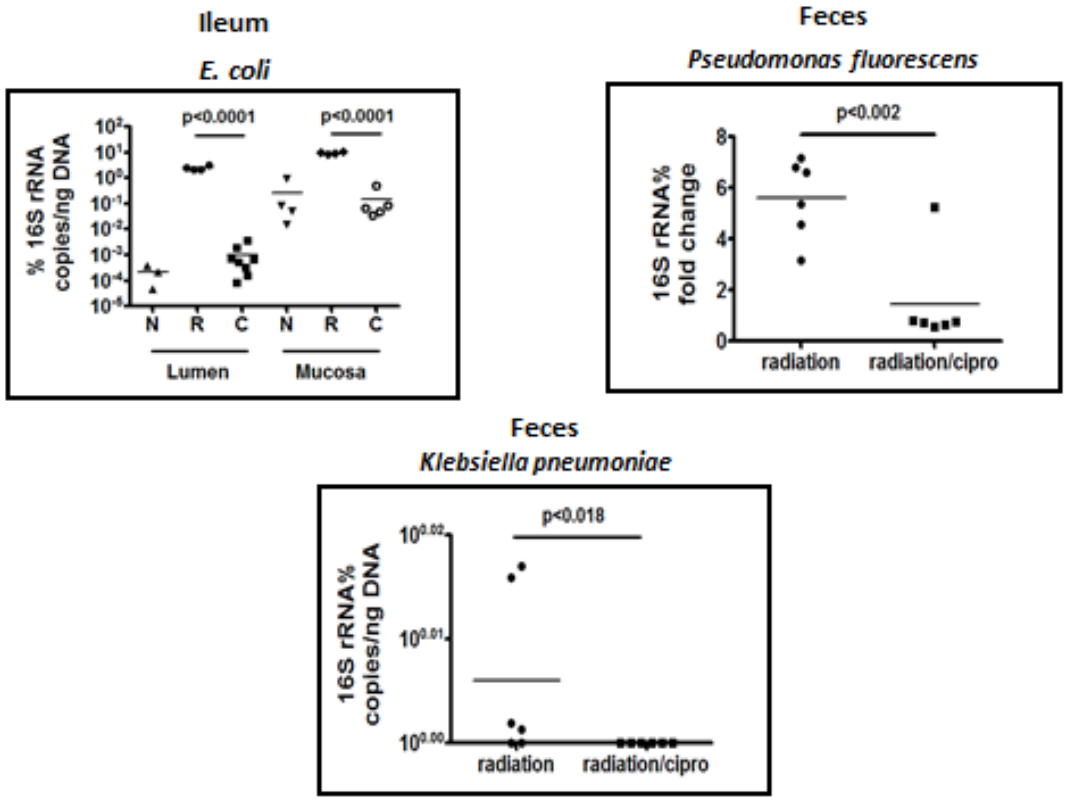

Figure 7.7. Ciprofloxacin administration prevents alterations in concentrations of specific intestinal bacterial groups following radiation exposure. (A) Quantitation of intestinal bacterial species are shown, using quantitative PCR of the 16S rRNA gene. Radiation exposure results in increases in intestinal populations Proteobacteria phylum members, and cipro largely prevents these increases. Copy number is normalized to total 16S.

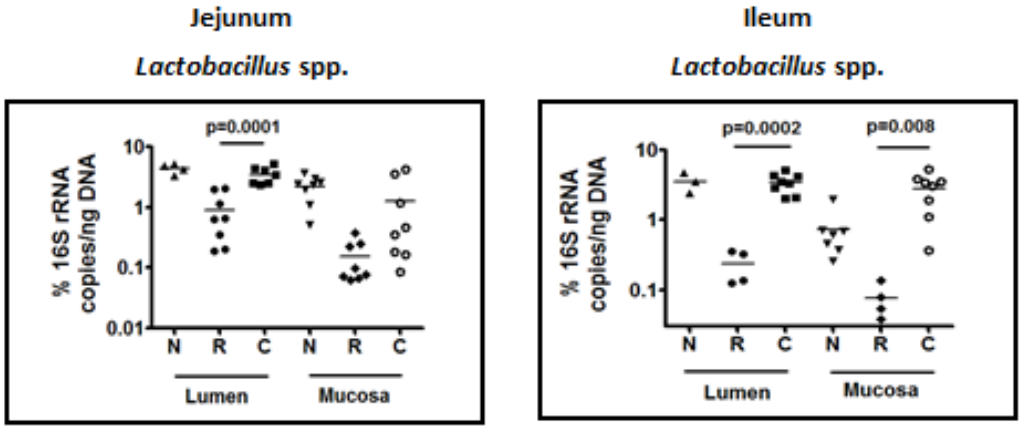

Figure 7.7. (B) Quantitation of intestinal bacterial species is shown, using quantitative PCR of the 16S rRNA gene. Radiation exposure results in decreases in Firmicutes phylum members, and cipro largely prevents these decreases. Copy number is normalized to total 16S.

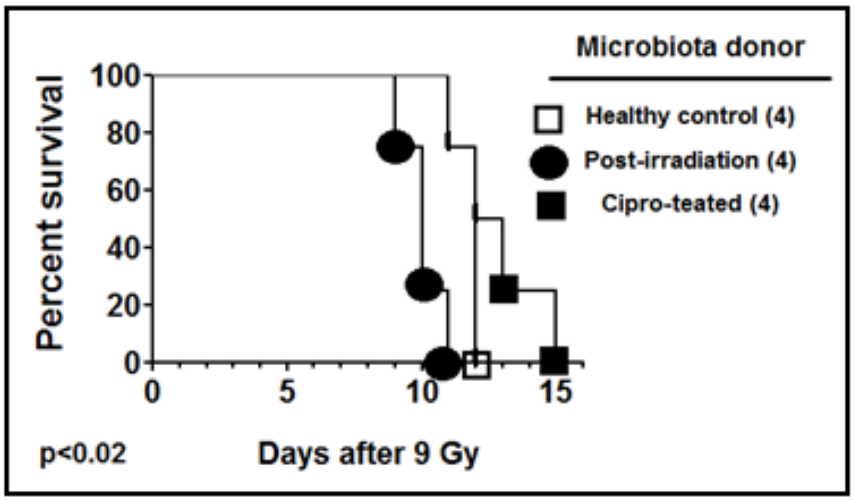

Figure 7.8. Effects of cipro on the intestinal microbiota directly impact the host response to radiation. GF WT mice received transplantation of 1) normal microbiota, 2) post-irradiation microbiota or 3) microbiota from ciprofloxacin-treated mice. Mice receiving microbiota from cipro-treated mice had prolonged survival after exposure to a lethal dose of irradiation compared to mice receiving normal microbiota or post-irradiation microbiota ($p<0.02$).

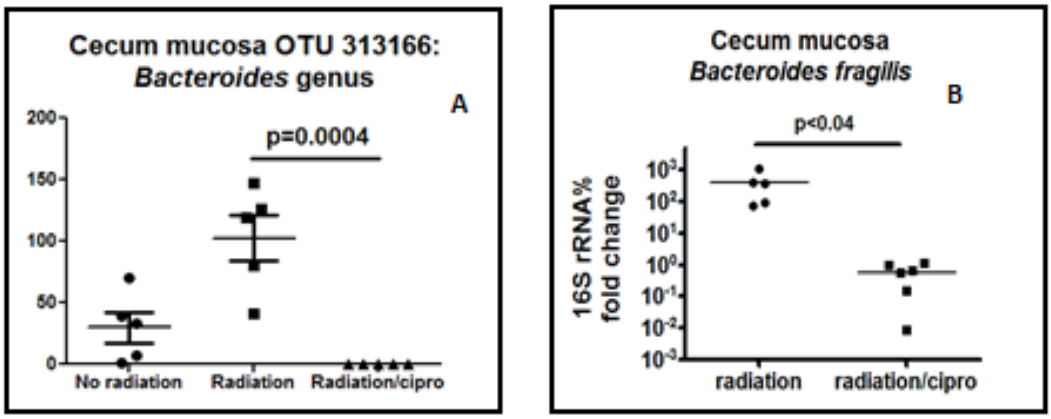

Supplementary Figure 7.1. Quantitation of intestinal bacterial species is shown, using 454 pyrosequencing (left) and quantitative PCR of the 16S rRNA gene (right). Radiation exposure results in increases in increases in intestinal *Bacteroides* species, and cipro largely prevents these increases. Copy number is normalized to total 16S.

Discussion

The human gut is the natural environment for a diverse and dynamic microbial ecosystem, whose structure and functions are presently a major target of biomedical research. A better understanding of the human microbiota and how to manipulate it safely may lead to better ways to prevent harm and promote health with minimum toxicity (1). We have utilized novel gene sequencing technologies and powerful bioinformatics analysis tools to provide insights into the composition, structure and activities of the gut microbiota in several rodent models of intestinal injury and inflammation, including the interleukin 10-deficient (IL-$10^{-/-}$) mouse model of chronic, spontaneous, immune-mediated colitis (chapter 4) and a radiation-induced gastrointestinal (GI) syndrome mouse model (chapters 6 and 7), as well as in humans with diarrhea-predominant irritable bowel syndrome (D-IBS; chapter 3). We have developed procedures for subjecting germ-free, selectively colonized, and conventionalized mice to manipulations while maintaining their gnotobiotic environments (chapters 4, 6 and 7). We have also validated procedures for transplanting cecal microbial communities into germ-free mouse recipients (chapters 6 and 7).

Collecting a stool sample is easy and noninvasive, and so unsurprisingly the great majority of the information that is available on the gut microbiota composition derives from studies on fecal samples that merely serve as surrogates for the colonic luminal microbiota (2, 3). However, the stool represents a significantly different environment than the intestinal mucosa, where host-microbial interaction takes place (4, 5). In addition, there are differences in bacterial concentrations, host cell exposure time to the microbiota, and mucin organization (6) between the colon and small intestine, and even between different regions of the colon (7). For these reasons, we have investigated bacterial communities in the jejunum, (chapters 6 and 7), cecum

(chapters 6 and 7), and colon (chapters 3, 6 and 7). The biological importance of differences between mucosa-associated and luminal bacteria is unclear (8-13), so we also studied microbial communities in both of these compartments (chapters 3, 6, and 7). All mouse experiments included age- and gender-matched, young adult animals, as it has been suggested that the age (14) or sex (15) of an adult may impact the microbiota composition. Finally, while high temporal stability has been observed in the adult microbiota (16), we have accounted for potential temporal variations in the microbiota by performing kinetic analyses, assessing microbial communities both at several time points in near succession, and over longer periods of time (chapters 4, 6 and 7).

Utilizing gnotobiotic animals, we demonstrated that commensal bacteria play a protective role early in the host response to radiation intestinal injury, by contributing to intestinal epithelial cell proliferation and limiting excessive intestinal epithelial cell apoptosis (chapter 6). We also showed that commensal bacteria contribute to the pathogenesis of the radiation GI syndrome, which had been shown previously by Gordon and Crawford (17). We subsequently confirmed our hypothesis that radiation induces a profound intestinal dysbiosis that can explain the dual role of gut bacteria early and late in the host radiation response, respectively (chapters 6 and 7).

We identified a reduction of enteric Firmicutes in both mice with immune-mediated colitis (chapter 4) and radiation intestinal injury (chapters 6 and 7; table 1), similar to that previously described in patients with Crohn's disease (18, 19). Within the Firmicutes phylum, we determined that *Lactobacillus reuteri* comprised the great majority of *Lactobacillus* spp. in the healthy C57BL/6 mouse intestinal tract and were largely eliminated in the gut following radiation (chapter 6). These data identify this bacterial species as an important potential therapeutic target for the radiation GI syndrome. It is possible that *L. reuteri* could provide

protection from radiation intestinal injury through a number of potential mechanisms, and selective colonization experiments involving *L. reuteri* monoassociated animals and animals dual associated with *L. reuteri* and a pathogenic bacterial strain could provide valuable information. *Lactobacillus* species are among the most frequently used bacteria in probiotic products (20), as they are regarded as safe for human use, even for immunocompromised individuals, children (21), neonates and the elderly (22). *Lactobacillus* species have been shown to provide benefits in humans with atopic dermatitis (23, 24), viral infections (25), and allergies (26), and they contribute to the treatment of *Helicobacter pylori* infection (27) and colitis (28) in mice, and gastric ulcers in rats (29). Mechanistically, *Lactobacillus* species possess the ability to adhere to intestinal epithelial cells via mannose-binding (30) and pili (31), enhance tight junctions (32, 33), modulate cellular pathways (34-38), induce production of mucin by goblet cells (39) and defensins by Paneth cells (40), modulate dendritic cell functions (41-43), stimulate production of IL-12 (44, 45) and IL-10 (45, 46) by monocytes/macrophages, degrade pro-inflammatory chemokines (47), produce bacteriocins (48-51), and improve gut function parameters (52-54). However, *L. reuteri* have not yet received a great deal of attention, although they have been shown to treat hypercholesterolemia (55). For the application of probiotic species, considerable *in vitro*, *in vivo*, and clinical evidence must justify their use (56), safety must be ascertained (22) and undesired effects must be identified (57).

We found that Enterobacteriaceae exist in very small concentrations in the healthy mouse gut, consistent with previous reports in humans and mice (58-60). In line with previous reports in human inflammatory bowel diseases (IBD) (61-67) and in chemical- (68, 69), pathogen- (70, 71), and immune defect-induced (72, 73) colitic mice, we observed dramatic increases in relative abundance of intestinal Enterobacteriaceae, particularly *Escherichia coli*, (members of the

Proteobacteria phylum), in mice exposed to radiation (chapters 6 and 7; table 1) and in mice experiencing spontaneous, chronic, immune-mediated intestinal inflammation (chapter 4; table 1). Hypotheses are emerging regarding mechanisms by which host responses shape the microbial community structure and drive the proliferation of Enterobacteriaceae, particularly *E. coli*, (which have been found in higher abundance in people with IBD [74-80]), in settings of intestinal injury, which certainly could pertain to the radiation GI syndrome. One recent report proposed that nitrate generated by the host as a by-product of inflammation can be used by *E. coli* and likely by other commensal Enterobacteriaceae to edge out competing microbes that rely on fermentation to generate energy for growth (81, 82). In fact, there is accumulating evidence that *E. coli* are able to thrive not only in the setting of intestinal inflammation, but in the setting of general stress directed by or at the host. For example, *E. coli* have been shown to be more abundant during pregnancy (83), weaning (84), fasting (85), and starvation (86), and following surgery (87). Furthermore, expression of *E. coli* stress genes is stimulated in the inflammatory environment (88).

The biodiversity in the human gut is a result of coevolution between host and microbe and has been shown to be stable over time in healthy individuals (89). Thus a departure from the normal biodiversity of the intestinal microbiota may reflect a disease state in the gut. We performed thorough analyses of intestinal microbial biodiversity in our studies, assessing both α- and β-diversity. A reduction in intestinal bacterial biodiversity is consistently present in children, adolescents (90-93), and twins with ulcerative colitis (94), as well as other subsets of IBD patients (95). In line with these previous studies in IBD, we found decreased fecal microbial biodiversity in patients with D-IBS (chapter 3; table 1) and in mice with spontaneous, chronic, immune-mediated colitis (chapter 4). We also noted differences in microbial biodiversity

between fecal and colonic mucosal communities, with decreased biodiversity in the colon compared to the feces (chapter 3). Interestingly, we found that radiation exposure largely resulted in increased biodiversity in the intestinal microbiota (chapter 6).

We characterized significant shifts in the composition of the microbiota in several forms of intestinal disease (table 1), including D-IBS (chapter 3), spontaneous, chronic, immune-mediated colitis (chapter 4), and radiation enteropathy (chapter 6 and chapter 7). What has been lacking in studies of human dysbioses is the determination of the biological and clinical significance of community imbalances. The question remains: Are the changes in intestinal microbiota that are observed in intestinal disorders necessary determinants of initiation and/or perpetuation of pathogenesis, or are the microbiota alterations simply consequences of chronic inflammation/injury? Frank et al. presented four possible causal relationships between intestinal disease and dysbiosis (96): 1) Dysbiosis is a primary trigger that leads to pathogenesis. 2) Disruption of the commensal microbial community and its functions contributes to the duration or severity of the disease state. 3) The pathological condition itself causes a secondary shift in microbial community structure that does not impact the pathogenesis of disease. 4) Dysbiosis arises in parallel with pathogenesis secondary to etiological factors but does not serve as a causal factor of disease.

The strongest evidence that dysbiosis contributes to human disease could be obtained through double-blind, randomized controlled experiments utilizing agents that create dysbiosis in healthy individuals or that normalize dysbiotic communities in diseased individuals (96). Under these conditions, any exact causal relationships that exist between dysbiosis exposure and subsequent pathological development could be defined. However, there are obvious ethical considerations that render these experiments difficult if not impossible to carry out in humans.

Alternatively, we designed experiments employing animal models of disease that contributed important insights into the timing and mechanistic basis of disease pathophysiology in relation to altered microbiota. We generated a mouse model of radiation intestinal injury and used molecular-based technologies to characterize a radiation-induced intestinal dysbiosis that closely matches that described in other intestinal disorders, namely IBD. We were able to utilize this model to artificially create a reproducible dysbiotic microbiota that we used in mechanistic studies incorporating microbiota transplantation and selective colonization of gnotobiotic mice, combined with targeted experiments to determine causal relationships and further define mechanisms of action (chapters 6 and 7).

Revisiting the aforementioned hypotheses offered by Frank et al., we can use our findings described within this thesis to begin to disavow some of the postulates while perhaps strengthening support for one supposition in particular. The first hypothesis is that dysbiosis is a primary trigger that leads to pathogenesis. First, we have shown that alterations in the gut microbiota that we identified in patients with IBS (chapter 3) and in mice with immune-mediated colitis (chapter 4) and radiation enteropathy (chapters 6 and 7) are very similar to those seen in human IBD (61, 62, 65, 97-99), as well as in a mouse model of *Clostridium difficile* colitis (100). One would expect that if dysbiosis is a primary trigger of disease, then each respective disease with unique pathophysiology would be caused by a singular dysbiosis with distinguishing features. Yet, this does not seem to be the case. Second, we performed longitudinal observational studies with conventionalized wild-type and (IL-10$^{-/-}$) mice in an attempt to assess the causal relationship between dysbiosis and the development of spontaneous, chronic, immune-mediated colonic inflammation in IL-10$^{-/-}$ mice (chapter 4). While exact timing of disease onset was

difficult to define, it did not appear that dysbiosis preceded the onset of colonic inflammation in these mice, suggesting that at least in this animal model, dysbiosis does not initiate disease.

The second hypothesis is that disruption of the commensal microbial community and its functions contributes to the duration or severity of the disease state. We have shown that changes in the microbial community structure characterized by an increased mucosal and luminal abundance of Enterobacteriaceae can be transferred to other animals, resulting in an exacerbation of intestinal injury (chapters 6 and 7). This phenomenon has been shown previously in an immunodeficient mouse that spontaneously develops colitis (72, 101). In addition, selective colonization gnotobiotic experiments revealed that individual bacterial species relevant to radiation dysbiosis, *E. coli* and *Enterococcus faecalis*, have differential abilities to induce radiation morbidity and mortality (chapter 6). Together these data support the hypothesis that dysbiosis and/or its components contribute to the severity of disease, and contradict the hypothesis that the pathological condition itself causes a secondary shift in microbial community structure that does not impact the pathogenesis of disease, as well as the hypothesis that dysbiosis arises in parallel with pathogenesis secondary to etiological factors but does not serve as a causal factor of disease.

One of the ultimate goals of these lines of research is to identify interventions that will alter dysbiosis and to determine whether these interventions alter the course of disease. As an example of a previous success story, past descriptions of phylum level changes in the intestinal microbiota during *C. difficile* infections, (reductions in Bacteroidetes and relative increases in Proteobacteria and Verrucomicrobia), resulted in the creation of a new macrocyclic, the Bacteroides-sparing antibiotic fidamoxicin, which reduced initial *C. difficile* infection relapse rates by 50% compared to the antibiotic vancomycin (102). We have identified an FDA-

approved antibiotic, the fluoroquinolone ciprofloxacin (cipro), which prevents radiation-induced shifts in the microbiota and rescues mice from the radiation GI syndrome (chapters 6 and 7). One of our aims is to guide the discovery of narrow-spectrum antibiotics that will even more optimally restore the normal gut microbiota in patients exposed to radiation or with other forms of intestinal injury.

Cipro prevents the radiation GI syndrome through several mechanisms (chapter 7). It prevents the development of sepsis, but interestingly there is a window of protection for the administration of cipro. If delivered 24 hours after radiation exposure or thereafter, protection is not seen. Furthermore, one dose delivered at one hour after radiation exposure was sufficient to protect not only irradiated mice from the GI syndrome, but also their untreated, irradiated cage mates. These findings strongly suggested that there is a cipro-preventable event(s) that occurs within the first 24 hours after radiation exposure that is critical to the pathogenesis of the GI syndrome. We identified a dysbiosis that ensues within the first 24 hours of radiation exposure, and we demonstrated that cipro inhibits this dysbiosis. It is reasonable to assume that as agents that lyse bacterial cells and/or prevent their proliferation, antibiotics are able to affect the composition of the microbiota, and unsurprisingly recent studies have shown that this is the case (103, 104). In fact, the administration of cipro to humans affected the majority of bacterial taxa in the gut (105). Importantly, we showed that cipro prevented the proliferation of *E. coli* observed in the gut after radiation. It has been proposed that antibiotic administration results in blooms of enteric commensal *E. coli* populations (106-109), but this was not the case with the delivery of cipro in our animal model of radiation enteropathy.

We found that radiation selectively reduces expression of α-defensins (chapters 6 and 7), antimicrobial peptides (AMPs) that are produced and secreted by small intestinal Paneth cells.

Delivery of cipro both preserves expression of these AMPs in SPF mice exposed to radiation and induces their expression in germ free mice, independent of the presence of microbes. This is important because a growing number of infections are caused by antibiotic-resistant bacteria and there is a shortage of new families of antibiotics that could compensate for resistance to existing antibiotics due to the high costs of development (110, 111). In addition, the administration of broad-spectrum antibiotics can lead to detrimental effects on the commensal microbiota (96, 112-113). As a result, there is a dire need for the development of new antimicrobials that can be used in clinical settings, and AMPs that are produced by intestinal epithelial cells or bacteria might warrant serious consideration as alternatives to traditional antibiotics. It is possible that antibiotics other than cipro have the ability to modulate the microbiota through similar direct effects on the host. To date, this has been largely unexplored.

We also identified a probiotic (VSL#3) that induces α-defensin expression in SPF mice, promotes eubiosis and mitigates the radiation GI syndrome (chapter 7). There is growing interest in developing strategies to therapeutically improve the physiological quality of the human gut microbial ecosystem. Various interventional approaches have emerged, including the use of probiotics, prebiotics or techniques for microbial reconstitution through fecal transplantation. These strategies are aimed at combatting overgrowth of opportunistic community members and/or providing metabolic substrates or live micro-organisms for the promotion of the growth and activity of beneficial species. Probiotics are defined as "live micro-organisms which, when administered in adequate amounts as part of food, confer a health benefit on the host" (114). Prebiotics are "selectively fermented ingredients that permit changes in the composition and/or activity of the intestinal microbiota that confer benefits upon host well-being" (115). An exciting

concept is that of the “synbiotic”: the combination of probiotics and prebiotics aimed at optimizing the impact of probiotics on the gut microbial ecosystem (116).

The results from our cecal content transplantation experiments demonstrate that the composition of the microbiota impacts the clinical response of the host to radiation (chapters 6 and 7). These data may guide the rational design of healthy, resilient and robust microbial communities that can be used to maintain or restore human health following radiation, and perhaps in patients suffering from intestinal diseases of other etiologies. Fecal microbiota transplantation (FMT) has been used sporadically over the last 50 years (117), but an epidemic of *C. difficile* infections in the USA and Europe (118-120) has resulted in the increased use of FMT to treat this disorder (121, 122), which is characterized by a dysbiosis (123) and is frequently unresponsive to antibiotics (102, 124). Three systematic reviews of recurrent *C. difficile* cases treated with FMT found that 83%, 90% and 92% of patients were cured, respectively (121, 125, 126). FMT induced response in 7 patients with ulcerative colitis in two studies (127, 128), but it has been suggested that repeated FMT may be required to effectively treat IBD (129).

Nonetheless, diseases that result from microbiota-related dysfunction invite the investigation of FMT as a potential treatment, including radiation intestinal injury. FMT overcomes a quantitative limitation of probiotic therapeutics: Oral probiotic doses are typically 3-4 orders of magnitude lower than the 100 trillion microorganisms that are native to the colon (121), and the numbers are likely further reduced after passage through the harsh environment of the stomach. In addition, probiotics rarely persist in the gut beyond 14 days (130), while donor flora persists at 24 weeks post-transplantation (131). When utilizing FMT, which can be delivered by colonoscopy (132-134) or retention enema (135), the donor microbiota should be optimized for the maximal benefit of the recipient. Next generation sequencing techniques

should be used to profile the donor stool to ensure a balance of biochemical pathways is present that will complement those of the host. The enterotypes (136) of the donor and recipient should also be considered. The history, screening of donors, pretreatment processes, patient preparation, routes of administration, and methodology for FMT have been reviewed (137-139), and formal standard practice guidelines for performing FMT have been published (140). However, the technical aspects of FMT are likely to rapidly evolve over the next few years with its increased use. Specifications for storage, quantification, and preparation of donor material should become more stringently standardized as FMT randomized controlled trials are performed for *C. difficile*, IBD, and other intestinal disorders, and the results are assessed along with molecular analyses of the microbiota.

It should be noted that radiation is delivered therapeutically during treatment of solid tumors of the abdomen and pelvis in fractionated doses of 1.5-2.0 Gy at a time. Our studies focused on single doses of 15 Gy because this is the minimum dose of radiation that universally causes the radiation GI syndrome in mice. Therefore, these studies are directly relevant to people who are exposed to large doses of radiation as a result of nuclear meltdown, terrorist attack, space exploration, or medical error. They may also be relevant to people who receive appropriately fractionated radiation doses, but who are exquisitely susceptible to radiation intestinal injury, due to genetic predispositions or other risk factors.

Future studies in these areas should include a focus on: 1) The effect of common intestinal diseases and potential therapies on functional secretion of AMPs by Paneth cells or colonocytes. Techniques must be developed that can accurately and reliably assess AMP secretion. 2) The role of compromised barrier function in these diseases. We did not assess

barrier function in our studies, but it is invariably important in the pathogenesis of these intestinal disorders, and it could prove to be a promising therapeutic target.

Our studies have improved the knowledge of how the host and bacteria interact during intestinal inflammation and injury and how the microbiota responds and are regulated in settings of irritable bowel syndrome, spontaneous, chronic, immune-mediated colitis, and radiation exposure. Given the abrupt rise in incidence and prevalence of intestinal disorders that appears to have coincided with socioeconomic development and dietary changes, expeditious progress in this area of research is crucial in order to impede the dramatic acceleration of the prevalence of these diseases. These data may yield valuable clinical tools in restoring a healthy microbiota to prevent or treat intestinal disorders without administering broad, immunosuppressive medications that are accompanied by severe side effects.

Disease	Bacteria	Effect	Location	Paper	Technique
IL-10$^{-/-}$	**Proteobacteria**	**Increased**	**Feces**	**IV**	**454**
Radiation	**Proteobacteria**	**Increased**	**SI, colon**	**VI, VII**	**454**
IL-10$^{-/-}$	***E. coli***	**Increased**	**Feces**	**IV**	**454, qPCR**
Radiation	***E. coli***	**Increased**	**SI, colon**	**VI, VII**	**454, qPCR**
Radiation	***K. pneumoniae***	**Increased**	**Feces**	**VI**	**qPCR**
Radiation	***P. fluorescens***	**Increased**	**Feces**	**VI**	**qPCR**
IL-10$^{-/-}$	**Firmicutes**	**Decreased**	**Feces**	**IV**	**454**
Radiation	**Firmicutes**	**Decreased**	**SI, colon**	**VI, VII**	**454**
Radiation	***Lactobacillus* spp.**	**Decreased**	**SI, colon**	**VI, VII**	**454, qPCR**
D-IBS	**Clostridiales**	**Decreased**	**Feces**	**III**	**T-RFLP**
IL-10$^{-/-}$	***Clostridium* spp.**	**Decreased**	**Feces**	**IV**	**454**
Radiation	***C. coccoides***	**Decreased**	**Feces**	**VI**	**qPCR**
IL-10$^{-/-}$	**Tenericutes**	**Increased**	**Feces**	**IV**	**454**
Radiation	***Bacteroides* spp.**	**Increased**	**Cecum, feces**	**VI**	**454, qPCR**
Radiation	***E. faecalis***	**Increased**	**Feces**	**VI**	**qPCR**
Radiation	***Porphyromonadaceae***	**Increased**	**Cecum**	**none**	**454**
IL-10$^{-/-}$	**Bacteroidetes**	**Decreased**	**Feces**	**IV**	**454**
IL-10$^{-/-}$	**Actinobacteria**	**Decreased**	**Feces**	**IV**	**454**
IL-10$^{-/-}$	**Verrucomicrobia**	**Decreased**	**Feces**	**IV**	**454**
IL-10$^{-/-}$	***Akkermansia***	**Decreased**	**Feces**	**IV**	**454**
Radiation	***Bifidobacterium* spp.**	**Decreased**	**Feces**	**VI**	**qPCR**
Radiation	**SFB**	**Decreased**	**Feces**	**VI**	**qPCR**
Radiation	**Lachnospiraceae**	**Decreased**	**Cecum**	**none**	**454**
D-IBS	**Biodiversity**	**Decreased**	**Feces**	**III**	**T-RFLP**
IL-10$^{-/-}$	**Biodiversity**	**Decreased**	**Feces**	**IV**	**454**
Radiation	**Biodiversity**	**Increased**	**SI, colon**	**VI, VII**	**454**

Table 1. Compositional shifts in the enteric microbiota in intestinal disorders. SI=small intestine; *E. coli=Escherichia coli*; *K. pneumoniae=Klebsiella pneumoniae*; *P. fluorescens=Pseudomonas fluorescens*; *C. coccoides=Clostridium coccoides*; *E. faecalis=Enterococcus faecalis*; SFB=segmented filamentous bacteria.

REFERENCES

1. Frierich MJ. Genomes of microbes inhabiting the body offer clues to human health and disease. JAMA 2013; 309: 1447-1449.

2. de Vos WM, de Vos EAJ. Role of the intestinal microbiome in health and disease: from correlation to causation. Nutr Rev 2012; 70: S45-S56.

3. Shanahan F. The colonic microbiota and colonic disease. Curr Gastroenterol Rep 2012; 14: 446-452.

4. Sweeney TE, Morton JM. The human gut microbiome- A review of the effect of obesity and surgically induced weight loss. JAMA Surg 2013; 148(6): 563-9.

5. Turnbaugh PJ, Ridaura VK, Faith JJ, et al. The effect of diet on the human gut microbiome: a metagenomic analysis in humanized gnotobiotic mice. Sci Transl Med 2009; 1(6): 6ra14.

6. Johansson ME, Larsson JM, Hansson GC. The two mucus layers of colon are organized by the MUC2 mucin, whereas the outer layer is a legislator of host-microbial interactions. Proc Natl Acad Sci U S A 2011; 108: 4659-65.

7. Hu S, Wang Y, Lichtenstein L, et al. Regional differences in colonic mucosa-associated microbiota determine the physiological expression of host heat shock proteins. Am J Physiol Gastrointest Liver Physiol 2010; 299: G1266-G1275.

8. Marchesi JR. Human distal microbiome. Environ Microbiol 2011; 13: 3088-3102.

9. Gillevet P, Sikaroodi M, Keshavarzian A, Mutlu EA. Quantitative assessment of the human gut microbiome using multitag pyrosequencing. Chem Biodivers 2010; 7: 1065-1075.

10. Van den Abbeele P, Van de Wiele, Verstraete W, Possemiers S. The host selects mucosal and luminal associations of coevolved gut microorganisms: a novel concept. FEMS Microbiol Rev 2011; 35: 681-704.

11. Durban A, Abellan JJ, Jimenez-Hernandez N, et al. Assessing gut microbial diversity from feces and rectal mucosa. Microb Ecol 2011; 61: 123-133.

12. Lyra A, Forssten S, Rolny P, et al. Comparison of bacterial quantities in left and right colon biopsies and faeces. World J Gastroenterol 2012; 18(32): 4404-4411.

13. Souza HL, de Carvalho VR, Romeiro FG, et al. Mucosa-associated but not luminal *Escherichia coli* is augmented in Crohn's disease and ulcerative colitis. Gut Pathogens 2012; 4: 21.

14. Drago L, Toscano M, Rodighiero V, et al. Cultivable and pyrosequenced fecal microflora in centenarians and young subjects. J Clin Gastroenterol 2012; 46: S81-S84.

15. Flak MB, Neves JF, Blumberg RS. Welcome to the microgenderome. Science 2013; 339: 1044-1045.

16. Jalanka-Tuovinen J, Salonen A, Nikkila J, et al. Intestinal microbiota in healthy adults: temporal analysis reveals individual and common core and relation to intestinal symptoms. PLoS ONE 2011; 6:e23035.

17. Crawford PA, Gordon JI. Microbial regulation of intestinal radiosensitivity. Proc Natl Acad Sci U S A 2005; 102(37): 13254-9.

18. Manichanh C, Rigottier-Gois L, Bonnaud E, et al. Reduced diversity of faecal microbiota in Crohn's disease revealed by a metagenomic approach. Gut 2006; 55: 205-211.

19. Kang S, Denman SE, Morrison M, et al. Dysbiosis of fecal microbiota in Crohn's disease patients as revealed by a custom phylogenetic microarray. Inflamm Bowel Dis 2010; 16: 2034-2042.

20. Selle K, Klaenhammer TR. Genomic and phenotypic evidence for probiotic influences of *Lactobacillus gasseri* on human health. FEMS Microbiol Rev 2013; 1-21.

21. Borrelio SP, Hammes WP, Holzapfel W, et al. Safety of probiotics that contain *Lactobacilli* or *Bifidobacteria.* Clin Infect Dis 2003; 36: 775-80.

22. Sanders ME, Akkermans LMA, Haller D, et al. Safety assessment of probiotics for human use. Gut Microbes 2010; 1: 164-185.

23. Drago L, Iemoli E, Rodighiero V, et al. Effects of *Lactobacillus salivarius* LS01 (DSM 22775) treatment on adult atopic dermatitis: a randomized placebo-controlled study. Int J Immunopathol Pharmacol 2011; 24: 1037-48.

24. Rosenfeldt V, Benfeldt E, Nielsen SD, et al. Effect of probiotic *Lactobacillus* strains in children with atopic dermatitis. J Allergy Clin Immunol 2003; 111: 389-95.

25. Leyer GJ, Li S, Mubasher ME, et al. Probiotic effects on cold and influenza-like symptom incidence and duration in children. Pediatrics 2009; 124: e172-e179.

26. Johansson MA, Sjogren YM, Persson J-O, et al. Early colonization with a group of Lactobacilli decreases the risk for allergy at five years of age despite allergic heredity. PLoS ONE 2011; 6: e23031.

27. Aiba Y, Suzuki N, Kabir AM, et al. Lactic acid-mediated suppression of *Helicobacter pylori* by the oral administration of *Lactobacillus salivarius* as a probiotic in a gnotobiotic murine model. Am J Gastroenterol 1998; 93: 2097-2101.

28. Macho Fernandez E, Valenti V, Rockel C, et al. Anti-inflammatory capacity of selected *Lactobacilli* in experimental colitis is driven by NOD2-mediated recognition of a specific peptidoglycan-derived muropeptide. Gut 2011; 60: 1050-1059.

29. Uchida M, Shimizu K, Kurakazu K. Yogurt containing *Lactobacillus gasseri* OLL 2716 (LG21 yogurt) accelerated the healing of acetic acid-induced gastric ulcers in rats. Biosci Biotechnol Biochem 2010; 74: 1891-1894.

30. Adlerberth I, Ahrne S, Johansson ML, et al. A mannose-specific adherence mechanism in *Lactobacillus plantarum* conferring binding to the human colonic cell line HT-29. Appl Environ Microbiol 1996; 62: 2244-51.

31. Lebeer S, Claes I, Tytgat HL, et al. Functional analysis of *Lactobacillus rhamnosus* GG pili in relation to adhesion and immunomodulatory interactions with intestinal epithelial cells. Appl Environ Microbiol 2012; 78: 185-193.

32. Anderson R, Cookson A, McNabb W, et al. *Lactobacillus plantarum* MB452 enhances the function of the intestinal barrier by increasing the expression levels of genes involved in tight junction formation. BMC Microbiol 2010; 10: 316.

33. Karczewski J, Troost FJ, Konings I, et al. Regulation of human epithelial tight junction proteins by *Lactobacillus plantarum in vivo* and protective effects on the epithelial barrier. Am J Physiol Gastrointest Liver Physiol 2010; 298: G851-G859.

34. van Baarlen P, Troost F, van der Meer C, et al. Human mucosal *in vivo* transcriptome responses to three *Lactobacilli* indicate how probiotics may modulate human cellular pathways. Proc Natl Acad Sci U S A 2011; 108 (Suppl 1): 4562-4569.

35. Wells JM. Immunomodulatory mechanisms of *Lactobacilli*. Microb Cell Fact 2011; 10 (Suppl 1): S17.

36. van Baarlen P, Troost FJ, van Hemert S, et al. Differential NF-κB pathways induction by *Lactobacillus plantarum* in the duodenum of healthy humans correlating with immune tolerance. Proc Natl Acad Sci U S A 2009; 106: 2371-2376.

37. Hasegawa M, Yang K, Hashimoto M, et al. Differential release and distribution of Nod1 and Nod2 immunostimulatory molecules among bacterial species and environments. J Biol Chem 2006; 281: 29054-29063.

38. Petnicki-Ocwieja T, Hrncir T, Liu YJ, et al. Nod2 is required for the regulation of commensal microbiota in the intestine. Proc Natl Acad Sci U S A 2009; 106: 15813-15818.

39. Mack DR, Ahrne S, Hyde I, et al. Extracellular MUC3 mucin secretion follows adherence of *Lactobacillus* strains to intestinal epithelial cells *in vitro*. Gut 2003; 52: 827-833.

40. Schlee M, Harder J, Koten B, et al. Probiotic *Lactobacilli* and VSL#3 induce enterocyte beta-defensin 2. Clin Exp Immunol 2008; 151: 528-535.

41. Mohamadzadeh M, Olson S, Kalina WV, et al. *Lactobacilli* activate human dendritic cells that skew T cells toward T helper 1 polarization. Proc Natl Acad Sci U S A 2005; 102: 2880-2885.

42. Meijerink M, van Hemert S, Taverne N, et al. Identification of genetic loci in *Lactobacillus plantarum* that modulate the immune response of dendritic cells using comparative genome hybridization. PLoS ONE 2010; 5: e10632.

43. Konstantinov SR, Smidt H, de Vos WM, et al. S layer protein A of *Lactobacillus acidophilus* NCFM regulates immature dendritic cell and T cell functions. Proc Natl Acad Sci U S A 2008; 105: 19474-19479.

44. Hessle C, Hanson LA, Wold AE. *Lactobacilli* from human gastrointestinal mucosa are strong stimulators of IL-12 production. Clin Exp Immunol 1999; 116: 276-82.

45. Rask C, Adlerberth I, Berggren A, et al. Differential effect on cell-mediated immunity in human volunteers after intake of different *Lactobacilli*. Clin Exp Immunol 2012; 172: 321-332.

46. Kaji R, Kiyoshima-Shibata J, Nagaoka M, et al. Bacterial teichoic acids reverse predominant IL-12 production induced by certain *Lactobacillus* strains into predominant IL-10 production via TLR2-dependent ERK activation in macrophages. J Immunol 2010; 184: 3505-3513.

47. Von Schillde MA, Hormannsperger G, Weiher M, et al. Lactocepin secreted by *Lactobacillus* exerts anti-inflammatory effects by selectively degrading proinflammatory chemokines. Cell Host Microbe 2012; 11: 387-396.

48. Corr SC, Li Y, Riedel CU, et al. Bacteriocin production as a mechanism for the anti-infective activity of *Lactobacillus salivarius* UCC118. Proc Natl Acad Sci U S A 2007; 104: 7617-7621.

49. Toba T, Yoshioka E, Itoh T. Potential of *Lactobacillus gasseri* isolated from infant feces to produce bacteriocin. Lett Appl Microbiol 1991; 12: 228-231.

50. Itoh T, Fujimoto Y, Kawai Y, et al. Inhibition of food-borne pathogenic bacteria by bacteriocins from *Lactobacillus gasseri*. Lett Appl Microbiol 1995; 21: 137-141.

51. Zhu WM, Liu W, Wu DQ. Isolation and characterization of a new bacteriocin from *Lactobacillus gasseri* KT7. J Appl Microbiol 2000; 88: 877-886.

52. Ouwehand AC, Tiihonen K, Saarinen M, et al. Influence of a combination of *Lactobacillus acidophilus* NCFM and lactitol on healthy elderly: intestinal and immune parameters. Br J Nutr 2009; 101: 367-375.

53. Ringel-Kulka T, Palsson OS, Maier D, et al. Probiotic bacteria *Lactobacillus acidophilus* NCFM and *Bifidobacterium lactis* Bi-07 versus placebo for the symptoms of bloating in patients with functional bowel disorders: a double-blind study. J Clin Gastroenterol 2011; 45: 518-525.

54. Olivares M, Diaz-Ropero MAP, Gomez N, et al. Oral administration of two probiotic strains, *Lactobacillus gasseri* CECT5714 and *Lactobacillus coryniformis* CECT5711, enhances the intestinal function of healthy adults. Int J Food Microbiol 2006; 107: 104-111.

55. Jones ML, Martoni CJ, Parent M, Prakash S. Cholesterol-lowering efficacy of a microencapsulated bile salt hydrolase-active *Lactobacillus reuteri* NCIMB 30242 yogurt formulation in hypercholesterolemic adults. Br J Nutr 2012; 107: 1505-13.

56. Salminen S, von Wright A, Morelli L, et al. Demonstration of safety of probiotics. A review. Int J Food Microbiol 1998; 44: 93-106.

57. Salminen MK, Tynkkynen S, Rautelin H, et al. *Lactobacillus* bacteremia during a rapid increase in probiotic use of *Lactobacillus rhamnosus* GG in Finland. Clin Infect Dis 2002; 35: 1155-1160.

58. Wu GD, Chen J, Hoffmann C, et al. Linking long-term dietary patterns with gut microbial enterotypes. Science 2011; 334: 105-108.

59. Faith JJ, McNulty NP, Rey FE, Gordon JI. Predicting a human gut microbiota's response to diet in gnotobiotic mice. Science 2011; 333: 101-104.

60. Eckburg PB, Bik EM, Bernstein CN, et al. Diversity of the human intestinal microbial flora. Science 2005; 308: 1635-1638.

61. Gophna U, Sommerfeld K, Gophna S, et al. Differences between tissue-associated intestinal microfloras of patients with Crohn's disease and ulcerative colitis. J Clin Microbiol 2006; 44: 4136-4141.

62. Frank DN, St Amand AL, Feldman RA, et al. Molecular-phylogenetic characterization of microbial community imbalances in human inflammatory bowel diseases. Proc Natl Acad Sci U S A 2007; 104: 13780-13785.

63. Krook A, Lindström B, Kjellander J, et al. Relation between concentrations of metronidazole and *Bacteroides* spp. in faeces of patients with Crohn's disease and healthy individuals. J Clin Pathol 1981; 34(6): 645-50.

64. Giaffer MH, Holdsworth CD, Duerden BI. The assessment of faecal flora in patients with inflammatory bowel disease by a simplified bacteriological technique. J Med Microbiol 1991; 35(4): 238-43.

65. Seksik P, Rigottier-Gois L, Gramet G, et al. Alterations of the dominant fecal bacterial groups in patients with Crohn's disease of the colon. Gut 2003; 52: 237-242.

66. Martin HM, Campbell BJ, Hart CA, et al. Enhanced *Escherichia coli* adherence and invasion in Crohn's disease and colon cancer. Gastroenterology 2004; 127: 80-93.

67. Eckburg PB, Relman DA. The role of microbes in Crohn's disease. Clin Infect Dis 2007; 44: 256-262.

68. Lupp C, Robertson ML, Wickham ME, et al. Host-mediated inflammation disrupts the intestinal microbiota and promotes the overgrowth of Enterobacteriaceae. Cell Host Microbe 2007; 2: 119-129.

69. Heimesaat MM, Fischer A, Siegmund B, et al. Shift towards pro-inflammatory intestinal bacteria aggravates acute murine colitis via Toll-like receptors 2 and 4. PLoS One 2007; 2(7): e662.

70. Stecher B, Robbiani R, Walker AW, et al. *Salmonella enterica* serovar Typhimurium exploits inflammation to compete with the intestinal microbiota. PLoS Biol 2007; 10: 2177-89.

71. Barman M, Unold D, Shifley K, et al. Enteric salmonellosis disrupts the microbial ecology of the murine gastrointestinal tract. Infect Immun 2008; 76(3): 907-15.

72. Garrett WS, Gallini CA, Yatsunenko T, et al. Enterobacteriaceae act in concert with the gut microbiota to induce spontaneous and maternally transmitted colitis. Cell Host Microbe 2010; 8: 292-300.

73. Wohlgemuth S, Haller D, Blaut M, Loh G. Reduced microbial diversity and high numbers of one single *Escherichia coli* strain in the intestine of colitic mice. Environ Microbiol 2009; 11: 1562-71.

74. Darfeuille-Michaud A, Neut C, Barnich N, et al. Presence of adherent *Escherichia coli* strains in ileal mucosa of patients with Crohn's disease. Gastroenterology 1998; 115(6): 1405-1413.

75. Darfeuille-Michaud A, Boudeau J, Bulois P, et al. High prevalence of adherent-invasive *Escherichia coli* associated with ileal mucosa in Crohn's disease. Gastroenterology 2004; 127(2): 412-421.

76. Sokol H, Lepage P, Seksik P, et al. Temperature gradient gel electrophoresis of fecal 16S rRNA reveals active *Escherichia coli* in the microbiota of patients with ulcerative colitis. J Clin Microbiol 2006; 44(9): 3172-3177.

77. Rolhion N, Darfeuille-Michaud A. Adherent-invasive *Escherichia coli* in inflammatory bowel disease. Inflamm Bowel Dis 2007; 13(10): 1277-1283.

78. Rhodes JM. The role of *Escherichia coli* in inflammatory bowel disease. Gut 2007; 56(5): 610-612.

79. Kotlowski R, Bernstein CN, Sepehri S, Krause DO. High prevalence of *Escherichia coli* belonging to the B2+D phylogenetic group in inflammatory bowel disease. Gut 2007; 56(5): 669-675.

80. Thomazini CM, Samegima DA, Rodrigues MA, et al. High prevalence of aggregative adherent *Escherichia coli* strains in the mucosa-associated microbiota of patients with inflammatory bowel diseases. IJMM 2011; 301(6): 475-479.

81. Winter SE, Winter MG, Xavier MN, et al. Host-derived nitrate boosts growth of *E. coli* in the inflamed gut. Science 2013; 339: 708-711.

82. Winter SE, Lopez CA, Baumler AJ. The dynamics of gut-associated microbial communities during inflammation. EMBO Rep 2013; 14: 319-327.

83. Santacruz A, Collado MC, Garcia-Valdes L, et al. Gut microbiota composition is associated with body weight, weight gain and biochemical parameters in pregnant women. Br J Nutr 2010; 104: 83-92.

84. Wu XY, Chapman T, Trott DJ, et al. Comparative analysis of virulence genes, genetic diversity, and phylogeny of commensal and enterotoxigenic *Escherichia coli* isolates from weaned pigs. Appl Environ Microbiol 2007; 73: 83-91.

85. Cray WC, Casey TA, Bosworth BT, Rasmussen MA. Effect of dietary stress on fecal shedding of *Escherichia coli* 0157:H7 in calves. Appl Environ Microbiol 1998; 64: 1975-9.

86. Monira S, Nakamura S, Gotoh K, et al. Gut microbiota of healthy and malnourished children in Bangladesh. Front Microbiol 2011; 2: 228.

87. Rocha F, Laughlin R, Musch MW, et al. Surgical stress shifts the intestinal *Escherichia coli* population to that of a more adherent phenotype: role in barrier regulation. Surgery 2001; 130: 65-73.

88. Patwa LG, Fan TJ, Tchaptchet S, et al. Chronic intestinal inflammation induces stress-response genes in commensal *Escherichia coli*. Gastroenterology 2011; 141(5): 1842-51.

89. Zoetendal EG, Akkermans AD, De Vos WM. Temperature gradient gel electrophoresis analysis of 16S rRNA from human fecal samples reveals stable and host-specific communities of active bacteria. Appl Environ Microbiol 1998; 64: 3854-3859.

90. Noor SO, Ridgway K, Scovell L, et al. Ulcerative colitis and irritable bowel syndrome patients exhibit distinct abnormalities of the gut microbiota. BMC Gastroenterology 2010; 10: 134.

91. Andoh A, Imaeda H, Aomatsu T, et al. Comparison of the fecal microbiota profiles between ulcerative colitis and Crohn's disease using terminal restriction fragment length polymorphism analysis. J Gastroenterol 2011; 46: 479-486.

92. Michail S, Durbin M, Turner D, et al. Alterations in the gut microbiome of children with severe ulcerative colitis. Inflamm Bowel Dis 2012; 18(10):1799-808.

93. Nemoto H, Kataoka K, Ishikawa H, et al. Reduced diversity and imbalance of fecal microbiota in patients with ulcerative colitis. Dig Dis Sci 2012; 57(11): 2955-64.

94. Lepage P, Hasler R, Spehlmann ME, et al. Twin study indicates loss of interaction between microbiota and mucosa of patients with ulcerative colitis. Gastroenterology 2011; 141: 227-236.

95. Qin J, Li R, Raes J, et al. A human gut microbial gene catalogue established by metagenomic sequencing. Nature 2010; 464: 59-65.

96. Frank DN, Zhu W, Sartor RB, Li E. Investigating the biological and clinical significance of human dysbioses. Trends Microbiol 2011; 19(9): 427-434.

97. Baumgart M, Dogan B, Rishniw M, et al. Culture independent analysis of ileal mucosa reveals a selective increase in invasive *Escherichia coli* of novel phylogeny relative to depletion of Clostridiales in Crohn's disease involving the ileum. ISME J 2007; 1: 403-418.

98. Walker AW, Sanderson JD, Churcher C, et al. High-throughput clone library analysis of the mucosa-associated microbiota reveals dysbiosis and differences

between inflamed and non-inflamed regions of the intestine in inflammatory bowel disease. BMC Microbiol 2011; 11: 7.

99. Peterson DA, Frank DN, Pace NR, Gordon JI. Metagenomic approaches for defining the pathogenesis of inflammatory bowel diseases. Cell Host Microbe 2008; 3: 417-427.

100. Reeves AE, Theriot CM, Bergin IL, et al. The interplay between microbiome dynamics and pathogen dynamics in a murine model of *Clostridium difficile* infection. Gut Microbes 2011; 2: 145-158.

101. Garrett WS, Lord GM, Punit S, et al. Communicable ulcerative colitis induced by T-bet deficiency in the innate immune system. Cell 2007; 131: 33-45.

102. Louie TJ, Miller MA, Mullane KM, et al. Fidamoxicin versus vancomycin for *Clostridium difficile* infection. N Engl J Med 2011; 364: 422-431.

103. Cotter PD, Stanton C, Ross RP, Hill C. The impact of antibiotics on the gut microbiota as revealed by high throughput DNA sequencing. Discov Med 2012; 13: 193-9.

104. Dethlefesen L, Relman DA. Incomplete recovery and individualized responses of the human distal gut microbiota to repeated antibiotic perturbation. Proc Natl Acad Sci U S A 2011; 108: 4554-4561.

105. Dethlefsen L, Huse S, Sogin ML, Relman DA. The pervasive effects of an antibiotic on the human gut microbiota, as revealed by deep 16S rRNA sequencing. PLoS Biol 2008; 6:e280.

106. Janczyk P, Pieper R, Souffrant WB, et al. Parenteral long-acting amoxicillin reduces intestinal bacterial community diversity in piglets even 5 weeks after the administration. ISME J 2007; 1: 180-3.

107. Antonopoulos DA, Huse SM, Morrison HG, et al. Reproducible community dynamics of the gastrointestinal microbiota following antibiotic perturbation. Infect Immun 2009; 77: 2367-75.

108. Pelissier MA, Vasquez N, Balamurugan R, et al. Metronidazole effects on microbiota and mucus layer thickness in the rat gut. FEMS Microbiol Ecol 2010; 73: 601-10.

109. Manichanh C, Reeder J, Gilbert P, et al. Reshaping the gut microbiome with bacterial transplantation and antibiotic intake. Genome Res 2010; 20: 1411-9.

110. White AR. Effective antibacterials: at what cost? The economics of antibacterial resistance and its control. J Antimicrob Chemother 2011; 66: 1948-1953.

111. Cooper MA, Shlaes D. Fix the antibiotics pipeline. Nature 2011; 472: 32.

112. Willing BP, Russell SL, Finlay BB. Shifting the balance: antibiotic effects on host-microbiota mutualism. Nature Rev Microbiol 2011; 9: 233-243.

113. Blaser M. Antibiotic overuse: stop the killing of beneficial bacteria. Nature 2011; 476: 393-394.

114. Fuller R. Probiotics in man and animals. J Appl Bacteriol 1989; 66: 365-78.

115. Roberfrold M, Gibson GR, Hoyles L, et al. Prebiotic effects: Metabolic and health benefits. Br J Nutr 2010; 104: S1-S63.

116. Schrezenmeir J, de Vrese M. Probiotics, prebiotics, and synbiotics- approaching a definition. Am J Clin Nutr 2001; 73(Suppl 2): 361S-4S.

117. Eiseman B, Silen W, Bascom GS, Kauvar AJ. Fecal enema as an adjunct in the treatment of pseudomembranous enterocolitis. Surgery 1958; 44: 854-859.

118. Ricciardi R, Rothenberger DA, Madoff RD, Baxter NN. Increasing prevalence and severity of *Clostridium difficile* colitis in hospitalized patients in the United States. Arch Surg 2007; 142: 624-631.

119. Jarvis WR, Schlosser J, Jarvis AA, Chinn RY. National point prevalence of *Clostridium difficile* in US health care facility inpatients. Am J Infect Control 2009; 37: 263-270.

120. Rupnik M, Wilcox MH, Gerding DN. *Clostridium difficile* infection: new developments in epidemiology and pathogenesis. Nat Rev Microbiol 2009; 7: 526-536.

121. Borody TJ, Khoruts A. Fecal microbiota transplantation and emerging applications. Nat Rev Gastroenterol Hepatol 2012; 9: 88-96.

122. Brandt LJ. Intestinal microbiota and the role of fecal microbiota transplant (FMT) in treatment of *C. difficile* infection. Am J Gastroenterol 2013; 108: 177-185.

123. Chang JY, Antonopoulos DA, Kalra A, et al. Decreased diversity of the fecal microbiome in recurrent *Clostridium difficile*-associated diarrhea. J Infect Dis 2008; 197: 435-438.

124. Kelly CP, LaMont JT. *Clostridium difficile*- more difficult than ever. N Engl J Med 2008; 359: 1932-1940.

125. Guo B, Harstall C, Louie T, et al. Systematic review: fecal transplantation for the treatment of *Clostridium difficile*-associated disease. Aliment Pharmacol Ther 2012; 35: 865-875.

126. Gough E, Shaikh H, Manges AR. Systematic review of intestinal microbiota transplantation (fecal bacteriotherapy) for recurrent *Clostridium difficile* infection. Clin Infect Dis 2011; 53: 994-1002.

127. Borody TJ, Warren EF, Leis S, et al. Treatment of ulcerative colitis using fecal bacteriotherapy. J Clin Gastroenterol 2003; 37: 42-47.

128. Bennet JD and Brinkman M. Treatment of ulcerative colitis by implantation of normal colonic flora. Lancet 1989; 1: 184.

129. Borody TJ, Campbell J. Fecal microbiota transplantation: current status and future directions. Expert Rev Gastroenterol Hepatol 2011; 5: 653-655.

130. Tannock GW, Munro K, Harmsen HJ, et al. Analysis of the fecal microflora of human subjects consuming a probiotic product containing *Lactobacillus rhamnosus* DR20. Appl Environ Microbiol 2000; 66: 2578-2588.

131. Grehan MJ, Borody TJ, Leis SM, et al. Durable alteration of the colonic microbiota by the administration of donor fecal flora. J Clin Gastroenterol 2010; 44: 551-561.

132. Lund-Tonnesen S, Berstad A, Schreiner A, Midtvedt T. *Clostridium difficile*-associated diarrhea treated with homologous feces. Tidsskr Nor Laegeforen 1998; 118: 1027-1030.

133. Persky SE, Brandt LJ. Treatment of recurrent *Clostridium difficile*-associated diarrhea by administration of donated stool directly through a colonoscope. Am J Gastroenterol 2000; 95: 3283-3285.

134. Brandt LJ, Borody TJ, Campbell J. Endoscopic fecal microbiota transplantation: "first-line" treatment for severe *Clostridium difficile* infection?" J Clin Gastroenterol 2011; 45: 655-657.

135. Kassam Z, Hundal R, Marshall JK, Lee CH. Fecal transplant via retention enema for refractory or recurrent *Clostridium difficile* infection. Arch Intern Med 2012; 172(2): 191-193.

136. Arumugam M, Raes J, Pelletier E, et al. Enterotypes of the human gut microbiome. Nature 2011; 473: 174-180.

137. Bakken JS. Fecal bacteriotherapy for recurrent *Clostridium difficile* infection. Anaerobe 2009; 15: 285-289.

138. Van Nood E, Speelman P, Kuijper EJ, Keller JJ. Struggling with recurrent *Clostridium difficile* infections: is donor feces the solution? Euro Surveill 2009; 14: 19316.

139. Landy J, Al-Hassi HO, McLaughlin SD, et al. Review article: faecal transplantation therapy for gastrointestinal disease. Aliment Pharmacol Ther 2011; 34: 409-415.

140. Bakken JS, Borody T, Brandt LJ, et al. Treating *Clostridium difficile* infection with fecal microbiota transplantation. Clin Gastroenterol Hepatol 2011; (9): 1044–1049